Investigation of engineering properties and vegetation performance of biochar-amended soil for the application in the bioengineered structures

A thesis

Submitted in the Partial Fulfilment of the Requirement for the Degree of

DOCTOR OF PHILOSOPHY

By

ROJIMUL HUSSAIN

(Roll No. 176104008)

Under the guidance of

Dr. Ravi K

Department of Civil Engineering

Indian Institute of Technology Guwahati

Guwahati-781039, Assam, India

January, 2022

DEDICATED TO MY BELOVED PARENTS

CERTIFICATE

This is to certify that the thesis entitled **"Investigation of engineering properties and vegetation performance of biochar-amended soil for the application in the bioengineered structures"** submitted by Rojimul Hussain to the Indian Institute of Technology Guwahati, for the award of degree of Doctor of Philosophy (PhD) in Civil Engineering is a record of bonafide research work carried out by him under my supervision and guidance. The thesis work, in my opinion, has reached the requisite standard fulfilling the requirement for the degree of Doctor of Philosophy.

The results contained in this thesis have not been submitted in part or full to any other University or Institute for award of any degree or diploma.

IIT Guwahati

Date: 12/01/2022

Dr. Ravi K

Associate Professor

Department of Civil Engineering

Indian Institute of Technology Guwahati

Guwhati-781039, Assam, India

DECLARATION

I do hereby declare that the content embodied in this thesis is the result of investigations carried out by me in the department of Civil Engineering, Indian Institute of Technology Guwahati, Guwahati, Assam, India.

In keeping with the general practice of reporting scientific observations, due acknowledgements have been made wherever the work described is based on the findings of other investigators.

IIT Guwahati **Rojimul Hussain**

Date: 12/01/2022

ACKNOWLEDGEMENTS

I would like to express my sincere gratitude to my thesis supervisor Dr. Ravi K for the excellent guidance and encouragement during the course of my research work. My association with him is truly memorable. Special thanks are given to my masters (M. Tech) co-supervisor Dr. Ankit Garg who helped in the preparation of research plan. I am grateful to my doctoral committee members Prof. Sreedeep S, Dr. Suresh Kartha and Dr. Pankaj Kalita for their valuable suggestions and encouragement at every stage of this research work.

I am indebted to my family members who have been my greatest source of joy. Thank you Abba, Maa, Ba and Dada for your constant support, prayers, love and encouragement, and believing and upholding me in the times of need.

Special thanks need to be mentioned for my research colleagues Sanandam Bordoloi and Vinay Kumar Gadi with whom I have learned a lot. I would like to acknowledge the support, friendship and love of my seniors and juniors in Indian Institute of Technology Guwahati namely Rohini, Siddarth, Anant, Abhishek, Bhanu, Dhanesh, Atma, Adnan, Utla, Deepak, Arnab, Himanshu, ankit, Kristy, Sameer, Sweta, Goswami, Dhritilekha. I am thankful to Samarjyoti Kalita, Hariram Upadhay, Reshima Begum and Asim Das for their help in carrying out experiments in the geotechnical engineering laboratory. I acknowledge the research facility offered by the Central Instrument Facility (CIF), IITG in completing the study.

I am also thankful to all the faculty members, staff members of Civil Engineering department, IIT Guwahati and to all those who have been related to this study, either directly or indirectly.

Rojimul Hussain

CONTENTS

LIST OF FIGURES

LIST OF TABLES

LIST OF SYMBOLS AND ABBREVIATIONS

Symbol/abbreviation	Description
ABA	Abscisic acid
AC	Ash content
AEV	Air entry value
ASTM	American Society for Testing and Materials
BAS	Biochar-amended soil
BET	Brunauer-Emmett-Teller
C	Carbon content
c	Cohesion
CBR	California bearing ratio
CEC	Cation exchange capacity
DST	Direct shear test
EC	Electrical conductivity
FESEM	Field emission scanning electron microscopy
FOS	Factor of safety
FTIR	Fourier Transform Infrared Spectroscopy
GSD	Grain size distribution
HCF	Hydraulic conductivity function
IPM	Instantaneous profile method
I_r	Infiltration rate
K_{sat}	Saturated hydraulic conductivity
K_{unsat}	Unsaturated hydraulic conductivity
LC	Leaves count
LL	Liquid limit
MB	Mesquite biochar
MDD	Maximum dry density
MDI	Mini disk infiltrometer
n	Fitting coefficient of SWRC
OMC	Optimum moisture content
PAWC	Plant available water content
PI	Plasticity index
PL	Plastic limit
PWP	Permanent wilting point

PY	Photosynthetic yield
PY(II)	Effective photosynthetic yield
RMD	Root mass density
SBB	Sugarcane bagasse biochar
SC	Stomatal conductance
SC_{max}	Maximum stomatal conductance
SC_{min}	Minimum stomatal conductance
SG	Specific gravity
SL	Shrinkage limit
SSA	Specific surface area
SWRC	Soil water retention characteristics or curve
UCS	Unconfined compressive strength
USCS	Unified Soil Classification System
USEPA	United State Environmental Protection Agency
VD	Vegetation density
VD_{max}	Maximum vegetation density
VD_{min}	Maximum vegetation density
VM	Volatile matter
WAC	Water absorption capacity
WHB	Water hyacinth biochar
XRD	X-Ray diffraction
θ_s	Saturated volumetric water content
α	Fitting coefficient of SWRC
θ_r	Residual volumetric water content
θ_{1500}	Volumetric water content at suction of 1500 kPa
ϕ	Angle of internal friction
Ψ_W	Suction at which the vegetation starts wilting
Ψ_{SCD}	Suction at which the SC starts decreasing
F_v/F_m	Maximum photosynthetic yield
F_m	Maximum fluorescence level
F_v	Intermediate fluorescence level
$(F_v/F_m)_{max}$, $(PY(II))_{max}$	Maximum of F_v/F_m and PY(II)
$(F_v/F_m)_{min}$, $(PY(II))_{min}$	Minimum of F_v/F_m and PY(II)
$\Psi_{(Fv/Fm)D}$, $\Psi_{(PY(II))D}$	Suction at which F_v/F_m and PY(II) start decreasing

ABSTRACT

Soil bioengineered structures are comprised of soil for stability and vegetation for protection. These structures are commonly adopted because of their multiple beneficial impacts. The stability and performance of these structures depend on the soil engineering properties and vegetation performance. Further, the vegetation performance i.e., the vegetation growth and health status are interrelated to the soil engineering properties. The vegetation in these structures provides additional stability and protection from erosion and failure. The vegetation roots act as soil reinforcement by anchoring or bridging the soil particles together through mobilization of its tensile strength. The root water uptake by the roots induces suction in soil that in turn increases soil shear strength or stability in terms of apparent cohesion. Further, the above ground mass of vegetation protects the soil surface from erosion along with the aesthetic view. Therefore, suitable growth and health status of vegetation are utmost important for the effective functioning of bioengineered structures. Many a times soil does not provide suitable condition for the growth and health status of vegetation and therefore several amendments have been adopted for improving the vegetation performance. Among these amendments, biochar has been regarded as more suitable soil amendment due to their stable structure i.e., microbial non-degradable and organic nature. Biochar is a carbon-rich material obtained after pyrolysis of biomass under oxygen deficit condition. The conversion of biomass into biochar is also the sustainable way of managing wastes, mitigating climate change and producing energy. Biochar as soil amendment is often used for soil carbon sequestration, improving the soil fertility as well as crop growth and yield, and removing the organic and inorganic pollutants from soil. Application of biochar as soil amendment majorly focused on loose agricultural soil. Soil in bioengineered structures is different from the agricultural soil i.e., often compacted for achieving stability and subjected to a prolong drying due to the irregular irrigation pattern. Therefore, the engineering properties of biochar-amended soil (BAS) and the vegetation performance in BAS need to be investigated under compacted state for ensuring effective stability and performance of bioengineered structures. In the present thesis work, the engineering properties i.e., the hydro-mechanical and physicochemical properties of biochar-amended compacted soil and the vegetation (grass species) growth and health status in biochar-amended compacted soil have been investigated for potential application in bioengineered structures. The results revealed that the amendment of biochar improved the soil engineering properties by increasing the soil pH, CEC, water retention capacity, shear strength and load bearing

capacity, and decreasing the dry density, infiltration rate, saturated hydraulic conductivity, unsaturated hydraulic conductivity and desiccation crack potential. Further, the biochar amendment found to be improved the vegetation performance by increasing the vegetation (roots and shoot mass) growth, delaying the wilting (higher permanent wilting point), decreasing the stomatal conductance (pathogen resistance or good health) and allowing complete photosynthetic activity at relatively large suction. The amendment of different types biochar found to be exhibited variable responses on the soil engineering properties and vegetation performance. Adversely, the undrained shear strength or UCS of the soil was found to be decreased after biochar amendment which needs to be further investigated. However, the magnitude of UCS obtained for 5% (w/w) biochar amendment rate was found to be higher than the minimum (200 kPa) required strength for most of the bioengineered structures and suggested by the united state environmental protection agency (USEPA). Based on the present thesis work, it is suggested to use 5% BAS in bioengineered structures; however, considering field trials before application would add more reliability.

Keywords: Bioengineered structures, Biochar, Biochar-amended soil, Soil engineering properties, Vegetation performance.

CHAPTER 1
INTRODUCTION

1.1 Background

Soil bioengineered structures, such as landfill cover, vegetated slopes and embankment, green roof, turf and golf green are often adopted throughout the world due to their multiple beneficial features. Bioengineered structures mainly consist of soil and vegetation. The soil component of the structure would impart the mechanical stability while the vegetation would help in improving the stability by root reinforcement and surface coverage. Proper functioning of these structures are utmost important as any failure could cause serious consequences to the human and the environment. For example, the failure of a sanitary landfill cover could lead to the emission of harmful greenhouse gases (CH_4 and CO_2) to the environment and could generate the excessive leachate by the ingress of water which in turn could pollute the ground water. The integrity of these structures are dependent on the engineering properties of the soil and the performance of the vegetation which in turn interrelated to the soil properties. Therefore, suitable soil engineering properties, such as physicochemical, hydraulic and mechanical properties are highly important for the proper functioning of these structures. Further, the improved vegetation performance i.e., the growth and health status are equally important which controls the most beneficial features including stability of these structures. Vegetation roots act as soil reinforcement i.e., anchor or bridge the soil particles together by mobilizing its tensile strength and increases the strength or stability which is called as reinforcing action (Wu et al., 1979). The root water uptake by the roots induces suction in soil which acts as apparent cohesion and increases the strength and stability (hydrologic action, Ng et al., 2013). The poor soil engineering properties and vegetation performance could lead to the instability and failure of these structures. Many a times for improving the performance of vegetation, soil is often amended with different types of amendments such as lime, compost, fertilizer, biochar etc. (Hargreaves et al., 2008; Abbas et al., 2018). However, among these, biochar is regarded as more suitable for soil amendment due to their stable structure i.e., microbial non-degradable and unique physicochemical properties (Sohi et al., 2012).

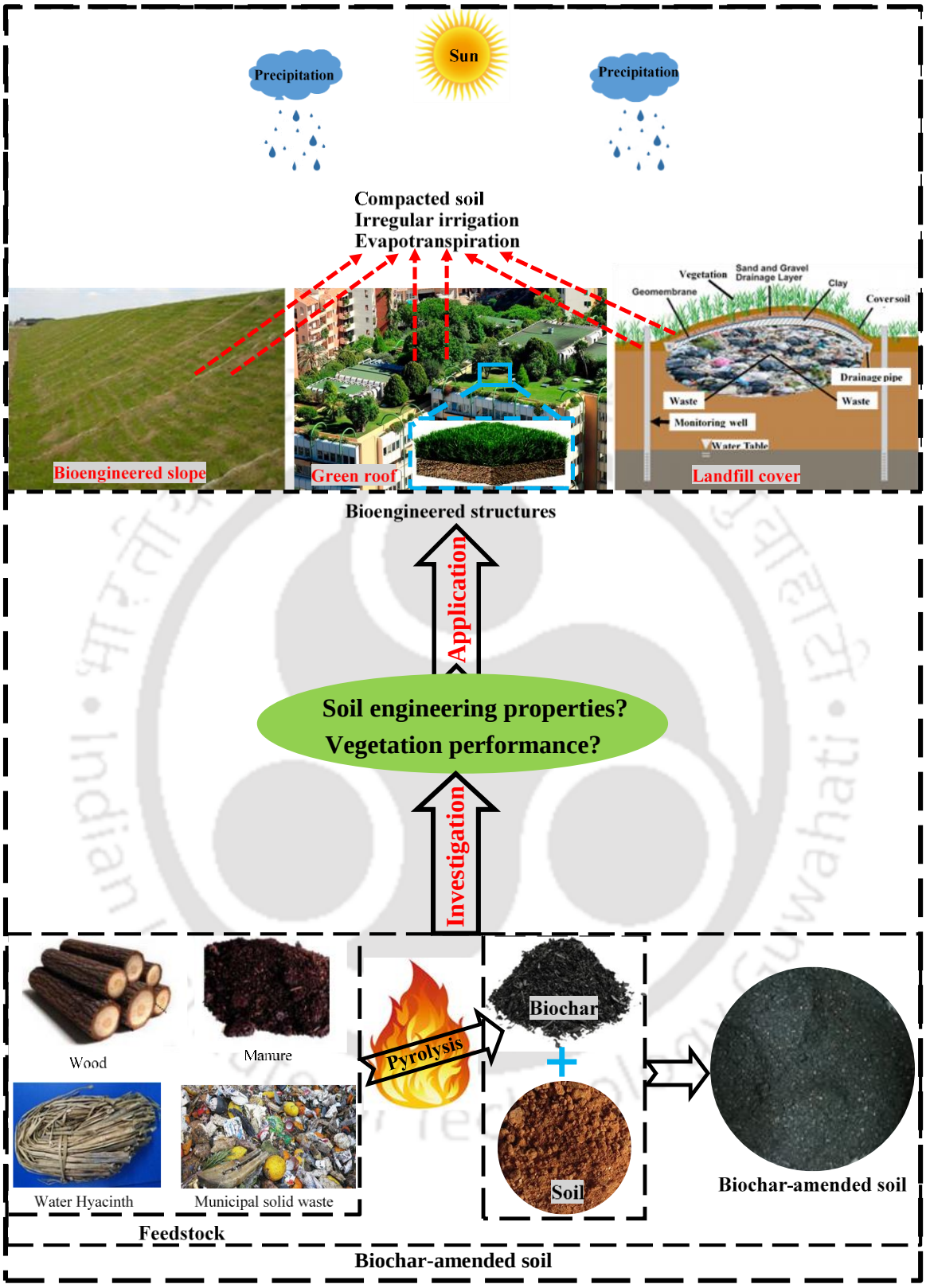

Fig. 1.1 Schematic diagram showing preparation and potential real field application of biochar

Biochar is a carbon-rich product obtained after pyrolysis of biomass, such as wood, manure or solid waste in a closed chamber with little or no oxygen environment (Lehmann and

Joseph, 2009). It has been proposed as soil amendment for carbon sequestration, improving soil fertility as well as vegetation growth and yield, improving nutrient retention and removing organic and inorganic (heavy metal) pollutants (Steinbeiss et al., 2009; Van Zwieten et al., 2010; Jeffery et al., 2011; Chen et al., 2012; Waqas et al. 2015; Vaughn et al., 2018). The high porosity, large specific surface area (SSA), high pH (alkaline), presence of surface functional groups (carboxyl, hydroxyl, and phenolic) and high nutrient content of biochar makes it suitable for soil amendment (Lehmann and Joseph 2009; Uzoma et al., 2011; Ahmad et al., 2014; Tan et al., 2015). Extensive literature is available where biochar amendment in soil found to be improved the soil properties (Lehmann et al., 2011; Lei and Zhang, 2013; Ahmad et al., 2014; Reddy et al., 2014; Wong et al., 2017; Garg et al., 2019; Ganesan et al., 2020). Therefore, biochar-amended soil (BAS) could be extended to bioengineered structures. Fig. 1.1 highlights the systematic production to potential application of biochar in bioengineered structures as an engineering material for improving their performances.

1.2 Motivation of the study

The amendment of biochar in soil i.e., the biochar-amended soil for improving the soil fertility was first adopted by the people of Amazonian region (Lehmann and Joseph, 2009). Biochar has been recognized as an effective tool for environmental management, such as waste management, climate change mitigation, energy production and soil improvement. Solid waste management is the crucial challenge faced by the modern-day cities due to their land scarcity and high population density (Ferronato et al., 2017). As a result, sustainable waste disposal strategies are becoming attractive solutions to improve solid waste management in urban areas (Zhao et al., 2009). Currently, landfilling, incinerating, and composting are the most common methods of waste disposal. Landfill waste disposal not only occupies a large amount of valuable land but could also cause pollution due to failure that threatens humans and the environment (Karakus et al. 2017). For example, the failure of the Manila landfill cover caused by the heavy rain in the Philippines in 2000 resulted in serious pollution of the environment (Karakus et al. 2007). Further, the incineration and open composting of waste generate greenhouse gases and foul smell to the environment (Xu et al., 2020). Therefore, the production of biochar is the potential best option for managing the waste originating from animals or plants, thus decreasing the associated pollution loading from the environment. The use of waste biomass in biochar production is not only

economical but also beneficial such as energy production and climate change mitigation (Barrow, 2012). The Pyrolysis of the waste biomass kills the any microbes present in that, thereby reducing the potential harmful environmental health effects (Lehmann and Joseph, 2009). However, the persistence of toxic heavy metals in biochar that develops from sewage sludge and municipal solid waste (Lu et al., 2012) must be carefully handled before long-term application to soil.

The application of biochar in soil is also one of the best ways to mitigate the climate change through sequestering the C in soil (Lehmann et al., 2008). The rapid climate change or the global warming is mainly caused by the piling of the greenhouse gases, such as CH_4, CO_2 and NO_2 gases. The long-term stability of biochar in soil is the key factor that decreases the emission of CO_2 into the atmosphere (Cheng et al., 2008; Singh et al., 2012). The pyrolysis of biomass into biochar produces lesser volume of CO_2 compared to that of incineration or open air combustion of biomass as observed from the Life Cycle Assessment (LCA) thus curtailing the stock of CO_2 in the atmosphere (Shen et al., 2020). The efficacy of biochar in reducing the concentration and emission of CH_4 gas in landfill liner system by adsorption and oxidation of CH_4 into CO_2 has been well documented (Reddy et al., 2014a; Sadasivam and Reddy, 2015 and Yargicoglu and Reddy, 2017). Further, the application of biochar reduced the emission of greenhouse gases (N_2O, CO_2 and CH_4) from the agricultural soil (Karhu et al., 2011). Therefore, the reduced greenhouse gases with biochar could effectively mitigate the climate change and hence its allied impact on the environment.

The application of biochar in soil and water could reduce the accumulation of organic and inorganic (heavy metals) pollutants through sorption thereby, lowering the toxicity in vegetation and animal by reducing the bioavailability of these pollutants (Qiao et al., 2017 and Zou et al., 2017). The amendment of biochar of high organic C content, internal porosity and pH improves the physicochemical and biological properties of agricultural soil (Ahmad et al., 2014). The biochar amendment increases the microbial population and activity by providing suitable habitant (porous structure) for microbes and improving the enzymatic activity in soil (Verheijen et al., 2010; Lehmann et al., 2011) that influences the biogeochemical processes, example vegetation growth in soil (Lehmann et al., 2011; Awad et al., 2012). The amendment of biochar of alkaline pH induces a liming effect on the acidic soil similar to adding lime in soil which is beneficial for the growth or productivity of vegetation (Reddy et al., 2014). The application of biochar in soil decreases the leaching of nutrients or improves the nutrient retention in soil (Beck et al., 2011; Major et al., 2012; Cheng et al.,

2017 and Lee et al., 2018), thereby higher stock of nutrient available in soil for the roots to uptake, as a result higher growth of vegetation. Biochar amendment improves the growth and yield of crops in agricultural soil by altering the physicochemical properties of the soil (Biederman and Harpole, 2013). Further, the inclusion of biochar in soil alters the pore structure or system and water affinity of the soil that in turn affects the soil water retention characteristics, hydraulic conductivity, infiltration rate and strength behavior (Laird et al., 2010; Uzoma et al., 2011; Lei and Zhang, 2013; Du et al., 2017; Moragues-Saitua et al., 2017; Suliman et al., 2017 and Wong et al., 2017). Major investigations on the impact of biochar as soil amendment were conducted for loose agricultural soil where soil does not compact and subjected to regular irrigation. However, the biochar effect on compacted soil suitable for bioengineered structures was rarely investigated. Reddy et al. (2014) and Sadasivam and Reddy. (2015) explored the biochar effect on methane oxidation and extraction in compacted landfill cover soil. Similarly, researchers (Wong et al., 2016; Bordoloi et al., 2018; Ni et al., 2018; Garg et al. 2019) have investigated the biochar effect on microbial activity and soil properties for intending application in landfill soil. Therefore, biochar-amended soil could be use in bioengineered structures where structural stability and vegetation growth are the major concerns. It would be the sustainable strategy for managing the waste, improving the soil properties and reducing the environmental pollution loadings. However, before that, the engineering properties of compacted biochar-amended soil and the vegetation performance in biochar-amended soil need to be investigated for ensuring the adequate stability and proper functioning of these structures.

1.3 Organization of the thesis

The **first chapter** presents the introduction of the study where motive and background for the study are highlighted.

Chapter 2 presents the detailed literature review of the studied topic. The influence of biochar amendment on various soil properties and vegetation performance was reviewed and discussed. The research gap has been identified and the objectives for the study set accordingly and presented in chapter 2.

Chapter 3 presents the detailed methodology used for evaluating the different soil properties and vegetation performance.

Chapter 4 discussed the results obtained for the physicochemical and microstructural properties of the different types biochar produced, different types soil tested and the biochar-amended soil.

Chapter 5 presents the results of saturated hydraulic conductivity and infiltration rate obtained for biochar-amended soil considering the effect of different biochar types, amendment rates, biochar particles size and the soil types.

Chapter 6 presents the results obtained for soil water retention characteristics (SWRC) and unsaturated hydraulic conductivity of the biochar-amended soil considering different biochar types, amendment rates and soil types, and measured under drying and wetting scenario.

Chapter 7 presents the results obtained for mechanical properties i.e., the shear strength and load bearing capacity of the biochar-amended soil considering different biochar types, amendment rates and soil types.

Chapter 8 presents the results obtained for the vegetation performance i.e., the vegetation growth and health status in biochar-amended soil considering different biochar types, amendment rates and soil types. Correlation among the soil properties and plant parameters are also presented.

Chapter 9 summarizes the major findings of the study and proposed future potential scope of works.

CHAPTER 2
LITERATURE REVIEW

2.1 Introduction

The initiation of every research work requires the information of past history and the current status. Considering this, the research work carried out by the past researchers was reviewed and elaborated in this chapter. The characteristics and production process of biochar, and the parameters influence the biochar properties are discussed in section 2.2. The influence of biochar amendment on the engineering behavior of soil, such as physicochemical, hydraulic and mechanical properties are elaborated in section 2.3, 2.4, 2.5 respectively. Further, the effect of biochar amendment on the performance of vegetation or plants is also discussed in section 2.6. After a substantial literature review, the research objectives of the present study are decided and presented in section 2.7.

2.2 Biochar: characteristics and production process

The application of biochar in the Amazonian region called “terra-preta de indio”, where dark black soils were prepared through slash-and-char technique has been reported in the literature (Lehmann and Joseph 2009). Several definitions of biochar have been forwarded by different authors; however, International Biochar Initiative (IBI) standardized the definition as ‘‘*a solid material obtained from the thermochemical conversion of biomass in an oxygen-limited environment’’* (IBI 2015). Fig. 2.1 highlights the physical appearance and internal structure of biochar.

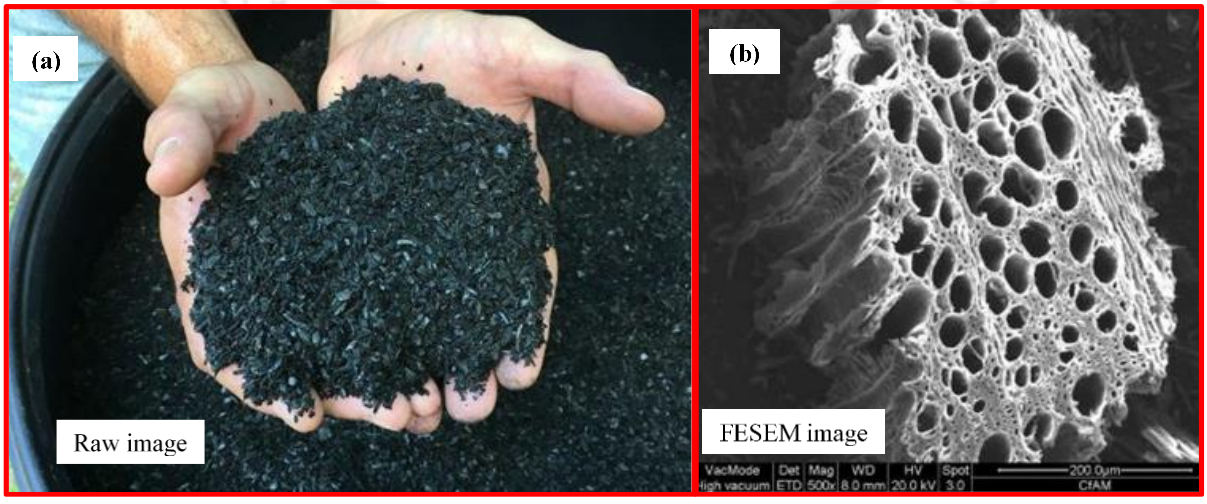

Fig. 2.1 Biochar (a) physical appearance and (b) internal structure.

In general, a wide range of feedstock, such as wood, manure, rice husk, straw, bagasse, plant residue, bamboo and municipal solid waste (MSW) are utilized in the production of biochar through thermochemical conversion (Tan et al. 2018). The plant-based feedstock mainly consists of cellulose, hemicellulose, and lignin, which are gradually degraded during thermochemical conversion process. The animal-based feedstock, like manure, mainly consist of organic matter or compound, which is less degradable (Ahmad et al. 2014). Similarly, the MSW is characterized by high salt content due to the presence of waste food (Zhou et al. 2015). The thermochemical conversion processes for the production of biochar include gasification and pyrolysis. The pyrolysis process of biochar can be slow pyrolysis or fast pyrolysis, where slow pyrolysis leaves higher biochar output (15–89%) compared to the fast pyrolysis (Tan et al. 2015). The characteristics of feedstock and the pyrolysis condition influence the physical and chemical properties of the biochar (Tomczyk et al. 2020).

Biochar derived from manure has been characterized by high nutrient content and cation exchange capacity (CEC) (Singh et al. 2010; Uzoma et al. 2011; Tan et al. 2018). A higher nutrient content in poultry litter biochar compared to the other biochar (sugarcane straw, rice hull and sawdust) was documented by Conz et al. (2017). Among plant-based feedstock, the pyrolysis of wood biomass leaves a higher carbon (C) content due to the abundant availability of lignocellulose content in wood biomass (Tan et al. 2018). Among four different (rice husk, rice straw, apple tree and oak tree) biochar tested, wood-based biochar showed higher C content (Jindo et al. 2014). The nutrient concentration, porosity and specific surface area (SSA) of biochar increases with the increase of pyrolysis temperature (Downie et al. 2009; Jindo et al. 2014; Tan et al. 2018). The breaking of aliphatic alkyl and ester groups with temperature causes a higher loss of volatile substances, such as cellulose and hemicellulose and therefore, the formation of micro-pores (Kim et al. 2013; Ahmad et al. 2014). However, the increase of pyrolysis temperature has a negligible influence on the SSA of biochar obtained from animal manure and solid waste due to nonexistence of lignocellulosic compound. In fact, a lower SSA compared to the plant-based biomass could be observed at higher pyrolysis temperature (Ahmad et al. 2014). The pH of biochar increases with pyrolysis temperature due to the release of higher nutrient or alkali salts at elevated pyrolysis temperature (Conz et al. 2017). CEC, that represents the negative surface charge of the biochar, may increase or decrease with pyrolysis temperature depending on the functional groups present in the biochar. In addition, the concentration of volatile matter decreases and the C content increases with elevated pyrolysis temperature, leading to a low concentration of

Oxygen (O) and Hydrogen (H) (Tan et al. 2015; Yargicoglu et al. 2015). Therefore, the physiochemical properties of biochar are mostly governed by the feedstock characteristics and the pyrolysis conditions. Thus, the selection of suitable feedstock and the pyrolysis condition through characterization is utmost important for specific application of biochar.

2.3 Physicochemical properties of BAS

The investigation of the physicochemical properties of soil after biochar amendment is crucial as the migration of gases, microbial activity, water retention, hydraulic conductivity and the growth and development of vegetation are dependent on the soil physicochemical properties (Wong et al., 2016, 2017, 2019; Chen et al., 2018; Bordoloi et al., 2019). The influence of biochar amendment on soil physicochemical properties was studied by past researchers, Table 2.1 highlights the elaboration of those studies. The dry or bulk density of soil was observed to be decreased after amendment of biochar. The lightweight of biochar relative to soil and internally porous structure of biochar causes reduction in mass and compressibility of BAS compared to bare soil; thus, lower dry density compared to bare soil. The pH of soil is often reported to be increased after biochar amendment. However, it is dependent on the pH of the soil and biochar. Biochar mostly exhibits neutral to alkaline pH and few exceptions acidic depending on the feedstock type. The amendment of alkaline biochar in acidic soil increases the pH, while for neutral to basic pH soil, the biochar amendment may not influence the pH. The specific gravity of soil also decreases after biochar amendment by the mass reduction due to replacement of soil by lightweight biochar. The atterberg limits i.e., liquid limit, plastic limit and shrinkage limit of soil, which are important engineering properties related to soil hydro-mechanical properties are also influence by the biochar amendment. The biochar amendment may increase or decrease the atterberg limits depending on the type of soil and biochar amended (Table 2.1). The amendment of biochar in course-grained soil (silt and sand) have the chance to increase the atterberg limit due to enhanced water absorption by the biochar as these soil showcase low atterberg limits. While clayey soils have the chance to decrease the atterberg limits, since clayey soil generally poses large liquid and plastic limit due to higher water adsorption capacity compared to biochar. Therefore, the physicochemical properties of BAS varies soil to soil and biochar to biochar. Thus, the effect of the biochar on physicochemical properties of a particular soil need to be investigated before applying in a specific purpose.

Table 2.1 Review of literature on the effect of biochar on soil physicochemical properties.

References	Soil type	Biochar			Parameter measured					
		Feedstock	Pyrolysis Tem, ˚C	Mix proportion	pH	SG	Density	LL	PL	SL
Yaghoubi and Reddy 2011	Silty clay	Wood pellets	520	5, 20% (w/w)	Increased	Decreased	-	Increased	Increased	-
Ibrahim et al. 2013	Sandy loam	Conocarpus	400	0.5, 1, 1.5, 2% (w/w)	-	-	Decreased	-	-	-
Zong et al. 2014	Silty clay	Wheat straw, woodchip, waste water sludge	500	2, 4, 6% (w/w)	-	-	-	Decreased	Decreased, Increased, Decreased	-
Reddy et al. 2015	Silty clay	Wood pellet	520	5, 10, 20% (w/w)	Increased	Decreased	No effect	Increased	Increased	-
Ajayi and Horn 2016	Fine sand, Sandy loam silt	Wood-chips	500-600	2, 5, 10% (w/w)	Increased	-	Decreased	-	-	-
Du et al. 2016	Silty loam, Loam	Peanut shells	350-500	Not available	No effect	-	Decreased	-	-	-
Zong et al. 2016	Sandy silt	Wheat straw, woodchip, waste water sludge	500	2, 4, 6% (w/w)	Increased	-	-	Increased	Decreased	-
Ahmed et al. 2017	Silt loam	Maple wood	500	2, 5, 10% (w/w)	-	-	Decreased	Increased	Increased	-
Moragues-saitua et al. 2017	Sandy clay loam, Loam	Miscanthus sp.	450	3.5, 10, 20 (Mg/ha)	-	-	No effect	-	-	-
Ni et al. 2018	Silty sand	Peanut-shell	500	10% (w/w)	-	-	Decreased	-	-	-
Williams et al. 2018	Clay	Pine wood	-	5, 10, 20, 30% (w/w)	-	-	Decreased	-	-	-

References	Soil type	Biochar			Parameter measured					
		Feedstock	Pyrolysis Tem, ˚C	Mix proportion	pH	SG	Density	LL	PL	SL
GuhaRay et al. 2019	Clay	Mesquite	500	5, 10% (w/w)	Increased	Decreased	Decreased	Decreased	Increased	-
Bora et al. 2020	Silty sand	Water hyacinth, peanut shell, sawdust, poultry litter	390, 510, 530, 450	5, 10% (w/w)	-	-	Decreased	Increased	Increased	Increased
Ganesan et al. 2020	Clayey sand	Cedar wood	350, 550	5, 10% (w/w)	-	-	Decreased	Increased	Increased	increased

LL- liquid limit, PL- plastic limit, SL- shrinkage limit, SG- specific gravity, Tem- temperature.

2.4 Hydraulic properties of BAS

Hydraulic properties of soil are indeed important that governs the movement of water through soil, stability of soil engineered structures and compressibility of soil. The root water uptake by plant roots and irrigation efficiency in agricultural field are also dependent on soil hydraulic behavior (Clarke and Townley Smith, 1986; Shwetha and Varija, 2015). Extensive research on hydraulic properties of soil has been conducted in conventional unsaturated and saturated soil mechanics (Fredlund and Rahardjo, 1993). Soil water retention characteristics or curve (SWRC), infiltration rate, unsaturated hydraulic conductivity and saturated hydraulic conductivity are the highly concerned hydraulic properties in conventional soil mechanics. The amendment of biochar of high porosity (Lehman and Joseph 2009) and water absorption capacity (Githinji, 2014) in soil could alter the soil hydraulic properties by changing the pore size network of the soil (Nimmo 1997; Downie et al. 2009; Verheijen et al. 2010). The influence of biochar on soil hydraulic properties has been reviewed and elaborated in detail below. Table 2.2 presents the review of literature on the influence of biochar amendment on the different soil hydraulic properties.

2.4.1 Soil water retention characteristics

Water retention characteristics of any geophysical material is represented by the relation of suction and water content. Commonly, for soil, the relation is termed as soil water retention curve (SWRC) and expressed by suction (Ψ) with volumetric (θ) or gravimetric water content (ω) or degree of saturation (S_r) or void ratio (e) (Ng and Pang, 2000 and Malaya and Sreedeep, 2011). The SWRC is highly important to estimate various parameters required to describe the unsaturated soil behavior (Marshall 1958; Mualem 1986 and Fredlund and Rahardjo 1993). The empirical prediction of shear strength and permeability function of unsaturated soil and solving unsaturated flow problems using deterministic and stochastic models requires SWRC as an input (Tamari et al., 1993). The optimum water retention in root zone defined by SWRC is utmost important for the growth and development of vegetation in bioengineered structures (embankment, green slopes and landfill cover), and agricultural system (Clarke and Townley Smith, 1986). Further, the simulation of root water uptake and the contaminant flow through barrier requires the SWRC as an input parameter (Cuenca et al. 1996; Sinowski et al. 2009). The SWRC of soil is influenced by many factors including soil type (texture), degree of compaction, compaction water content, measuring path (drying/wetting) and the instrument employed for measurement (Marinho and Stuermer 2000; Ng and Pang 2000; Lu and Likos 2004; Sreedeep and Singh 2011).

Table 2.2 Review of literature available on biochar effect on soil hydraulic properties

References	Soil type	Biochar			Parameter measured			
		Feedstock	Pyrolysis Tem, ˚C	Mix proportion	K_{sat}	K_{unsat}	Infiltration	SWRC
Busscher et al. 2010	Loamy sand	Pecan	700	11, 22, 44 (Mg/ ha)	-	-	No effect	-
Uzoma et al. 2011	Sand	Black locust	300, 400, 500	10, 20 (Mg/ha)	Decreased	Decreased	-	Increased
Kameyama et al. 2012	Clay	Sugarcane bagasse	400,500,600, 700,800	1, 3, 5, 10% (w/w)	Increased	Increased	-	Increased
Herath et al. 2013	Silt loam	Corn Stover	350, 550	10, 11 (Mg/ha)	Increased	-	-	-
Ibrahim et al. 2013	Sandy loam	Conocarpus	400	0.5, 1, 1.5, 2% (w/w)	Decreased	-	Decreased	Increased
Lei and Zhang 2013	Loam	Dairy manure, Woodchip	300, 500, 700	5% (w/w)	Increased	-	-	Increased
Ouyang et al. 2013	Silty clay, Sandy loam	Dairy manure	500	2% (w/w)	No effect	-	-	Increased
Barnes et al. 2014	Sand, Clay	Mesquite wood	400	10% (w/w)	Decreased, Increased	-	-	-
Carvalho et al. 2014	Sand	Eucalyptus wood	450	8, 16, 32 (t/ha)	-	-	-	No effect
Githinji 2014	Sand	Peanut hulls	500	25, 50, 75, 100% (v/v)	Decreased	-	Decreased	-
Hardie et al. 2014	Sandy loam	Acacia tree	550	-	-	No effect	-	No effect
Prober et al. 2014	Clay loam	Green-waste	600	20 (t/ha)	-	-	Increased	-
Rogovska et al. 2014	Loam	Hardwood wood chip	500-575	19, 38, 58, 77, 96 (Mg /ha)	-	-	No effect	Increased

References	Soil type	Biochar			Parameter measured			
		Feedstock	Pyrolysis Tem, ˚C	Mix proportion	K_{sat}	K_{unsat}	Infiltration	SWRC
Sun and Lu 2014	Clayey silt	Crop straw, Woodchips, Wastewater-sludge	500	2, 4, 6% (w/w)	-	-	-	Increased
Castellini et al. 2015	Clay	Prunings of trees	500	0.5, 1, 2, 3% (w/w)	No effect	Negligible effect	-	Increased
Jeffery et al. 2015	Sand	Hay	400, 600	1, 5, 20, 50 (t/ha)	No effect	-	-	No effect
Ojeda et al. 2015	Sandy loam	Sewage sludge, Poplar, Pine wood	500-550	1% (w/w)	-	-	-	No effect
Ajayi and Horn 2016	Fine sand, Sandy loam silt	Wood-chips	500-600	2, 5, 10% (w/w)	Decreased, Increased	-	-	Increased
Andrenelli et al. 2016	Silty clay loam	Pelletize wheat-bran	800, 1200	14 (Mg/ha)	-	-	-	Increased
Du et al. 2016	Silty loam, Loam	Peanut shells	350-500	Not available	Decreased	-	-	Increased
Lim et al. 2016	Coarse sand, Fine sand, Silt loam, Clay loam	Hardwood wood pellets, Pine wood chips, Hardwood chips, Oat hulls	500	1, 2, 5% (w/w)	Decreased, Decreased, Increased, Increased	-	-	-
Novak et al. 2016	Sandy loam	Pine chips, Poultry litter	500	2% (w/w)	-	-	Increased	-
Igalavithana et al. 2017	Sandy loam	Corn residue	500	2.5, 5, 7.5, 10% (w/w)	Decreased	-	-	-

References	Soil type	Biochar			Parameter measured			
		Feedstock	Pyrolysis Tem, ˚C	Mix proportion	K_{sat}	K_{unsat}	Infiltration	SWRC
Moragues-saitua et al. 2017	Sandy clay loam, Loam	Miscanthus sp.	450	3.5, 10, 20 (Mg/ha)	No effect	-	-	Increased
Obia et al. 2017	Sandy loam, loamy fine sand	Corn cobs	350	1.7, 2, 3.4, 4% (w/w)	Decreased, No effect	-	-	-
Suliman et al. 2017	Sand	Pine wood, Pine bark, Hybrid poplar wood	350, 600	2% (w/w)	-	-	-	Increased
Wong et al. 2017	Kaolin clay	Peanut-shell	500	5, 20% (w/w)	-	-	-	Increased
Bordoloi et al. 2018	Sandy Clay	Water hyacinth	300-350	2, 5, 10, 15% (w/w)	-	-	-	Increased
Villagra-Mendoza and Horn 2018	Sand, Sandy loam	Mango wood	600	2.5, 5% (w/w)	Decreased	Increased, No effect	-	Increased
Wong et al. 2018	Kaolin clay	Peanut-shell	500	5, 20% (w/w)	Increased	-	-	-
Wanniarachchi et al. 2019	Loam sand	Pine wood	500	20 (Mg/ha)	No effect	Decreased	Decreased	-

Note: '-'Not measured, Tem- Temperature, SWRC- Soil water retention curve

These factors mainly influence the pore geometry or network of the soil that ultimately alters the SWRC (Hillel 1982; Nimmo, 1997 and Verheijen et al., 2010). Experimental measurement of SWRC both in laboratory as well as in field has been well established. Drying (desorption) and wetting (adsorption) are the two process commonly adopted in measurement of SWRC (Lu and Likos, 2004). Experimental technique of measurement mainly includes axis translation technique (Hilf 1956) and vapour equilibrium technique (Tang & Cui 2005), based on which several measuring devices, such as pressure plate apparatus (Gardner 1956), thermocouple psycrometer and various electronic sensors were developed. However, measurement of wide range of suction using these techniques is tedious and time consuming (Casini et al. 2013). Therefore, several mathematical models (functions) have been developed to obtain wide range of suction in a shorter duration (Brooks & Corey 1964; van Genuchten, 1980).

The amendment of highly porous biochar in soil alters the soil pore size network. The change in pore size distribution or network could affect the soil matric suction and hence, the SWRC as highlighted in Fig. 2.2.

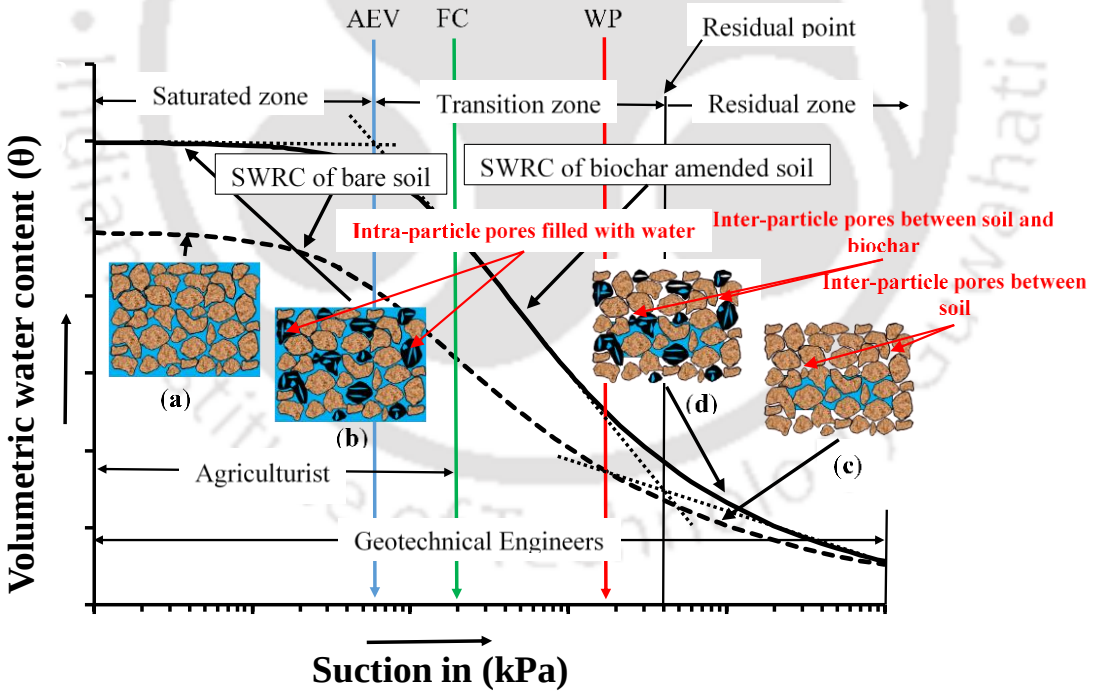

AEV- Air entry value, FC- Field capacity, WP- Wilting point

(**a**) Saturated bare soil, (**b**) Saturated biochar amended soil

(**c**) Bare soil at higher suction, (**d**) Biochar amended soil at higher suction

Fig. 2.2 Diagram showing the effect of biochar on saturated to dry state of a soil along the SWRC

The large SSA of biochar due to the high porosity or the presence of intra-particle pores (pores within biochar skeleton, (Lehmann and Joseph, 2009; Gao and Masiello, 2017)) modifies the pore size distribution or the total porosity in soil-biochar composites (Nimmo, 1997; Verheijen et al., 2010). In addition, the pore size distribution may also be changed by the alteration of inter-particle pores (pores between soil-soil or soil-biochar particles, (Gao and Masiello, 2017; Liu et al., 2017)) which is dependent on the relative size of biochar particles, soil texture and aggregate stability of the soil (Ouyang et al., 2013; Barnes et al., 2014; Sun and Lu, 2014; Liu et al., 2017). The change in pore size or the porosity affects the capillary action of the soil, thereby altering the SWRC (Fredlund and Rahardjo, 1993; Eden et al., 2017). The change in capillary action or the matric suction can be understood by the relationship given below:

$$\Psi m = \frac{4T \cos \theta}{d} \qquad (2.1)$$

where ψ_m is the matric suction (in kPa), T is the surface tension of water (equal to 0.072 N/m at 20˚C), θ is the contact angle between the water-air interface and soil-biochar surface, and d (in m) is the pore diameter. Extensive study on the effect of biochar on SWRC has been undertaken in the recent past and some of these studies are highlighted in Table 2.2. It could be observed from Table 2.2 that some researchers found an increased water retention of the soil after amendment of biochar, while some others also mentioned a no influence of biochar on the water retention. Moreover, it has been observed from the critical assessment of the literature (Table 2.2) that the influence of biochar on the SWRC varies with many factors, such as relative size of the soil and biochar particles, compaction density and water content, type of biochar or feedstock and pyrolysis temperature, amendment rate and aging of the biochar.

Unlike fine-grained soil, coarse-grained soil constitutes of large inter-pores (pores between particles) and retain less water due to the absence of any charge on its surface. The amendment of biochar in coarse-grained soil often increases the water retention (Busscher et al. 2010; Basso et al., 2013). However, the application of biochar may reduce or may not influence the water retention of fine-grained soils, which are characterized by higher water retention. The amendment of biochar of particle size smaller than the particles size of coarse-grained soil may reduce the porosity of the soil through filling or blocking of the inter-pores (Ajayi and Horn 2016). This is resulting in higher suction in pore spaces (see from Eq. (2.1)) and concurrently, some water would retain in the intra-pores present in biochar skeleton,

hence, increase in water retention (Chen et al. 2010). Whereas, in fine-grained soils that have particles of size smaller than the biochar particles may lead to a higher porosity or increase pore space due to the formation of macro aggregate (Lei and Zhang 2013; Sun and Lu 2014). As a consequence, a decrease or no change in water retention could occur. Therefore, the increase in water retention due to biochar inclusion is expected to be higher in coarse-grained soil compared to the fine-grained soil (Ouyang et al. 2013; Du et al. 2016; Moragues-Saitua et al. 2017). Ouyang et al. (2013) mentioned a relatively higher water retention in sandy loam soil compared to that of silty clay soil while investigating the SWRC of biochar amended silty clay and sandy loam. Irrespective of soil type, the SWRC varies with the particle size of biochar. The number of intra-pores present in biochar is dependent on the particle size of the biochar (Liu et al. 2017). It implies that the biochar with larger particle size generally exhibits a higher numbers intra-pores and hence, retain more water as compared to biochar of smaller particle size. The reduction of biochar particle size by breaking or grinding of the parent biochar for various application could lead to a destruction of intra-pores and hence, lower SSA and water retention (Spokas et al. 2014). Liu et al. (2017) reported an increase in water retention with increased particle size of the biochar while investigating the effect of three different particle size of biochar on the SWRC of a sandy soil.

The density or compaction condition of soil has a strong influence on the SWRC (Ng and Pang 2000), since the pore size of soil changes with the compaction density. The size of pores decreases with density due to the expulsion of air from the pores (Ranjan and Rao 2007). The effect of biochar on the SWRC of soil is thought to vary with compaction density. Wong et al. (2017) investigated the effect of density and initial moisture content on the SWRC of biochar-amended clay. A higher water retention in soil compacted at lower density compared to the soil compacted at higher density was reported. At low compaction density, the formation of macro aggregate leads to the higher pore spaces for the biochar-amended clay to retain water in inter-pores (Sun and Lu 2014). However, at higher density, the effect of macro aggregates suppressed leading to the lesser pore spaces hence, lower water retention (Wong et al. 2017).

The amendment of biochar derived from plant-based feedstock showed higher water retention compared to biochar derived from manure-based feedstock (Lei and Zhang 2013; Suliman et al., 2017). Biochar produced from plant-based feedstock exhibits a higher porosity (intra-pores) with larger SSA and charge density on surface (Liang et al. 2006; Githinji 2014) compared to manure-based feedstock leading to the higher water retention. The water

retention increases with elevated pyrolysis temperature of plant-based biochar (Andrenelli et al. 2016; Suliman et al. 2017). The increase of pyrolysis temperature accelerates the degradation rate of lignocellulosic components present in plant-based feedstock leading to the formation of more numbers of intra-pores with large SSA hence, higher water retention (Kim et al. 2013). Whereas, in manure-based biochar, the absence of lignocellulosic component causes no effect of elevated pyrolysis temperature (Ahmad et al. 2014). Moreover, the hydrophobic nature of biochar decreases with increase in pyrolysis temperature, which may also cause a higher water retention (Suliman et al. 2017).

The amendment rate and the aging of biochar affect the SWRC (Barnes et al. 2014; Ajayi and Horn 2016; Paetsch et al. 2018). An increased water retention with increase in amendment rate of biochar is often reported by researchers (Abel et al. 2013; Sun and Lu 2014; Moragues-Saitua et al. 2017). At identical density, the application of biochar at higher rate (20% w/w) showed a significant increase in water retention whereas, a low amendment rate (5%) showed no significant change (Wong et al. 2017). The aging or weathering of biochar with time in field causes change in physiochemical properties (Sorrenti et al. 2016) and disintegration of biochar into smaller particles (Spokas et al. 2014). This process leads to a decrease in porosity by the destruction of biochar intra-pores and clogging of soil macro-pores (Liu et al., 2017). The decreased porosity due to aging affects the SWRC (Paetsch et al., 2018). A higher water retention (plant available water) was observed in a three years aged BAS over a fresh BAS (Paetsch et al. 2018).

In contrast, a group of researchers (Table 2.2) mentioned a no or negligible effect of biochar on the SWRC. The non-wettability or hydrophobic nature of the biochar caused by the formation of some surface functional groups could be attributed to the no biochar effect. The hydrophobicity of biochar prevents water from entering into the biochar intra-pores leading to no change in SWRC (Jeffery et al. 2015). Further, the low amendment rate of biochar which may not be sufficient could also be attributed to the no change in the SWRC (Carvalho et al. 2014). The existing literatures mainly focused on the agricultural soil system (i.e., loose soil or low density and design life) compared to bioengineered structures where soil compacted at higher to moderate density and the design life is very high. In addition, a higher amendment rates of biochar were adopted in many literatures which may not be feasible for large structures such as bioengineered structures (Yu et al. 2013; Liu et al. 2014). Therefore, further research is needed to consider the above discussed factors, which are utmost important for bioengineered structures.

2.4.2 Unsaturated hydraulic conductivity

The unsaturated hydraulic conductivity (K_{unsat}) of soil is a vital hydraulic property that governs the transient seepage through the soil, infiltration of water into the soil, water uptake by plant roots, water flow through earthen channels and wells and evaporation from the soil surface (Fredlund and Rahardjo 1993; Ranjan and Rao 2007; Gadi et al. 2016). The stability of engineered structures, such as compacted embankments and slopes, when subjected to a rainfall loading is highly dependent on the hydraulic conductivity (Leung and Ng 2013; Leung et al. 2016). This is because the magnitude and distribution of pore-water pressure (PWP) and suction during rainfall events controlled by the hydraulic conductivity. The K_{unsat} of soil is affected by many factors, including void ratio, suction or water content and net stress (Romero et al. 1999; Ng and Leung 2012; Gallage et al. 2013). Experimental measurement of K_{unsat} both in laboratory and field has been documented in literatures. It includes steady state measurement technique such as constant head method, constant flow method and centrifuge method, and transient state technique such as horizontal infiltration method, outflow method and instantaneous profile method. Moreover, estimation K_{unsat} from measured saturated hydraulic conductivity (K_{sat}) and SWRC using different empirical, macroscopic and statistical models (for e.g. Richards (1931), Gardner (1958), Brooks and Corey (1964) and Marshall, (1958) model) also well established (Lu and Likos, 2004).

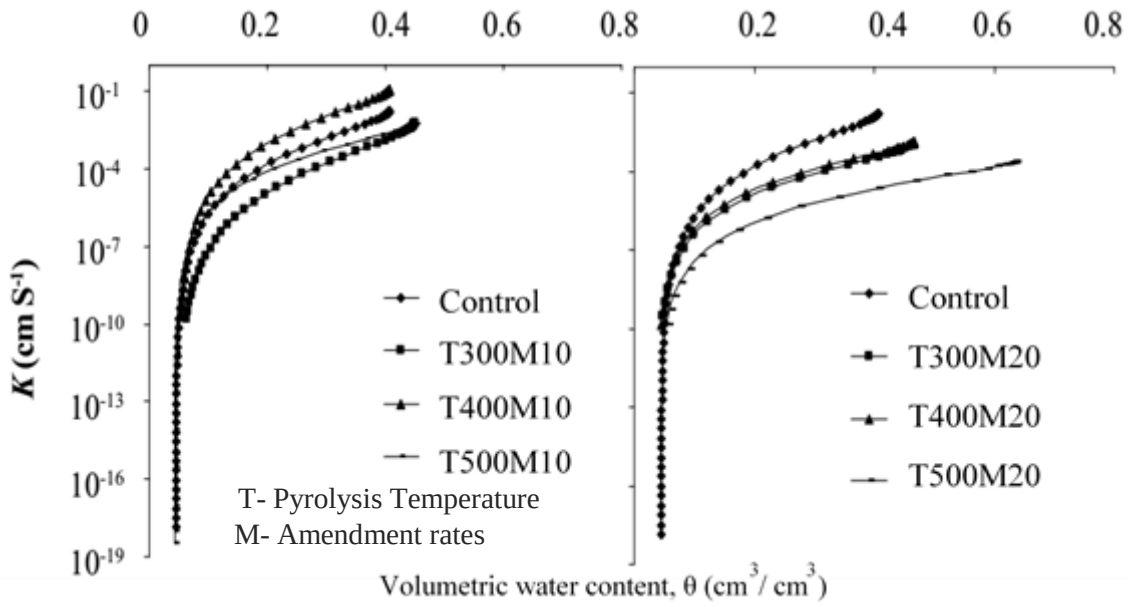

Fig. 2.3 Effect of Biochar amended at different rates on unsaturated hydraulic conductivity (K_{unsat}) of a sandy soil (after Uzoma et al., 2011).

The amendment of biochar could also affect the hydraulic conductivity (Downie et al. 2009; Lei and Zhang 2013; Wong et al. 2017). Soil most often remains in dry or unsaturated state that necessitates the study of the K_{unsat} of BAS. Limited literatures are available where the K_{unsat} of soil amended with biochar has been investigated. Table 2.2 highlights the review of currently available literature. As shown in Fig. 2.3, Uzoma et al. (2011) estimated K_{unsat} of sandy soil amended with biochar at different rate using unit step outflow method and reported a lower K_{unsat} in BAS compared to the control soil. Moreover, distinct effect of biochar on K_{unsat} was observed when a higher rate (20 Mg ha^{-1}) of biochar was amended over a low rate (10 Mg ha^{-1}). In clayey soil amended with biochar at 1,3,5 and 10% (w/w), Kameyama et al. (2012) measured the K_{unsat} using multistep outflow method and found increased K_{unsat} in 5 and 10% BAS compared to the bare soil. While, for biochar content below 5% a combined increase and decrease (based on the potential range) of the K_{unsat} compared to the control soil was observed.

In contrast, study by Castellini et al. (2015) reported a negligible change in K_{unsat} compared to bare clayey soil when biochar of 1 and 3% (w/w) was amended for observing the K_{unsat} using unit hydraulic gradient (UHG) method. Further, Hardie et al. (2014) concluded after estimating the K_{unsat} from infiltration measurement that the inclusion of biochar in sandy loam soil had no effect on K_{unsat}. Therefore, the effect of biochar on K_{unsat} varies with the type of soil and the biochar amendment rate. The comparison among the currently available literature is difficult due to the variation in test sample density, biochar amendment rate, biochar type and the K_{unsat} measurement methodology (indirect measurement). Hence, further research is needed to investigate the influence of biochar on the K_{unsat} by considering identical sample density, different soil type, different biochar type and amendment rate along with suitable direct measurement technique like instantaneous profile method (IPM, Leung et al. 2016). Unlike indirect measurement by other methods, such as outflow and horizontal infiltration method, the IPM is a typical transient-state testing method and directly measures the K_{unsat} (Leung et al. 2016). Moreover, the IPM is applicable for all type of soil and higher suction range along with both drying and wetting paths. Whereas, the other methods are limited to relatively coarse-grained soil, lower suction range (restriction in air entry disk) and single path such as drying in outflow and wetting in horizontal infiltration method (Lu and Likos 2004).

2.4.3 Saturated hydraulic conductivity

The measurement of K_{sat} has been reported long back (Klute 1965; Bouma et al. 1979). It controls the seepage through dams and agricultural land, drainage through embankment and slopes, percolation loss through water storage system and flow through wells (Klute 1965). Experimental measurement of K_{sat} using Darcy's law both in laboratory as well as in-situ (field) has been well documented in literature (Klute, 1986 and Angulo-Jaramillo et al., 2000). In addition, estimation of K_{sat} by empirical correlation with soil pore size and grain size distribution also reported by researchers. Laboratory measurement of K_{sat} includes constant-head method and falling-head method where suitability of these methods depends on soil texture. While, the in-situ method of measurement includes auger-hole method, pump test of wells and use of Guelph permeameter (Ibrahim and Aliyu, 2016). The K_{sat} of soil is affected by many factors, including particle size distribution, pore size and bulk density (Mbagwu,1995). In general, coarse-grained soil (sand, gravel) exhibits a higher K_{sat} compared to fined grained soil (clay, silt). The larger pore size of coarse-grained soil compared to the fine-grained soil that provides more passage to flow water leads to a higher K_{sat} (Suleiman and Ritchie 2001; Zeleke and Si 2005). The bulk density or density of soil negatively correlates with the K_{sat} i.e., with increase in bulk density the K_{sat} decreases due to the reduction of pore volume or void ratio (Ranjan and Rao 2007).

When biochar of high porosity and large SSA is amended with soil, the K_{sat} of the soil may change due to the modified pore size distribution of the BAS. Extensive research on the influence of biochar on soil K_{sat} has been undertaken in the recent past (Table 2.2).

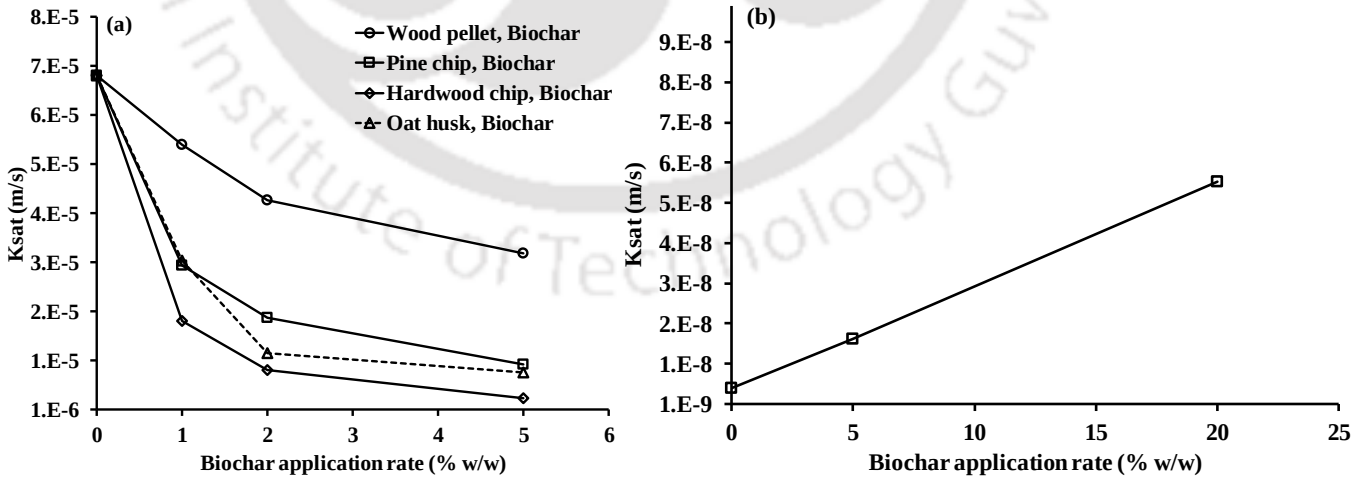

Fig. 2.4 Effect of Biochar amended at different rate on saturated hydraulic conductivity (K_{sat}) of (a) sandy soil (after Lim et al., 2016) and (b) clayey soil (after Wong et al., 2018).

Some group of researchers have reported increased K_{sat} of soil after biochar amendment, while some others have demonstrated that the addition of biochar may reduce the K_{sat} (Fig.

2.4a-b) or have no significant effects on the K_{sat} (Table 2.2). The application of biochar in coarse-textured soil, such as coarse sand, medium sand, fine sand, and sandy loam soil reduces the K_{sat} (Table 2.2). Lim et al. (2016) investigated the effect of four distinct biochar amended at 1, 2 and 5% (w/w) on the K_{sat} of coarse sand and observed a significant decrease in K_{sat} with increase in amendment rate of all the biochar (Fig. 2.4a). Similarly, Igalavithana et al. (2017) mentioned a decrease in K_{sat} with increase in the biochar amendment rate while studying the K_{sat} of sandy loam soil amended with biochar of corn residue at 2.5, 5, 7.5 and 10% (w/w). The decrease of K_{sat} in biochar-amended coarse-grained soil could be attributed to the filling or clogging of soil inter-pores by the fine biochar particles (Barnes et al. 2014; Igalavithana et al. 2017). Most of the existing literature reported about the application of biochar particles size <2 mm. The smaller (<2 mm) particles of biochar compared to the soil could fill the pore spaces of the coarse soil that have possibly reduced the porosity of the soil and hence, decreased the K_{sat}. In addition, the rapid disintegration of some unstable biochar particles may also clog the soil pores, as a consequence decrease in K_{sat} (Barnes et al. 2014). The increase of tortuosity due to increased micro-pores in soil or pore clogging upon biochar inclusion lead to the decrease in K_{sat} (Barnes et al. 2014; Lim et al. 2016).

In contrary, the K_{sat} increases when biochar is amended in fine-textured soil, such as loam, silt loam, silty clay loam, clay loam, and clay (Table 2.2). Herath et al. (2013) mentioned higher K_{sat} in silty loam soil amended with biochar derived from corn stover and pyrolysed at 350 and 550˚C compared to control soil. Similarly, Wong et al. (2018) reported an increase in K_{sat} with increased biochar amendment rate (Fig. 2.4b) while investigating the K_{sat} of compacted clayey soil amended with peanut-shell biochar at 5 and 20% (w/w). The increase of K_{sat} in biochar-amended fine-grained soil could be attributed to the application of larger size biochar particles compared to the fine-grained soil that increases the porosity (Herath et al. 2013; Wong et al. 2018) and hence, the K_{sat}. However, the smaller fine-grained soil (clay, <2 µm) particles could also entrap in the biochar intra-pores (~10 µm) that may contrarily reduce the porosity. Further, the increase of K_{sat} could also be due to the formation of macro aggregates when biochar amended in fine-grained soil (Wong et al. 2017).

Comparatively, some literatures documented a no change in K_{sat} of soil after biochar amendment (Table 2.2). In these studies, the considered amendment rates of biochar were lower (0.5-2% (w/w)) compared to the others (5-20%) that have possibly unable to influence the K_{sat}. Therefore, the influence of biochar on K_{sat} of soil depends primarily on the soil type, biochar particles size and amendment rate. Moreover, from the existing literature, it is

difficult to differentiate the effect of biochar on K_{sat} with respect to different soil type, biochar type and amendment rate. This is mainly due to the variation in the test sample compaction density which is very sensitive to the K_{sat} (Mbagwu 1995). Hence, further research is needed to investigate the effect of biochar on K_{sat} of soils with same compaction density, different biochar type and amendment rate.

2.4.4 Infiltration

The rate of ingress of water from the surface into the soil is known as infiltration (Hillel 2004). The knowledge of infiltration is important as it governs surface runoff, groundwater storage, and the overall soil water management (Githinji 2014; Bordoloi et al. 2017). The measurement of infiltration both in the laboratory and field has been well documented in the past (Angulo-Jaramillo et al. 2000; Angulo-Jaramillo et al. 2016). The monitoring of infiltration rate (I_r) using free ponding method (Wooding 1968; Haverkamp et al. 1990), ring infiltrometer (Leung et al. 2015) and tension disk infiltrometer (especially, mini-disk infiltrometer) (Bhave and Sreeja 2013; Bordoloi et al. 2017) has been well established. The I_r of soil mainly depends on the hydraulic conductivity or the pore size of the soil (Kutilek 2004). In addition, factors, including soil moisture content, depth of groundwater table, soil temperature and the air entrapped in pores also affect the I_r (Angulo-Jaramillo et al. 2000; Bhave and Sreeja 2013). In the recent past, the effect of biochar on the soil water infiltration has been investigated by many researchers and some of these are presented in Table 2.2. The inclusion of biochar in soil may increase, decrease or may not influence the I_r (Table 2.2).

To measure I_r, Githinji. (2014) conducted infiltration test using a mini-disk infiltrometer on sand amended with peanut hulls biochar at 25, 50, 75 and 100% (v/v) and concluded of decreased I_r with increased amendment rate of biochar. Similarly, Ibrahim et al. (2013) reported a decrease in I_r with increase in biochar amendment rate while monitoring infiltration rate in sandy loam soil amended with Conocarpus biochar at 0.5, 1, 1.5 and 2% (w/w) using mini-disk infiltrometer. However, at lower amendment rate, the variation in I_r was observed negligible. The reduced I_r in BAS compared to control soil could be attributed to the higher hydrophobicity of the applied biochar, or may be due to the filling or blocking of soil pores by the smaller biochar particles. In contrast, Novak et al. (2016) measured I_r in sandy loam soil amended with pine chips and poultry litter biochar at 2% (w/w) and observed an increase in I_r during the water flow in the initial stage and thereafter a decrease with the

further flow of water. However, the amendment of poultry litter biochar showed no significant change in the I_r.

Furthermore, Busscher et al. (2010) and Rogovska et al. (2014) documented a no significant effect of biochar addition on the I_r while measuring the infiltration rate in loamy sand mixed with pecan biochar and loam soil amended with hardwood biochar at different amendment rate. Therefore, the effect of biochar on soil I_r could be highly influenced by the biochar type and amendment rate. The mechanism of changing I_r after biochar amendment is not clear yet. In addition, the application of biochar at higher rate could only influenced the I_r, which may not be feasible for many large scale (field) applications. Hence, further research is needed to investigate and understand the effect of biochar on soil water I_r and the possible mechanism underneath the alteration in I_r by considering different soil type, biochar type and amendment rate.

2.5 Mechanical behavior of biochar amended soil

The mechanical properties of soil include the shear strength and compressibility on which the stability and performance during and after construction of the soil structure depend. In general, the stability of soil structure is expressed in terms of factor of safety (FOS), which is defined as the ratio of resisting force (shear strength) to the driving force (shear stress) (Fredlund et al. 2012). The compressibility behavior of soil is used to compute the settlement of soil structure due to self-weight and under external loading conditions (Horn and Lebert 1994; Ranjan and Rao 2007). The computation of settlement from compressibility could help in controlling the differential settlement of the structure that causes a decrease in strength of the soil and formation of cracks (Burland 1990; Tang et al. 2008). Studies have shown that the application of biochar to a landfill cover soil could significantly enhance the rate of methane oxidation through enhanced air permeability and methanotrophic population (Sadasivam and Reddy 2014; Reddy et al. 2014; Wong et al. 2016). However, the feasibility of biochar in engineered systems e.g., landfill cover and manmade slopes or embankment depends on the stability and performance (indirectly, strength and compressibility) of these structures. Therefore, it is important to understand and quantify the effect of biochar amendment on the strength and compressibility characteristics of soil. The influence of biochar on the strength and compressibility of soil is elaborated in detail below with the help of Table 2.3, highlighting the review of some of the existing literature.

Table 2.3 Review of literature on mechanical behavior of BAS

References	Soil type	Biochar			Parameter measured			
		Feedstock	Pyrolysis Tem, ˚C	Mix proportion	Shear strength		Compressibility	Desiccation crack
					Cohesion C (kPa)	Friction angle ϕ (˚)		
Busscher et al. 2009	Sand	Pecan	700	0.5, 1, 2% (w/w)	Decreased	Decreased	-	-
Haque et al. 2014	Clay	Green waste	-	10, 20% (w/w)	Increased	-	-	-
Zong et al. 2014	Clay	Woodchip, Wheat straw, Wastewater sludge (WS)	500	2, 4, 6% (w/w)	Decreased	Increased	-	Decreased
Reddy et al. 2015	Silty clay	Wood pellet	520	5, 10, 20% (w/w)	Increased	Increased	Decreased	-
Sadasivam and Reddy 2015a	Silty clay	Pine and Fir wood	520	2, 5, 10% (w/w)	Increased	Increased	Increased	-
Sadasivam and Reddy 2015b	Silty clay	Hardwood	500	10% (w/w)	Increased	Increased	-	-
Zong et al. 2016	Silt loam	Woodchip, Wheat straw, WS	500	2, 4, 6% (w/w)	Decreased	No effect	-	-
Ahmed et al. 2017	Silt loam	Maple wood	500	2, 5, 10% (w/w)	Decreased	Decreased	-	-
Bordoloi et al. 2018	Sandy Clay	Water hyacinth	300-350	2, 5, 10, 15% (w/w)	-	-		Decreased
Pardo et al. 2018	Sand	-	470	3, 5% (w/w)	Increased	-	-	-
GuhaRay et al. 2019	Clay	Mesquite	500	5, 10% (w/w)	Increased	-	-	-
Ganesan et al. 2020	Clayey sand	Cedar wood	350, 550	5, 10% (w/w)	Decreased	Decreased	-	Decreased

Note: '-'-Not measured, Tem- Temperature

2.5.1 Shear strength and stability of bioengineered slopes

The influence of biochar on soil shear strength investigated by various researchers are summarized in Table 2.3. The effect of biochar on soil shear strength varies with the soil and biochar type (Table 2.3).

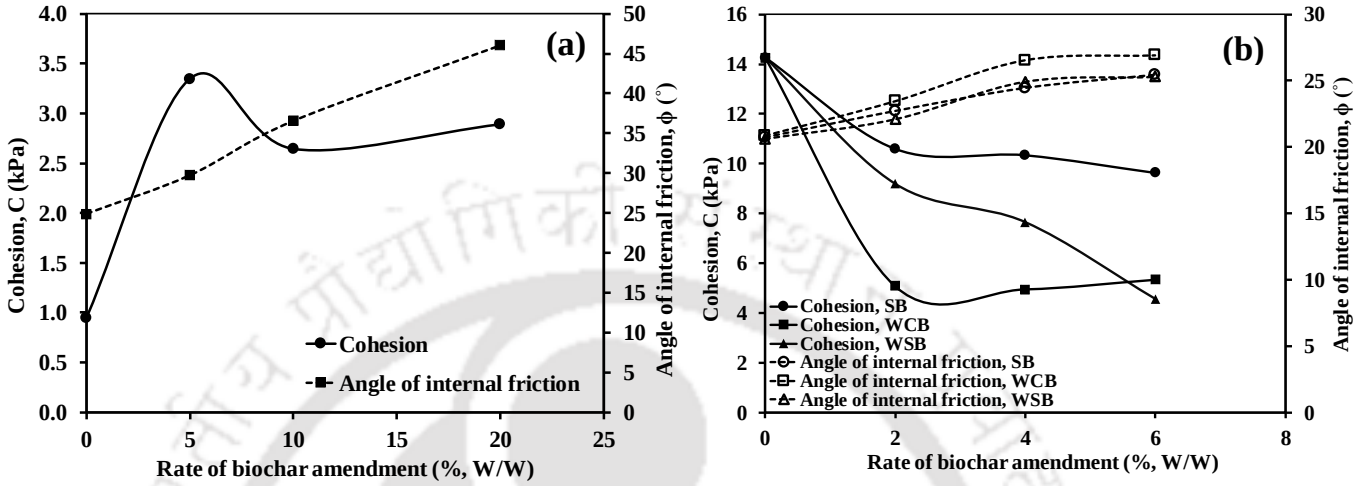

Fig. 2.5 Effect of Biochar amended at different rate on shear strength of (a) silty clay (after Reddy et al., 2015) (b) clay (after Zong et al., 2014).

Fig. 2.5(a-b) shows the effect of biochar on shear strength of silty clay (after Reddy et al., 2015) and clay (after Zong et al., 2014). As highlighted in Fig. 2.5, the improvement in the shear strength (parameters c and ϕ) of silty clay after biochar amendment was reported by Sadasivam and Reddy (2015a) and Reddy et al. (2015). In clayey soil, Zong et al. (2014) found decreased cohesion (c) and increased angle of internal friction (ϕ) after amendment of woodchip, straw, and wastewater sludge biochar (Fig. 2.5b), while Haque et al. (2014) reported increased shear strength (UCS, unconfined compressive strength) after adding green waste biochar. Zong et al. (2016) mentioned a no influence of biochar on the ϕ of silty loam soil. However, Ahmed et al. (2017) reported reduced shear strength of the same soil after wood biochar amendment. Similarly, in sandy soil, Busscher et al. (2010) observed decreased c and ϕ after biochar amendment while Pardo et al. (2018) found increased c. Further, the existing literature adopted only the conventional testing methods where the effect of suction, which is an important factor contributing to the shear strength was not considered. It is also evident from literature that the biochar amendment could increase water retention and infiltration in soil which may in turn increase the pore water pressure and decrease the suction depending on the hydraulic conductivity (Ibrahim et al. 2013; Chen et al. 2016).

Hence, further studies are needed to investigate and understand the effect of biochar on soil shear strength by considering suction or moisture content.

Generally, the shear strength of soil is used to calculate the factor of safety (FOS) for assessing the stability of soil structure (slopes). The FOS for an unsaturated cohesive soil slope is written as follows (Zhang et al. 2014):

$$\boldsymbol{FOS} = \frac{\boldsymbol{c'}}{\boldsymbol{\gamma_t \times H \times sin\alpha \times cos\alpha}} + \frac{\boldsymbol{tan\phi'}}{\boldsymbol{tan\alpha}} + \frac{\boldsymbol{\Psi \times tan\phi b}}{\boldsymbol{\gamma_t \times H \times sin\alpha \times cos\alpha}} \qquad (\mathbf{2.2})$$

Where c' is the cohesion of the soil, φ' is the angle of internal friction of the soil, φ^b is the angle indicating the increase in shear strength relative to matric suction (u_a - u_w), γ_t is total unit weight, α is slope angle, ψ = (u_a - u_w) is suction and H is depth of slip surface. For a bioengineered slope, where vegetation is grown over the slope, the changes in FOS can be written as (Wu et al. 1979):

$$\boldsymbol{FOS} = \frac{\boldsymbol{c'}}{\boldsymbol{\gamma_t \times H \times sin\alpha \times cos\alpha}} + \frac{\boldsymbol{cr}}{\boldsymbol{\gamma_t \times H \times sin\alpha \times cos\alpha}} + \frac{\boldsymbol{tan\phi'}}{\boldsymbol{tan\alpha}} + \frac{\boldsymbol{\Psi \times tan\phi b}}{\boldsymbol{\gamma_t \times H \times sin\alpha \times cos\alpha}} \qquad (\mathbf{2.3})$$

Where γ_t is total unit weight (includes weight of soil and vegetation) and c_r is the cohesion due to root strength ($c_r = T_r \times (A_r/A) \times (cos\theta \times tan\phi' + sin\theta)$), θ is the angle of distortion of roots with respect to the vertical, (A_r/A) is the root area ratio and T_r is the tension in roots. It can be observed from Eq. (3) that the vegetation improves the slope stability through root reinforcement and hydrologic process (transpiration or root water uptake). Vegetation roots act as a tensile reinforcement in soil and mobilize its tensile strength through interface friction between soil and root surface for improving soil shear strength or stability (Bordoloi et al. 2018a). The root water uptake and transpiration (stomatal conductance) by plants lead to a decrease in water content in the root zone of soil, as a consequence a higher suction generates (retain) in soil (Garg et al. 2015) and hence, higher shear strength or stability (Fredlund and Rahardjo 1993).

The inclusion of biochar in soil is shown to improve vegetation growth (biomass) and roots development, improve plant health condition (transpiration and photosynthetic yield) and reduce soil bulk density (Kamman et al. 2011; Liu et al. 2013; Baronti et al. 2014; Bruun et al. 2014; Akhtar et al. 2015; Gavili et al. 2018; Rizwan et al. 2018). The higher growth of plant biomass and roots along with improved health condition in BAS potentially lead to a higher stability of slopes (Gray 1974; Wu et al. 1979; Cammeraat et al. 2005). Further, the

reduced bulk density of BAS may also improve the stability (from Eq. (2.2) and (2.3)). However, the influence of reduced bulk density on soil shear strength would be critical for assessing the overall stability. Therefore, comprehensive studies are needed to investigate the shear strength of BAS by incorporating vegetation for potential application in bioengineered slopes.

2.5.2 Compressibility

Compressibility is the phenomenon refers to the decrease of soil volume due to expulsion of air and water under variable loading condition. The compressibility behavior of soil is an important parameter that requires for the design of stable soil structures, such as slopes, embankment, landfill cover and foundation base (Ranjan and Rao 2007). The higher compressibility of soil may cause differential settlement leading to a decrease in strength and the formation of cracks (Burland 1990; Tang et al. 2008). Recently, literatures are witnessed the amendment of biochar in soil for various purpose especially, in landfill cover (Reddy et al. 2014). The amendment of biochar in soil could alter the compressibility behavior of the soil. Therefore, the study of the influence of biochar on soil compressibility is necessary for feasible utilization of biochar in soil structures. To date, a few studies are available (Table 2.3), where the compressibility behavior of BAS has been investigated.

Sadasivam and Reddy. (2015) reported increased compressibility and thereby, decreased constrained modulus (inverse of slope of the axial strain and normal stress plot) of silty clay after amending with four different biochar at 2, 5 and 10% (w/w) under two levels of moisture content (dry and 25% of Water Holding Capacity, WHC). The higher porosity and lower density of soil after biochar amendment compared to the control soil attributed to the increased compressibility (Cao et al. 2014; Omondi et al. 2016). However, at higher initial moisture level (i.e., 25% WHC), biochar amendment led to the decrease in compressibility possibly due to the formation of bonding between the particles of biochar and soil in the presence of water (Bazargan et al. 2014). Similarly, Reddy et al. (2015) documented decreased compressibility or settlement of silty clay with increase in wood pellet biochar amendment rate from 5% to 20% (w/w) under 20% initial moisture content. Further, the compressibility was found to be increased with decrease in biochar particle size. Therefore, the effect of biochar on soil compressibility behavior is inconclusive i.e., it may increase or decrease the soil compressibility depending on the type, particle size and amendment rate of the biochar. Hence, comprehensive studies are needed to investigate and

understand the influence of biochar on soil compressibility by considering different type of soil and biochar.

2.5.3 Desiccation crack

Desiccation crack is the discontinuity or fracture mostly observed in fine-grained soil upon drying. Cracks develop in soil when the tensile stress generated in soil due to loss of moisture (increase suction) from the surface overcomes the tensile strength of the soil (Corte and Higashi 1964). The presence of desiccation crack affects the performance of many soil structures including landfill liner, slurry wall, pond liner and slopes such as embankment and dams (Miller 1988). The presence of cracks increases the water infiltration through soil structures (Li and Zhang 2011). The higher infiltration of water through the landfill cover soil could lead to the generation of excessive leachate, which is harmful to the integrity of the liner (Albright et al. 2006; Costa et al. 2013). In addition, the higher water infiltration could reduce the soil shear strength potentially lead to the failure of the soil structures (Lee et al. 1988; Talbot and Deal 1993). In an agricultural system, the higher infiltration of water and solute through soil cracks leads to the drought stress and nutrient leaching (Thomas and Phillips 1979; Coles and Trudgill 1985).

The amendment of biochar in soil could reduce the tendency of crack formation (Kumar et al. 2020). Biochar is reported to be capable of increasing the water retention of soil when amended to soil due to their relatively higher porosity and large SSA, which is against the formation of cracks by water loss or drying (Bordoloi et al. 2018; Garg et al. 2019). Limited literatures are available (Table 2.3), where the influence of biochar on desiccation cracks has been investigated. For example, Zong et al. (2014) investigated the crack potential of clayey soil amended with 2, 4 and 6% (w/w) wheat straw, woodchips, and wastewater sludge biochar and reported decreased cracks (crack area and line density) in BAS with increase in biochar amendment rate. Further, biochar made from wheat straw (SB) showed highest crack reducing ability among the biochar tested. Similarly, the other literature (Table 2.3) also reported a decreased soil cracks after biochar amendment. The lower cracking tendency in BAS is attributed to the higher water retention and reduced shrinkage-swelling behavior of soil after biochar amendment (Lu et al. 2014; Zhang et al. 2020). However, in the existing literature, the test samples were mostly prepared in slurry form and the sample size was small with no control on density, which may not be relevant in engineering application. In fact, in engineering applications, soil is often compacted and a certain minimum volume

called representative elementary volume (REV) is required for defining cracks (Li and Zhang 2011). Therefore, further research is needed to investigate the effect of biochar on desiccation crack potential of compacted soil by considering standard sample size, different biochar type and amendment rate along with multiple drying-wetting cycles.

2.6 Influence of biochar on vegetation performance

2.6.1 Significance of vegetation in bioengineered structure

The integrity of bioengineered structures depends mainly on the soil engineering behavior and vegetation performance (Gadi et al. 2016). Vegetation performance implies the function of vegetation in improving the stability of the bioengineered structures through root reinforcement and hydrological process (Wu et al. 1979; Garg et al. 2015). The performance of vegetation depends on the growth and development of the vegetation which can be quantified by the growth and health condition of the vegetation (Sotir 1990; Vergani and Graf 2016). Therefore, the proper growth and health condition of vegetation along with the improved quality of soil are highly important for the effective functioning of bioengineered structures. In the recent past, many researchers explored the growth (crop yield) and health condition of vegetation in BAS which has been reviewed and presented in Table 2.4. Frequently, an improved plant growth and health condition after biochar amendment were reported (Table 2.4). The rich nutrient content and higher water retention of biochar provides higher available water and nutrient to the plants and improves the aeration (nitrogen content) in root zone (Lehmann et al. 2003; Rondon et al. 2007; Amonette and Joseph 2009; Atkinson et al. 2010; Major et al. 2012). However, the effect of biochar on vegetation growth and health condition depends on many factors (Table 2.4) that need to be considered. Thus, the vegetation growth and health condition in BAS and influencing factors have been reviewed and elaborated in detail below.

2.6.1.1 Vegetation growth or yield

In literature, vegetation growth is expressed as plant (dry) biomass yield, leaf area index (LAI), vegetation density (VD) and root biomass (Jeffery et al. 2011; Lehmann et al. 2011; Gadi et al. 2017; Werner et al. 2018). Plant biomass is defined as the above ground mass of the plant including shoot and leaves (except grains, in case of crop species) (Kamman et al. 2011). However, for a crop species, the growth is represented by crop yield (Jeffery et al. 2011) that indicates the output of crop grain per unit of ground area.

Table 2.4 Review of literature on vegetation performance in BAS

References	Soil type	Biochar			Plant type	Parameter measured				
						Vegetation growth			Vegetation health condition	
		Feedstock	Pyrolysis Tem, ˚C	Mix proportion		Biomass yield	Crop yield	Root growth	SC	PY
Kamman et al. 2011	Sand	Peanut hull	498	100, 200 (t/ha)	*Chenopodium quinoa*	Increased	-	Increased	Decreased	Decreased
Gravel et al. 2013	-	Balsam fir, Spruce	475	1% (v/v)	Pepper, basil, lettuce, geranium coriander	No change No change Decreased No change Increased	-	Decreased	-	-
Baronti et al. 2014	Sandy clay loam	Orchard pruning	500	22, 44 (t/ha)	Vitis vinifera (L.)	-	-	-	Increased	Increased
Bruun et al. 2014	Sand	Wheat straw, Hardwood	730, 480	0.5, 1, 2, 4% (w/w)	Spring Barley	No effect	Increased	Increased	-	-
Xie et al. 2014	-	Wood	-	5% (w/w)	Beans	Increased	Increased	-	-	-
Akhtar et al. 2015	Sandy loam	Hardwood	500	5% (w/w)	Maize	Increased	-	Increased	Increased	Increased
Egamberdieva et al. 2016	Silty sand	Maize, Wood	600, 850	1, 2, 3% (w/v)	Soybeans	No change	-	No change	-	-
Gale et al. 2016	-	Wood	422, 475, 575	5, 10, 20, 50 (t/ha)	Ryegrass, Clover	Decreased	-	Decreased	-	-

References	Soil type	Biochar			Plant type	Parameter measured				
						Vegetation growth			Vegetation health condition	
		Feedstock	Pyrolysis Tem, ˚C	Mix proportion		Biomass yield	Crop yield	Root growth	SC	PY
Abdul and Abdul 2017	Silty clay	Fruit bunch, Rice husk	350, 500, 650	-	Rice	Increased	Increased	-	-	-
Hunter et al. 2017	Silt loam	Cherry wood	375, 475, 575	1, 2, 3% (w/w)	Lettuce (lactuca sativa)	Decreased	-	-	-	-
Trupiano et al. 2017	-	Orchard pruning	500	6.5% (w/w)	Lettuce	Increased	-	Increased	Increased	-
Abbas et al. 2018	Sandy clay loam	Rice straw	450-550	3, 5% (w/w)	Maize	Increased	Increased	Increased	Increased	Increased
Anyanwu et al. 2018	-	Rice husk	380	0.5, 1, 5, 10, 25, 50% (w/w)	Rice, Tomato	Increased	-	No change	-	-
Gavili et al. 2018	Silty clay	Cattle manure	600	1.25, 2.5, 5% (w/w)	Spinach	No effect	-	-	Increased	-
Gonzaga et al. 2018	Sand	Coconut husk, Orange bagasse, Pinewood chips	500	5, 10, 20, 60 (t/ha)	Maize	Increased, No effect, No effect	-	-	-	-
Pandit et al. 2018	Silt loam	Weed (*Eupatorium adenophorum*)	600-700	0.5, 2% (w/w)	Maize	Increased	-	-	Increased	-

References	Soil type	Biochar			Plant type	Parameter measured				
						Vegetation growth			Vegetation health condition	
		Feedstock	Pyrolysis Tem, ˚C	Mix proportion		Biomass yield	Crop yield	Root growth	SC	PY
Rizwan et al. 2018	-	Rice straw	450	3, 5% (w/w)	Rice	Increased	-	-	Increased	Increased
Zheng et al. 2018	Silty clay	Peanut shell	350	1.5, 5, 10% (w/w)	Sesbania, Seashore mallow	Increased	-	Increased	-	-
Tanure et al. 2019	Sandy loam	Eucalyptus bark	350	0.5, 1, 2, 4, 6% (w/w)	Maize	Increased	-	Increased	Increased	Increased
Pokovai et al. 2020	Silty loam	Wood chips	600	0.5, 2.5, 5% (w/w)	Pepper	Increased	-	Increased	-	-

Note: '-' -Not measured, Tem- Temperature, SC- Stomatal conductance, PY- Photosynthetic yield.

The LAI, defined as the one-sided green leaf area per unit ground surface area in broadleaf canopies, indicates the plant growth in terms of leaf area and requires for evaluating the transpiration rate (Allen 1998; Gadi et al. 2016). The growth of non-crop species, especially grass species where shoot and leaves are not distinct, is expressed as vegetation density (VD) (Gadi et al. 2018). The VD is defined as the ratio of total green surface area of vegetation to the total ground surface area considered (Bordoloi et al. 2018). The LAI and VD can be measured by using image analysis technique, which is a superior technique compared to the traditional biomass measurement technique in terms of non-destructiveness and less time consumption (Gadi et al. 2018). The growth of vegetation highly depends on the growth and distribution of roots (Coppin et al. 1990; Bruun et al. 2014). The growth of roots is presented by root biomass, defined as the mass of entire roots. It is also quantified as root length density (RLD, defined as the total length of roots per unit volume of soil) and root area index (RAI, defined as the ratio of root surface area to the soil surface area surrounded by the roots) (Gadi et al. 2016). Therefore, the investigation of growth and development of roots is necessary for assessing the vegetation growth, root water uptake and reinforcing potential in the soil.

In the recent past, the growth of vegetation in BAS has been investigated by many researchers where an increased vegetation or crop yield was mostly reported (Table 2.4). In meta-analysis performed on published literatures, Liu et al. (2013) and Jeffery et al. (2011) concluded that the application of biochar in soil improves the overall vegetation growth and yield by 10 to 11%. The amendment of biochar in agricultural soil improved the growth of Tendergreen plant while showed negligible impact on blue lake plant (Xie et al. 2014).

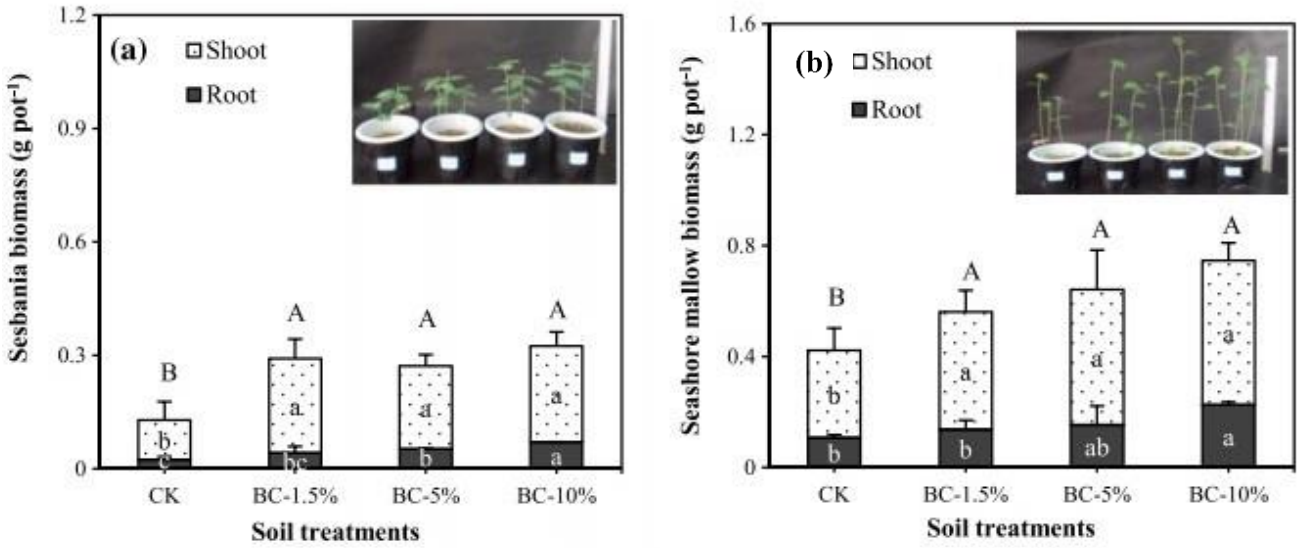

Fig. 2.6 Effect of Biochar addition on growth (biomass) of (a) Sesbania and (b) Seashore mallow (Zheng et al., 2018).

As presented in Fig. 2.6(a-b), Zheng et al. (2018) reported the higher plant biomass growth (characterized by shoot length, root length, root surface area and leaf surface area) of Seashore mallow compared to the Sesbania plant in biochar-amended silty clay and the growth was higher with larger biochar amendment rates. Similarly, Gonzaga et al. (2018) documented an increased biomass of maize due to application of coconut husk biochar, while the amendment of orange bagasse and pinewood chips biochar showed no influence on the maize biomass. Further, some researchers observed an improvement in vegetation growth only when an organic or inorganic compost was added along with the biochar (Wang et al. 2012; Qayyum et al. 2017; Vaughn et al. 2018). In fact, Hunter et al. (2017) mentioned a decreased plant dry biomass yield of Lettuce plant in biochar-amended silty loam compared to the control soil. Therefore, it is clear from the literature that the influence of biochar on vegetation growth is highly dependent on the type and amendment rate of biochar and the type of vegetation grown. Hence, the selection of suitable biochar type and amendment rate along with the vegetation type is highly important for the efficient performance of bioengineered structures.

2.6.1.2 Vegetation health condition

The health condition of vegetation is often examined through the monitoring of some crucial plant parameters such as stomatal conductance (SC) and photosynthetic yield (PY) (Krupa et al. 2001; Rahnama et al. 2010). The drought (abiotic) stress monitored in the root zone also indicates the plant health condition. However, the drought stress is indirectly related to the SC. SC (mmol water m^{-2} s^{-1}) is defined as the rate of water vapor exiting through stomata or the rate of CO_2 entering into the stomata of a plant leaf (Caplan and Yeakley 2010). Moreover, the SC essentially represents the leaf level transpiration rate (T_r) of the plants. Adequate transpiration of water through stomata is very important for the survival (plant metabolism) of any plants (Mathur and Vyas 1995; Masle et al. 2005). Transpiration is responsible for the expulsion of excess water from the plants to the atmosphere that creates free space in the stomatal guard cell for entering CO_2, which is the main substrates for photosynthesis (Hopkins 1999; Sinha, 2004). The transpiration is also related to the root water and nutrient uptake which are responsible for the development of plant tissue (Kramer 1969). Photosynthetic yield or efficiency (PY) is defined as the fraction of light energy (in terms of quantum) converted into chemical energy during photosynthesis process in plants (Bordoloi et al. 2018a). The PY is highly important for plants, as the rate of photosynthesis

i.e., rate of conversion of CO_2 into glucose is controlled by the available chemical energy (converted from the light (photon) energy) (Liu et al. 2016). The higher PY in plant leads to the higher rate of photosynthesis (Zhu et al. 2010).

The SC and PY are often affected by many factors including drought or water stress. The deficit of water or drought stress in soil have strong influence on SC and PY, since the root water uptake related to SC and PY is highly affected by the drought stress (Kammann et al., 2011 and Gavili et al., 2018). Literatures are available where influence of biochar amendment on alleviating drought stress and plant health condition was investigated, some of them are reviewed and presented in Table 2.4. The amendment of biochar made from several feedstock and at different rates enhanced the PY and SC (T_r) of plants grown in various soil type (Table 4). In contrary, literature (Kammann et al., 2011) also reported decreased PY and T_r (SC) of plants (*Chenopodium quinoa*) when biochar (peanut hull) was incorporated in sandy soil. Therefore, it is cleared from the literature that the incorporation of biochar mostly improves the plant health condition. However, currently limited literatures are available and the properties of biochar varies with feedstock and pyrolysis temperature. Hence, to better understand the influence and mechanism of biochar on vegetation health, more comprehensive research by considering different soil, biochar and vegetation type is needed.

2.7 Critical appraisal from the literature review

The properties of biochar are highly dependent on the type of feedstock, pyrolysis temperature and residence time. Biochar produced from plant-based feedstock shows higher porosity and specific surface area (SSA), whereas biochar produce from manure shows higher nutrient content. Similarly, biochar derived from solid waste characterized by high salt content. The increase of pyrolysis temperature increases the porosity, SSA and pH of plant-based biochar, while have no effect on manure based biochar. The polycyclic aromatic hydrocarbons (PAHs) and dioxins could also be generated as by-products during production of biochar, which are also function of feedstock and pyrolysis condition and harmful towards the environment. Therefore, selection of proper feedstock and pyrolysis condition is important for producing the biochar.

The influence of biochar amendment on soil hydraulic properties was found to be dependent on many factors. Biochar amendment may increase, decrease or may not influence the soil hydraulic properties depending on the type of soil where biochar amended, feedstock type and pyrolysis condition of the biochar, amendment rate and particles size of the biochar,

and the compaction state adopted for testing. The particle size of soil and biochar controls the porosity which in turn affects water flow path. Further, the hydrophobic nature of few biochar that arises due to some surface functional groups (aliphatic) could also lead to the no influence of biochar on soil hydraulic properties. The application of biochar in soil alters the shear strength of the soil, i.e. Shear strength parameters may increase or decrease after biochar inclusion depending on factors such as soil and biochar type, amendment rates and particle size of biochar. The tendency of desiccation crack formation in soil decreases after biochar amendment i.e., biochar mitigates crack formation and the efficacy varies with the type of biochar amended. The influence of biochar on soil compressibility is inconclusive due to limited numbers of studies were undertaken i.e., biochar amendment may increase or decrease the soil compressibility depending on biochar type, particle size and amendment rate.

The amendment of biochar in soil increases soil fertility as well as vegetation growth and yield, while it is highly controlled by the type and amendment rate of biochar and the type of vegetation grown. The incorporation of biochar mostly improves the plant health condition as well as alleviates the drought stress. However, limited studies were undertaken due to which clear judgment may not be appropriate. The currently available literature reported the vegetation performance and hydro-mechanical properties of the BAS focusing mainly on loose agricultural soil where soil is maintained in loose state and irrigates frequently i.e., induces a low suction. However, soil in bioengineered structures is often compacted for achieving structural stability and subjects to a large suction due to prolong drying (lesser or rare irrigation). Therefore, the hydro-mechanical properties and vegetation performance of the biochar-amended compacted soil considering large suction range need to be investigated. Based on which the objectives of the study are decided and presented below.

2.8 Objectives and Scope of work of the study

The broad objectives of the study are as follows

1) Production of biochar from locally available waste biomass and its characterization.

To attain the objective, the scope of work involved are

i) Production of biochar from waste sugarcane bagasse and water hyacinth biomass through pyrolysis using pyrolyzer.

ii) Characterization of the biochar obtained after pyrolysis.

2) Investigation of hydraulic and mechanical properties of compacted biochar-amended soil.

To meet the second objective, the following scope of work involved

Fig. 2.7 presents the diagrammatic representation (flow chart) of the scope of works.

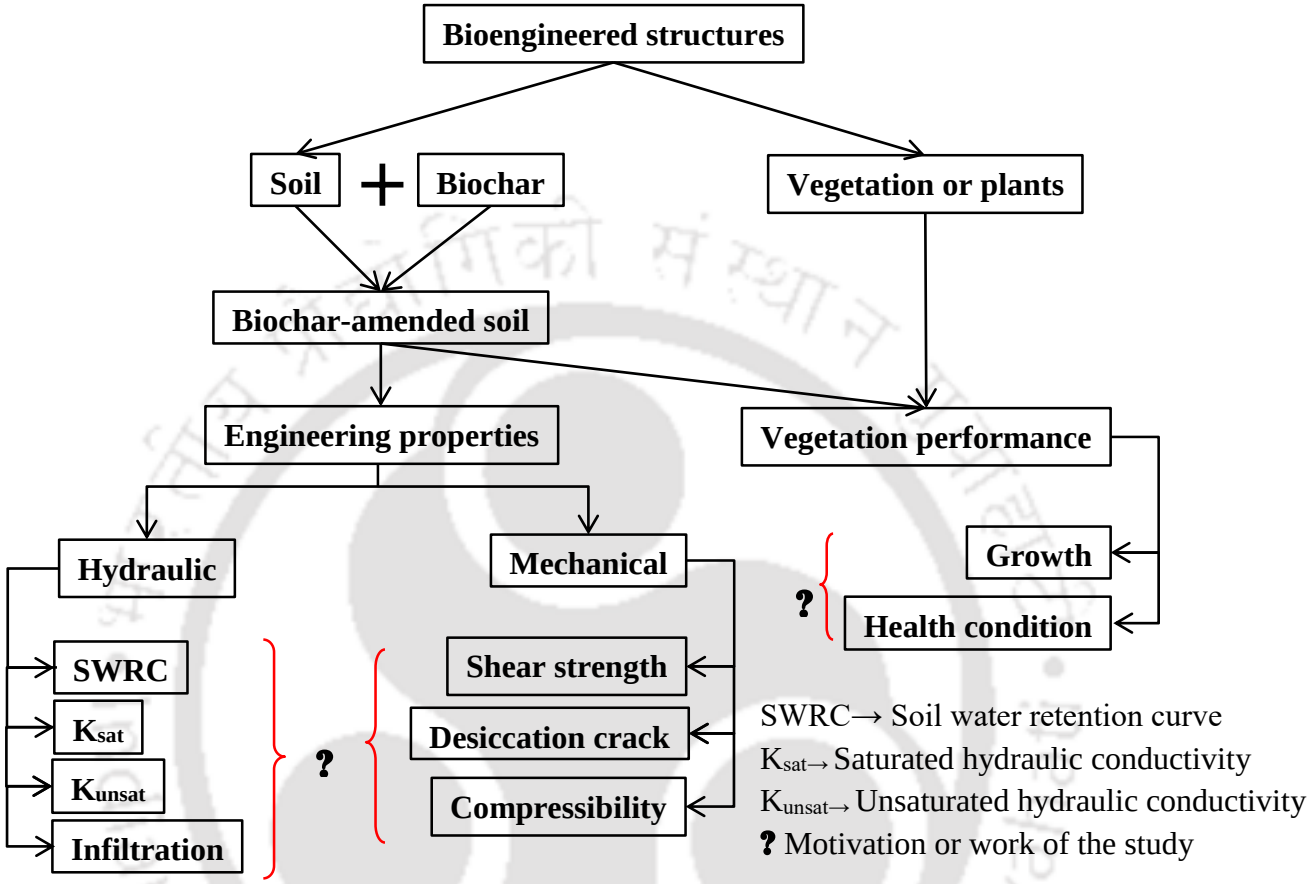

Fig. 2.7 Importance of biochar-amended soil in terms of engineering properties and vegetation performance for potential application in bioengineered structures.

i) Establishment of soil water retention curve (SWRC) using compacted soil column, for different type of soil by amending different type and proportion of biochar.

ii) Measurement of unsaturated hydraulic conductivity using instantaneous profile method, for different type of soil by amending different type and proportion of biochar.

iii) Measurement of saturated hydraulic conductivity, for different type of soil by amending different type and proportion of biochar.

iv) Measurement of infiltration rate using mini disk infiltrometer, for different type of soil by amending different type and proportion of biochar.

v) Evaluation of strength characteristics of BAS through laboratory unconfined compression test (UCS), direct shear test and California bearing ratio (CBR) test.

vi) Evaluation of desiccation crack potential in BAS using image processing technique.

3) Monitoring of vegetation performance in compacted biochar-amended soil.

Similarly, to attain the third objective, the following scope of work involved

i) Measurement of vegetation growth through image processing technique.

ii) Monitoring of plant health through the measurement of plant parameters such as stomatal conductance and photosynthetic yield using Leaf Porometer and Mini-Pam yield analyzer.

iii) Evaluation of plant survivability under drought stress in biochar-amended soil.

CHAPTER 3
MATERIALS AND METHOD

3.1 Introduction

The materials used and the experimental methodology adopted for the thesis work are presented here in this chapter. The methodology includes the geotechnical exploration of BAS i.e., the physicochemical and hydro-mechanical properties of soil after biochar amendment. The methodology of growing and monitoring performance of vegetation in BAS are also presented.

3.2 Materials

3.2.1 Soil

In the present study, two different soils, one from inside the campus of Indian Institute of Technology (IIT) Guwahati and another from the river bed of Brahmaputra river located in the North-eastern province of India (26.19˚N, 91.69˚E) were collected. These are the dominant soils used for the construction activity and growing vegetation in the region. Dead roots, stones and any other impurities were manually removed from the soils. Thereafter, characterized for the physicochemical properties based on the standard procedure prescribed by ASTM standard (ASTM C128-15; ASTM D422–63-07; ASTM D698-12; ASTM D854-10; D4318-10; ASTM D4972-18). The photographic view of the soils is presented in Fig. 3. 1.

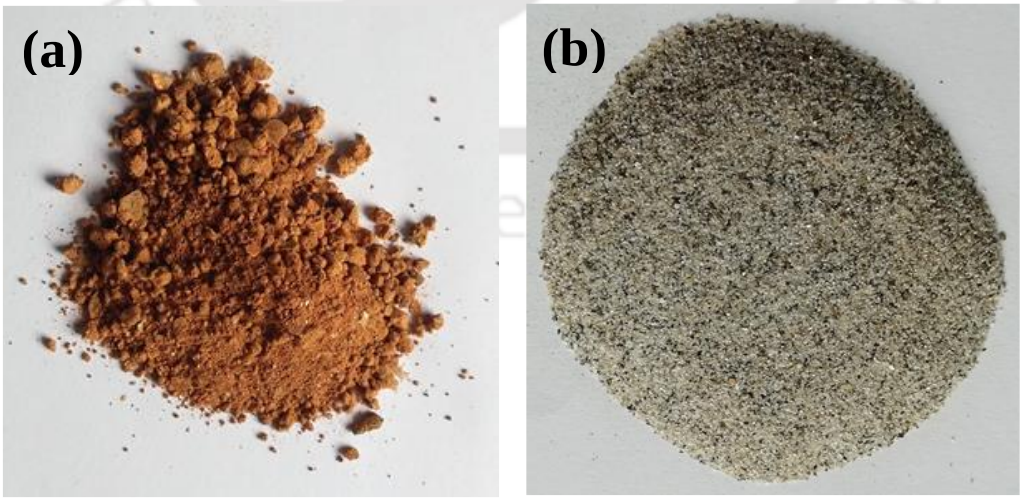

Fig. 3.1 Images of (a) Silty sand from IIT Guwahati campus, (b) Sand from Brahmaputra river.

3.2.2 Biochar

3.2.2.1 Preparation of feedstock

In the present study, one commercial biochar produced from hardwood of mesquite (*Prosopis juliflora*, Greenfield Eco Solutions Pvt. Ltd.) and two other in-house produced biochar from water hyacinth (*Eichhornia crassipes*) and sugarcane bagasse (*Saccharum officinarum*) were used. Mesquite is a fast-growing terrestrial invasive weed found in many parts of the world and poses a serious threat to the native biodiversity (Angalaeeswari and Kamaludeen 2017). Similarly, water hyacinth (WH) is also an aquatic invasive weed that can multiply its mass within 2 weeks and can thus, pose a threat to the aquatic ecosystem. Every year millions of dollars are invested to control and clear WH infestation from water bodies (Simberloff et al., 1997). Further, the disposal of WH in soil decomposes the biomass carbon readily and release to the atmosphere due to degradation (Masto et al., 2013). Sugarcane bagasse (SCB) is the waste byproduct that remains after extraction of juice from sugarcane in sugar industries. Each year a huge quantity of SCB is generated and the management of which is a challenging task. Therefore, the utilization of these biomasses as feedstock could at least control their effect on the ecosystem. The WH plants as feedstock was collected from place near to the campus of Indian institute of technology (IIT) Guwahati (26.19˚N, 91.69˚E). All the required WH plants were collected from the same water body to minimize any genetic variation. The sugarcane bagasse (SCB) was collected from a local market in Guwahati (26.186˚N, 91.7454˚E). The raw WH plants and SCB were sun-dried and chopped into smaller (20-40 mm) pieces. The chopped biomass was then oven-dried at 105˚ C for 12 hours. The dried samples were stored in airtight containers at ambient temperature before they were pyrolysed in a fixed bed reactor. Fig. 3.2 highlights the preparation of the feedstock.

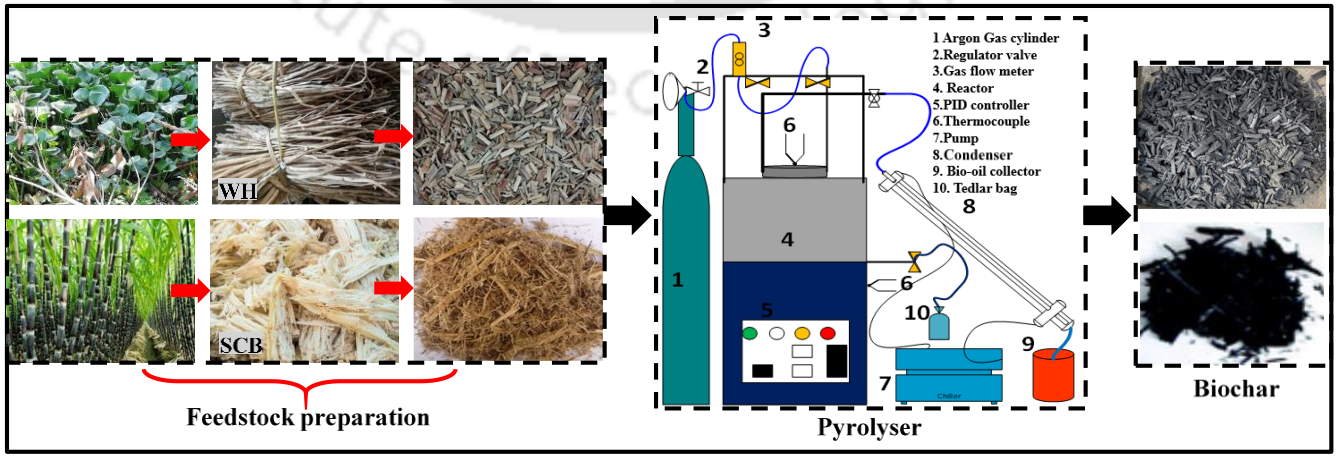

Fig. 3.2 Feedstock preparation to biochar production.

3.2.2.2 Pyrolyser and pyrolysis of the feedstock

The pyrolysis of the feedstock was carried out using a fixed batch pyrolyser as shown schematically in Fig. 3.2. The pyrolyser was designed with an electrically heated rotary tube furnace (6.28 m^3) and a microprocessor based digital PID (proportional integral derivative) temperature controller (PXF9, FUJI electric, Shinagawa, Tokyo, Japan) with thyristor power drive (accuracy of ±1° C). The microprocessor consists a single program of 64 segments that programmes heating, cooling, and holding time. A 4 kW heater (P610C; ULVAC-RIKO, Yokohama, Japan) heats the feedstock in the reactor. Thermocouple positioned at 15 mm from the inner surface of the quartz tube reactor monitors the pyrolysis temperature inside the furnace. A maximum temperature of 1350˚ C can be reached with a continues working temperature of 1150° C by using silicon carbide heating elements (solid rod type). The pyrolysis was performed by taking a maximum of 500 g feedstock at 400° C with a heating rate of 10° C/min for one hour. During pyrolysis, argon gas (150 mL/min) was supplied continuously from the top of the pyrolysis tube reactor. With the inert gas passes over the feedstock, the feedstock heated once the preheating takes place at the sides of the reactor. The syngas and volatiles formed were swept away by the inert gas into a condensation system consisting of chilled water bath (collection of bio-oil). The maximum quantity of biochar produced or yield (%) was determined using Equation (3.1) by considering the mean of triplicates:

$$\%\, \boldsymbol{Yield_{Biochar}} = \frac{\boldsymbol{Mass_{Biochar}}}{\boldsymbol{Mass_{Biomass}}} \times \mathbf{100} \qquad (\mathbf{3.1})$$

The biochar obtained was pulverized, pass through 4.75 mm sieve and stored in air tight containers for subsequent use.

3.2.3 Plant species

In the present study, a non-crop species, broadleaf carpet grass or cow grass (*Axonopus compressus*) was used to investigate the performance of vegetation in BAS. It is a perennial grass with fibrous root system and spreads by creeping stolon and underground rhizomes. The roots mainly grow within the top 40 cm soil depth and have a high tensile strength of 51-60 MPa (Zhang et al.,2014). The easy and abundant availability, drought tolerance characteristics and the land rehabilitation and reforestation ability of the grass species led their use in the stabilization (erosion control) of slopes in South–East Asia (Beard and Green,

1994; Carrow, 1996). Further, the selected grass as a non-crop species requires less maintenance in terms of nutrient supplement and water irrigation that makes them more suitable for bioengineered structures.

3.3 Methodology

3.3.1 Physicochemical and microstructural properties of the soil, biochar and BAS

The grain size distribution (GSD) of the soils, biochar and biochar (5%, 10% and 15% w/w) amended soils were analysed according to ASTM D-422-63-07. The specific gravity was determined as per the procedure recommended by ASTM D-854. Density bottle method was adopted for the measurement of the specific gravity, where pre-mixed soil-biochar samples with added water were taken in a density bottle and kept for 24 hours for removing entrapped air and the corresponding specific gravity was measured. The consistency or Atterberg limits, i.e., the liquid limit (LL), plastic limit (PL) and shrinkage limit (SL) of the bare and BAS were determined according to the ASTM D-4318. The LL was determined by using both the cone penetrometer and Casagrande apparatus. The compaction characteristics of the bare and biochar-amended silty sand were determined by standard proctor test as per the procedure described in ASTM D-698-12. Similarly, for the pure sand, relative density test according to ASTM D4253-16 was conducted. The water absorption capacity was determined according to the standard procedure mentioned in ASTM C128-15, where 20 g of oven dried bare or BAS samples were soaked in water for a period of 72 hours. Thereafter, the excess water was drained out from the samples using a filter paper and the corresponding mass of the samples were recorded. The mass of water absorbed with respect to the dry mass of the samples are reported as water absorption capacity. The pre-determined quantity of soil and biochar were mixed thoroughly before starting all the experiments. Analyses were triplicated and the average value is reported.

The elemental composition of the biochar was determined by the combustion technique using an elemental analyser as described in Bird et al. (2017). Ash content was measured by ammonium acetate method described in ASTM E1755-01 (2007). The pH and electrical conductivity (EC) of the bare and BAS was determined according to ASTM D 4972-18. Measurements were taken in pre-shaken (24 hours) samples with a material: water ratio of 1:10 using an electrode connected to a pH meter and electrical conductivity meter (Jindo et al. 2014). The CEC was determined by ammonium acetate method as described in ASTM D 7503-18. The contact angle of wetting in biochar was determined by sessile drop

method described in Jeffery et al. (2015). Where a smooth surface of biochar was prepared on a microscopic glass slide, and a droplet of water of volume 0.03 ml was deposited on the surface. The images of the droplet were captured by a high-resolution camera and analysed in image j software for getting the contact angle between the tangent line drawn through the curve (referring the water surface) and the horizontal line (presenting the glass slide).

The morphology of the soil and biochar was studied by field emission scanning electron microscopy (FESEM) analysis using a Sigma-300 (Zeiss) variable pressure field emission scanning electron microscope operated with 2-10 kV accelerating voltage. Images were captured at several magnifications ranging from 50X to 50KX. Before capturing the images, the oven dried (48 hours) samples were pass through 150-micron sieve to minimize particle size effect. X-ray diffraction (XRD) test was conducted for identifying the major mineralogical component of the soil and biochar. Dry powdered samples were placed on a flat holder and scanned between 5-90˚ using an X-ray diffractometer (28 Bruker AXS D8 model, Billerica, MA). The functional groups present in the biochar and soil were identified by Fourier transforms infrared spectroscopy (FTIR) test using Fourier transform infrared spectrophotometer (IRAffinity-1, Shimadzu, Japan). Oven-dried samples were uniformly mixed with KBr in a 1:100 sample to KBr ratio as per the KBr pellet method and the corresponding FTIR spectra were recorded for the entire range of wave number in transmittance mode (Gupt et al., 2018). The specific surface area (SSA) of the soil and biochar was determined by using a Brunauer-Emmett-Teller (BET) surface area analyzer (Autosorb IQ MP, Quantachrome, Florida) according to the procedure mentioned in Brunauer et al. (1938).

3.3.2 Hydraulic properties

3.3.2.1 Saturated hydraulic conductivity

The saturated hydraulic conductivity (K_{sat}) of the bare and BAS was measured using a rigid-wall permeameter in accordance with the standard testing procedure described in ASTM D5856-15. Soil and biochar at 5%, 10% and 15% (w/w) were dry mixed in an aluminium pan thereafter water corresponding to 0.9MDD and MDD was added and mixed uniformly. The mixtures were then statically compacted at 0.9MDD and MDD in a PVC mould of size 50 mm diameter and 160 mm length up to a depth of 80 mm. The details of the experimental setup are presented in Fig. 3.3.

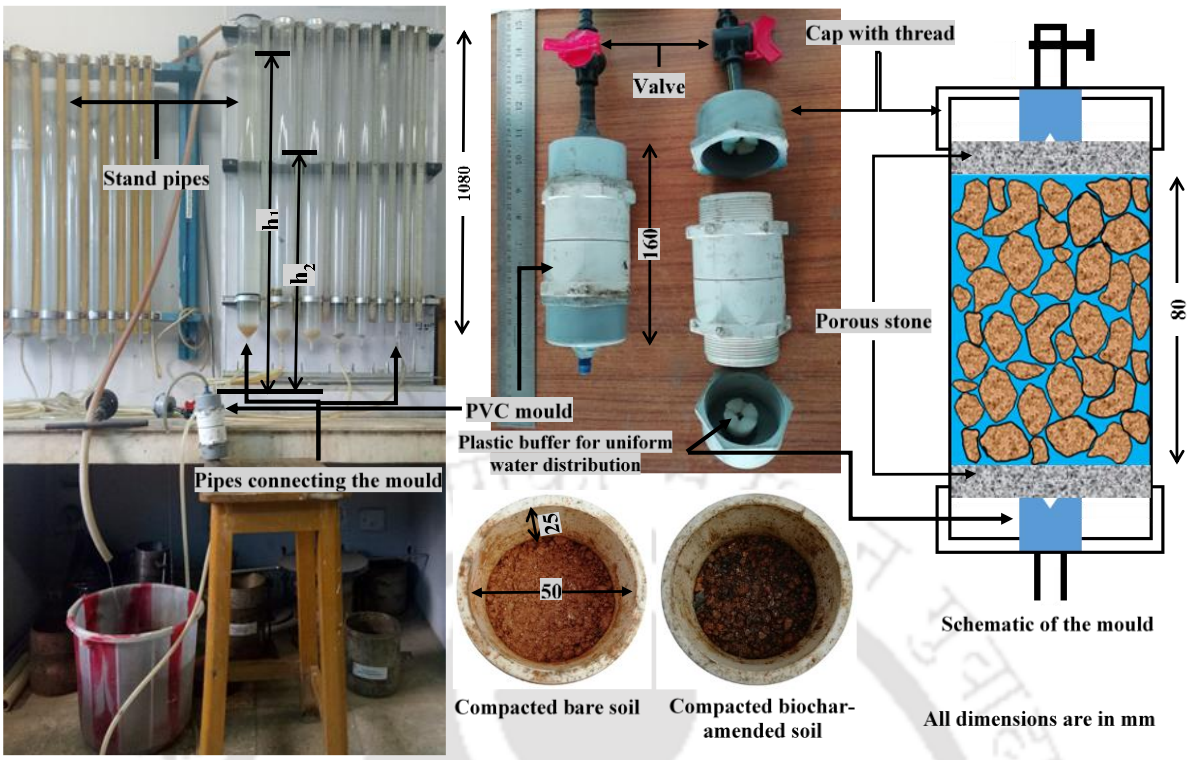

Fig. 3.3 Experimental setup adopted for the measurement of permeability.

The selection of compaction density of 0.9MDD and MDD, and the corresponding water content was to represent the compaction criteria adopted for many geotechnical and geoenvironmental structures, as reported in the literature (Goldsmith et al., 2001, Li et al., 2016). A relative compaction of 95% (i.e., 0.95MDD) was reported to be suitable for the adequate growth and development of non-crop species in man-made slopes by the previous researchers (GCO, 2000, Ni et al., 2016, Ni et al., 2018). Moreover, the selection of biochar amendment rate of 5%, 10% and 15% was based on the trial study conducted for the tested biochar. The amendment of biochar beyond 15% was observed to lead to the non-uniformity of the soil-biochar mix due to lower specific gravity of the biochar compared to the soils. In literature, a maximum biochar amendment rate of 20 to 30% (w/w) was also reported (Williams et al., 2018, Wong et al., 2018). Three independent replicates for each biochar amendment rate were prepared. All the compacted samples were then saturated by allowing water from bottom to the top on an average for 4 days. After saturation, the hydraulic conductivity of the biochar-amended silty sand was determined by measuring the flow rate under a falling head condition. Whereas, for biochar-amended sand, the flow rate was measured under a constant head condition due to the higher rate of flow. The K_{sat} of the silty sand was calculated using the following equation (Klute, 1986):

$$k = \left(\frac{a \times L}{A \times t}\right) ln\left(\frac{h_1}{h_2}\right) \qquad (3.2)$$

where k is the hydraulic conductivity (m/s), a is the cross-sectional area of the standpipe (m^2), L is the length of the sample (m), A is the cross-sectional area of the sample (m^2), h_1 and h_2 are the initial and final water head with respect to the outflow (m), t is the time for the hydraulic head difference to decrease from h_1 to h_2.

Similarly, for the sand, the K_{sat} was calculated as follows:

$$k = \frac{V \times L}{A \times \Delta h \times t} \qquad (3.3)$$

where k is the hydraulic conductivity (m/s), V (m^3) is the volume of water passes through the sample in a known time t (s) and Δh is the hydraulic head difference (m).

3.3.2.2 Infiltration rate

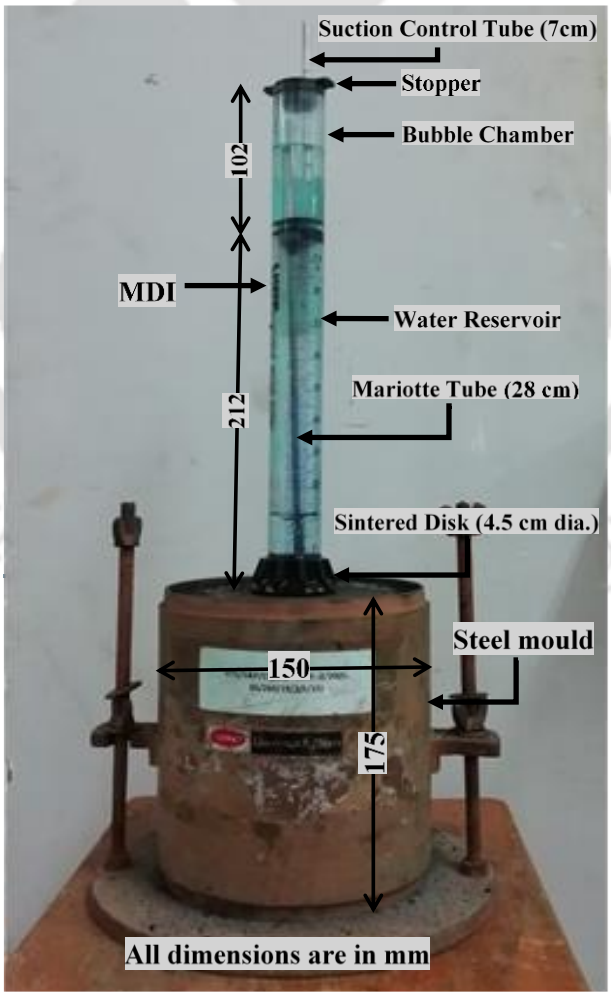

Fig. 3.4 Experimental setup adopted for the measurement of infiltration rate (I_r).

The infiltration rate of the bare and BAS was measured using a mini-disk infiltrometer (MDI), as shown in Fig. 3.4. Soil was compacted at 0.9MDD and MDD and their corresponding moisture content in a steel cylindrical mould of size 15 cm diameter and 17.5 cm length. The MDI was chosen due to its simplicity to use in the laboratory and there is no need of auguring or disturbing the sample. Before starting the measurement, the bubble chamber and the reservoir of the MDI were filled with water and a suction head of 2 cm was applied through the suction control tube. The application of the suction head was basically to minimize any flow of water through macro-pores. A similar suction head of 2 cm was found to be adopted by the previous researchers (Fodor et al., 2011, Bordoloi et al., 2017). Thereafter, the water filled MDI was placed vertically straight on the compacted soil surface (Fig. 3.4) for ensuring proper contact between the sintered disk and the soil surface. The responses of the cumulative volume of water infiltrate (V) with time (t) were recorded at an interval of 60 seconds for the silty sand and 10 seconds for the pure sand. The recorded cumulative volume of water infiltrate (V) was plotted against the time (t) and the obtained V-t responses were fitted with a second-degree polynomial equation. To compare the infiltration rate of bare and biochar amended soil, a same second-degree polynomial equation was maintained for all the V-t responses of bare and biochar amended soil. The polynomial equation was further differentiated with respect to time (t) to obtain the slope of the plot i.e., dV/dt for calculating infiltration rate, I(t) as shown in equation 3.4 below:

$$\boldsymbol{I(t) = \frac{1}{A}\frac{dV}{dt}} \qquad (\mathbf{3.4})$$

Where (dV) is the change of volume of water infiltrated within a given time (dt), and A is the cross-sectional area of the infiltrometer. Similar approach of evaluating infiltration rate was adopted by previous researchers (Leung et al., 2015, Bordoloi et al., 2017).

3.3.2.3 Soil water retention characteristics (SWRC)

3.3.2.3.1 Preparation of soil column

The test setup used in the present study is presented in Fig. 3.5 (a-b). PVC mould of size 250 mm diameter and 500 mm length with base plate were fabricated for preparing compacted soil column. Although the soil hydraulic properties are scale-dependent, the mould dimension was selected to maintain one-dimensional flow conditions. Six numbers of holes were drilled in the diametrical direction of the mould at a depth of 150, 250 and 350 mm from the base of the mould for accommodating suction and moisture content sensors.

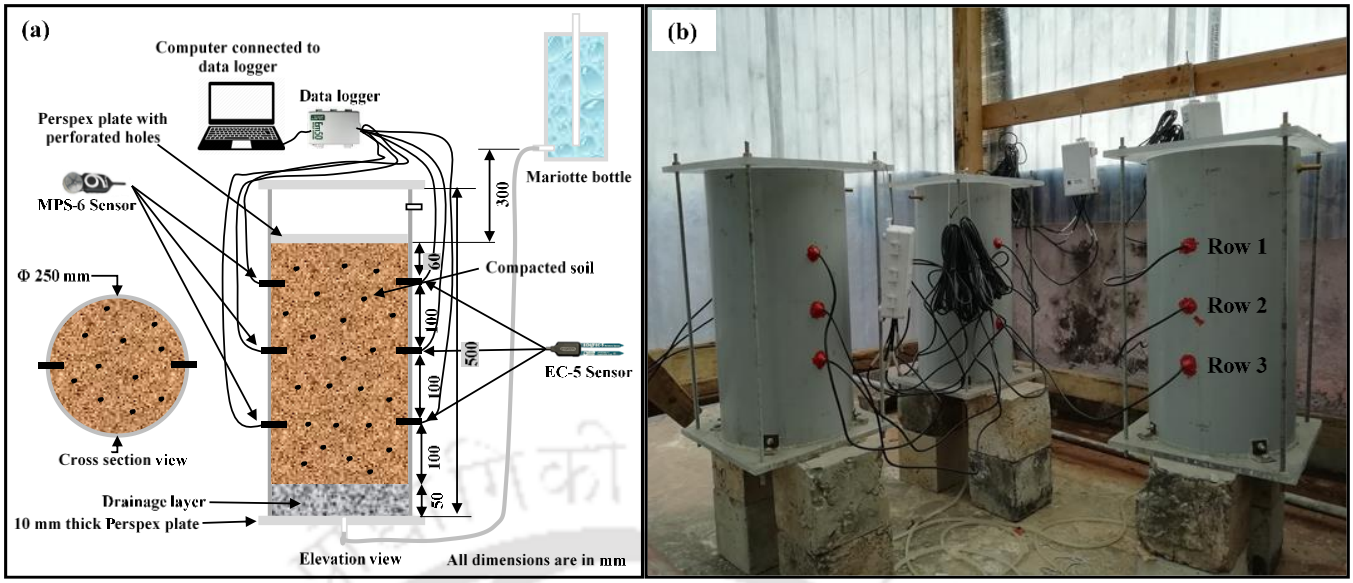

Fig. 3.5 (a) schematic diagram of the experimental setup adopted and (b) setups under transparent house.

Holes were also drilled to allow water to flow in and excess water to flow out. For BAS, the soil and biochar at 5%, 10% and 15% (w/w) were dry mixed in an aluminum pan. Thereafter, water corresponds to 0.9MDD obtained from the standard Proctor test (compaction curve) was added, mixed uniformly and incubated for a period of 24 hours by sealing inside a desiccator for moisture equilibration. The mixture was then statically compacted at a dry density equal to 0.9MDD in three layers up to a height of 410 mm from the base of the mould using soil compression testing machine (Aimil, India) and applying a vertical force of 47-50 kN. For pure sand, the mixture was statically compacted at a dry density equal to 0.9MDD obtained from the relative density test. Before compacting the soil columns, a drainage layer of 50 mm thick with gravel was placed at the bottom of the mould for uniform distribution of water entering into the soil. The sensors for monitoring suction and moisture content were installed while compacting the soil column. The sensors are described in the next section below. Perspex plate (10 mm thick) one with perforated holes and another without holes were placed on the top of the compacted soil and the mould, respectively and buffer supports were placed in between the plates for minimizing the evaporation of water from the soil and controlling any volume change or swelling of soil during wetting.

3.3.2.3.2 Monitoring of suction, water content and establishment of soil water retention curve (SWRC)

The matric suction (ψ_m) was monitored using TEROS-21 sensors while the volumetric water content (θ) was monitored using EC-5 volumetric water content sensors (METER Group, inc., 2019, USA). The EC-5 sensors could measure volumetric water content in the range of 0 to 100% with an error of ±3% and the TEROS-21 sensors could measure the matric suction in the range of 9 to 10^5 kPa with an error of ±10%. These sensors were placed during compaction of the soil/soil-biochar mixture at 60, 160 and 260 mm from the surface of the compacted soil as shown in Fig. 3.5. However, before installation, soil specific calibration for all the sensors were performed for minimizing any variation or error in reading. The selection of spacing of 100 mm between sensors was based on the influence zone of the moisture sensors, which is approx. 25 mm radial distance. To prevent any possible leakage of water during experimentation, the open space surrounding the sensor body was sealed beforehand using a plastic sealant (Anabond glue, Fig. 3.5b). Duplicate columns for each treatment of bare (0%), 5% and 10% biochar-amended silty sand and pure sand were tested.

All the compacted soil columns were placed in a transparent roofed house (Fig. 3.5b) maintained at the atmospheric condition and protected from natural precipitation. The average relative humidity and temperature were measured by microclimate monitoring station (Decagon devices). For measuring the drying SWRC, all the soil columns were initially irrigated using a controlled head mariotte bottle with a flow rate of 100 ml/min until the suction read by the TEROS-21 sensor reached a minimum value of around 9 kPa (minimum range of the sensor) or near saturation. Thereafter, all the saturated soil columns were undergone continuous drying until the suction reached a nearly constant peak value. Similarly, for wetting SWRC, all the dried soil columns were subjected to a bottom to up saturation using a controlled head mariotte bottle with a flow rate of 100 ml/min until the suction reached a minimum value of around 9 kPa or near saturation. The TEROS-21 and EC-5 sensors were connected to EM-50 data loggers for continuous monitoring of suction and moisture content at an interval of initially 10 minutes, thereafter varied up to 1 hour.

The suction and volumetric water content data obtained from the data loggers were plotted and fitted to van Genuchten (1980) model using RETC software (van Genuchten et al., 1991) as given below:

$$\boldsymbol{\theta} = \left\{\left[\frac{\mathbf{1}}{\mathbf{1} + (\boldsymbol{\alpha} \times \boldsymbol{h})^{\boldsymbol{n}}}\right]^{\boldsymbol{m}} \times (\boldsymbol{\theta_s} - \boldsymbol{\theta_r})\right\} + \boldsymbol{\theta_r} \qquad (\mathbf{3.5})$$

where θ (m^3/m^3) is the volumetric water content at any suction, α (m^{-1}) is the shape parameter of the SWRC, h (m) is the suction head, n is the shape parameter, m (=1-1/n) is also the shape parameter, θ_s (m^3/m^3) is the saturated volumetric water content and θ_r (m^3/m^3) is the residual volumetric water content. The corresponding fitting parameters with uncertainties were obtained at 95% confidence interval. The plant available water content (*PAWC*) was calculated from the field capacity (FC) and permanent wilting point (PWP). Based on the literature (Colman, 1947; Jamison and Kroth, 1958; Cassel and Nielsen, 1986), the FC is considered as 10 kPa for pure sand and 33 kPa for silty sand. The PWP is considered to be 1500 kPa (Feddes, 1978). The difference in water content at 1500 kPa and 10 kPa for pure sand or 33 kPa for silty sand is reported as *PAWC*.

3.3.2.4 Unsaturated hydraulic conductivity

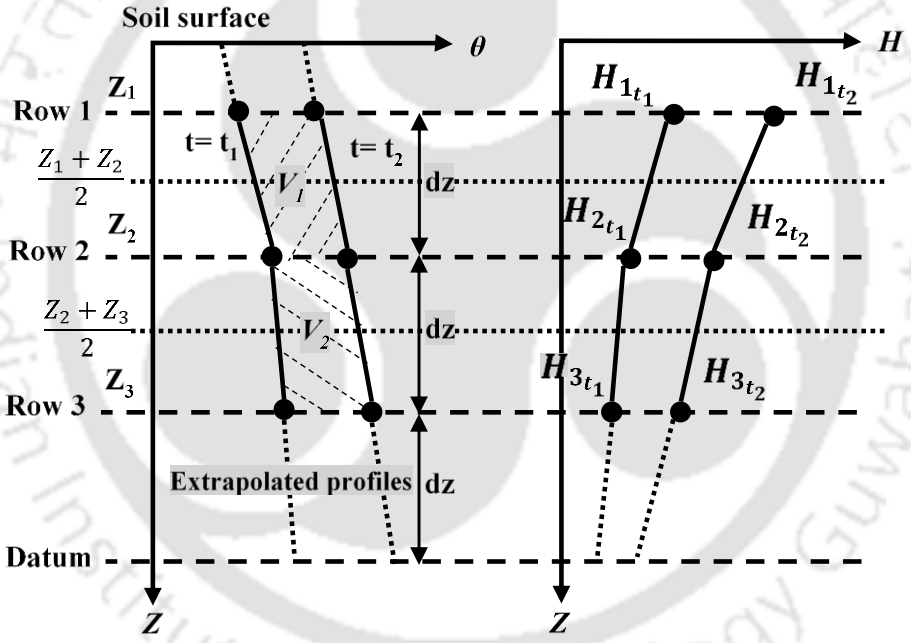

Fig. 3.6 Arbitrary instantaneous profiles of VWC (θ) and hydraulic head (H) at elapsed times $t = t_1$ and t_2, along a one-dimensional soil column.

In the present research work, the unsaturated hydraulic conductivity (K_{unsat}) was derived from the suction and moisture content data using instantaneous profile method (IPM) according to the procedure reported by Leung et al. (2016). Arbitrary profiles of the water content and hydraulic head are highlighted in Fig. 3.6. The K_{unsat} was estimated with the help of Equation 3.6-3.9 as follows:

$$k_{z_{avg}.t_{avg}} = \frac{V/_{\Delta t}}{i_{z_{2}.t_{avg}} - i_{z_{1}.t_{avg}}} \qquad (3.6)$$

$$i_{z_{avg}.t_{avg}} = \frac{1}{2}\left[\left(\frac{H_{1.t_1} - H_{2.t_1}}{Z_{1.t_1} - Z_{2.t_1}}\right) + \left(\frac{H_{1.t_2} - H_{2.t_2}}{Z_{1.t_2} - Z_{2.t_2}}\right)\right] \qquad (3.7)$$

where $k_{z_{avg}.t_{avg}}$ is the unsaturated hydraulic conductivity (K_{unsat}) between any two rows of sensors in 'm/s', V (i.e., V_1, V_2, shaded area in Fig. 3.6) is the change of total water volume between two sensors and time interval Δt, $i_{z_{avg}.t_{avg}}$ is the hydraulic gradient at depth Z_{avg}, H (*i.e.*, H_1, H_2, H_3)= $[Z+(\psi/\gamma_w)]$ is the hydraulic head in 'm', Z (*i.e.*, Z_1, Z_2, Z_3) is the potential head or height from the datum in 'm' and ψ is the matric suction in 'kPa'. The change in water volume V_1 was calculated as follows:

$$V_1 = \left[\frac{\left(\theta_{1,t_2} - \theta_{1,t_1}\right) + \left(\theta_{2,t_2} - \theta_{2,t_1}\right)}{2}\right] dz \qquad (3.8)$$

where θ (i.e., θ_1, θ_2, θ_3) is the volumetric water content in 'm^3/m^3' and dz is the spacing between two sensors in 'm'. Similarly, V_2 was calculated. The hydraulic gradient at any sensor depth (i.e., i_1, i_2, i_3) was calculated as follows:

$$i_{z.t_{avg}} = \frac{1}{2}\left[\left(\frac{H_{t_1}}{Z_{t_1}}\right) + \left(\frac{H_{t_2}}{Z_{t_2}}\right)\right] \qquad (3.9)$$

Finally, the K_{unsat} was calculated from equation 3.6 by putting the values obtained from equation 3.8 and 3.9.

3.3.2.5 Determination of porosity

The porosity of the samples after completion of saturated permeability test was measured by a conventional helium gas porosimeter as described in Pal et al. (2018). The method involves the intrusion of helium gas into the soil pores comprising open and interconnected pores, and recording of the change in pressure due to the intrusion of gas in the pores. Based on the principle of Boyle's law, the solid volume or the porosity was determined from the observed pressure difference and the bulk sample volume. All the samples were freeze-dried at -80° C for 4 days in a Freeze dryer (CoolSafe 100-9 Pro, Labogene, Bjarkesvej 5, Allerod, Denmark) before the porosity measurement.

3.3.3 Mechanical properties

3.3.3.1 Direct shear test

The direct shear test on bare and biochar-amended silty sand and pure sand was conducted according to ASTM D3080-02 standard. The samples of BAS were prepared by dry mixing of biochar at 5%, 10% and 15% (w/w) with the soils. For silty sand, water corresponds to 0.9MDD obtained from proctor test (compaction curves) was added to the samples and kept in a desiccator for moisture equilibration. After that, the samples were compacted in a direct shear box of area 36 cm^2 and depth 4 cm, confirming a dry density of 0.9MDD. Notably, the samples of pure sand were prepared at air-dry state (without adding extra water) and compacted at 0.9MDD obtained from the relative density test. The compacted samples were sheared under normal stress of 49, 98 and 147 kPa, and a constant displacement rate of 1.25 mm/min, simulating the field condition for most geotechnical structures as per the code (ASTM) referral. The direct shear apparatus is equipped with multiple strain rate option. However, the strain rate of 1.25 mm/min was selected so that undrained and abrupt failure condition does not occur. A similar strain rate of 1.25 mm/min was considered by the past researchers (Bordoloi et al. 2017; Mukherjee and Mishra 2019). Stress-strain responses were recorded by mechanical dial gauge mounted along the shear box until shear displacement equivalent to 10% of the sample size undergone. Tests were replicated thrice and the average value is reported. The shear strength parameters i.e., the cohesion (c) and the angle of internal friction (ϕ) were computed by fitting the peak shear stress and the corresponding normal stress into Mohr-coulomb failure criteria.

3.3.3.2 Unconfined compression test

To observe the undrained shear strength, unconfined compression test or UC test was conducted as per the provision of ASTM D2166-00 standard for bare soil and biochar amended soil. The samples of soil-biochar-composite were prepared first by mixing biochar at 5, 10 and 15% (w/w) with soil. Thereafter, water was added to the samples and stored in a desiccator for 24 hours by sealing inside the plastic bags for moisture equilibration. The samples of bare soil and the soil-biochar composite were compacted at two different densities (i.e., 0.9MDD and MDD) and their corresponding moisture content (obtained from compaction curves) in a cylindrical mold allowing static compaction from both the ends. These densities were selected to observe the effect of density on the shear strength of the

BAS by replicating the compaction density (0.9MDD- MDD) adopted for most geotechnical structures (Goldsmith et al. 2001; Li et al. 2016; GCO, 2000).

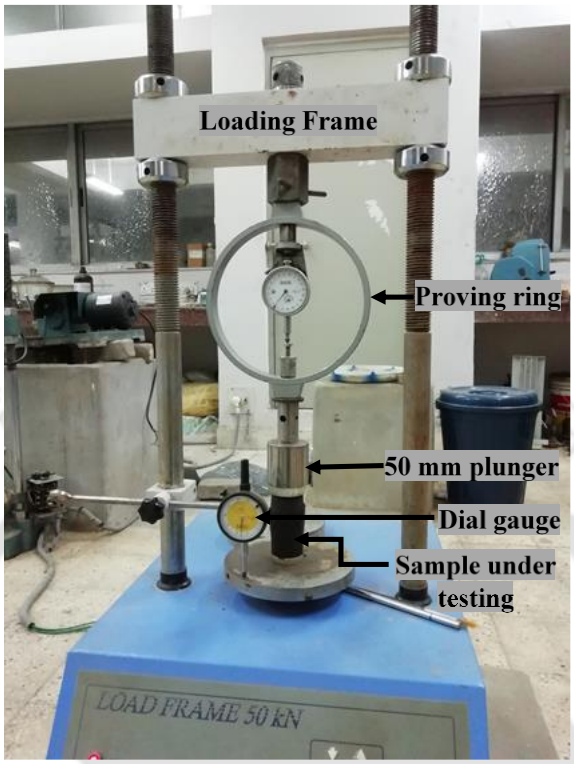

Fig. 3.7 Unconfined compression testing machine shearing samples.

The compacted samples (38 mm diameter and 76 mm length) were then sheared in a UC testing machine under a constant strain rate of 1.25 mm/minute as shown in Fig 3.7, and their corresponding stress-strain responses were recorded. Three replicate samples for bare and each BAS under each density condition were tested.

3.3.3.3 California bearing ratio test

The California bearing ratio or CBR test on bare and BAS was conducted according to ASTM D1883-16. The water mixed bare and BAS were kept in a desiccator for 24 hours to achieve uniform distribution of water throughout the soils. Samples for pure sand were prepared at air-dry state. Thereafter, compacted at dry density of 0.9MDD and MDD in a cylindrical mold. All the compacted samples were soaked in water for 96 hours i.e., soaked CBR test. The soaked CBR test was selected to understand the performance of embankment material of bare and BAS under worst possible condition (IRC:37 2012). A 50 mm diameter plunger was allowed to penetrate on the surface of the compacted soaked samples at a deformation rate of 1.25 mm/min until a final penetration depth of 12.5 mm was reached and

the load versus deformation response recorded. Test on each sample repeated thrice and the average value is reported.

3.3.3.4 Monitoring of desiccation crack

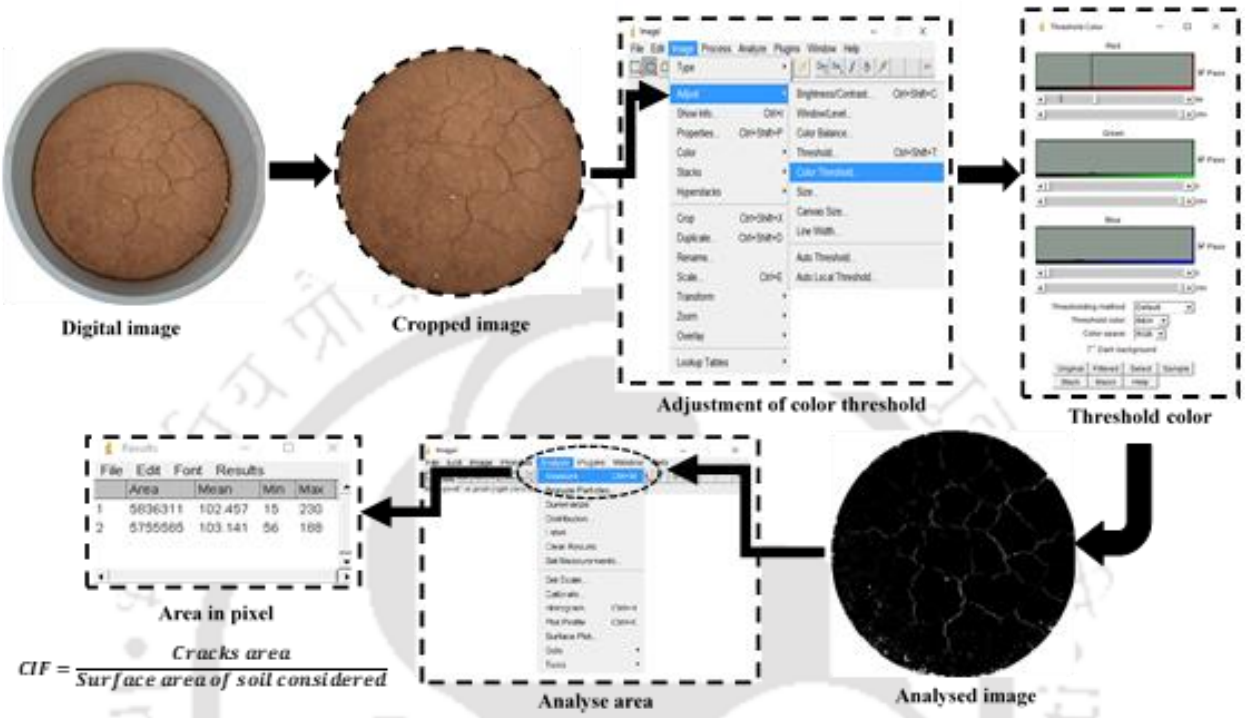

Fig. 3.8 Process of analyzing crack (CIF) using colour threshold technique in image j.

In the present research work, the surface cracks developed during the drying phase of the samples were quantified by crack intensity factor (CIF). The CIF is the ratio of the total crack area to the surface area of the soil considered. Images of the compacted soil surface were captured daily using a commercial DSLR camera (Canon EOS 600D with lens range 18-55 mm and resolution of 72 dpi) mounted on an adjustable steel frame. Images were captured from the same height for minimizing any variation in pixel count or area of the images. The captured images were analyzed for cracks using an open-access image processing software image j (Rasband 2011) as per the procedure described in Gadi et al. (2017). Fig. 3.8 shows the stepwise procedure adopted for analyzing the image for crack quantification. Digital images captured by the camera were imported into the image j software and then cropped for removing the boundary shrinkage. The area (in pixel) of the cropped image was measured and taken as the total soil surface area. In the next step, the cropped images were adjusted to color threshold using RGB color space and the corresponding area of cracks was measured. Thereafter, the CIF was calculated as the ratio of cracks area (A_C) to the total soil surface area (A_T) i.e.,

$$CIF(\%) = \frac{A_C}{A_T} \times 100 \qquad (3.10)$$

3.3.4 Vegetation performance

3.3.4.1 Preparation of soil column and growing of vegetation

Vegetation were grown in the same soil column compacted and used for K_{unsat} measurement as shown in Fig. 3.9. The preparation of the soil column is already explained in section 3.3.2.3.1.

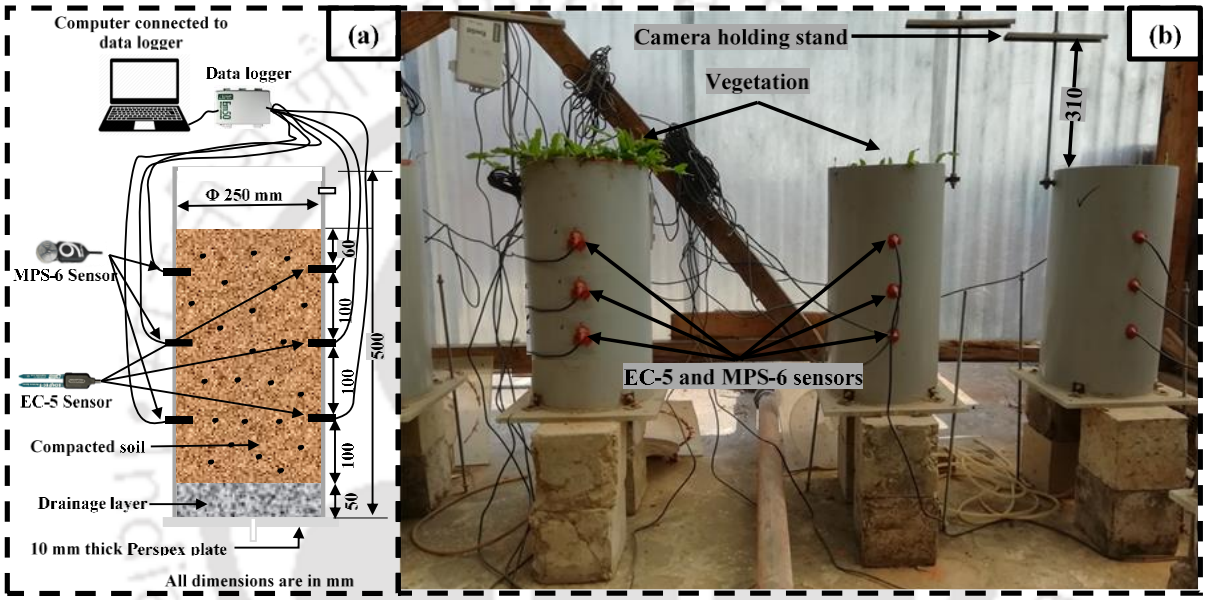

Fig. 3.9 Experimental setup used for growing vegetation, (a) schematic diagram and (b) real image.

All the columns were irrigated with water thereafter, three numbers of individual grass with equal numbers of leaves were transplanted in each column by digging small holes on soil surface. The columns were kept under a transparent-roofed house where samples were protected from natural precipitation however accessed to the sun light and open air circulation i.e., maintained with natural environmental condition. The air temperature, relative humidity and solar radiation were monitored using microclimate monitoring system (Meter Inc. USA). The free or potential water evaporation was measured by weight difference technique. Fig. 3.10 (a-d) highlights the variation of daily average temperature, relative humidity and solar radiation and potential evaporation with time during the growth period.

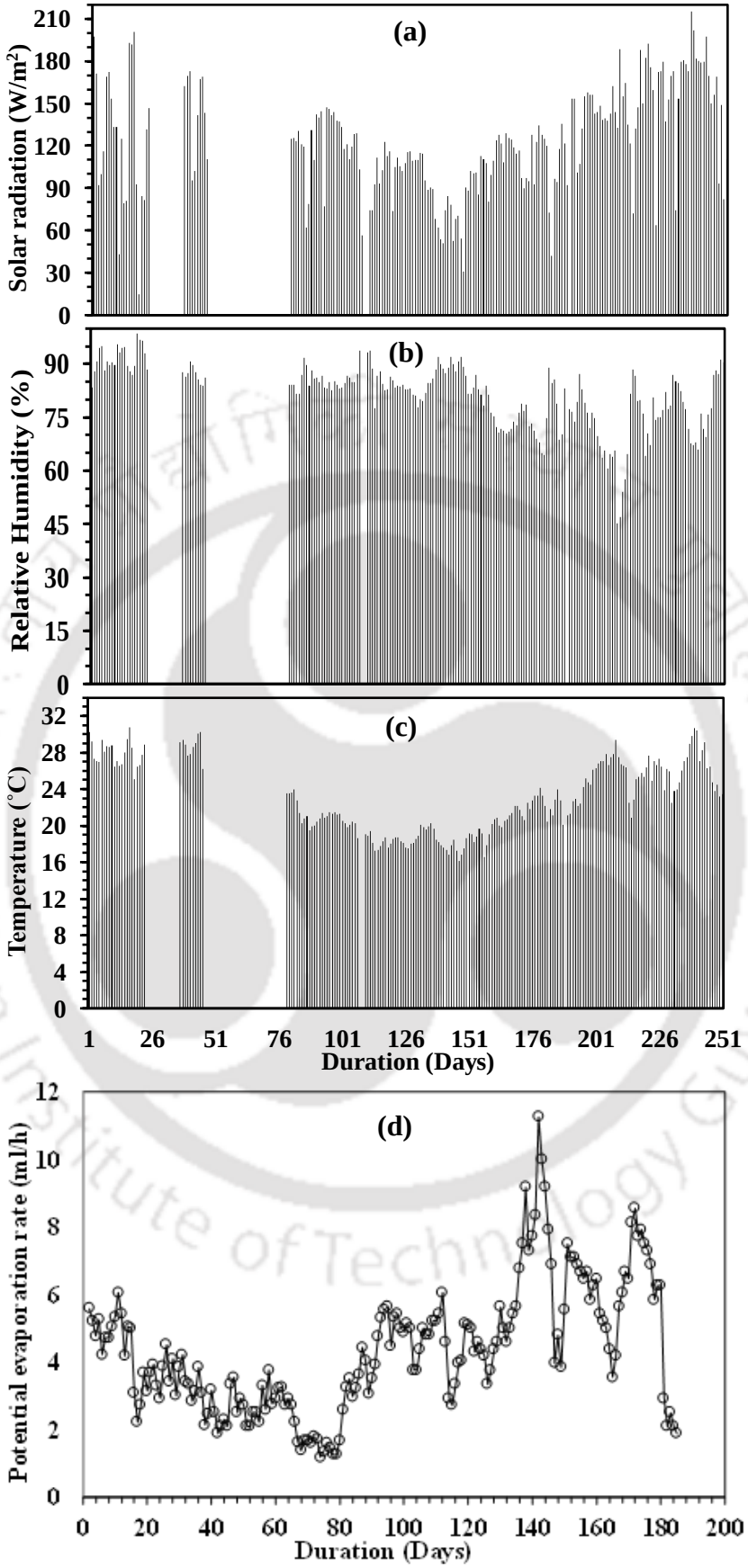

Fig. 3.10 Variation of daily average solar radiation (a), relative humidity (b), temperature (c) and potential evapotranspiration (d) with time.

Equal amount of water (250 ml) was irrigated one-day interval in all the columns for maintaining moisture content at around field capacity or near saturated in the root zone. Irrigation was continued till the vegetation near completely covered the soil surface i.e., fully grown over the columns. After completely covered by the vegetation, all the columns were subjected to drought state i.e., no water was irrigated and the plants progressively wilted. The growth and health parameters were monitored both in the growing and wilting phase of the plants.

3.3.4.2 Quantification of plant growth

The growth of the vegetation was quantified by the vegetation density (VD), leaves count, shoot and root biomass and root mass density (RMD). VD (m^2/m^2) on a surface is defined as the ratio of area covered by the vegetation (A_v) and the total soil surface area (A_s) considered (Gadi et al., 2018). VD was measured from the captured images of the column surface by image analysis technique as highlighted in Fig. 3.11.

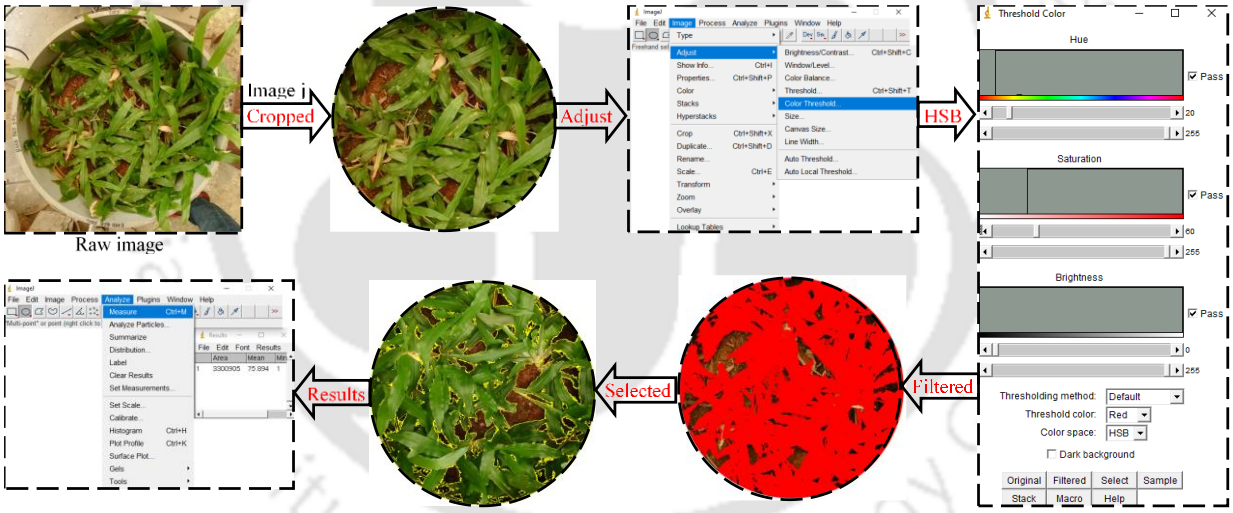

Fig. 3.11 Determination of VD by image analysis technique.

Images were captured using digital camera (Canon EOS 600D) in two days interval from a same elevation (400 mm, Fig. 3.9) from the soil surface to minimize any observational error. To process the image, the camera captured image was loaded into Image J (open source) image processing software and cropped to only account the soil surface area. The pixel area of the cropped image was counted which is the total soil surface area, A_s. In the next step, the cropped image was adjusted to color threshold using HSB (Hue, Saturation and Brightness) color space and the corresponding pixel area of the vegetation (A_v, red) was counted. Finally, the VD was calculated as follows:

$$VD(\%) = \frac{Av}{As} \times 100 \qquad (11)$$

The number of leaves or the leaves count of the all bare and amended soil were taken in seven-day interval. The dry biomass of the shoot and roots after complete wilting of the grass was determined according to the method described in Abbas et al. (2018). The above ground biomass (shoot) of the grass was cut and washed with distilled water. The roots along the depth were collected after taking out the soil and washed with 1% HCL and distilled water. The dry mass of roots was measured for each 2 cm depth and the total roots mass per unit volume of soil is presented as RMD. Finally, the total dry weights (oven-dried at 60˚ C) of the shoot and roots were recorded after constant drying (negligible to no change in the mass) of the samples.

3.3.4.3 Measurement of stomatal conductance and photosynthetic yield

Stomatal conductance (SC) and photosynthetic yield (PY) was measured using leaf porometer (Meter Inc. USA) and MINI-PAM-II (Heinz Walz Gmbh, Effeltrich, Germany) instrument as shown in Fig. 3.12. Leaf porometer gives the SC of leaves based on the measured relative humidity and temperature by the sensors placed across the leaf in series.

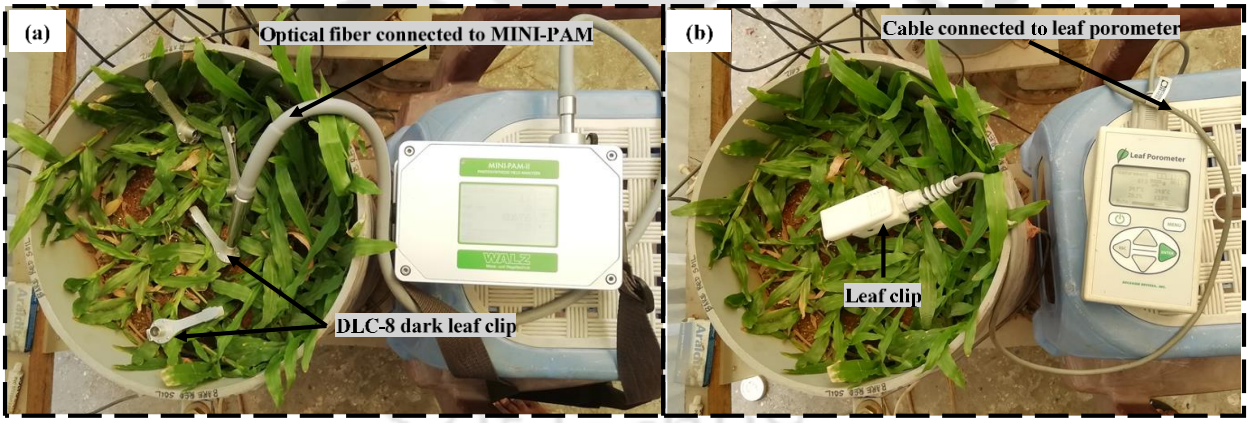

Fig. 3.12 Measurement of (a) PY by MINI-PAM and (b) SC by Leaf porometer.

To start the measurement of SC, the desiccant chamber in the porometer was filled with fresh desiccant and then calibrated with filter paper and deionized water for reliable measurement as suggested by the manufacturer. With the porometer calibrated, the leaf was placed in the leaf clip and the measurements were taken. Conductance was measured at the bottom of the grass leaf (abaxial conductance) due to presence of higher numbers of stomata in the bottom surface of the grass leaves which is protected from the direct sun light. Large numbers of leaves are available in a single column and measuring SC in all is time consuming. Further,

SC varies with the leaf age, time of measurement (diurnal variation) and location of the leaves (under light or shade). Therefore, four numbers of leaves with relatively same age and at different location (both shade and light) were selected. Measurements were taken within 10 AM to 1 PM of the day to avoid the effect of diurnal variation. As grass leaves wilt gradually with time, taking measurement in the same selected leaves for the entire monitoring period was not possible. Hence, the leaves were changed as the selected leaves start wilting. However, at the end, when all the leaves were wilted measurement was taken in wilted leaves.

The MINI-PAM could measure many photosynthetic parameters based on the chlorophyll fluorescence technique; however, in the present study, maximum yield (F_v/F_m), effective yield (Y(II)) and the photosynthetic efficiency were measured in dark actinic condition. The F_v/F_m is the maximum light absorption and utilization (in photosynthesis) capacity of leaves and occurs just after dark adaptation. Y(II) is the photochemical utilization of the absorbed light by the leaves under light condition. The photosynthetic efficiency was determined by measuring the light curve, which is the relationship between the electron transfer rate (ETR) and light intensity expressed as photosynthetic active radiation (PAR). For measuring the photosynthetic parameters, the selected leaves (the same considered for SC measurement) were clamped using DLC-8 dark leaf clip with a moveable shuttle and allowed to adapt dark for 15 minutes. With the leaves dark adapted, the optical fiber connected to the MINI-PAM was positioned in the clip and the readings were recorded after opening the shuttle (Fig. 3.12). Measurements were taken on adaxial (top surface) leaf side due to the direct exposure of sun light (higher density of chlorophyll). The dark period of 15 minutes was selected based on the trial measurement where no significant difference in readings of dark adapted between 10 to 30 minutes was observed and also adapted by the past researchers (Sobrado, 2008; Kalaji et al., 2014).

CHAPTER 4
PHYSICOCHEMICAL AND MICROSTRUCTURAL PROPERTIES OF BIOCHAR AND BAS

4.1 Introduction

This chapter presents the results obtained for the physicochemical and microstructural analysis of the soil, biochar and BAS. The evaluation of physicochemical and microstructural properties of the soil or BAS is necessary as the hydro-mechanical and biological properties of soils are dependent on physicochemical and microstructural properties. The physicochemical properties, such as GSD, specific gravity, consistency limits, compaction characteristics, water absorption capacity, pH, EC, CEC, elemental composition and wettability characteristics (contact angle), and microstructural properties, such as mineralogical composition (XRD), surface area (BET), functional groups (FTIR), and surface morphology (FESEM) were evaluated. The biochar exhibits distinct physical appearance and material properties compared with the soil therefore, the effect of biochar amendment on the soil physicochemical properties was evaluated and discussed in detail below.

4.2 Physical properties

The soil collected from the Brahmaputra river was characterized to be poorly graded sand, SP based on the Cu and Cc value of 1.35 and 0.87 respectively and the soil collected from the campus was classified as silty sand, SM (USCS; ASTM D2487-11). Other properties are discussed in the below sections.

4.2.1 Specific gravity

The specific gravity (SG), water absorption capacity, liquid limit, plastic limit and shrinkage limit of the soil, biochar and BAS are presented in Table 4.1. The SG of the bare silty sand and pure sand was observed to be 2.68 ± 0.10 and 2.63 ± 0.14 respectively. The SG of the biochar tested was found to be much lower (46-70%) than the soils. The distinct material and the porous nature or presence of intra-pores in biochar, which could be seen from the FE-SEM images attributed to the lower SG of biochar compared to the soils.

Table 4.1 Effect of biochar on physical properties of the soils.

Properties	Biochar type	Soil type	Biochar amendment rate				
			0% (Bare)	**5%**	**10%**	**15%**	**Only biochar**

Specific gravity	MB	Silty sand	2.68±0.10	2.59±0.04	2.47±0.09	2.30±0.16	1.44±0.10
		Sand	2.63±0.14	2.60±0.05	2.49±0.01	2.42±0.02	
	WHB	Silty sand	2.68±0.10	2.51±0.05	2.42±0.03	2.28±0.04	0.80±0.05
	SBB	Silty sand	2.68±0.10	2.53±0.05	2.44±0.02	2.29±0.04	1.11±0.20
Water absorption capacity (%)	MB	Silty sand	36±1.4	51±3.5	58±2.5	72±3	156±11
	WHB	Silty sand	36±1.4	46±3	60±5	104±6	564±16
	SBB	Silty sand	36±1.4	59±1.5	79±5	98±0.5	633±3.4
Liquid limit (LL), %	MB	Silty sand	50±0.3	51 ±0.4	53±0.4	55±0.4	-
	WHB	Silty sand	50±0.3	54 ±0.5	61 ±0.6	73 ±0.8	
	SBB	Silty sand	50±0.3	56 ±0.4	68 ±0.5	79 ±0.4	
Plastic limit (PL), %	MB	Silty sand	30±1.1	32 ±0.5	36±0.1	38±0.7	-
	WHB	Silty sand	30±1.1	34 ±0.4	43±0.6	51±0.4	
	SBB	Silty sand	30±1.1	36 ±1	41 ±0.6	48 ±0.5	
Shrinkage limit (SL), %	MB	Silty sand	27±0.2	30 ±0.70	33±0.31	35±0.40	-
	WHB	Silty sand	27±0.2	33 ±0.8	45±0.9	63±1	
	SBB	Silty sand	27±0.2	38 ±1.1	52 ±0.4	69 ±0.2	
Plasticity index (PI), %	MB	Silty sand	20	19	17	17	-
	WHB	Silty sand	20	20	18	22	
	SBB	Silty sand	20	20	27	31	

Note: Value in table represents the average value ± standard deviation.

The WHB exhibited the lowest SG among the different biochar tested while the MB showed the highest. The soft sponge like structure of WH and hard wood structure of mesquite resulted in lowest and highest SG after pyrolysis. The SG of the soils was observed to be decreased when biochar of 5%, 10% and 15% (w/w) was amended (Table 4.1). The replacement of heavy (higher specific gravity) soil particles with the light (lower specific gravity) and porous biochar particles that allows higher air entrapment attributed to the decreased SG after biochar amendment (Reddy et al. 2015). Similarly, difference between the SG of different BAS could be observed due to the variation in the SG of different biochar.

4.2.2 Water absorption capacity

The water absorption capacity (WAC) is the ability of the material to absorb water in its pores when the material is in saturated or water submerged condition. The silty sand exhibited the WAC of 36 ± 1.4% and the WAC of the biochar tested was found to be very high (difference of 120-597%) compared to the soil. Among the biochar tested, SBB

exhibited the highest (633 ± 3.4%) WAC while the MB showed the lowest (156 ± 11%). The porous structure of biochar that allows higher storage of water due to presence of intra-pores attributed to the higher WAC. Moreover, the lower lignin content (18-24%) and higher cellulose content (45-55%) in sugarcane bagasse biomass compared with the other biochar led to the higher porosity after pyrolysis and hence the higher WAC (Rainey, 2009). In literature, Chen et al. (2010) also reported WAC of 500% for SBB. The amendment of 5%, 10% and 15% biochar (all biochar) increased the WAC of the soil (Table 4.1). The replacement of lower water absorptive soil particles by the higher absorptive biochar particles after amendment resulted in higher stored water or WAC in BAS (Brockhoff et al. 2010). The higher WAC of BAS could be beneficial for assisting the growth of vegetation in bioengineered structures or in drought-prone areas (Beck et al. 2011).

4.2.3 Consistency limits

The liquid limit (LL) of the soil was observed to be 49.9 ± 0.3%. The amendment of 5%, 10% and 15% biochar increased the LL in the range of 11% to 58% (Table 4.1). The higher water absorption capacity of BAS compared to bare soil attributed to the increased LL. The intra-pores in biochar increases the porosity and specific surface area (SSA) of the soil after amendment (Downie et al. 2009) that allows a greater amount of water to be entrapped within it, as the case reported by Sridharan et al. (1988) for bare soil. Thus, the larger SSA with surface functional groups attract more water in its pores and hence, the higher LL. The increase in LL of the soil due to biochar amendment was found to be dependent on biochar type. Among the biochar tested, SBB showed the highest increment (58%) while the CB showed the lowest (11%). The difference in porosity among the biochar as evident from the WAC led to the variation in LL among the different BAS. The LL of soil gives an indirect assessment of water storage capacity, shear strength, swelling, shrinkage and compressibility of the soil (Sharma and Bora 2003; Yilmaz 2006). Thus, the increased LL due to the biochar amendment in the present study indicates an improvement in water retention and shear strength that could be beneficial for stability and vegetation growth in bioengineered structures.

The plastic limit (PL) of the soil was observed to be 29.9 ± 1.1%. PL test on only biochar showed that biochar is non-plastic. The amendment of 5%, 10% and 15% different biochar increased (26% - 62%) the PL of the soil (Table 4.1). The amendment of non-plastic and highly porous biochar in the soil replaced the relatively plastic soil particles and absorbed

more water and hence led to the lower plasticity at higher water content or higher PL (Reddy et al. 2015). The increased PL due to biochar amendment indicates reduced cohesive nature of the soil. Considering the effect of biochar type, the highest increment in PL was observed with WHB amendment, whereas the lowest was exhibited by the MB. The plasticity index (PI) presented in Table 4.1 showed a decreasing trend with the amendment of MB and an increasing trend with the amendment of SBB.

The shrinkage limit (SL) of the soil was observed to be 27.3 ± 0.2%. The SL of the soil was found to be increased (30-152%) when different biochar of 5%, 10% and 15% was amended. Further, the amendment of SBB showed the higher increment in the SL compared with the other biochar (Table 4.1). The higher porosity or the increase of intra-porosity in BAS due to internally porous biochar structure stores more water and restricts the volume change (shrinkage) compared with the bare soil that have led to the higher SL in BAS. During test sample preparation, the addition of water in bare soil caused the water to be stored in inter-pores (pores between particles) that have led to the higher volume increase. However, in BAS, a fraction of water was stored within the intra-pores of biochar which led to the lower increase in volume. During drying phase, the evaporation of water from the inter-pores of bare soil led to the higher shrinkage or lower water content (SL); while in BAS, water was likely to be escaped from the intra-pores and caused a lower shrinkage or volume decrease and higher water content (SL). Similarly, the variation in the porosity among the different biochar types led to the different SL after amendment. The trends observed for Atterberg limits in the present study are found to be consistent with the literature (Reddy et al., 2015; Guharay et al., 2019; Joyti bora et al., 2020; Kumar et al., 2020).

4.2.4 Grain size distribution

Fig. 4.1 (a-d) highlights the GSD curves of different biochar and biochar-amended silty sand and pure sand. The SBB showed relatively lesser fine (<0.075 mm) content compared with the other biochar (Fig. 4.1a). The amendment of 5%, 10% and 15% different biochar was observed to shift the GSD curve of both the silty sand and pure sand downward. The increase of larger size particles in the GSD of amended soil compared to bare soil attributed to the downward shift. The silty sand had relatively higher (49%) fine content compared to biochar (13%). The GSD curves of the silty sand and pure sand amended with 5% biochar (MB) of different particles size are presented in Fig. 4.2 (a-b). The GSD curve of the silty sand (Fig. 4.2a) shifted downward when biochar of particles size larger than 0.425 mm was amended.

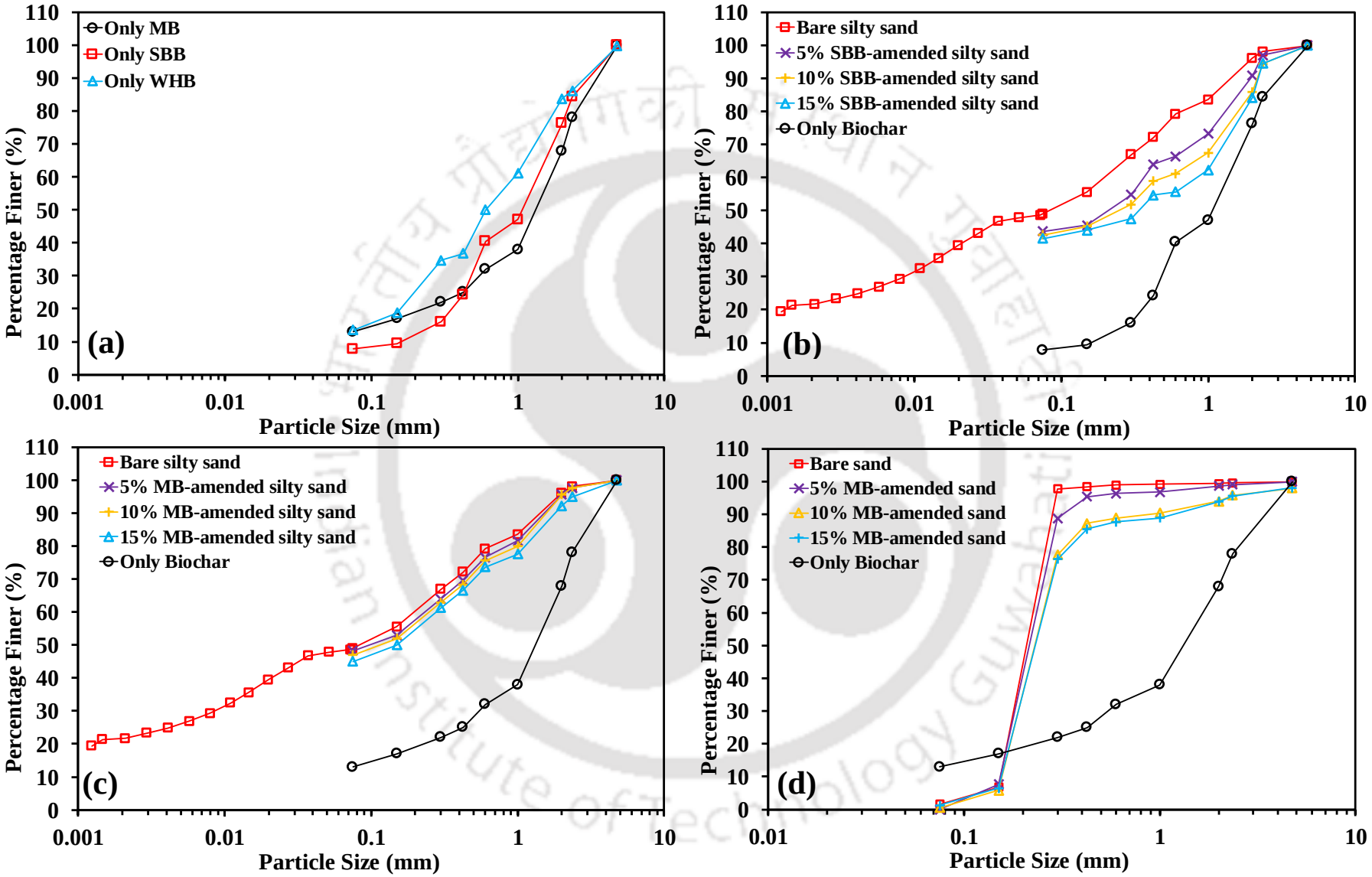

Fig. 4.1 GSD of (a) different biochar, (b) SBB-amended silty sand, (c) MB-amended silty sand and (d) MB-amended sand.

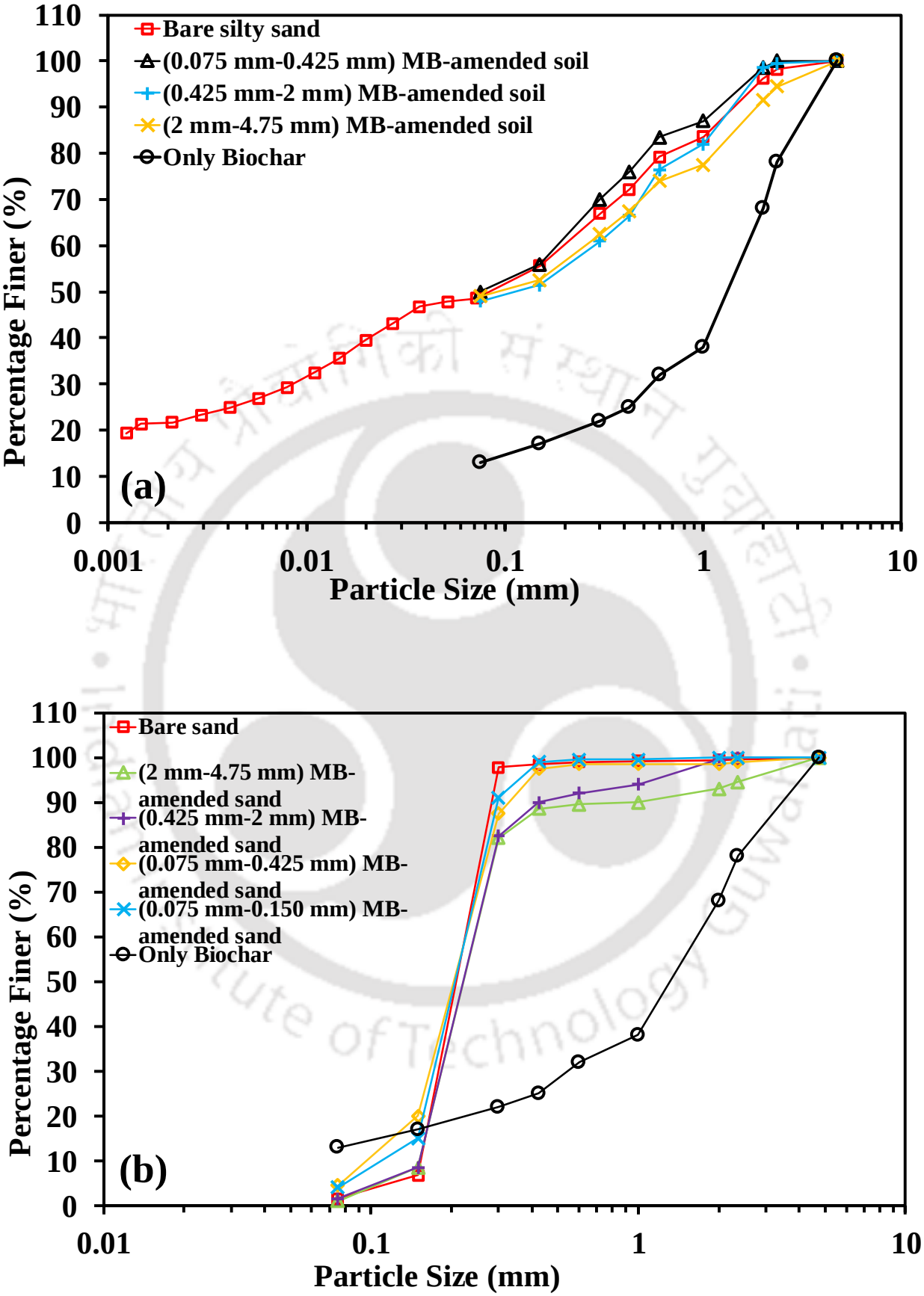

Fig. 4.2 Influence of different particles size of biochar (MB) on the GSD of (a) silty sand (b) pure sand.

Similarly, the amendment of biochar of particles size smaller than 0.425 mm shifted the GSD curve upward. The increase of the number of larger size particles in the GSD of amended soil compared to the bare soil shifted the GSD curve downward while the increase of smaller size particles shifted the GSD curve upward. In Fig. 4.2b for pure sand (particles size mostly around 0.150 mm), the amendment of biochar of particles size larger than 0.425 mm added some larger size particles in the GSD due to which the GSD curve shifted downward. However, the amendment of biochar of particles size smaller than 0.150 mm increased some finer particles in the GSD as the GSD curve shifted upward (near toe of the curve).

4.2.5 Compaction characteristics

The variation of maximum dry density (MDD) and optimum moisture content (OMC) of silty sand, and the maximum and minimum dry density of pure sand after biochar amendment are presented in Fig. 4.3a and Fig. 4.3b respectively. The MDD of the silty sand was observed to be 1.72 Mg/m^3 and the amendment of 5%, 10% and 15% different biochar decreased (5-31%) the MDD. Similarly, the pure sand exhibited the maximum dry density of 1.55 Mg/m^3 and decreased (9-19%) when biochar was amended. The minimum dry density was observed to be 1.38 Mg/m^3 and decreased (8-19%) after biochar amendment (Fig. 4.3b). Among the different biochar types tested, the highest decrease in MDD of silty sand was observed with the amendment of SBB while the lowest was found to be with WHB. A decreasing trend of dry density of clayey soil (Williams et al., 2018), completely decomposed granite (CDG, Ni et al., 2018) and silty sand (Bora et al., 2020) due to biochar amendment was also reported in the literature. The replacement of soil particles of higher specific gravity with the biochar particles of lower specific gravity (Table 4.1) after amendment attributed to the decreased dry density. Further, the higher porosity of BAS compared to bare soil (as evident from the WAC, Table 4.1) due to internally porous biochar reduced the compressibility of the composite during compaction by higher air entrapment in pores and hence, lower dry density or MDD (Reddy et al. 2015). Although, the WHB exhibited the lowest specific gravity compared with the other biochar (Table 4.1), the higher compressibility or lower porosity of WHB amended-soil during compaction led to the lowest decrease in the MDD.

The OMC of the soil as highlighted in Fig. 4.3a was observed to be increased (5% - 106%) after amendment of 5%, 10% and 15% different biochar. A higher increase in the OMC was observed with SBB, whereas the MB showed the lowest increment in OMC. Ni et al. (2018) reported an increased OMC due to biochar amendment. However, researchers (Reddy et al. 2015 and Williams et al. 2018) also reported negligible change in the OMC after biochar amendment, which is generally not expected for highly porous BAS.

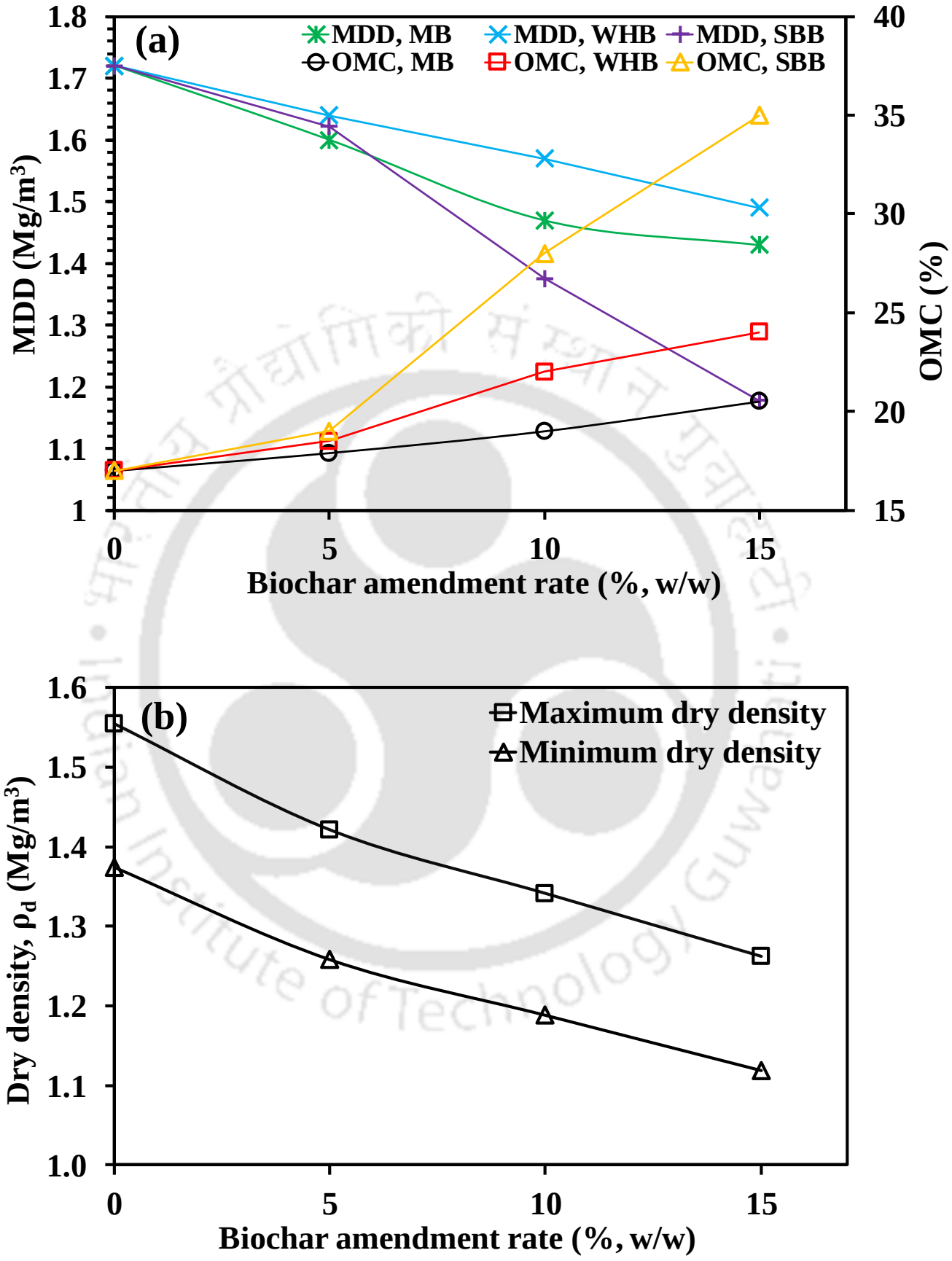

Fig. 4.3 Variation of MDD and OMC with biochar amendment in (a) silty sand (b) pure sand.

The higher water storage or absorption capacity (Table 4.1) of the biochar due to higher porosity and large SSA attributed to the increased OMC of the soil after biochar amendment (Guo et al. 2014). The SBB exhibited the highest WAC among all the tested biochar due to higher porosity and lower specific gravity which led to the highest increment in OMC. The decreased dry density and increased OMC of the soil after biochar amendment could promote the vegetation growth in bioengineered structures by improving root growth, water retention and air circulation or aeration.

4.3 Chemical properties

Table 4.2 highlights the elemental composition and other chemical properties of the biochar. Biochar yield was observed to be higher with WH (33%) compared to the other biochar. The higher yield of WHB could be attributed to the lower cellulose content in WH. Relatively higher carbon content was observed in MB while the WHB showed the lowest. The MB was produced from wood biomass compared with the other biochar made from soft non wood biomass that gave higher carbon content due to higher release of hydroxyl functional groups and the evaporation of volatile matter in the form of condensable and non-condensable gases.

Table 4.2 Elemental composition and other chemical properties of different biochar tested.

	SBB	**WHB**	**CB**
Elemental composition (%)			
Carbon (C)	65	53.4	71.5
Oxygen (O)	30	42.8	-
Hydrogen (H)	3.9	1.99	-
Nitrogen (N)	0.16	1.82	0.19
Molar ratios			
H:C	0.72	0.45	-
C:N	542	34.22	382
O:C	0.35	0.6	-
Yield (%)	25	33	-
Ash content (%)	1	11	1.9
Volatile matter (%)	22.6	30	-
SSA (m^2/g)	41	30.15	21.54

The lowest carbon content in WHB was further confirmed by the higher volatile matter (Table 4.2). The higher volatile matter in WHB was ascribed to incomplete carbonization. The lower H:C ratio in WHB indicates that there is an extremely condensed aromatic structure due depolymerization of the feedstock after pyrolysis. The Higher O/C ratio in

WHB indicates the lower aromaticity or the presence of higher hydrophilic surfaces than the other biochar (Aboulkas et al., 2017). The Ash content (AC) presented in Table 4.2 showed a very high AC in WHB while lowest in SBB. Ash is the non-combustible material, which significantly determines a material's heating value. Additionally, handling and processing of feedstock with high ash content (AC) is a contentious issue because they require more recurrent deposit removal and maintenance on boiler due to slagging (Kim et al., 2015; Nurmi, 2015). The variation in AC among the biochar was attributed to the different alkali and alkali earth metals in feedstock, which help in the formation of ash (Han et al., 2018). Biochar with high AC would be more preferred for bioengineered structures due to added fertilizer effects to the vegetation.

Table 4.3 presents the chemical properties of the soil, biochar and BAS. The bare silty sand and sand exhibited the pH value of 4.31 ± 0.05 and 6.24 ± 0.06 respectively while the biochar showed comparatively higher pH value (7.9-9.6). Among the tested biochar, SBB exhibited the highest pH value, while CB showed the lowest. The observed variation in pH among the biochar was mainly attributed to the differences in feedstock properties.

Table 4.3 Effect of biochar amendment on the chemical properties of the soils.

Properties	Biochar type	Soil type	Biochar amendment rate				
			0% (Bare)	**5%**	**10%**	**15%**	**Only biochar**
pH	MB	Silty sand	4.31±0.05	5.52±0.13	6.6±0.06	7±0.06	7.9±0.3
		Sand	6.24±0.06	7.76±0.14	7.89±0.07	8.01±0.07	
	WHB	Silty sand	4.31±0.05	6.7±0.03	7.2±0.05	7.63±0.03	9±0.32
	SBB	Silty sand	4.31±0.05	6.13±0.04	7.09±0.01	7.4±0.01	9.6±0.01
EC (dSm^{-1})	MB	Silty sand	0.04±0.003	0.12±0.013	0.2±0.02	0.34±0.01	1.5±0.01
		Sand	0.034±0.001	0.14±0.001	0.23±0.01	0.29±0.003	
	WHB	Silty sand	0.04±0.003	0.12±0.01	0.24±0.02	0.37±0.006	1.9±0.02
	SBB	Silty sand	0.04±0.003	0.12±0.008	0.34±0.07	0.46±0.034	3.2±0.028
CEC (meq/100 g)	MB	Silty sand	2.4	3	2.8	3.5	10
	WHB	Silty sand	2.4	9.5	12.8	15	27
	SBB	Silty sand	2.4	12	16	20	44

The amendment of 5%, 10% and 15% biochar increased the pH value of the silty sand (28-77%) and pure sand (24-28%) from acidic to a near neutral state. The increment was

observed to be higher in WHB amended soil, while the lowest was with MB. Thus, the amendment of alkaline biochar in the soil neutralized the acidity of the soil. This could be attributed to the presence of negatively charged surface functional groups on biochar surface that have bind the H^+ ions from the soil sample, thereby reducing the H^+ ion concentration in the sample and hence increased the pH value after amendment (Gul et al., 2015). In literature, the pH of soil was reported to be increased most of the time when biochar was amended (Yaghoubi and Reddy 2011; Reddy et al. 2015). Thus, the trends observed for pH in the present study are consistent with the literature. The increase of soil pH, mostly for acidic soil after biochar amendment is somewhat similar to the liming action of soil and could be beneficial for increasing the microbial activity and growth of vegetation (Hanson and Hanson 1996). Growth and development of vegetation are crucial for bioengineered structures, which prefers soil media to be in neutralize state; thus, BAS could be a good option for bioengineered structures in terms of pH modification.

The electrical conductivity (EC) value of the soil, biochar and BAS is highlighted in Table 4.3. The bare silty sand and pure sand exhibited the EC value of 0.04 ± 0.003 and 0.034 ± 0.001 respectively and amendment of 5%, 10% and 15% biochar increased the EC value of the soil. The higher EC value of the biochar compared to the soil attributed to the increased EC of the soil after biochar amendment. The presence of positive or negatively charged surface functional group that increased charge content in biochar attributed to the higher EC compared with the soil. Simply, the higher EC indicates the presence of higher salt content.

The CEC value obtained for the soil, biochar and BAS are also presented in Table 4.3. The bare soil showed a CEC value of 2.43 meq/100 g while the biochar exhibited CEC value in the range of 10-44 meq/100 g. The highest CEC was observed in SBB (44 meq/100 g) and the lowest was in CB (10.1 meq/100 g). The soil exhibited relatively lower CEC value compared to biochar attributing the lower clay content or lesser negative charge content in the soil. However, the presence of surface functional groups with a net negative charge (especially, O-) in biochar attributed to the higher CEC value of biochar. The amendment of biochar at 5%, 10% and 15% in the soil increased the CEC value, as mentioned in Table 4.3. The higher CEC value of biochar compared with the soil enhanced the soil CEC value after amendment. As CEC specifies the capability of biochar to absorb the nutrients (cation); therefore, amendment of biochar to soil of lower CEC could hold nutrients like K+ and NH4+. In addition, the addition of biochar with higher CEC could prevent the leaching of the

nutrients, thus reducing the groundwater pollution and higher soil fertility and vegetation growth could be observed in bioengineered structures (Bera et al., 2018).

4.4 Microstructural properties

Fig. 4.4 highlights the FESEM images of the soil and biochar.

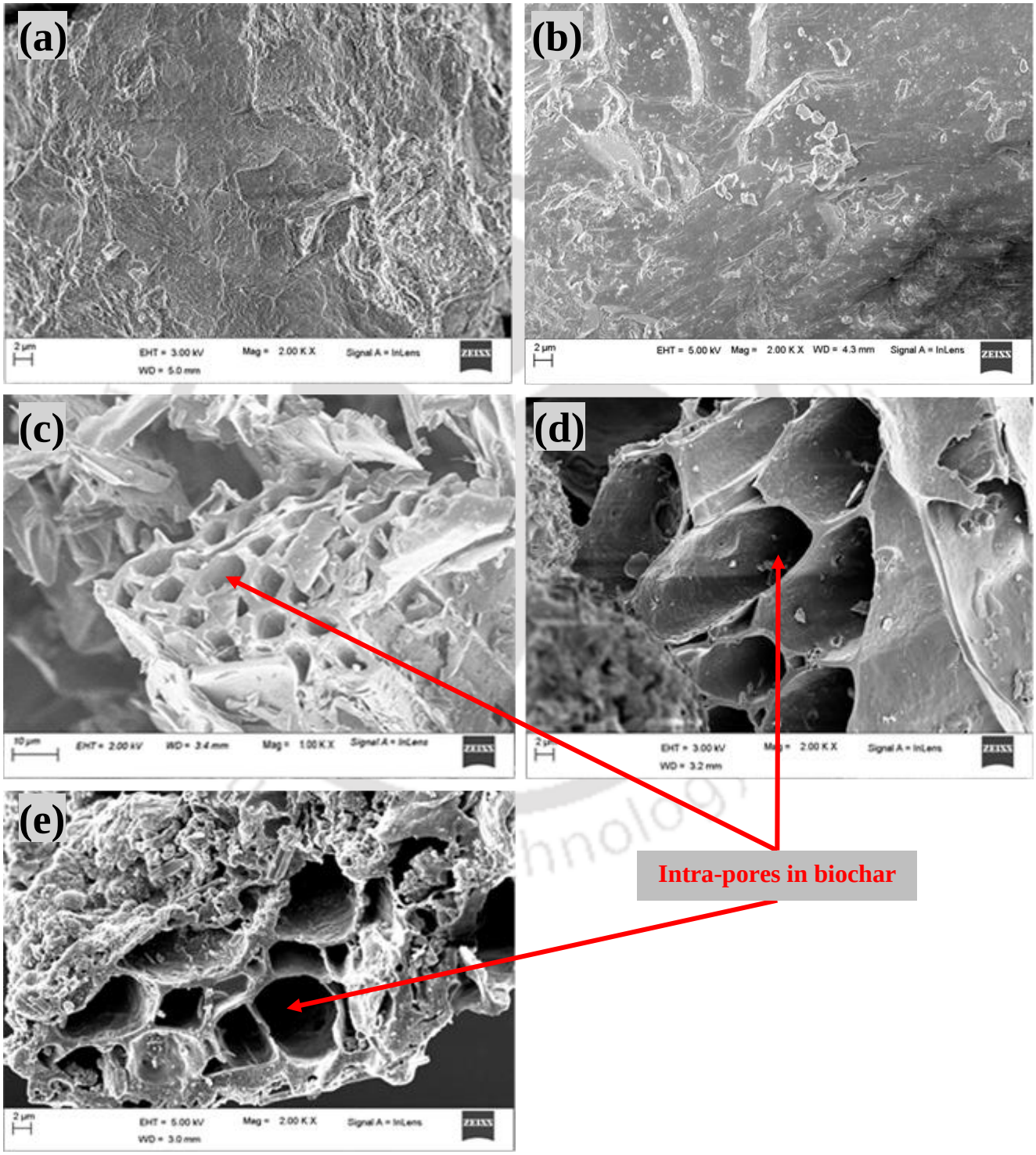

Fig. 4.4 FESEM images of (a) silty sand, (b) pure sand, (c) SBB, (d) WHB and (e) MB.

The internally porous structure or the intra-pores (~2-10 µm) within the skeleton of the biochar could be observed from figure while in the soils, no intra-pores could be seen. The pores were formed due to the degradation of feedstock or release of volatile matter from the feedstock (in the form of H_2O, CH_4 and CO) during pyrolysis (Yang et al., 2018). The SBB showed relatively smaller and thick-walled pores compared to the other biochar which led to the higher surface area. The variation in the morphological structures of the biochar was attributed to the different degree of mass conversion and de-volatilization process of organic materials in the feedstock. The diverse structure and distribution of pores detected in different biochar affirmed the heterogeneous nature of the biomass. The SSA of the silty sand and pure sand was found to be 14 and 6.8 m^2/g. The SSA of the biochar presented in Table 4.3 was observed to be higher compared to the soils. The intra-pores in biochar divides the skeleton into multiple channels like honeycomb due to which higher SSA was observed. The SBB showed the highest SSA among the biochar owing to the large number of smaller size pores in SBB as seen from the FESEM images. The SSA is a crucial indicator of the adsorption (water and nutrient) ability of the biochar thus it is essential to understand since it would determine their applications in vegetated soil based on the water use efficiency and nutrient uptake. Further, the SSA determines the ability of biochar in removing greenhouse gases (GHGs), organic pollutant and heavy metal ions from soil.

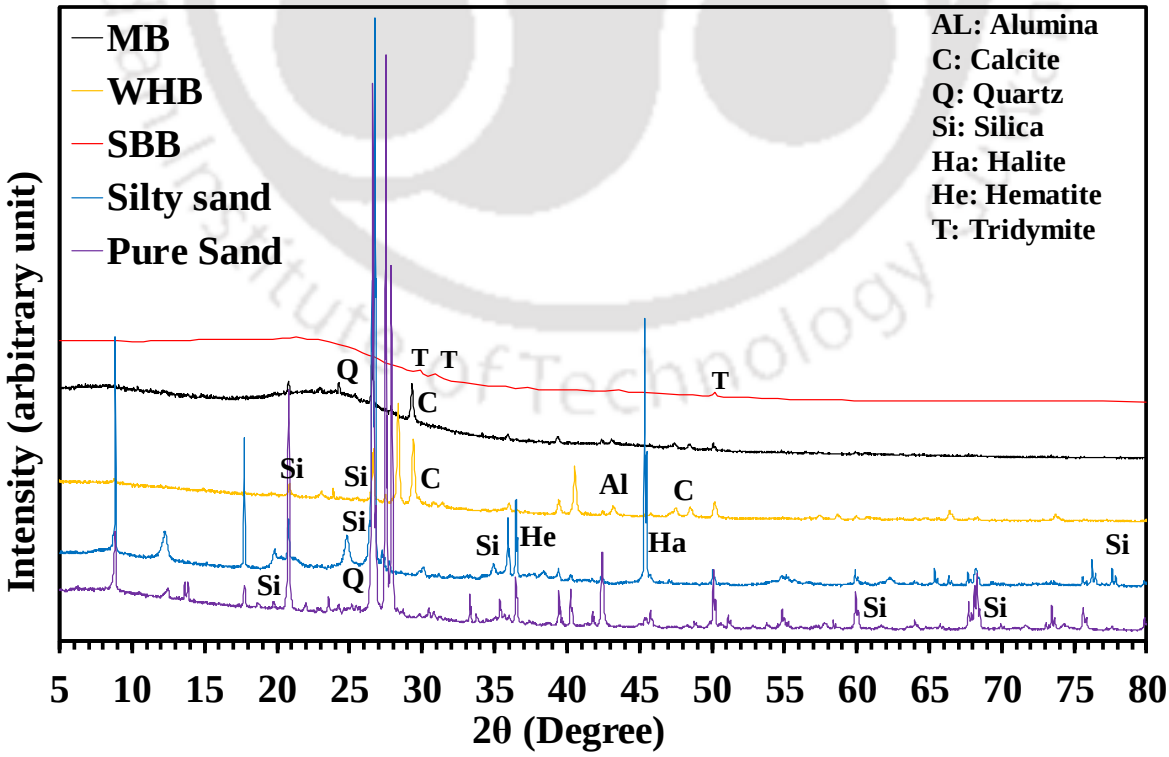

Fig. 4.5 XRD pattern of the soils and biochar.

Fig 4.5 highlights the XRD patterns of the soils and biochar. The peaks are marked and highlighted in the figure. The XRD patterns of the soils confirmed the crystalline structure relative to the biochar as large number of peaks were observed for the soils. Similarly, the XRD patterns of the SBB indicated the entirely amorphous structure based on the fewer peaks recorded while the WHB were relatively crystalline (Zeidabadi et al., 2018). The analysis of the XRD patterns confirmed the presence of mainly calcite mineral in all the biochar, except SBB where tridymite (SiO_2) was the dominant mineral. The carbonation of oxides of calcium during pyrolysis leaves the calcite mineral in biochar (Song et al., 2019). The soils i.e., silty sand and the pure sand consist of silica and quartz as the major mineral.

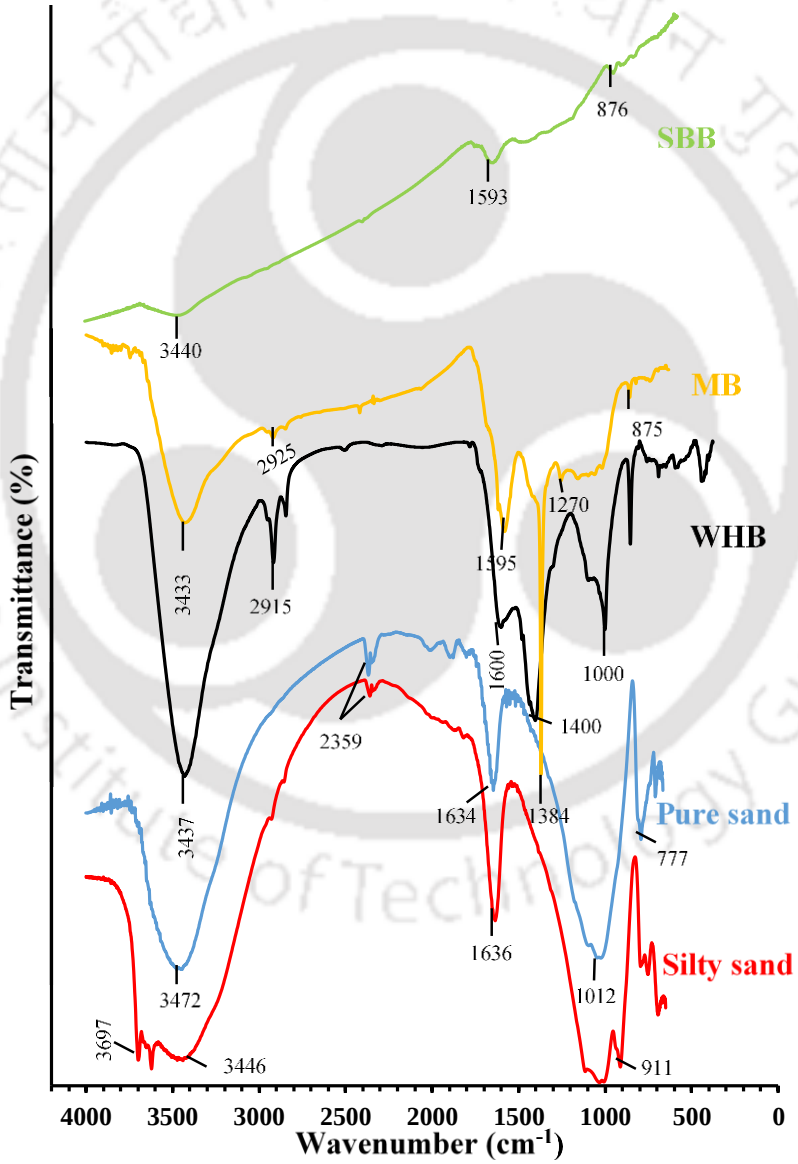

Fig. 4.6 FTIR spectra of the soils and biochar.

The FTIR peaks observed in the soils and biochar are marked and highlighted in Fig. 4.6. The broad peaks at web number 3433, 3472, 3440, 3437 cm^{-1} in biochar and the soils are due to

the intermolecular or intramolecular hydroxyl (OH) stretching. The hydroxyl (OH) group is responsible for the attraction of water molecules by the formation of hydrogen bonding i.e., hydrophilicity (Van der Spoel et al., 2006). The peaks at ~2900 cm^{-1} in the biochar are due to the aliphatic C–H bond of alkanes (Das and Sarmah, 2015). The presence of aliphatic functional group is often responsible for the biochar hydrophobicity (Gray et al., 2014). However, the hydrophobicity due to aliphatic functional group is not intrinsic or permanent rather vanishes with the flooding or wetting of water (Das and Sarmah., 2015). Peaks at 2359 cm^{-1} in the soils are due to C=O (symmetric) group, while peaks at ~1600 cm^{-1} represents the C=O stretching (Guharay et al., 2019). The C=O primarily represents ionisable carboxyl groups and associated with hydrophilicity (Gray et al., 2014). The peaks at ~1000 cm^{-1} confirms the C-O-C stretch associated with cellulose, hemicelluloses and lignin in the biochar (Masto et al., 2013). Peaks at ~875 cm^{-1} are due to the asymmetric bending of calcite groups (Angalaeeswari and Kamaludeen, 2017). Peaks at 1012, 911 and 777 cm^{-1} are confirming the Si–O (quartz) stretching and Si–O bending in soils (Gnanasaravanan and Rajkumar, 2013).

4.5 Summary and conclusions

The physicochemical and microstructural properties of the soil, biochar and BAS were evaluated and presented. The microstructural analysis revealed the distinct material characteristics or properties of the biochar compared to the soil. The FESEM analysis showed the porous structure of the biochar while the XRD and FTIR analysis confirmed the different material properties. Further, variation in the material properties was observed with the different feedstock type. The amendment of the biochar altered the physicochemical properties of the soils. The consistency limits, water absorption capacity (WAC), pH, electrical conductivity (EC), cation exchange capacity (CEC) of the soils increased in the range of 30-1050% while the specific gravity and dry density decreased by 9-31% after biochar amendment. Further, the effect of biochar on the soil physicochemical properties was found to be biochar or feedstock type dependent. The distinct material and structural properties of the biochar contributed to the altered physicochemical properties of the soils after biochar amendment. The physicochemical properties of soil are interrelated to the hydro-mechanical properties and have strong influence on the microbial diversity, and growth and development of vegetation in soil. Therefore, the altered physicochemical properties, especially increased WAC, CEC, pH and decreased dry density could be beneficial for the growth and development of vegetation in bioengineered structures.

CHAPTER 5
SATURATED HYDRAULIC CONDUCTIVITY AND INFILTRATION RATE OF BAS

5.1 Introduction

The saturated hydraulic conductivity (K_{sat}) and infiltration rate (I_r) are the crucial soil properties that defines the movement of water through soil pores and related to the stability of the soil structures or bioengineered structures. The ingress and seepage of water through landfill system, dam and other bioengineered slopes controlled by the K_{sat} and I_r of the soil in these structures. In literature, the K_{sat} and I_r of soil were often reported to be increased after biochar amendment. While literature also reported the decrease or no change of the K_{sat} and I_r of soil after biochar amendment. The different soil type exhibits distinct K_{sat} and I_r. The difference in particles size, production temperature and feedstock type of biochar could results in variable impact on soil after amendment. Therefore, the evaluation of soil K_{sat} and I_r after biochar amendment by considering different influencing factors is necessary for application in bioengineered structures. The influence of different biochar type and amendment rates on K_{sat} and I_r were evaluated for silty sand and pure sand and the results obtained are presented and discussed in this chapter. Further, the effects of biochar particles size on the K_{sat} of soils were evaluated. The porosity of the BAS was evaluated to understand the change in the K_{sat} and I_r after biochar amendment. Statistical analysis was carried out to see the significance level of the data.

5.2 Influence of soil type, biochar type and amendment rate on K_{sat}

Fig. 5.1 (a-b) presents the K_{sat} of the silty sand and the pure sand amended with 5%, 10% and 15% WHB, MB and SBB biochar under different (0.9MDD and MDD) compaction state. The bare silty sand exhibited a K_{sat} value of 8.2×10^{-7} (m/s) at 0.9MDD and 3.7×10^{-8} (m/s) at MDD. The amendment of 5 to 15% biochar initially decreased ($P>0.05$) the K_{sat} of the silty sand at 5% biochar, being lower than the bare silty sand. However, the further increase of biochar amendment rate from 5% to 15% increased ($P>0.05$) the K_{sat}, being higher than the bare silty sand (Fig 5.1a). Similarly, as presented in Fig. 5.1b, the bare sand exhibited a K_{sat} value of 3.3×10^{-4} (m/s) at 0.9MDD and 2.1×10^{-4} (m/s) at MDD. The amendment of 5 to 15% biochar decreased ($P<0.05$) the K_{sat} of the sand i.e., a lower K_{sat} in all biochar-amended sand compared to the bare sand could be observed.

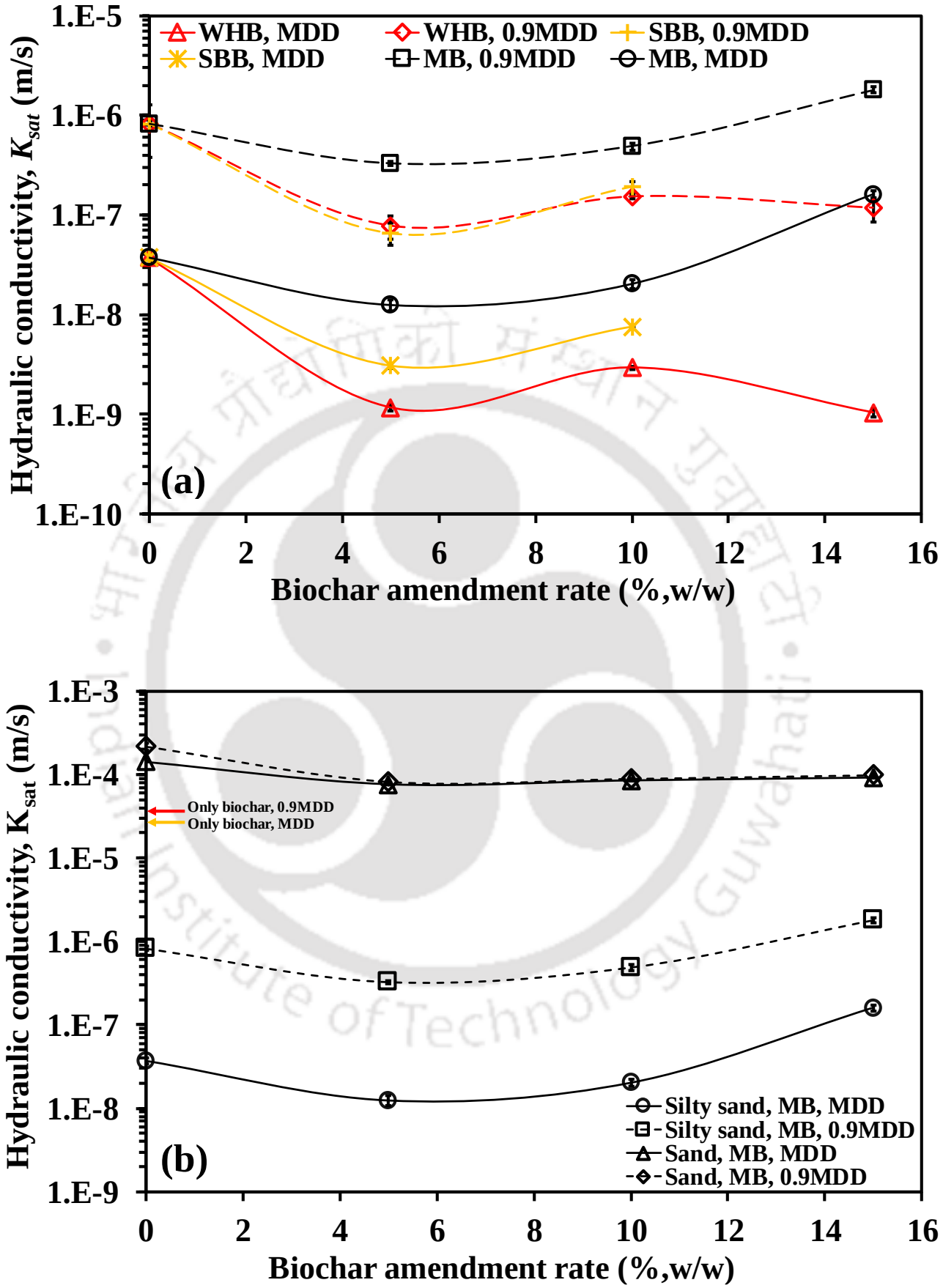

Fig. 5.1 Variation of K_{sat} with (a) biochar type and amendment rate and (b) soil type.

A slight increase (P>0.05) in the K_{sat} when biochar amendment rate was raised from 5% to 15% could be seen in Fig. 5.1b. The MB-amended soil exhibited the highest K_{sat} while the WHB-amended soil showed the lowest among the biochar tested. The decrease of K_{sat} in both the soils after biochar amendment was attributed to the lower porosity of the BAS compared to the bare soil upon wetting or flowing of water, as presented in Table 5.1.

Table 5.1 Porosity of the silty sand amended with MB

	Compaction state	Biochar amendment rate			
Porosity (%)		**Bare**	**5%**	**10%**	**15%**
	0.9MDD	33.1	29.8	34.6	37.2
	MDD	30.5	28.4	30	35.3

A similar trend like K_{sat}, initially decreased (P<0.05) porosity of the silty sand after biochar amendment thereafter increased (P<0.05) with further increase in biochar amendment rate could be observed (Table 5.1). Therefore, it is clear from Fig 5.1 and Table 5.1 that the change of soil K_{sat} after biochar amendment was mainly due to the alteration of porosity or pore size distribution of the soil. The porosity of the biochar-amended sand was not determined due to experimental limitation of being non self-standing behaviour of sand. However, it was bound to decrease upon wetting due to particular rearrangement, as the samples of sand were prepared in the air-dry state. Even though the porosity of the compacted BAS was higher than the bare soil due to decreased dry density (Fig. 4.3a-b), the flow of water during the test reduced the porosity possibly through clogging of the pore spaces (especially inter-pores) by the smaller soil or biochar particles and hence reduced K_{sat} similar to the case reported for biochar-amended sand in Novak et al. (2016). The marginal increase of K_{sat} at biochar 5% to 15% was attributed to the increased porosity (Table 5.1) possibly due to the biochar intra-pores or increased number of larger size inter-pores between soil or biochar particles. As observed from Fig. 4.1, the increase of biochar amendment rate from 5% to 15% shifted the GSD curve of the soils below, indicating an increase of larger size particles in the BAS compared to the bare soil that has the possibility of forming larger size inter-pores and hence, the higher porosity. The SBB and WHB made up of softwood compared to MB of hardwood that have crushed into smaller particles during compaction and hence reduced the porosity. Further, the smaller size intra-pores in SBB and WHB compared to MB (Fig. 4.4) made the flow path more tortuous and hence the lower K_{sat} in SBB and WHB-amended soil relative to MB-amended soil.

Considering the soil type, differences in K_{sat} of the silty sand and pure sand after biochar amendment could be observed (Fig. 5.1b) due to the variation in the GSD or indirectly the pore size distribution (PSD) of the silty sand and pure sand after biochar amendment (Fig. 4.1). The bare silty sand presence particles of all sizes (clay, silt and sand), whereas the bare sand exhibited particles of a same size within 150-300 µm (poorly graded). Therefore, the amendment of biochar in the pure sand added some missing particles in the GSD or led to the uniform GSD (Fig. 4.1d) which in turn decreased the porosity and hence, the K_{sat} compared to the bare sand. While in silty sand, the amendment of biochar added particles of the same size as already present in the GSD of bare silty sand thus led to the increased porosity and hence the K_{sat} compared to the bare silty sand. Wong et al. (2018) reported lower porosity and larger pore size in biochar-amended kaolin clay obtained by mercury intrusion porosimetry test. The amendment of biochar of larger particles size (<425 µm) in smaller size (< 2 µm) clay increased the pore size from mesopores (0.01-0.1 µm) to macropores (0.1-4 µm) while the entrapment of smaller clay particles in the biochar pores reduced the porosity.

Considering the compaction density, the increase of biochar amendment rate showed the similar trend for both the soil types. The influence of compaction density on the K_{sat} of BAS was found to be significant ($P<0.05$) and higher in silty sand while in sand, it is observed to be negligible or not significant ($P>0.05$) (Fig. 5.1a-b). The increase of compaction density from 0.9MDD to MDD reduced the K_{sat} in silty sand due to the decreased porosity with increased compaction density (Table 5.1). While in biochar-amended sand, the increase of compaction density showed no comparable difference in K_{sat}, possibly due to the nearly same porosity of the samples at 0.9MDD and MDD after wetting by water during the test as the samples for sand were prepared in air-dry state. The wetting of the dry packed sand samples caused the sand particles rearrangement by the reduction of frictional resistance that have led to the repacking and reformation of the pores in sand samples. The degree of particular rearrangement of sandy soil varies with the magnitude of packing density. In literature, Lei and Zhang. (2013) reported a trend of increased K_{sat} of biochar-amended silty sand while Igalavithana et al. (2017) reported the decreased K_{sat} of the same type of soil. In addition, studies by Uzoma et al. (2011), Barnes et al. (2014), Githinji (2014) and Lim et al. (2016) had also reported the decreased trend of K_{sat} in sandy soil after biochar amendment. Thus, the trends observed for K_{sat} in the present study are consistent with the literature. The decreased K_{sat} of the soils after biochar amendment could improve water retention or available water in soil pores which in turn could assist the growth of vegetation in bioengineered structures.

5.3 Effect of biochar particles size on K_{sat}

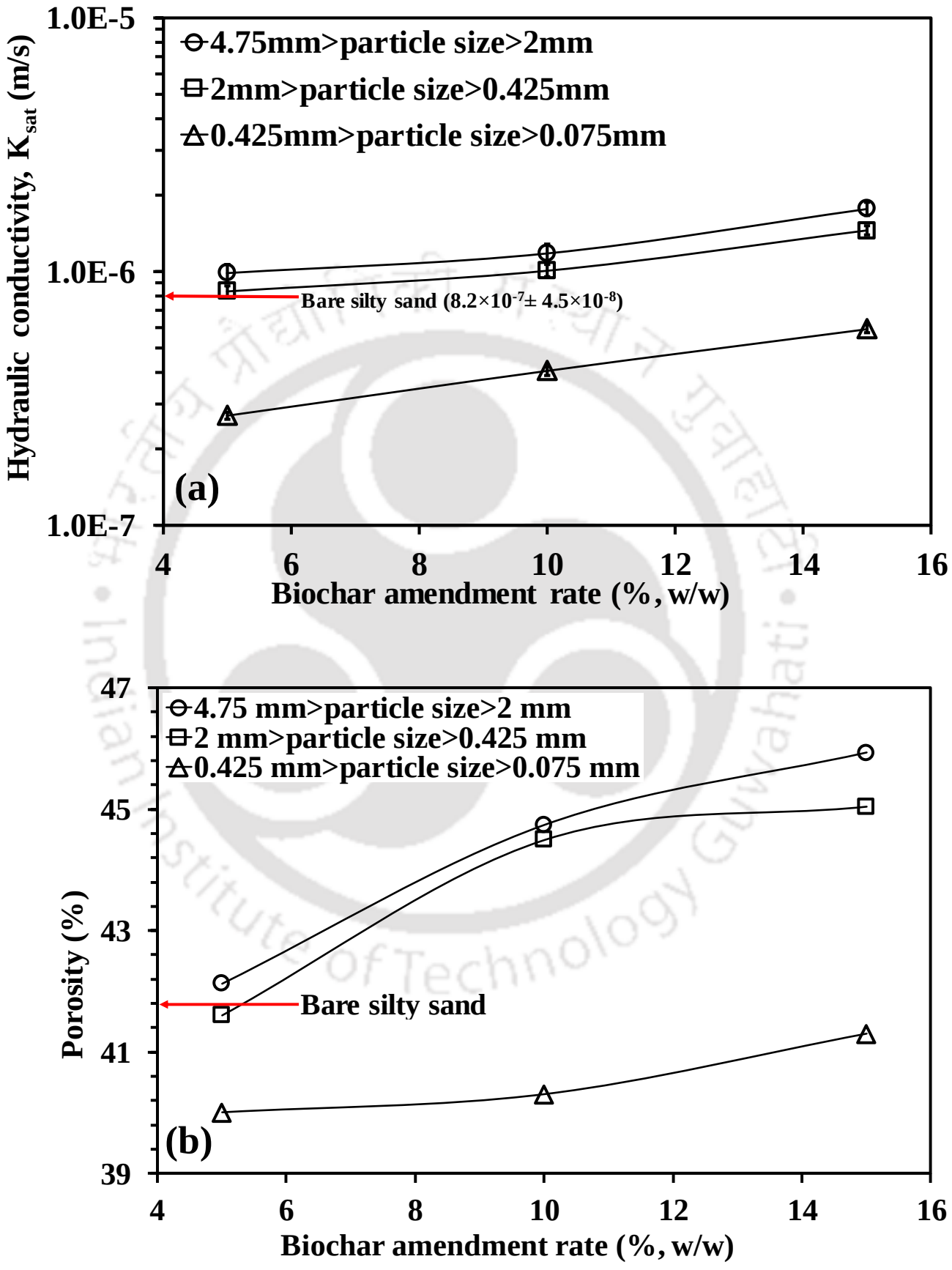

Fig. 5.2 Influence of biochar (MB) particles size on (a) K_{sat} and (b) porosity of silty sand.

Figure 5.2(a-b) show the K_{sat} and porosity of the silty sand amended with 5%, 10% and 15% fine (0.075-0.425 mm), medium (0.425-2 mm) and large (2-4.75 mm) biochar or MB. The bare silty sand exhibited the K_{sat} value of 8.2×10^{-7} m/s and it increased to 1.4×10^{-6} m/s and 1.8×10^{-6} m/s in medium and large biochar and decreased to 5.9×10^{-7} m/s in fine BAS when biochar amendment rate was increased to 15%. Considering the biochar particles size, the amendment of biochar with larger size particles of 0.425-2 mm and 2-4.75 mm showed a higher K_{sat} ($P<0.05$) compared to the K_{sat} of the bare soil. However, the change was observed to be negligible in the case of 5% biochar amendment rate. This higher K_{sat} was attributed to the increased porosity or pore volume of the BAS with larger biochar particles, which is evident from the porosity results presented in Fig. 5.2b. The bare silty sand exhibited a porosity of 41.8%, evaluated from the initial sample compaction dry density and specific gravity using the fundamental correlation among the dry density, specific gravity and porosity. The porosity increased to 45% and 45.9% in 15% BAS with larger biochar particles. The bare soil consists of 6% particles within the size range of 2-4.75 mm, 20% within 0.425-2 mm and remaining 74% below these size ranges (i.e., <0.425 mm, Fig. 4.1). Therefore, the amendment of medium (0.425-2 mm) and large (2-4.75 mm) biochar increased the numbers of larger size particles (>0.425 mm) in the GSD as seen from Fig. 4.1(b-c) that have possibly increased the porosity by forming larger size inter-pores between soil and biochar particles. Further, the intra-pores (mostly ~0.010 mm, Fig. 4.4) in biochar have also been contributed to the increased porosity; however, the soil consists of 20% fine content (clay, <0.002 mm) that could settle inside the biochar intra-pores as observed for pure Kaolin clay in Wong et al. (2018). The tendency of settlement is expected to be negligible in the present study, as the clay content was far lower than the content in pure clay (100%). The change in the porosity was observed to be more prominent when biochar amendment rate raised from 5% to 15% (Fig. 5.2b) and resulted in higher K_{sat}.

The amendment of the fine (0.075-0.425 mm) biochar decreased the K_{sat} ($P<0.05$) compared to the bare soil. The lowest K_{sat} was observed with 5% biochar and increased with an increase in amendment rate from 5% to 15%. The decreased porosity of the soil after amendment of fine (0.075-0.425 mm) biochar as shown in Fig. 5.2b attributed to the lower K_{sat} in fine BAS. The decreased porosity could be due to the formation of smaller size inter-pores compared to the bare soil or clogging of inter-pores that have made the flow path more tortuous and hence reduced the flow velocity or the K_{sat}. However, the impact of clogging pores was found to be lowered after biochar amendment rate raised from 5% to 15%. Therefore, the amendment of biochar in soil could have the possibilities of either increase or decrease the K_{sat} depending on the biochar particles size.

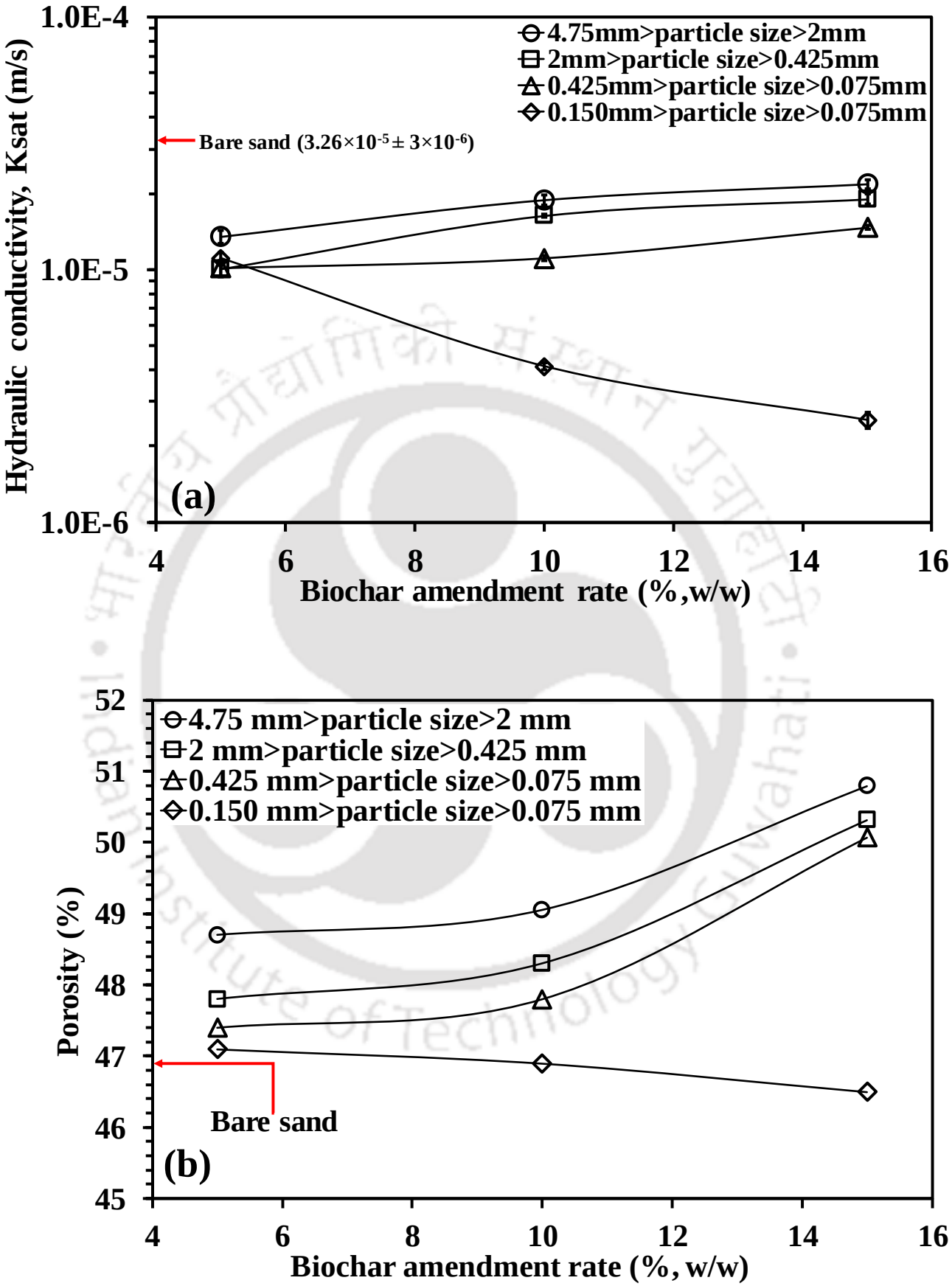

Fig. 5.3 Influence of biochar (MB) particles size on (a) K_{sat} and (b) porosity of sand.

The variation of the K_{sat} and porosity of the bare sand and sand amended with 5%, 10% and 15% biochar of particles size 0.075-0.15 mm, 0.075-0.425 mm, 0.425-2 mm and 2-4.75 mm are depicted in Fig. 5.3a-b. The bare sand exhibited the K_{sat} of 3.3×10^{-5} m/s and it decreased after biochar of irrespective of particles size was amended. Lowest K_{sat} of 2.5×10^{-6} m/s ($P<0.05$) was found in 15% smallest particles size (0.075- 0.150 mm) biochar-amended sand. The lower K_{sat} in biochar-amended sand compared to the bare sand could be attributed to the decreased porosity of the biochar-amended sand upon water wetting, since the samples of biochar-amended sand were compacted in air-dry state. The bare sand exhibited the porosity of 47.2%, computed from the compaction density and it increased to 50% and 50.8% in 15% biochar-amended sand with biochar of larger particles size i.e., 0.425-2 mm and 2-4.75 mm (Fig. 5.3b). Even though the porosity in compacted biochar-amended sand samples was higher (Fig. 5.3b), the flow of water during the test possibly reduced the pores size and hence the porosity in biochar-amended sand by filling or clogging the pore spaces thereby lower K_{sat} compared to the bare sand. The bare sand mainly (97%) consists of particles size within 0.150-0.425 mm (Fig. 4.1d) and the addition of larger particles size biochar (i.e., >0.150 mm) reduced the pore spaces or porosity possibly by filling the inter-pores between larger biochar particles with the smaller sand particles. While, in sand amended with smaller particles size (<0.150 mm) biochar, the decreased porosity could be due to the filling of inter-pores between sand particles by the smaller biochar particles. The decreased porosity and tortuous flow path of the sand after amendment of biochar of different particles size hindered the water flow path and hence lower K_{sat} compared to the bare sand.

Considering the particles size of the biochar, the influence of biochar particles size on K_{sat} was found to be minimum at 5% biochar amendment; however, significant difference in K_{sat} was observed when amendment rate increased from 10% to 15%. The amendment of biochar of particles size larger than 0.150 mm increased the K_{sat} ($P<0.05$) and particles size smaller than 0.150 mm decreased the K_{sat} ($P<0.05$) of the sand. The negligible effect of biochar particles size at 5% biochar content could be attributed to the low amendment rate. The increased K_{sat} at 10% and 15% larger particles size (>0.150 mm) biochar-amended sand was attributed to the increased porosity of the same compared with the porosity of 5% biochar-amended sand as shown in Fig. 5.3b. Similarly, the decreased K_{sat} with smaller particles size (<0.150 mm) biochar was attributed to the decreased porosity at higher amendment rate (Fig. 5.3b). At higher amendment rate i.e., 10% and 15%, the larger particles size (>0.150 mm) biochar caused the formation of larger size inter-pores compared to the

inter-pores in 5% biochar-amended sand and hence higher porosity. However, smaller particles size (<0.150 mm) biochar caused the filling or blocking of the inter-pores at a higher extend compared to that of 5% amendment rate that have led to the lower porosity. Similarly, in literature, Lim and Spokas (2018) and de Jesus Duarte et al. (2019) reported the variable responses of biochar on the K_{sat} of soil due to the different particles size of biochar where amendment of biochar particles size smaller than the soil particles reduced the K_{sat}. Trifunovic et al. (2018) reported of decreased K_{sat} of sand after amendment of fine biochar and increased K_{sat} after amendment of coarse biochar. Thus, the trends observed in the present study are consistent with the literature.

5.4 Influence of soil type, biochar type and amendment rate on I_r

Fig. 5.4 (a-b) highlights the variation of infiltration rate (I_r) with biochar type, amendment rate and soil type at 0.9MDD and MDD compaction states. The bare silty sand exhibited an infiltration rate of 6.1×10^{-8} (m/s) at 0.9MDD and 4×10^{-8} (m/s) at MDD. Similarly, the bare sand (Fig. 5.4b) showed an infiltration rate of 1.2×10^{-6} (m/s) at 0.9MDD and 8.15×10^{-7} (m/s) at MDD. It could be observed that the amendment of 5%, 10% and 15% biochar decreased ($P<0.05$) the I_r in both the soils under all compaction states. The increase of biochar amendment rate reduced the dry density (Fig. 4.3) and increased the porosity (Table 5.1) of the soil that should have increased the I_r. However, the amendment of the biochar reduced the pores size and made the pore size network complex due to the intra-pores which in turn led to the more tortuous flow path or increased the tortuosity and hence the lower I_r. Among the biochar tested, the WHB or SBB exhibited smaller particles size due to crushing (softwood) during compaction and smaller intra-pores (Fig. 4.4) which blocked the pores and increased the tortuosity higher extend and hence the lowest I_r. The hydrophobic nature of biochar could also reduce the soil I_r after amendment by hindering the flow of water in soil (Ibrahim et al 2013; Githinji, 2014). However, the biochar tested in the present study was found to be hydrophilic in nature due to presence of water absorptive functional groups (Fig. 4.6).

The different soil type tested, the amendment of biochar showed similar trend of decreased I_r in all the soil type. However, a higher decrease or steep change with increase in amendment rate could be observed in silty sand relative to the pure sand. Considering the compaction density, a similar trend of decreased ($P<0.05$) I_r with an increase in density from 0.9MDD to MDD could be observed in both the soils and with all the biochar types.

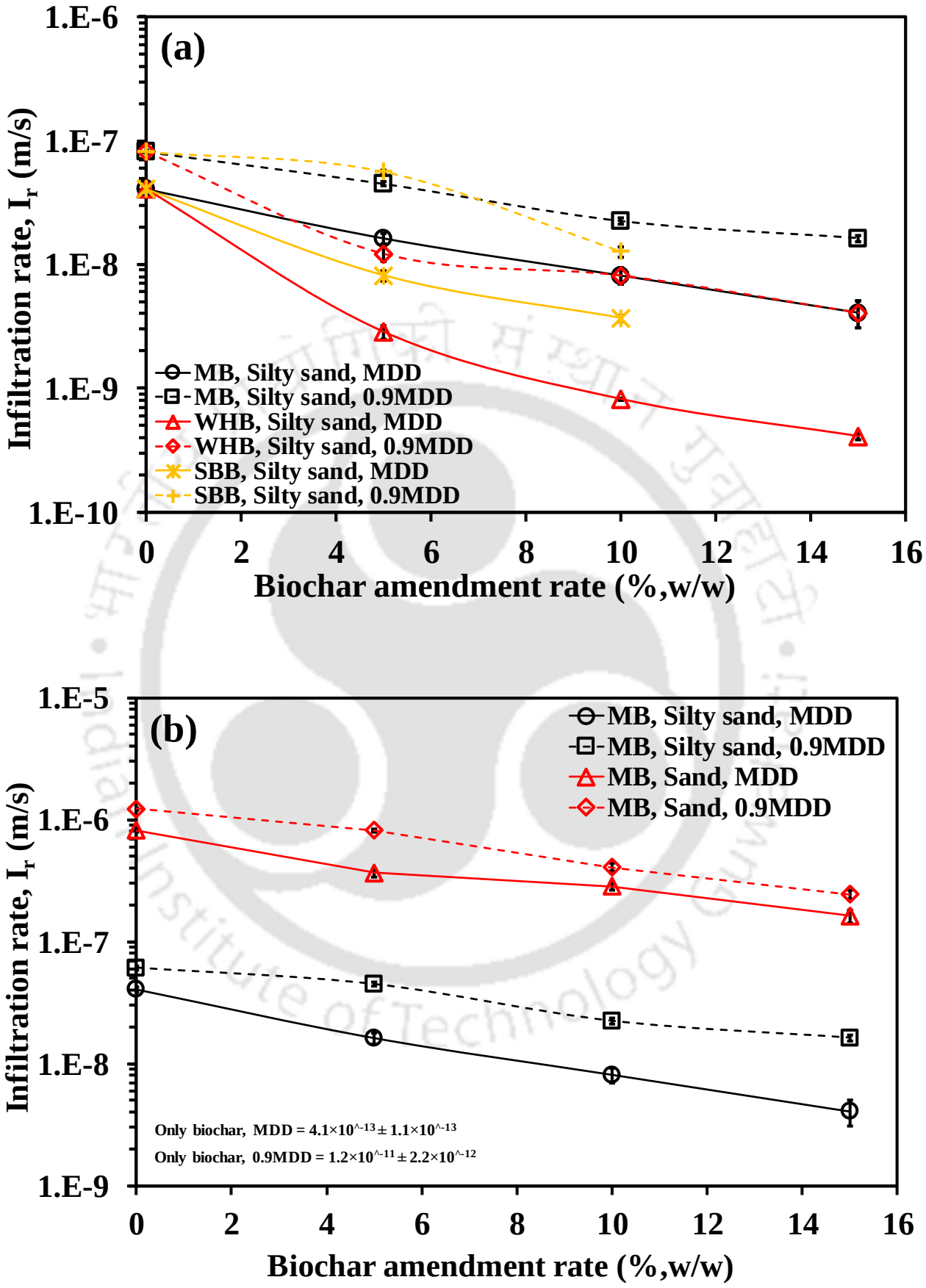

Fig. 5.4 Influence of (a) biochar type and (b) soil type on I_r.

This was mainly due to the decreased pore spaces or porosity of the soil with increase in compaction density which have blocked or retard the water entering in soil and hence lowered the I_r. Further, the influence of compaction density on I_r was found to be more prominent in silty sand and with WHB compared to the pure sand (Fig. 5.4a-b). The silty sand of more sensitive to compaction density as it presents particles of diverse size range relative to sand of majorly single particles size. With increase in compaction density, the smaller size particles of WHB after compaction affects the pores system higher extend and hence the larger difference in I_r between the WHB-amended silty sand compacted at 0.9MDD and MDD. Similarly, the decrease of I_r in sand amended with different types of biochar was also reported by the past researchers (Githinji, 2014, Ibrahim et al., 2013, Gopal et al., 2019). Therefore, the trends are consistent with the literature. The decreased infiltration rate in sand after biochar amendment could be useful of reduced leachate formation and excess pore water pressure in bioengineered structures due to limited ingress of water.

5.5 Variation of I_r with suction in BAS

The variation of infiltration rate (I_r) with suction for bare and 5% and 10% (w/w) WHB and MB-amended soil are presented in Fig. 5.5. The I_r obtained at different suction for bare and different BAS was fitted to an exponential equation and the R^2 value was found to be 0.8 for bare soil and 0.64 - 0.73 for other amended soil.

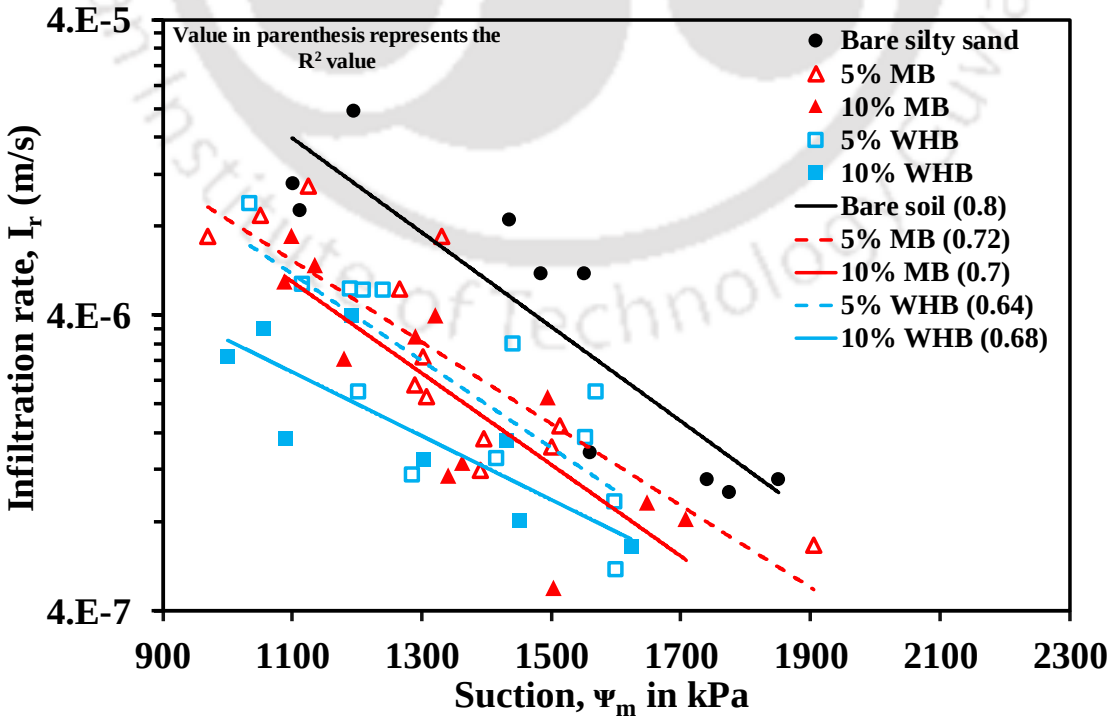

Fig. 5.5 Variation of infiltration rate with suction in different BAS.

It is clear from the Fig. 5.5 that the I_r of the bare and amended soil decreased with the progressive increase of suction. Although, the I_r of soil could increase with increase in suction due to higher water affinity or adsorption tendency at higher suction, the I_r was observed to be decreased. This could be due to the blockage of pores by the entrapped air at higher suction which have resisted the flow of water into the pores, thereby, reduced the I_r (Fredlund et al. 2012). A lower I_r in BAS compared to the bare soil similar to the reported in the previous section could be observed, and the increase of biochar amendment rate from 5% to 10% further decreased the I_r. The decrease of inter-pore size or the blockage of inter-pores by the settlement of smaller biochar or soil particles that have made the flow path tortuous attributed to the decreased I_r in BAS. Among the biochar tested, WHB amended soil showed lower I_r compared to the MB amended soil. The smaller particles of WHB compared to the MB (Fig 4.1a) decreased or blocked the inter-pores to a higher extent in WHB-amended soil which in turn led to the lowest I_r. Thus, the trends are consistent with that presented in the previous section and the literature (Ibrahim et al. 2013; Novak et al. 2016).

5.6 Summary and conclusions

The saturated hydraulic conductivity (K_{sat}) and infiltration rate (I_r) of different soils amended with different types biochar are presented. The K_{sat} of the soils i.e., silty sand and pure sand found to be decreased by around one order of magnitude after amendment of biochar of different types. The biochar amendment rates showed strong influence as relatively lower amendment rate (5%) exhibited lesser impact on K_{sat} while the higher amendment rates (>5%) showed significant changes. The different biochar types exhibited variation in K_{sat} as the WHB-amended soil showed the lowest K_{sat} among the biochar types tested. The biochar particles size showed strong influence on the K_{sat} as the amendment of larger size particles increased the K_{sat} while smaller size particles decreased the K_{sat}. The I_r was observed to be decreased by around two order of magnitude after amendment of biochar and similar to the K_{sat}, the I_r also influenced by the different biochar types, amendment rates and the soil types. The I_r at different suction in BAS was evaluated and found to be decreased with the increase of biochar amendment rates. The lower K_{sat} and I_r in BAS relative to bare soil could be beneficial of reduced leachate and excess pore water pressure generation due to lower ingress of water, and could store water due to low hydraulic conductivity (K_{sat}) which in turn could assist the growth of vegetation in bioengineered structures, especially landfill cover.

CHAPTER 6
SWRC AND UNSATURATED HYDRAULIC CONDUCTIVITY OF BAS

6.1 Introduction

The soil water retention characteristics (SWRC) has importance equally in geotechnical, geo-environmental and agricultural engineering. The estimation of various soil parameters involving unsaturated soil behavior needs SWRC as input (Marshall 1958; Mualem 1986; Fredlund et al., 2012). Further, the SWRC gives a useful information on water retention in root zone, which is highly important for the growth of vegetation in bioengineered structures and agricultural soil (Clarke and Townley-Smith 1986). The unsaturated hydraulic conductivity (K_{unsat}) of soil is a vital hydraulic property that governs the transient seepage and infiltration rate of soil, root water uptake and evaporation or evapotranspiration from soil (Fredlund and Rahardjo 1993; Ranjan and Rao 2007; Gadi et al. 2016). The amendment of biochar is reported to influence these soil properties i.e., the SWRC and K_{unsat}. Further, depending on the soil type, biochar type and amendment rates, the amendment of biochar may not influence the SWRC and K_{unsat}. Therefore, the investigation of SWRC and K_{unsat} of soil amended with biochar of different types and amendments rates is necessary for application in bioengineered structures. The results of SWRC and K_{unsat} of different soils amended with 5%, 10% and 15% WHB, SBB and MB are presented here in this chapter. The K_{unsat} was evaluated by using instantaneous profile method (IPM).

6.2 Influence of biochar type and amendment rates on SWRC

Fig. 6.1(a-c) highlights the SWRCs of the bare and 5% and 10%, (w/w) WHB, SBB and MB-amended silty sand. The fitting parameters of the SWRCs are presented in Table 6.1. The effect of biochar on these fitting parameters such as, saturated water content (θ_s), air entry value (AEV), coefficient or slope n and residual water content (θ_r) is discussed next. The bare silty sand exhibited the θ_s of 36% and it was observed to increase ($p = 0.02 < 0.05$) with the increase of amendment rates from 5% to 10% of all the biochar. The higher porosity with large SSA due to the intra-pores in biochar (Fig. 4.4) and the water absorptive surface functional groups (Fig 4.6) allowed higher water storage or absorption in biochar compared to the soil as seen from water absorption capacity results (Table 4.1). The biochar with higher porosity and water absorption capacity increased the total porosity and hence, the θ_s in the BAS relative to the bare soil.

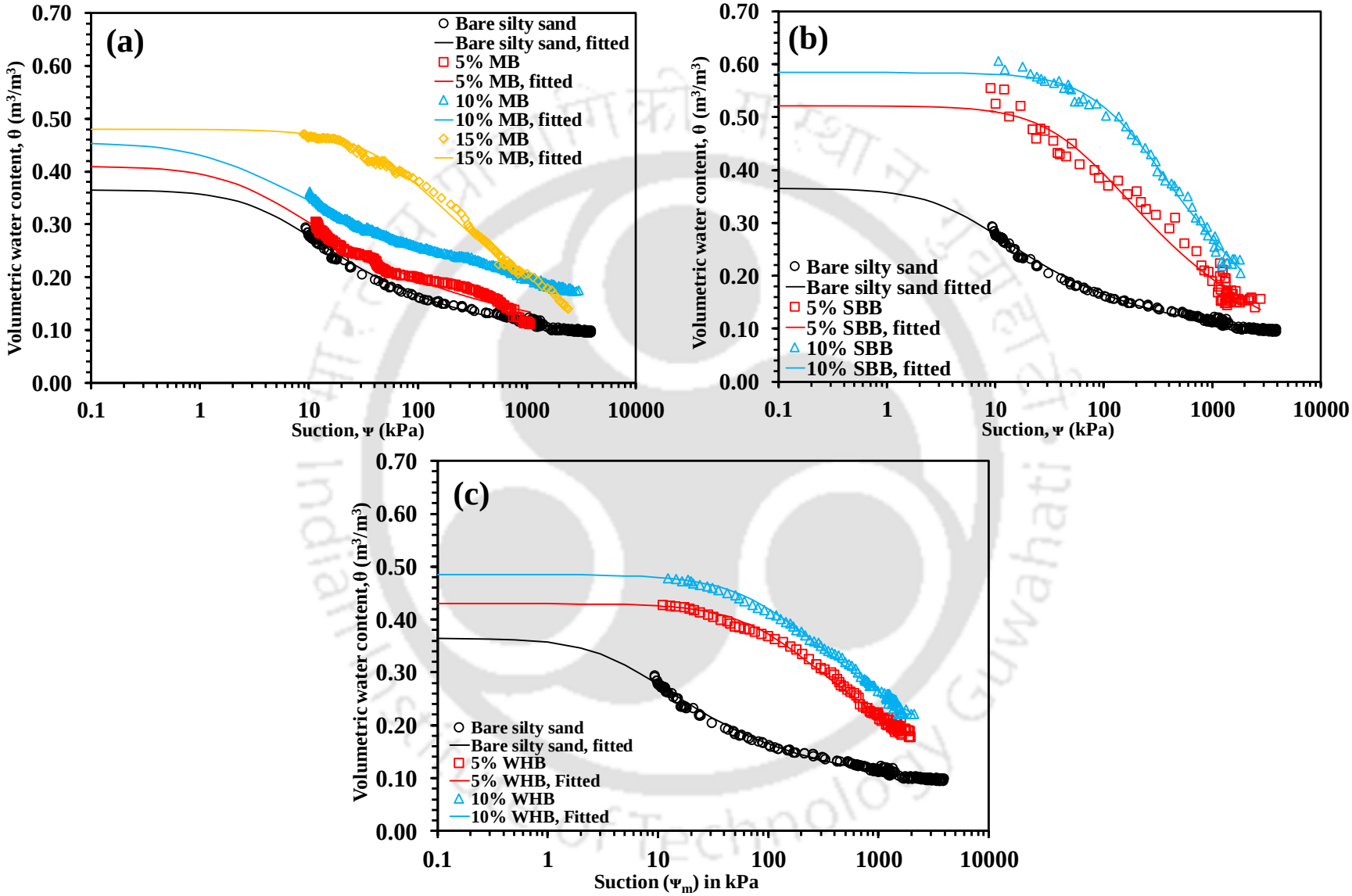

Fig. 6.1 Variation of SWRC in silty sand amended with (a) MB, (b) SBB and (c) WHB.

Table 6.1 Fitting parameters of SWRCs fitted using van Genuchten (1980) model.

Type	Biochar (%)	θ_s (%)	θ_r (%)	α (kPa^{-1})	AEV (kPa)	n (-)	m=(1-1/n)	R^2 value	θ_{1500} (%)	PAWC (%)
Bare soil	0	36.5	7.7	0.198	5.1	1.40	0.28	0.99	10	9
WHB	5	43	0	0.009	46	1.32	0.24	0.99	20	21
	10	48.5	0	0.010	42	1.28	0.22	0.99	24	22
MB	5	41	7	0.316	3.2	1.29	0.23	0.98	12	12
	10	45.5	9	0.592	1.7	1.19	0.16	0.99	18	13.5
	15	48	0	0.016	25	1.32	0.24	0.99	18	26
SBB	5	52	0	0.017	59	1.35	0.26	0.98	17	29
	10	58.4	0	0.006	164	1.42	0.29	0.99	24	33

AEV- Air entry value, PAWC- plant available water content.

Among the biochar types tested, SBB-amended soil showed the highest θ_s whereas the MB-amended soil exhibited the lowest (Table 6.1). The higher porosity as observed from the highest water absorption capacity (Table 4.1) and larger SSA due to the smallest size intra-pores in SBB (Fig. 4.4) led to the highest θ_s in SBB-amended soil. The higher porosity of SBB-amended soil was also evident from the lowest dry density (Fig. 4.3a). The higher porosity in SBB-amended soil occurred either by the reformation of larger size inter-pores between soil and biochar particles, or due to the higher intra-porosity by the more numbers of smaller size intra-pores in SBB (relative to other biochar). The higher θ_s in BAS implies the more quantity of water in soil that can be utilized for the growth of vegetation.

The bare soil showed the air entry value (AEV) of 5.1 kPa and observed to increase in the range of 500-3800% after amendment of biochar (all types). The higher AEV in BAS could be attributed to the smaller pore size in BAS compared to the bare soil. The amendment of biochar reformed the pores to the complex pores size network i.e., the settlement of smaller soil or biochar particles in the inter-pores and the smaller size intra-pores possibly led to the smaller size pores in BAS (Abel et al. 2013; Andrenelli et al. 2016). In smaller pores, water held tightly by larger suction due to capillary action and requires a higher pressure (air pressure) for escape compared to the larger pores in bare soil; thereby, higher AEV (Fredlund et al. 2012). The SBB-amended soil showed relatively higher AEV among the biochar tested. The smaller size intra-pores (Fig. 4.4) and smaller size particles after compaction of SBB relative to other biochar caused the smaller size pores in SBB-amended soil as smaller size particles could also settle in the inter-pores; thereby, higher AEV. The higher AEV in

biochar-amendment soil implies the prolong holding of water in BAS or would remain saturated for a longer duration compared to the bare soil.

The value of parameter 'n' or the slope of the SWRC was found to be 1.4 in bare silty sand decreased after the amendment of biochar of all types (Table 6.1). Slight difference in the n among the different biochar types could also be observed. The n is related to the pore size distribution of the soil. The smaller pore size in BAS compared to the bare soil or the decrease of pore size of the soil after biochar amendment caused the lower n in BAS. The amendment of the biochar reformed the size of the pores in soil by settling smaller size biochar or soil particles in the inter-pores or forming smaller size inter-pores and adding the intra-pores which have resulted in increased total porosity but decreased pore size compared to the bare soil (Andrenelli et al. 2016). The parameter 'n' physically represents the desaturation rate under drying and re-saturation rate under wetting of soil; thus, the lower 'n' value in BAS in the present study implies a slow de-saturation of the soil or slow release of water from the soil after AEV.

The residual water content (θ_r) was observed to be 0 (from the fitting) for most of the amended soil (Table 6.1). However, these were not the actual representative of θ_r. The actual θ_r corresponds to a very large suction which might not be reached in the present study and is difficult to measure due to the limitation in most of the measuring instrument. The peak or maximum suction measured in the present study was in the range of 2000-3000 kPa (Fig. 6.1). Therefore, the effect of biochar on θ_r could not be explained rather the water content at suction of 1500 kPa (i.e., θ_{1500}) which is often considered as wilting point for most of the plant species (Feddes et al. 1978) could better define the effect of biochar on water retention at large suction. Hence, instead of θ_r, the θ_{1500} is considered only for comparing the results of water retention at higher suction between bare and BAS. The bare soil exhibited θ_{1500} of 10% and increased in the range of 20-140% after amendment of biochar. Moreover, among the biochar tested, WHB-amended soil exhibited the highest θ_{1500} equally the SBB-amended soil. The smaller size pores could be the intra-pores retained water at higher suction due to their smaller size and hence the higher θ_{1500} in BAS. The smaller size pores held water tightly due to the capillary action and minimizes the water evaporation, and hence, higher water retention. The smaller size pores in WHB and SBB-amended soil due to the smaller size particles of SBB and WHB after compaction and smaller size intra-pores in SBB and WHB led to the higher θ_{1500} in WHB and SBB-amended soil.

Overall, the amendment of biochar improved the water retention of the soil and the amendment of SBB showed the highest improvement among the biochar tested. The trends of increased water retention of soil after biochar amendment were also reported by the previous researchers (Bordoloi et al. 2018b; Ni et al. 2018). Therefore, the trends observed for SWRC in the present study are consistent with the literature. The improved water retention in BAS could assist the growth of vegetation in bioengineered structures by reducing the irrigation demand and the effect of drought stress.

6.3 Variation of SWRC in biochar-amended soils under drying and wetting path

Fig. 6.2 (a-f) highlights the SWRCs of 5% and 10% MB-amended silty sand and pure sand measured at different depth under drying and wetting process. The fitting parameters of the SWRC are presented in Table 6.2. The effect of biochar on the SWRC fitting parameters, are discussed next. It is clear from the data presented in Table 6.2 that the θ_s of the silty sand and pure sand increased from 35% to 46% and 41% to 50% under drying process, and 33% to 43% and 40% to 51% under wetting process respectively after amendment of 10% biochar. The magnitude of θ_s was observed to be higher in pure sand compared to silty sand under both bare and amended state, and the rate of increment in θ_s due to biochar amendment was observed to be higher in silty sand compared to pure sand. The amendment of biochar showed no comparable change in the air entry value (*AEV*) of the soils as a bare minimum difference (physically may not be significant) between the data of bare and BAS could be observed from Table 6.2. The change in '*n*' due to biochar amendment was observed to be inconsistent in the silty sand while it decreased significantly from 1.76 to 1.34 under drying and 2.01 to 1.42 under wetting process in pure sand after 10% biochar amendment. The magnitude of '*n*' was observed to be higher in pure sand compared to the silty sand. The amendment of biochar increased the residual water content (θ_r) of the silty sand from 7% to 16% under drying and 9% to 17% under wetting process. Similarly, the θ_r increased from 1% to 5% under drying and 2% to 6% under wetting in pure sand respectively. Among the soil type tested, the rate of increment in θ_r due to biochar amendment was observed to be higher in pure sand.

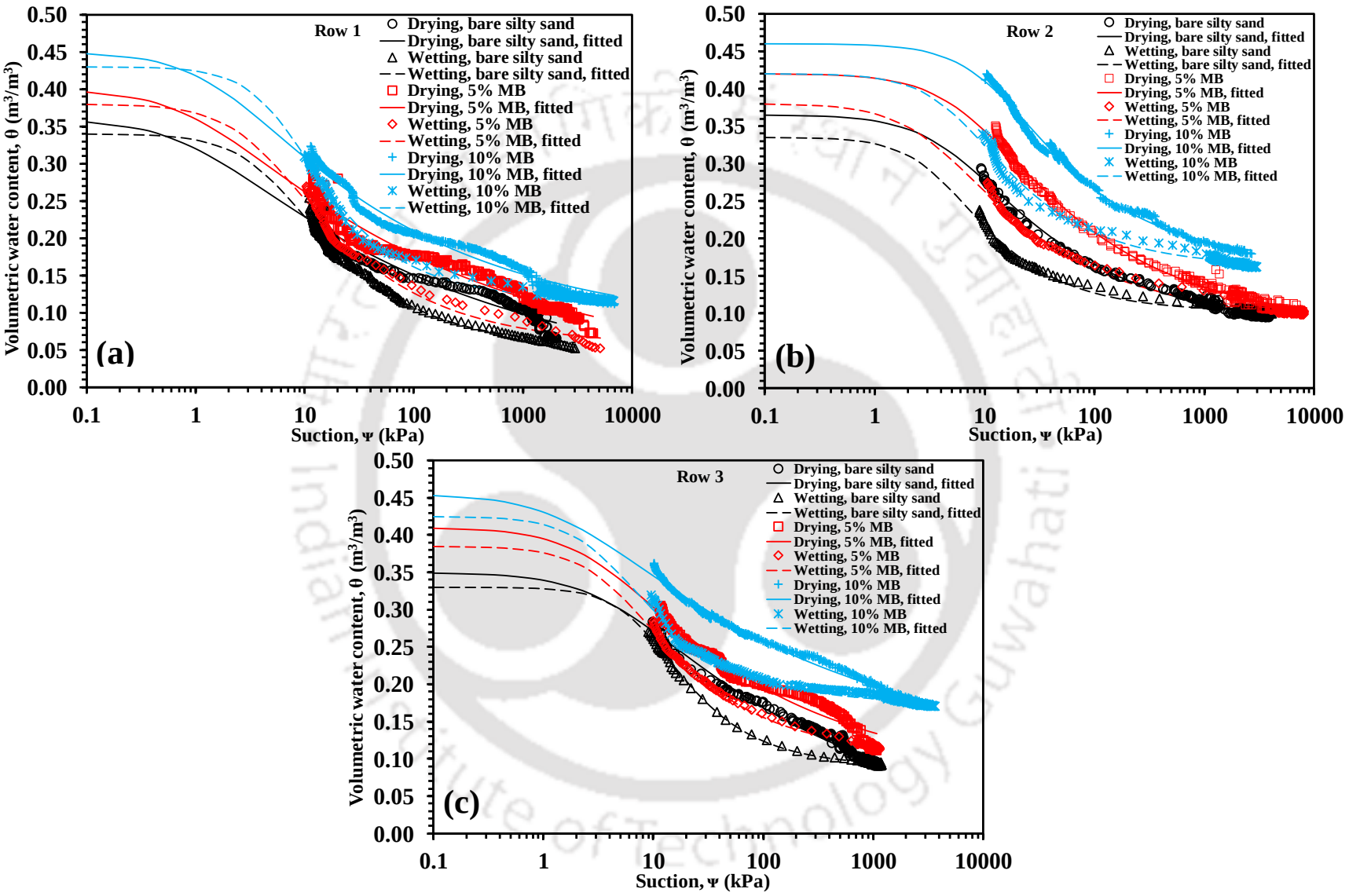

Fig. 6.2. Spatial variation of SWRCs in silty sand (a, b, c).

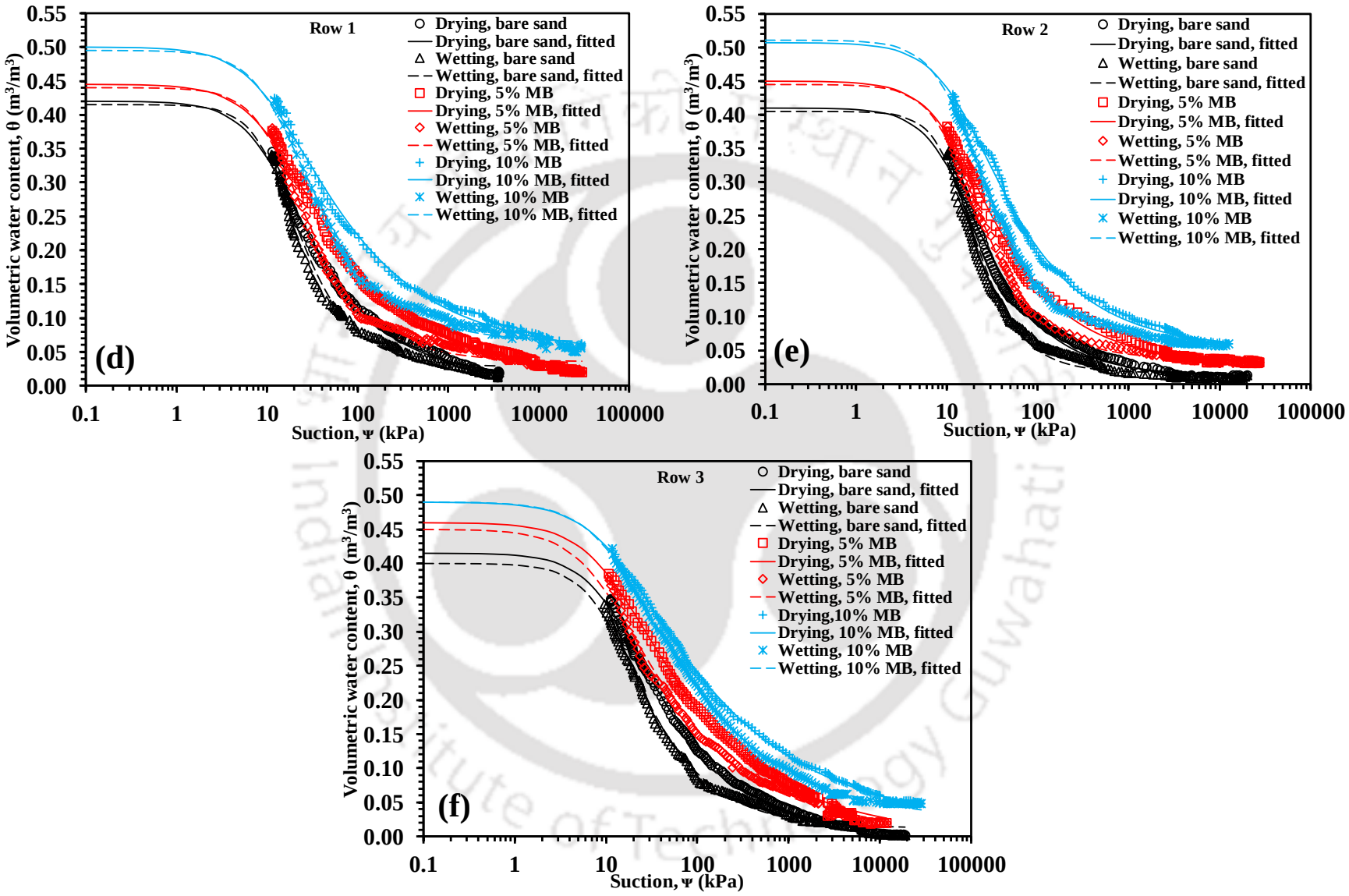

Fig. 6.2. Spatial variation of SWRCs in pure sand (d, e, f).

Table 6.2 Fitting parameters of SWRCs of the different soils amended with MB.

Soil type	Process	Sensor layer	BC (%)	θ_s (m^3/m^3)	θ_r (m^3/m^3)	α (m^{-1})	AEV (kPa)	n (-)	m(-)	R^2	PAWC (%)
Silty sand	Drying	Row 1	0	0.36	-	10.8	0.9	1.190	0.16	0.96	7.8
			5	0.40	0.02	9.8	1	1.19	0.16	0.95	8
			10	0.45	0.08	6.2	1.6	1.25	0.2	0.97	10
		Row 2	0	0.365	0.077	1.94	5.1	1.40	0.28	0.99	8.9
			5	0.42	0.079	1.37	7.2	1.36	0.27	0.99	11.5
			10	0.46	0.165	0.80	12.3	1.51	0.34	0.99	13
		Row 3	0	0.35	-	2.37	4.2	1.230	0.19	0.98	11
			5	0.41	0.07	3.1	3.2	1.29	0.23	0.98	12
			10	0.455	0.09	5.8	1.7	1.19	0.16	0.99	13.5
	Wetting	Row 1	0	0.34	0.051	1.97	5	1.55	0.35	0.98	6.7
			5	0.38	0.055	2.4	4.1	1.47	0.32	0.98	7.5
			10	0.43	0.12	1.57	6.2	1.70	0.41	0.99	8.2
		Row 2	0	0.335	0.102	2.4	4	1.69	0.41	0.99	5
			5	0.38	0.091	2.9	3.4	1.43	0.30	0.99	6.8
			10	0.42	0.161	1.73	5.7	1.59	0.37	0.99	8
		Row 3	0	0.33	0.09	1.09	9	1.81	0.45	0.99	6.4
			5	0.385	0.103	2.12	4.6	1.55	0.35	0.99	7.9
			10	0.425	0.173	2.7	3.7	1.62	0.38	0.98	8.8

Pure sand	**Drying**	**Row 1**	**0**	0.42	0.011	0.87	11.3	1.62	0.38	0.99	31
			5	0.445	0.017	0.84	11.7	1.48	0.32	0.99	32
			10	0.50	0.047	0.86	11.4	1.43	0.30	0.99	33.2
		Row 2	**0**	0.41	0.011	0.83	11.8	1.76	0.43	0.99	31.7
			5	0.45	0.030	0.78	12.6	1.62	0.38	0.99	32.5
			10	0.507	0.052	0.67	14.6	1.57	0.36	0.99	34.8
		Row 3	**0**	0.415	-	0.80	12.4	1.550	0.36	0.99	31
			5	0.46	-	0.85	11.5	1.410	0.29	0.99	31.5
			10	0.49	0.012	0.81	12.1	1.340	0.26	0.99	33
	Wetting	**Row 1**	**0**	0.415	0.028	0.73	13.4	2.00	0.50	0.99	31
			5	0.44	0.035	0.69	14.2	1.81	0.45	0.99	32.5
			10	0.495	0.063	0.70	14	1.67	0.40	0.99	33
		Row 2	**0**	0.405	-	0.73	13.4	2.01	0.50	0.98	31.6
			5	0.445	0.036	0.74	13.2	1.90	0.47	0.99	32.5
			10	0.511	0.060	0.69	14.2	1.82	0.45	0.99	35.5
		Row 3	**0**	0.40	0.012	0.84	11.7	1.73	0.42	0.99	31
			5	0.45	0.007	1.05	9.3	1.46	0.31	0.99	32
			10	0.49	0.020	0.76	12.9	1.420	0.3	0.99	33.3

Note: BC- Biochar content.

The *PAWC* of the silty sand and pure sand was observed to be increased from 9% to 13% and 32% to 35% under drying process, and 5% to 8% and 32% to 36% under wetting process after amendment of biochar. The biochar-driven increase in *PAWC* was found to be higher in silty sand. Larger magnitudes of *PAWC* in pure sand compared to silty sand could be seen from Table 6.2. Further, no compareable difference in data could be seen along the depth or in different rows of the sensors as presented in Table 6.2.

Table 6.3 Effect of biochar on the porosity of the soils.

Properties	Soil type	Biochar amendment rate			
		Only Biochar	**0% (Bare)**	**5%**	**10%**
Intra porosity (%)	Silty sand	1.8	-	-	-
	Pure Sand		-	-	-
Total porosity (%)	Silty sand	-	41.4	44.4	47
	Pure Sand	-	47	50.4	52
Inter porosity (%)	Silty sand	-	41.4	42.6	45.2
	Pure Sand	-	47	48.6	50.2

The amendment of biochar increased the total porosity of the soils (Table 6.3) as computed from the fundamental correlation using the respective initial compaction dry density and the measured specific gravity values. The total porosity comprised of inter-porosity by inter-pores and intra-porosity by intra-pores. The inter-porosity was calculated by deducting the measured (helium porosimeter) intra-porosity from the total porosity. The higher total porosity in BAS was attributed to the decreased dry density of the soils after biochar amendment (Fig. 4.3). The initial compaction density was different among the soil columns due to the decreased dry density of BAS. The intra-pores in biochar (Fig. 4.4) added the intra-porosity (1.8%) after amending to soil and increased the soil SSA, as it is evident from the higher water absorption capacity of biochar compared to the soils (Table 4.1). The amendment of biochar increased the numbers of larger-sized particles in GSD (shifted below, Fig. 4.1) that have generated larger size or more numbers of inter-pores compared to the bare soil after compaction and hence, increased the inter-porosity. The increased total porosity with larger *SSA* (Table 4.2) and the presence of water absorptive surface functional groups (Fig. 4.6) allowed larger quantity of water to be stored and hence, the higher θ_s. The larger magnitude of θ_s in pure sand compared to the silty sand was attributed to the lower initial compaction density of pure sand under both bare and amended state (Fig. 4.3) which led to

the higher total porosity and hence, the θ_s. The observed higher improvement in θ_s of silty sand over pure sand was due to the higher increase of inter-porosity by the formation of larger size or more numbers of inter-pores in silty sand after biochar amendment (Table 6.3). The amendment rates of biochar were maintained same for both the soils; ideally, the intra-porosity should remain same. The silty sand consists of considerably higher (49%) fines content compared to the pure sand (1.6%) and thus have the chance to form larger size inter-pores after biochar amendment (Fig. 4.1).

The decrease of '*n*' after biochar amendment was attributed to the reduced pore size in BAS relative to the bare soil due to the addition of intra-pores (<10 µm, Fig. 4.4) and the settlement of smaller soil or biochar particles in the inter-pores or reformation of inter-pores after biochar amendment (Abel et al., 2013; Andrenelli et al., 2016). The larger size inter-pores and non-uniform pore size distribution of pure sand due to presence of single-sized particles relative to the silty sand of all particles size ranges (Fig. 4.1) caused the steeper slope or larger magnitude of '*n*' in pure sand compared to the silty sand. The amendment of biochar in pure sand decreased the inter-pores size i.e., formed smaller-sized inter-pores and modified the pore size distribution towards uniformity which have caused the '*n*' to change larger extend in pure sand compared to the silty sand of relatively uniform pore size distribution. Sun and Lu (2014) reported an increased total porosity with reorganization of pore size into small and larger sizes in silty clay due to biochar amendment. Similarly, Wong et al. (2018) mentioned a changed pore size distribution of kaolin clay from dominant 0.05−0.06 µm pores to 0.1–4 µm pores, i.e., the pore size increased due to biochar amendment.

The increase of θ_r in biochar-amended soils was attributed to the smaller size residual pores which could be inter-pores or intra-pores that have retained water at larger suction due to their smaller size or diameter. The smaller-sized pores held water tightly due to strong capillary action (Fredlund et al., 2012) and resisted the water evaporation, thus higher water retention. The bare pure sand showed lower θ_r compared to the silty sand (Table 6.2) due to their large pores size. However, the amendment of biochar decreased the pores size higher extend in pure sand compared to the silty sand which have led to the higher θ_r in biochar-amended pure sand compared to silty sand, i.e., the efficacy of biochar in improving θ_r was observed to be higher in pure sand. The higher *PAWC* in BAS indicates the higher stored water for vegetation to readily use during drought state. The vegetation has strong influence

in bioengineered structures, in terms of improving structural stability through root reinforcement and hydrological process (Hussain et al., 2020a).

Difference in SWRC parameters was observed due to drying and wetting process (Table 6.2). Clearly, the effect of hysteresis could be observed in both the soils with or without biochar amendment (Fig. 6.2a-f). The hysteresis loop is observed to be wider in silty sand compared to the pure sand. The change in soil structure due to particular rearrangement or "ink-bottle" effects, volume change, entrapment of air and alteration in wetting characteristics (contact angle) during drying-wetting led to the hysteresis in the SWRC (Fredlund et al., 2012). Although the swelling of samples during wetting was restrained by the confinement, a small volume change due to shrinkage during drying could be possible in silty sand with clay and silt fraction, since the samples of silty sand were prepared with an addition of initial moisture content. However, the shrinkage was expected to be negligible due to the absence of higher swelling clay minerals and the presence of confinement. The shrinkage along with the change in pore size distribution due to particular rearrangement by the dying and followed by wetting led to the wider hysteresis loop in silty sand relative to the pure sand. In pure sand, only particular rearrangement during wetting caused the hysteresis and the absence of shrinkage-swelling led to the lower hysteresis effect compared with silty sand. The soils in the columns were compacted layer wise to maintain the uniformity that have caused no comparable variation in SWRC or the parameters along the depth in the columns.

6.4 Unsaturated Hydraulic conductivity of BAS

Fig. 6.3 (a-h) highlights the variation of unsaturated hydraulic conductivity (K_{unsat}) with suction, i.e., the hydraulic conductivity function for bare and biochar (5% and 10%, w/w) amended silty sand and pure sand under drying and wetting condition. The saturated hydraulic conductivity (K_{sat}) of the bare and biochar-amended silty sand and pure sand are also presented in figure for reference. The K_{unsat} was found to be reached the maximum near to K_{sat} at around 9 kPa (Fig. 6.3). In drying state, the K_{unsat} decreased in both the soils with the increase of suction (Fig. 6.3 a-b, e-f). The magnitude of K_{unsat} was recorded as low as 10^{-12} m/s in the present study. However, literature (Meerdink et al., 1996; Li et al., 2009; Uzoma et al., 2011) reported K_{unsat} value lower than 10^{-12} m/s. The magnitude of K_{unsat} varies soil to soil and depends on the range of suction measured i.e., at large suction, the K_{unsat} could be very low.

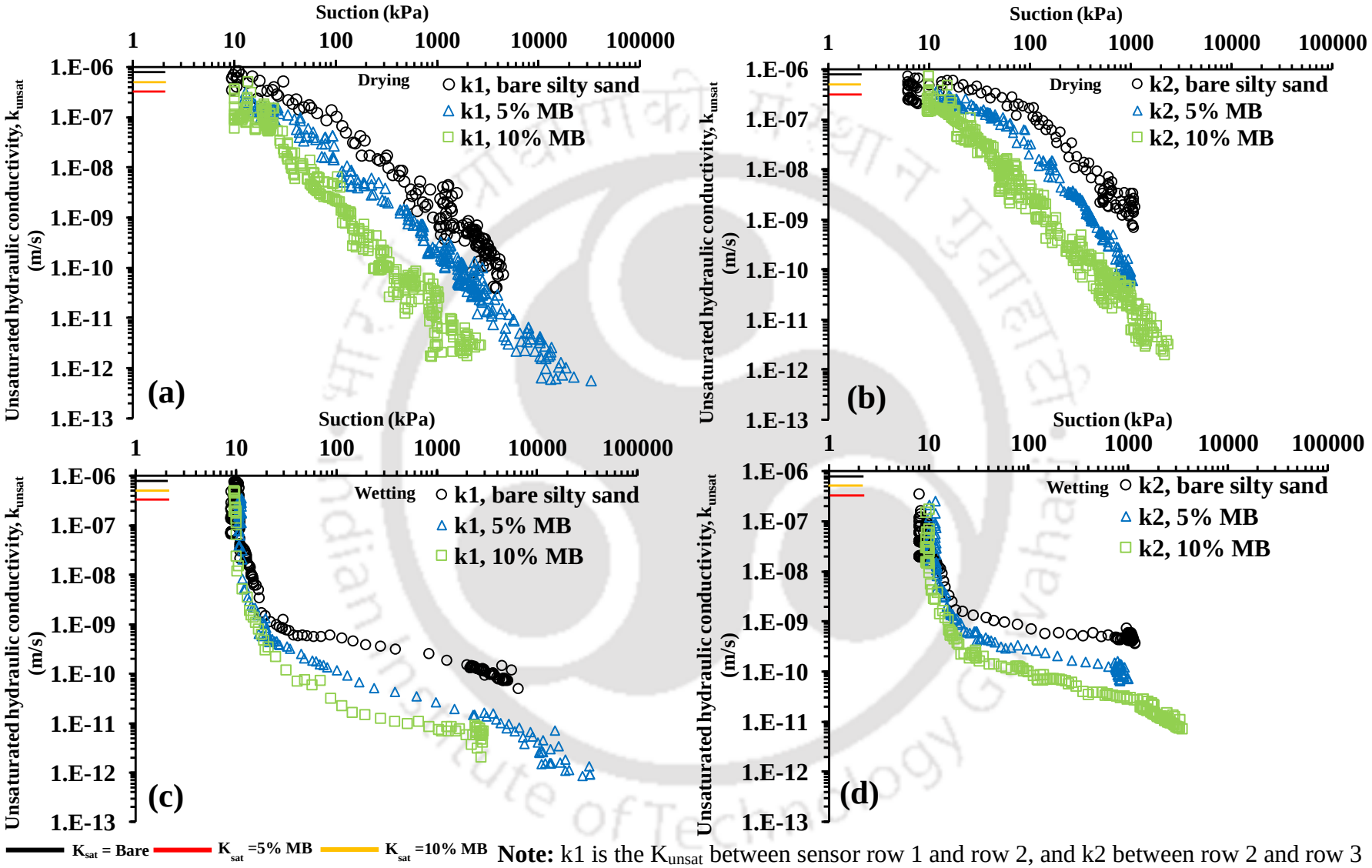

Fig. 6.3 Soil hydraulic conductivity function (SHCF) for the silty sand drying (a, b) and wetting (c, d).

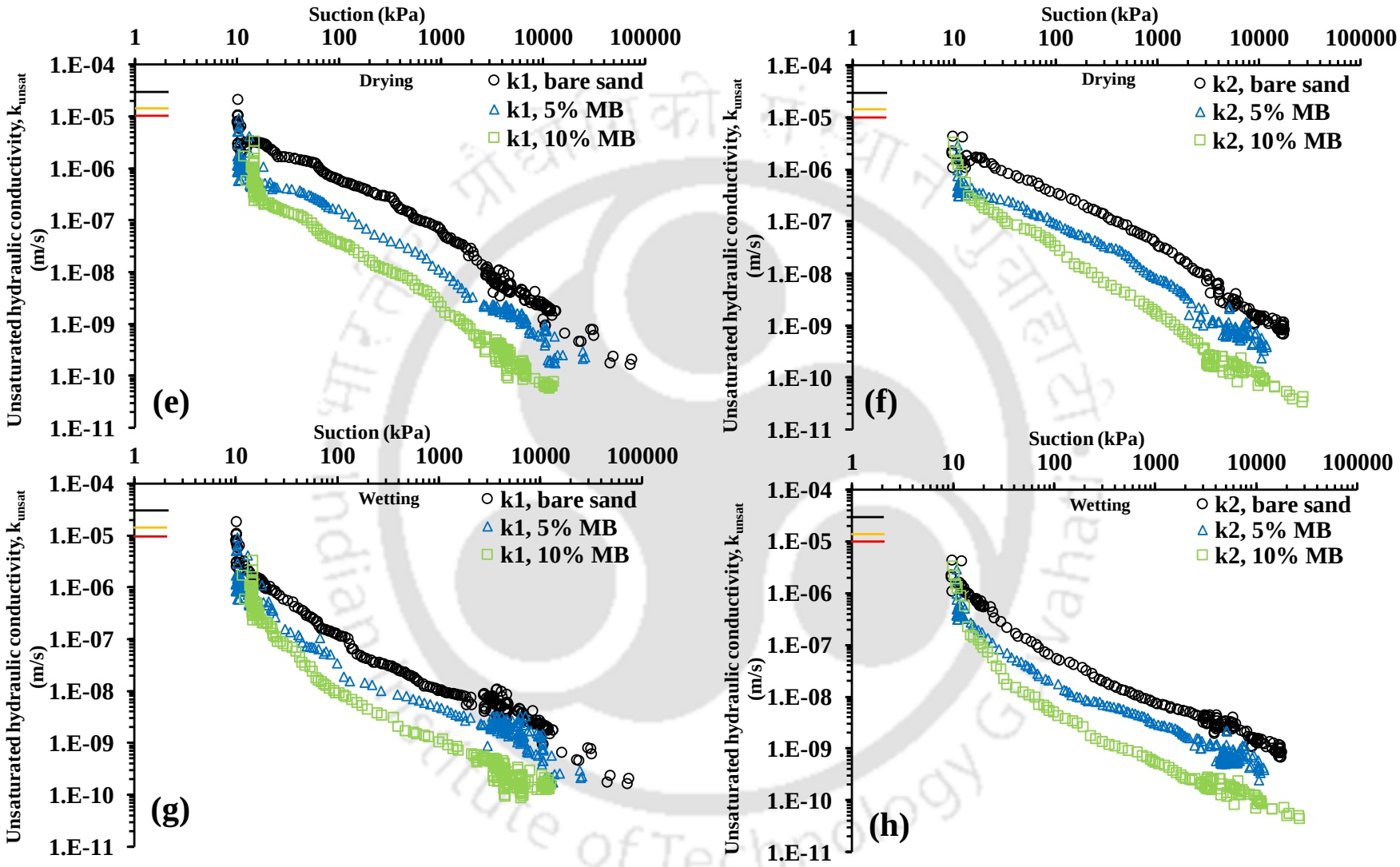

Fig. 6.3 Soil hydraulic conductivity function (SHCF) for the pure sand drying (e, f) and wetting (g, h).

The increase of suction allows more air bubbles to entrap in soil. These entrapped air bubbles block the hydraulic flow path, thereby increased the tortuosity of water flow paths and decreased the K_{unsat}. Further, the amendment of biochar decreased the K_{unsat} in both the soils under drying and wetting condition, and the rate of decrement in K_{unsat} was observed to be higher with the larger biochar amendment rate (Fig. 6.3). The amendment of the biochar in soils reorganized the pore structure or pore size distribution of the soils by adding smaller size intra-pores and possibly reforming smaller size inter-pores as observed by Sun and Lu (2014) for silty clay which have led to the increased tortuosity or tortuous flow path and hence, reduced K_{unsat}. Sun et al. (2015) and Blanco-Canqui (2017) reported an increased tortuosity in sandy soil after biochar amendment that affects the water flow path. The lower K_{unsat} of BAS compared to the bare soil was also justified from the delayed wetting and drying of BAS observed from the lower n value and higher AEV as presented in Table 6.2.

A steep change of K_{unsat} with suction could be observed in silty sand (Fig. 6.3a-d) relative to the pure sand (Fig. 6.3e-h) under drying and wetting condition which have ensured the uniform and smaller pores size in silty sand compared to the pure sand; thereby, a small change in suction or pore water led to the sharp change in the K_{unsat}. The magnitude of the hydraulic conductivity (K_{unsat} or K_{sat}) found to be always including drying and wetting process higher (~one-order) in pure sand compared to silty sand due to their highly porous structure that provides larger passage for water to flow. Differences or hysteresis could be observed in the hydraulic conductivity function of the soils under drying and wetting process, i.e., at any suction, the magnitude of K_{unsat} in drying state (Fig. 6.3a-b, e-f) was always higher than that of the wetting state (Fig. 6.3c-d, g-h). In addition, the effect of hysteresis was observed to be more pronounced in lower suction range relative to the large suction range. The lower volumetric water content along the wetting path due to the change in pore structure, contact angle, and the entrapment of air during drying and wetting process led to the lesser hydraulic flow path and hence, the lower K_{unsat} in wetting process. The influence of the altered pore structure or capillarity found to be more strong at lower suction range compared to the large suction that it has caused the higher hysteresis effect at lower suction range (Hillel, 1998; Al-Mahbashi et al., 2018). The deviation of wetting path K_{unsat} from the drying path (hysteresis) was observed to be more in silty sand compared to the pure sand and attributed to the higher change in pore structure due to particular rearrangement in silty sand of containing fines (clay and silt). The fine-grained soil generally undergoes higher structural changes or particular rearrangement due to their mineralic action (Al-Mahbashi et al., 2018).

There was no comparable variation observed in the K_{unsat} between three rows of sensors along the depth (i.e., k_1 and k_2 in Fig. 6.3a-h) in a same soil column under either of drying or wetting conditions which have ensured the maintenance of uniform soil compaction along the depth. Overall, the amendment of biochar decreased the K_{unsat} of the soils and the decreasing rate varies with the soil type.

6.5 Summary and conclusions

The SWRC and unsaturated hydraulic conductivity of different types biochar-amended soils are presented. The amendment of the biochar improved the water retention on an average 30-150% as quantified by the fitting parameters, and decreased the K_{unsat} by one-two order of magnitude of the compacted soils. The effect of biochar amendment on the water retention and the K_{unsat} was found to be varied with the biochar amendment rates. The different biochar types showed the variable effect on the water retention i.e., among the different biochar types tested, the amendment of SBB showed the highest improvement in the water retention of the soils. Similarly, among the soil types tested, the amendment of biochar (MB) showed higher improvement in water retention of pure sand. Further, relatively higher decrease of K_{unsat} was observed in silty sand compared to the pure sand after biochar amendment. Thus, the biochar amendment was found to be improved the water retention and decreased the K_{unsat} of the compacted soil tested over a large or wide suction range which are again vary with the factors, such as biochar types, biochar amendment rates and soil types. Therefore, the higher water retention and lower hydraulic conductivity (K_{unsat}) of compacted BAS relative to bare soil could be useful in assisting the growth of vegetation and lowering the ingress of surface water in bioengineered structures.

CHAPTER 7
STRENGTH, LOAD BEARING CAPACITY AND DESICCATION POTENTIAL OF BAS

7.1 Introduction

The mechanical properties of BAS i.e., the shear strength, load bearing capacity and desiccation crack potential are crucial on which the stability of the bioengineered structures depend. Biochar is porous and light in weight, and decreases the dry density of soil after amendment. Therefore, the influence of biochar on the shear strength, load bearing capacity and desiccation crack potential of soil need to be investigated for application in bioengineered structures. The strength and load bearing capacity of BAS were evaluated by the past researchers and where inconclusive results have been reported. The influence of biochar on shear strength and load bearing capacity would be different with soil types. In addition, the amendment of different biochar types would affect the soil shear strength and load bearing capacity differently. Thus, the effect of biochar amendment on shear strength, load bearing capacity and desiccation potential of different soils by considering different biochar types was investigated in the present study and the results of which are presented here in this chapter. The shear strength was evaluated by the conventional unconfined compression test and small direct shear test, load bearing capacity was evaluated by California bearing ratio (CBR) test and the desiccation crack potential was evaluated by the non-destructive image analysis technique.

7.2 Shear strength of different types BAS

Fig. 7.1(a-f) highlights the stress-strain responses of the bare, 5%, 10% and 15% (w/w) MB, SBB and WHB-amended soil. The peak stress of each response was noted and presented as unconfined compressive strength (UCS). Irrespective of compaction density, the failure or ultimate strain i.e., the strain at peak stress was observed to be increased with the increase of biochar amendment rate from 5% to 15%. The higher ultimate strain in BAS indicates the increased ductility, and could be attributed to the higher compacting water content and lower dry density of BAS samples especially with higher (15%) amendment rate compared to the bare soil or samples with lower amendment rate. The higher molding water content and lower density of BAS samples were due to the higher OMC and lower MDD biochar amended soil relative to bare soil (Fig. 4.3), as the samples were compacted based on the compaction parameters i.e., MDD and OMC. The higher water content with lower density (higher

porosity) assisted the soil-biochar composites to undergo a higher particular rearrangement or deformation without failure which have resulted in higher strain at failure. Thus, the amendment of biochar or the increase of biochar amendment rates improved the ductility of the soil under shearing.

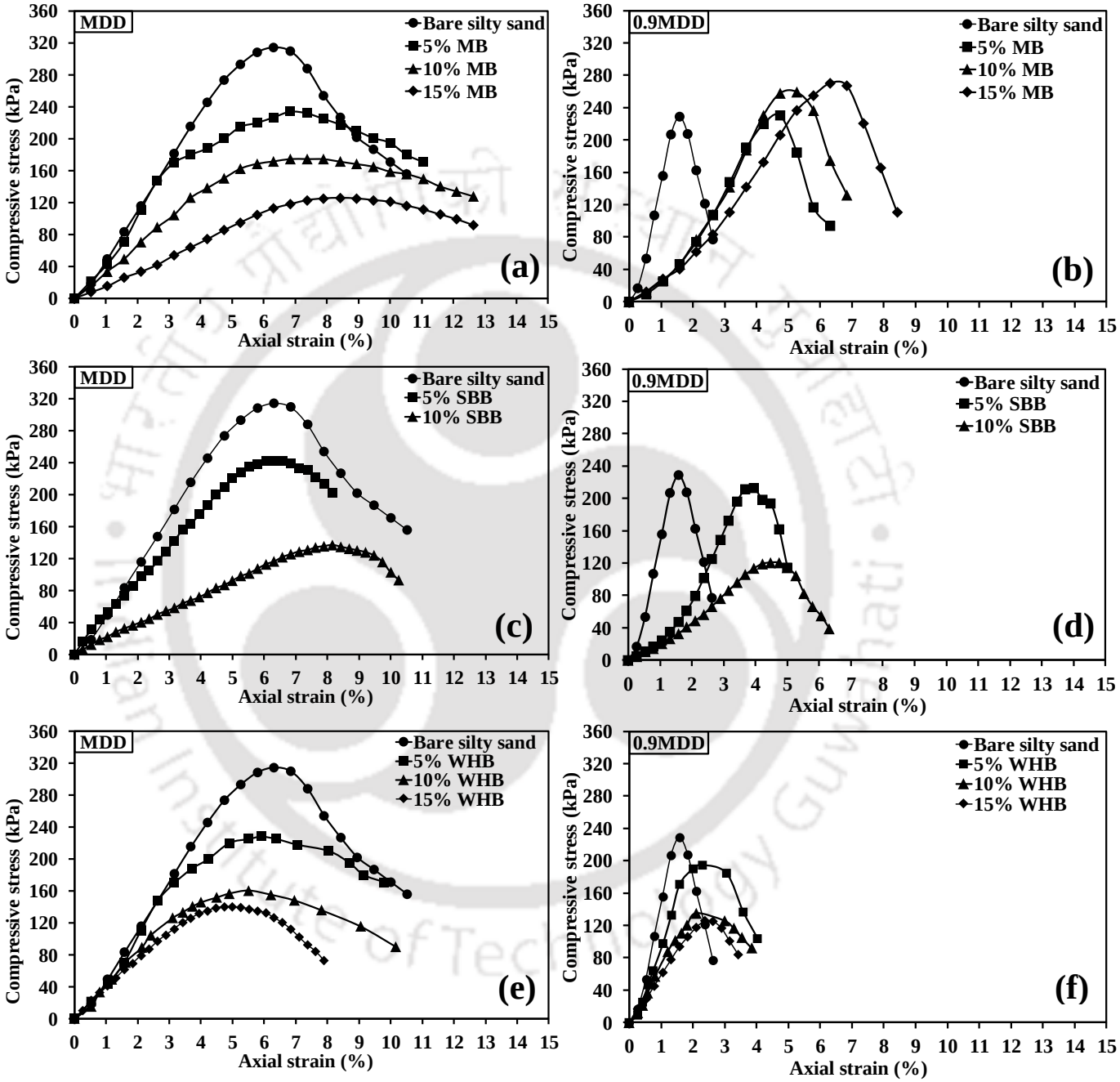

Fig. 7.1 Stress-strain responses of the different BAS (a-b) MB, (c-d) SBB and (e-f) WHB.

Further, the magnitude of ultimate strain was observed to be lower in less compacted i.e., 0.9MDD soils compared to the higher compaction (MDD, Fig. 7.1). The lower ultimate strain at lower compacting density was attributed to the brittleness behavior of the samples by the lower water content with higher porosity or voids. The samples were compacted at dry side of

the OMC and the lower density have higher porosity so the catastrophic or brittle failure (lower strain) could be expected. Fig. 7.2 presents the variation of the shear strength (UCS) in different types BAS under different compaction density.

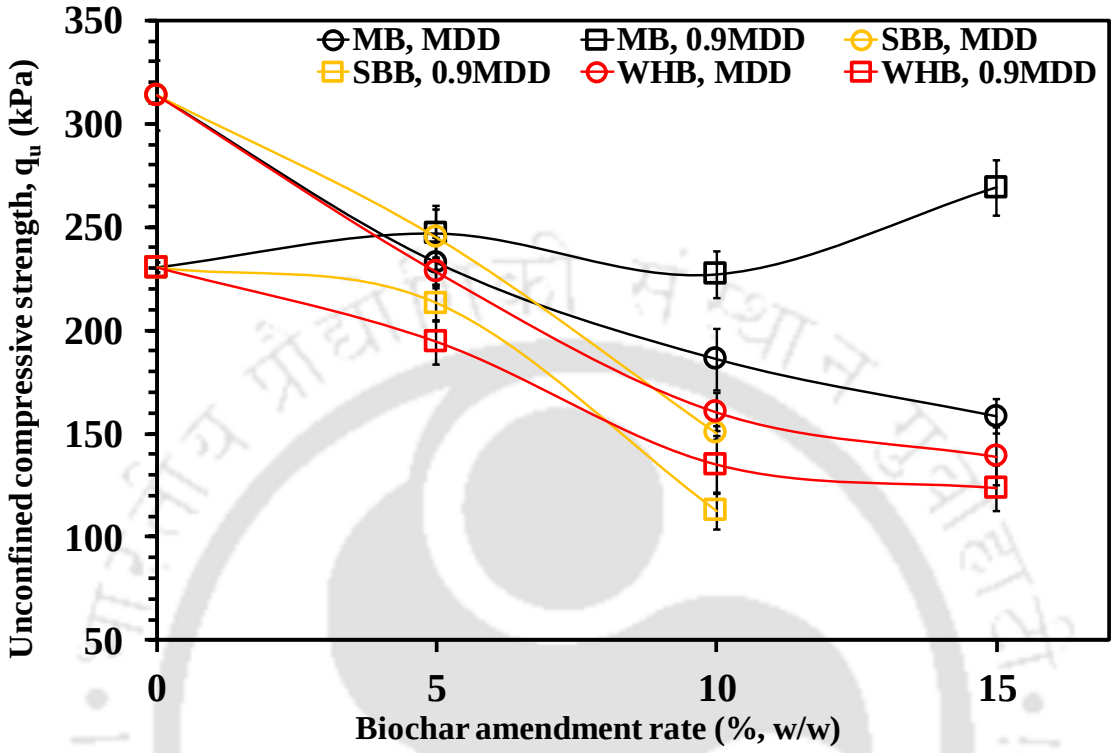

Fig. 7.2 Variation of UCS in different BAS.

The bare silty sand showed the UCS value of 314 kPa at compaction density MDD and 228 kPa at 0.9MDD respectively. The amendment of 5% to 15% biochar regardless of biochar types decreased the UCS of the soil in the range of 22-56% at MDD state and 7-51% at 0.9MDD. Exception, the MB-amended soil and compacted at 0.9MDD exhibited an increased UCS compared to the bare soil. Among the biochar types tested, the amendment of SBB showed the higher decrease in the UCS compared with the other biochar types. Ideally, the UCS is considered to be undrained behavior of soil and primarily related to the cohesion parameter of the soil. The decreased soil dry density or increased porosity after biochar amendment (Fig. 4.3) caused an increase in the inter particular distance, and reduction in Vander wall and electrostatic attraction and thus the reduction in the cohesion or UCS. The lowest dry density of SBB-amended soil compared to the other BAS (Fig. 4.3) led to the lowest UCS in SBB-amended soil. Considering the compaction density, the soil samples compacted at 0.90MDD showed lower UCS compared to the samples compacted at MDD. The lower initial water content in samples compacted at 0.9MDD compared to that of at

MDD caused the decrease in cohesion and an early or brittle failure of the samples, and hence the lower UCS (Malizia and Shakoor 2018).

Overall, the biochar amendment decreased the UCS of the soil and the increase of biochar amendment rate from 5% to 15% further decreased the UCS. In literature, Haque et al. (2014) reported the decreased trend of UCS in clayey soil amended with 10 to 20% (w/w) biochar. Similarly, Bora et al. (2020) also mentioned the decreased UCS of soil after amendment of water hyacinth biochar. However, literature (Sudhakar et al., 2017; GuhaRay et al., 2019) also reported the increase of UCS of soil after biochar amendment. Thus, the trends observed for UCS in the present study are consistent with the literature. The decreased shear strength or UCS of the soil after biochar amendment is not beneficial for stability point of view; however, at lower biochar amendment rate (5%), the variation in UCS among the different biochar types was observed to be negligible and the decrease with respect to bare soil was optimal i.e., showed a UCS value higher than 200 kPa which is satisfactory for most of the bioengineered structures (Daniel and Wu, 1993; Bello, 2011).

7.3 Influence of biochar amendment on the shear strength of different types soils

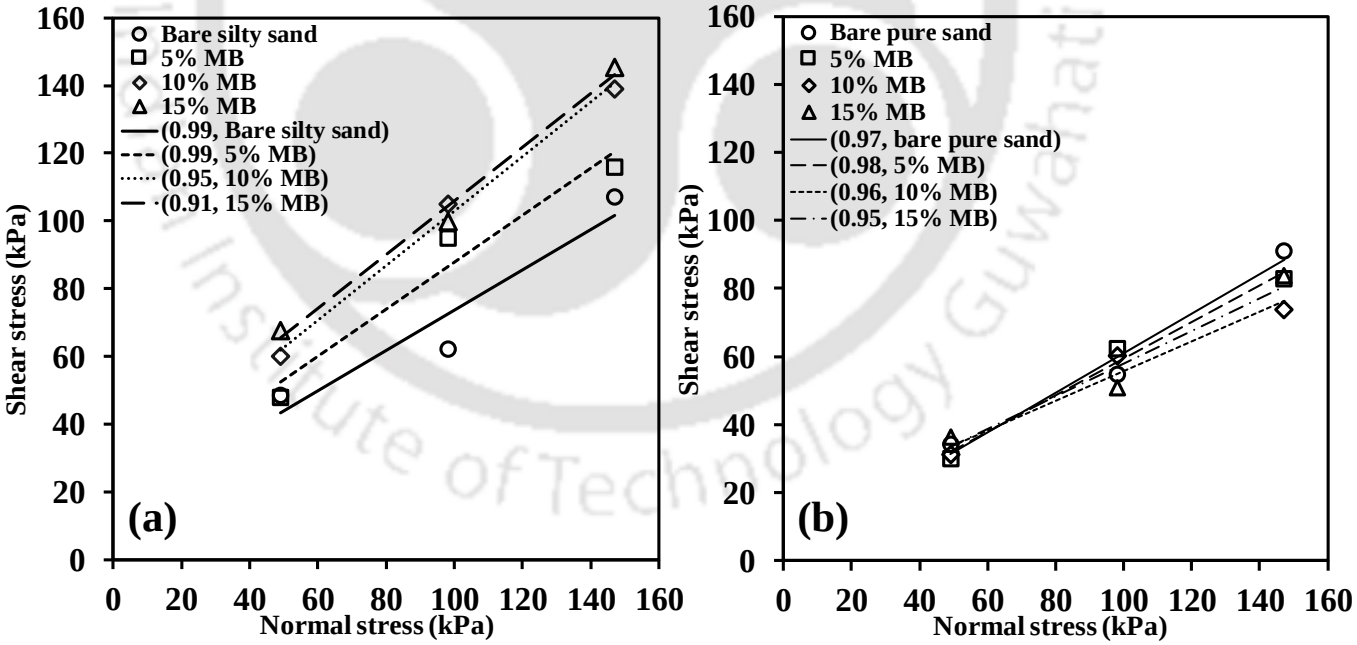

Fig. 7.3 Failure envelopes of MB-amended soil (a) silty sand and (b) pure sand.

Fig. 7.3 (a-b) presents the Mohr-Coulomb failure envelope obtained by plotting shear stress and normal stress for bare and MB-amended silty sand and pure sand. The failure envelope is observed to be shifted upward in silty sand and downward in pure sand with the increase of biochar amendment rates from 5% to 15%. The shear stress was observed to be lower in pure

sand compared to the silty sand as the failure envelopes in pure sand are located below the failure envelopes of silty sand.

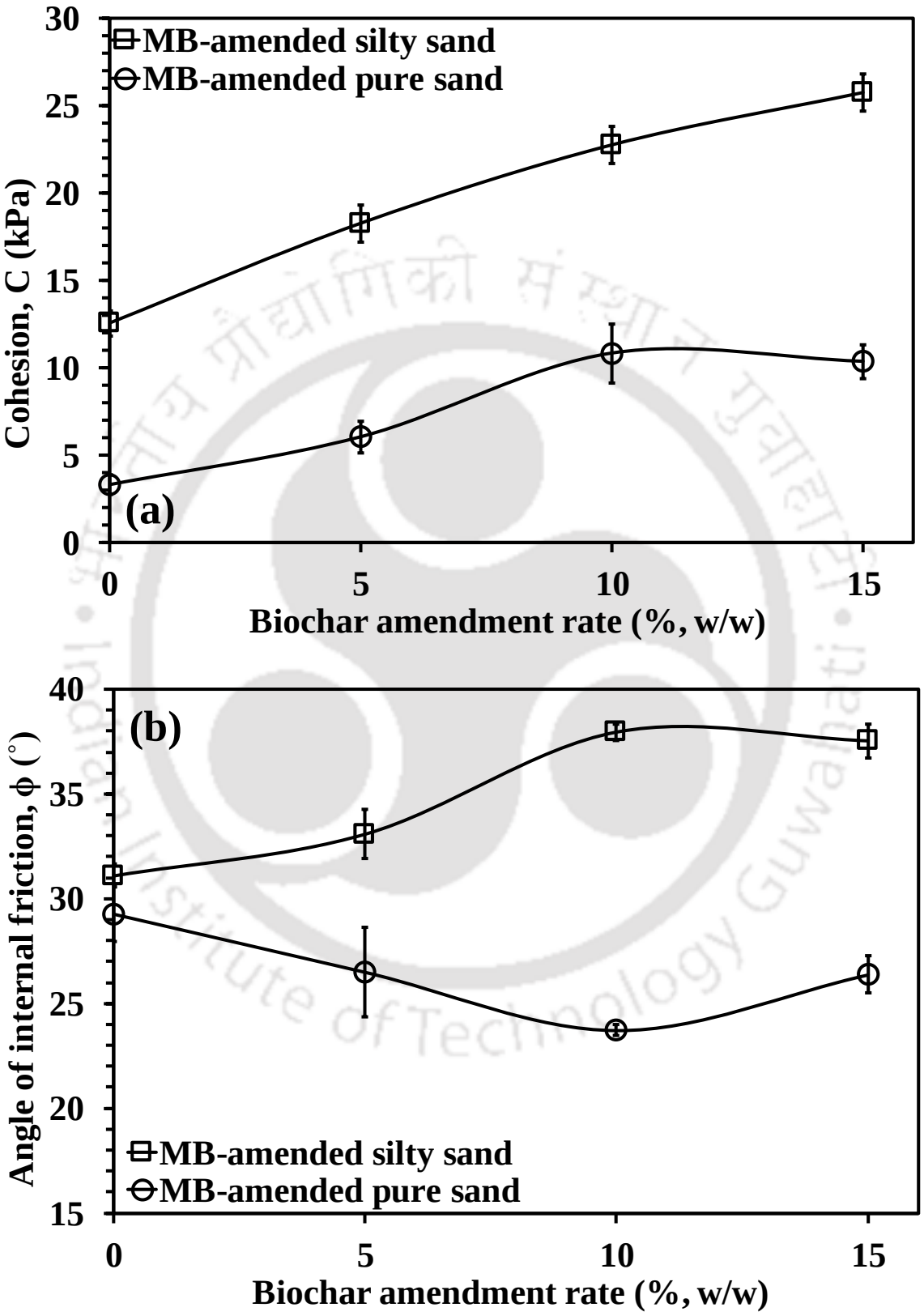

Fig. 7.4 Variation of shear strength (a) cohesion and (b) angle of internal friction in MB-amended silty sand and pure sand.

The shear strength parameters cohesion (c) and angle of internal friction (ϕ) are obtained from the failure envelopes, and the variation of c and ϕ with the amendment rates of biochar (MB) are highlighted in Fig. 7.4 (a-b). The bare silty sand and pure sand showed the c value of 12.5 ± 0.7 kPa and 3.3 ± 0.6 kPa. The c increased to the maximum of 25.8 kPa in silty sand when biochar of 15% (w/w) was amended, while in pure sand, the c increased to the maximum of 10.8 kPa at 10% biochar content and the further increase of amendment rate to 15% showed no change in c (Fig. 7.4a). The magnitudes of c were observed to be higher in silty sand both bare and biochar-amended state compared to the pure sand due to the presence of clay fraction in silty sand which offers true cohesion. The surface functional groups present in the biochar (Fig. 4.6) are positive or negatively charged i.e., the hydroxyl (OH) and carbonyl (C=O) are polar in nature with both negative and positively charged, and the carboxyl (C-O) group is negatively charged (Zuend et al. 2011; Uchimiya et al. 2012). The inter particular or electrostatic attraction was developed between the soil (clay) and biochar particles in the case of silty sand, and among the biochar particles in case of pure sand by the positive or negatively charged functional groups in biochar (Ranjan and Rao, 2007; Fredlund et al., 2012). In addition, the normal loads applied during sample compaction and shearing reduced the inter-particular distance and improved the particle interlocking by the settlement of smaller particles into larger pore spaces, especially in biochar-amended silty sand that have clay particles (Sadasivam and Reddy 2015). The minimum inter particular distance with electrostatic attraction in BAS increased the bonding among the soil and biochar particles and hence, the c (Sun and Lu 2014). In another way, the samples were prepared at dry side of OMC i.e., partially saturated state and the amendment of biochar decreases the pore size but increases the porosity of soil (Sun and Lu, 2014; Hussain et al., 2020d). Therefore, the BAS had the higher suction compared to the bare soil due to smaller pores size which have induced apparent cohesion in BAS and hence higher c. According to unsaturated soil mechanics, the suction induces apparent cohesion in soil by pulling the soil particles together (Fredlund et al., 2012). Further, the samples were sheared under confined condition (DST) therefore the biochar induced cohesion could be the apparent cohesion.

The bare silty sand and pure sand showed ϕ value of 31.1±0.5˚ and 29.3 ± 1.3˚ respectively. The ϕ value in the silty sand increased to the maximum of 37.9±0.4˚ at 10% (w/w) biochar content thereafter remained nearly same with further increase of biochar amendment rate. In contrast, the amendment of biochar in pure sand decreased the ϕ to the minimum of 23.7±0.3˚ at 10% biochar content and further increase of biochar amendment

rate to 15% increased the ϕ, however, the magnitude was lower than the bare pure sand. The silty sand presents considerable (49%) amount of fines fraction of which 20% clay content (Fig. 4.1) that have lower frictional resistance compared to the biochar. The rough surface due to internally porous structure (Fig. 4.4) and angular shape of the biochar (MB) relative to the silty sand increased the surface frictional resistance or interlocking among the particles in silty sand after amendment and hence, higher ϕ in biochar-amended silty sand. However, in the case of pure sand, the large granular sand particles offered higher frictional resistance compared to the biochar which have resulted in lower ϕ in biochar-amended pure sand. The trends of increased c and ϕ in silty clay due to biochar amendment were observed by the past researchers (Zong et al. 2014; Reddy et al. 2015); further, no change of ϕ in silty loam soil after biochar amendment was also reported (Zong et al. 2016). Further, similar to the biochar-amended soil, the amendment of diatomite in soil was reported to be reduced the soil dry density and increased the c and ϕ and hence the shear strength of soil (Burger et al., 2001; Aksakal et al., 2013; Wiemer and Kopf, 2017). Thus, the trends are found to be consistent with the literature. The improved c and ϕ or the shear strength of the soils after biochar amendment could enhance the stability of bioengineered structures.

7.4 Influence of the altered shear strength on the stability of a hypothetical slope

In order to see the significance of the improved shear strength or parameters after biochar (MB) amendment on the stability, an infinite slope stability analysis was conducted using the obtained c and ϕ. In general, the stability of any slopes is represented by a factor of safety (FOS). The FOS for cohesive soil slope when the water table located below the slip surface is written as follows (Ranjan and Rao 2007)

$$FOS = \frac{c'}{\gamma_t \times H \times sin\alpha \times cos\alpha} + \frac{tan\phi'}{tan\alpha} \qquad (7.1)$$

where c' is the cohesion, φ' is the angle of internal friction, γ_t is total unit weight, α is slope angle and H is the depth of slip surface. When the water table located at the top of slip surface i.e., at the worst condition the FOS is written as

$$FOS = \frac{c'}{\gamma_{sat} \times H \times sin\alpha \times cos\alpha} + \left[\frac{\gamma'}{\gamma_{sat}} \frac{tan\phi'}{tan\alpha}\right] \qquad (7.2)$$

where γ_{sat} is the saturated unit weight and γ' is the submerged unit weight. The FOS was computed by assuming three slope scenario or angle (2H:1V, 1H:1V and 3H:1V), a depth of slip surface of 1.5 m, and the water table located below and top of the slip surface. The total

unit weight for the analysis was calculated from the dry density obtained at different biochar content. The saturated and submerged unit weight were calculated from the fundamental relationships among γ, e, G and S_r. The results or the evaluated FOS are presented in Table 7.1. The stability analysis was not conducted for the pure sand i.e., conducted only for the silty sand since the silty sand is more preferable over pure sand for the construction of slopes or embankments.

Table 7.1 Factor of safety (FOS) computed from equation 1 and 2 for bare and biochar amended silty sand.

Slope angle	**Type**	**Biochar content (%)**	**FOS**	**% increase in FOS due to biochar amendment**		
				Total	By increased c and ϕ	By decreased density
Water table below the failure surface						
2H:1V or 27˚	Bare soil	**0**	2.44	0	0	0
	BAS	**5**	3.23	32	27	5
		10	4.18	71	56	15
		15	4.54	87	68	19
1H:1V or 45˚	Bare soil	**0**	1.62	0	0	0
	BAS	**5**	2.23	38	32	6
		10	2.92	81	62	19
		15	3.23	100	76	24
3H:1V or 18.44˚	Bare soil	**0**	3.50	0	0	0
	BAS	**5**	4.58	31	26	5
		10	5.91	69	55	14
		15	6.40	83	65	18
Water table at the top of failure surface (Worst condition)						
2H:1V or 27˚	Bare soil	**0**	1.64	0	0	0
	BAS	**5**	2.21	35	32	3
		10	2.77	69	63	6
		15	3.05	86	78	8
1H:1V or 45˚	Bare soil	**0**	1.15	0	0	0
	BAS	**5**	1.61	39	36	3
		10	2.04	77	68	9
		15	2.27	97	86	11

Slope angle	Type	Biochar content (%)	FOS	% increase in FOS due to biochar amendment		
				Total	By increased c and ϕ	By decreased density
3H:1V or 18.44˚	Bare soil	**0**	2.31	0	0	0
	BAS	**5**	3.08	33	31	2
		10	3.85	67	62	5
		15	4.23	83	76	7

As presented in Table 7.1, the bare soil exhibited the FOS of 3.5, 2.44 and 1.62 under dry scenario while 2.31, 1.64 and 1.15 under worst scenario at 3H:1V, 2H:1V and 1H:1V slope angles. It increased to 6.4, 4.54 and 3.23 under dry, and 4.23, 3.05 and 2.27 under worst scenario after amendment of 15% biochar. Thus, the FOS increased with the increase of amendment rates of biochar from 5% to 15% in all three slope angles and under both dry and worst scenario (Table 7.1). The increase of FOS in BAS was contributed by the both increased shear strength parameters (c and ϕ) and decreased dry density of the soil after biochar amendment as could be seen from Equation 1 and 2. The individual contribution of increased shear strength parameters on the increasing FOS was evaluated by keeping the total unit weight of all bare and BAS same (constant) as of the bare soil. Similarly, the contribution of the decreased dry density on increased FOS was evaluated and reported in Table 7.1. The contribution of the increased shear strength parameters was observed to be higher over the decreased dry density in increasing the FOS (Table 7.1).

In general, the design of slope or landfill cover requires a minimum acceptable FOS of 1.5 for static analysis using the limit equilibrium method (Sadasivam and Reddy 2015). In the present study, the FOS was found to be 7.3-327% higher than the 1.5 in all biochar amended soil under all slope angles and water table scenario. The lowest FOS under steepest slope angle and worst condition was observed to be 7.33%, 36% and 51.33% higher than 1.5 in 5%, 10% and 15% BAS respectively. Hence, the BAS at all amendment rates satisfied the design criteria. Therefore, the BAS could be utilized in slope or embankment construction. However, in the present study, the shear strength parameters (c, ϕ) were not determined under saturated state and the undrained strength (UCS) showed a decreasing trend after biochar amendment. Thus, the shear strength or the c and ϕ of the BAS under saturated state need to be investigated which would better describe the biochar effect under water submergence.

7.5 Load bearing capacity of BAS

The load-bearing capacity of the soil was evaluated by the CBR test.

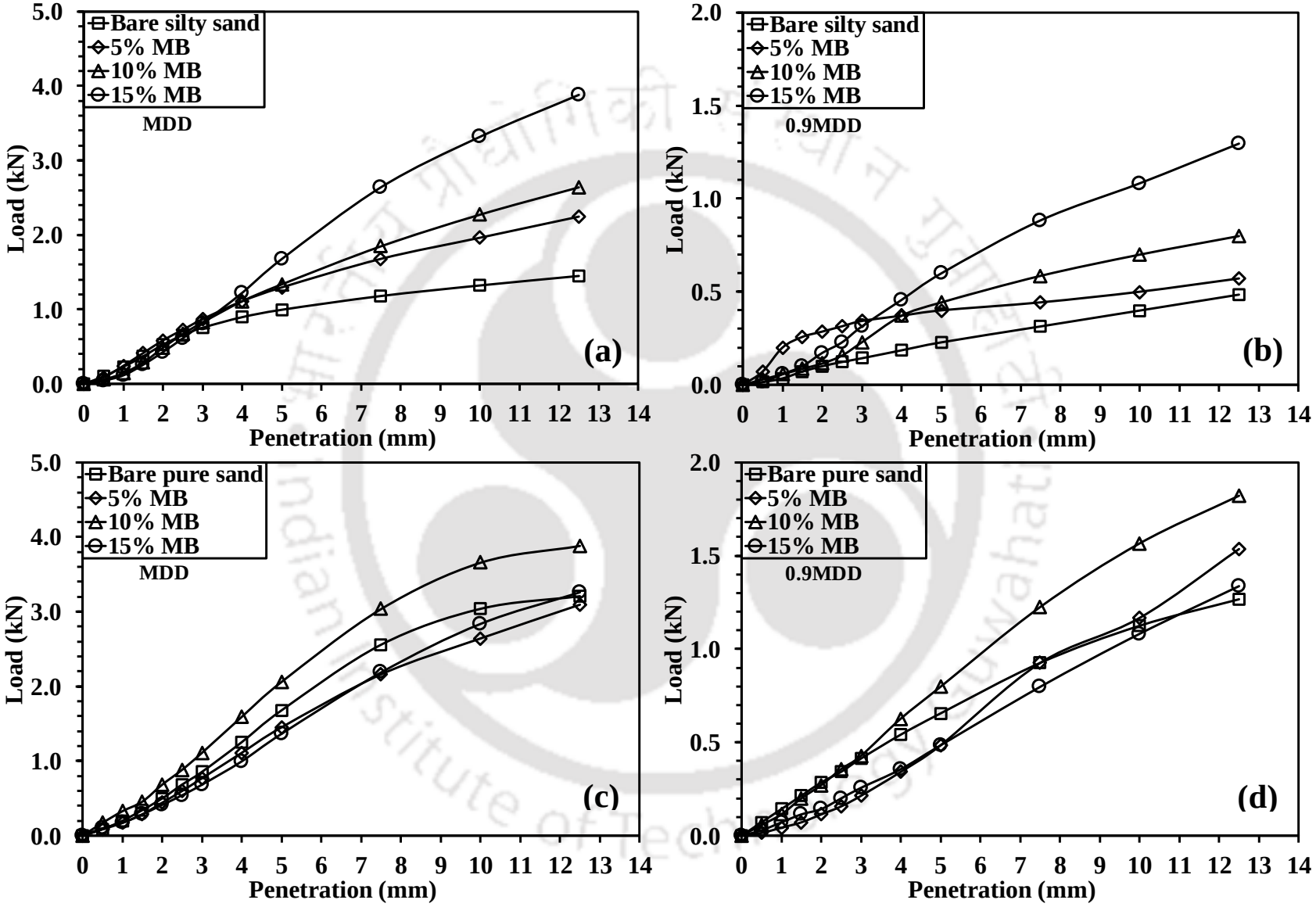

Fig. 7.5 Load-penetration responses of (a-b) Silty sand and (c-d) Pure sand.

The load-penetration responses of the bare and biochar-amended silty sand and pure sand under different compaction state are shown in Fig. 7.5 (a-d). The load-bearing capacity of the soils was observed to be increased with the increase of biochar amendment rates from 5 to 15% (Fig. 7.5). The highest load bearing capacity was observed with 15% biochar in silty sand and 10% biochar in pure sand. Relatively lower load bearing capacity was observed in soils compacted at 0.9MDD due to the loose state of soil at 0.9MDD. The load bearing capacity was further quantified by CBR value as the design and construction of embankments are based on the CBR value. The CBR values obtained for bare and biochar-amended soils are presented in Fig. 7.6 (a-b).

The soaked (96 hours) CBR value was found to be higher (20-165%) in BAS indicating the decreased tendency of compressibility of soil under load due to biochar amendment. The magnitude of the CBR value was found to be higher than 5 at MDD compaction state (Fig. 7.6a-b) which have satisfied the minimum required CBR value of 5 for non-cohesive soil (RDSO, 2018). The only biochar without soil exhibited the higher CBR value compared to the bare soils except for the pure sand at MDD which have shown higher CBR value compared to the biochar (Fig. 7.6a-b). The enhanced cohesion (Fig. 7.4a) due to the bonding between the soil and biochar particles of positive or negatively surface charged (functional groups) and the improved particles interlocking due to the higher frictional resistance (Fig. 7.4b) between soil and biochar particles of rough surface (Fig. 4.4) attributed to the higher load bearing capacity or CBR value in BAS (relative to bare soil). The samples in CBR test were confined by the mould and tested in the presence of vertical normal load therefore unlike undrained strength (UCS), the cohesion and frictional resistance were expected to be higher similar to the obtained by direct shear test (Fig. 7.4a-b). Further, the biochar absorbed and stored water under soaked condition due to the internally porous structure with surface functional groups (Fig. 4.4 and Fig. 4.6) that have resisted the penetration under load (Sadasivam and Reddy 2015). However, in the case of bare soil, the water soaking caused the lubrication (surface wetting) of the soil particles and led to the higher/excessive movement of soil particles or settlement under lighter load compared to the only biochar or BAS. The increase of CBR value in pure sand was observed to be restricted to 10% biochar content i.e., there was no further increase of CBR value observed at biochar content higher than 10% (Fig. 5b). This could be due to the lost effect of sand-biochar particles interlocking beyond 10% amendment.

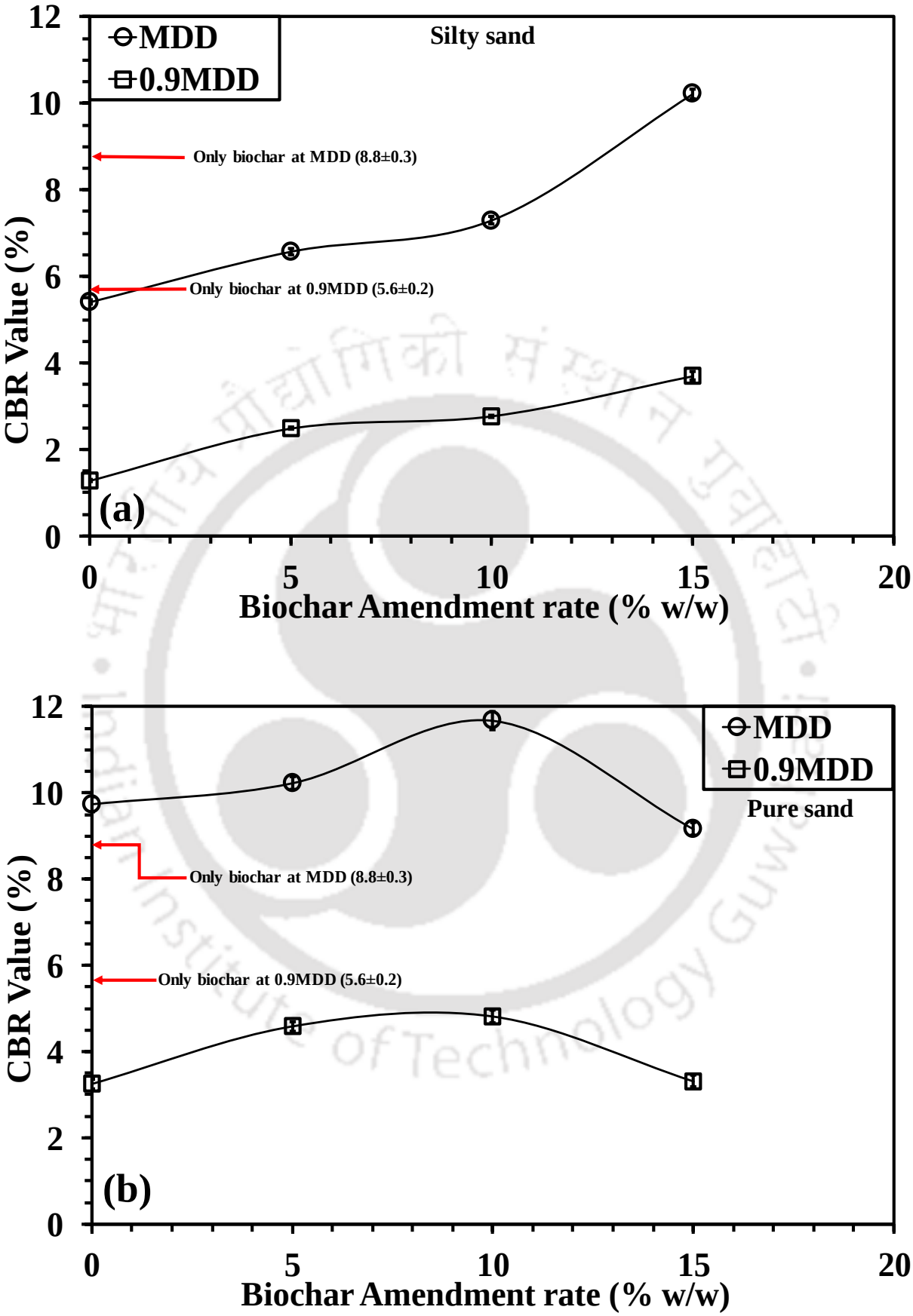

Fig. 7.6 Variation of CBR value with amendment rate of biochar (MB) in (a) silty sand and (b) pure sand.

The trend of increased CBR value of clayey soil amended with wood biochar was also reported by the past researcher (GuhaRay et al. 2019). Therefore, the construction of embankments with BAS would be beneficial due to the improved CBR value that will require lesser pavement or embankment thickness, as the IRC: 37-2012 (Guidelines for the design of flexible pavement) reported the lower thickness requirement of embankment component constructed with material of higher CBR value. Further, the improved CBR value due to biochar amendment was observed at both 0.9MDD and MDD compaction states which have satisfied the design criteria of embankments i.e., generally, design at compaction density between 0.9MDD and MDD (RDSO 2018; IRC: 37 2012).

7.6 Influence of biochar on soil desiccation cracks

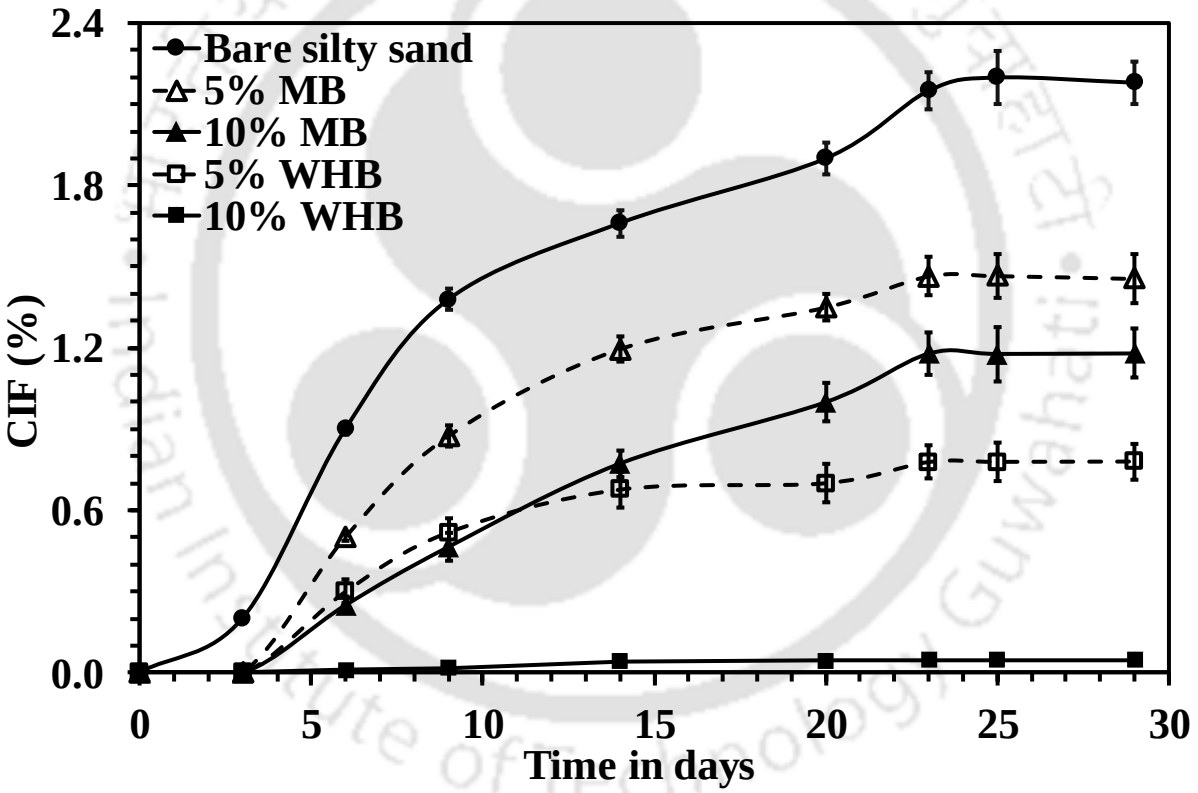

Fig. 7.7. Variation of desiccation cracks (CIF) with time in different types BAS.

Fig. 7.7 presents the variation of crack intensity factor (CIF) with time for bare, and 5% and 10% BAS. In figure, the time zero represents the day of wetting or saturation of the bare and amended soil samples. The CIF was observed to be zero for all bare and BAS on day zero which indicates the saturated condition of the samples. The zero CIF was found to be continued up to day 4 after saturation in BAS, indicating a prolonged saturation of BAS compared to the bare soil which is also supported by the higher AEV in BAS (Table 6.1).

With the increase of time after saturation, the CIF was found to be increased in all bare and BAS and became constant after reaching a peak value of 2.2 ± 0.1 in bare soil and 0.78 ± 0.07 to 1.47 ± 0.08 in BAS. The maximum CIF was observed to be 2.2 ± 0.1 in bare soil and this could be the maximum crack potential of the soil under the specified compaction state and boundary condition. In a previous study on silty clay compacted at the same compaction state of the present study, Bordoloi et al. (2018a) reported a maximum CIF value of 2.65 ± 0.56. However, in the present study soil consist of lower (49%) fine (<0.075 mm) content against higher (75%) content in Bordoloi et al. (2018a). Therefore, a lower CIF was acceptable as soil with lower fine content exhibits lesser cracks compared to soil with higher fine content (Yesiller et al. 2000). The increase of CIF with time was attributed to the decreased soil strength by alternate drying after wetting, and the increased tensile stress in soil surface. The shrinkage of soil due to drying causes the breaking of micro bonds and rearrangement of the soil structure and hence decreases the soil strength. Further, the drying or evaporation of water with time causes the generation of higher suction which in turn develops large tensile stress in the soil surface (Tang et al. 2010). Importantly, the tensile stress developed due to suction was maximum at peak CIF and thereafter, further increase of suction causes no change in the tensile stress and hence, in the CIF (Yesiller et al. 2000).

The amendment of the biochar (WHB, MB and SBB) decreased the CIF i.e., the CIF was observed to be lower in BAS compared to the bare soil. The improved water retention in BAS relative to bare soil (Fig. 6.1, Table 6.1) attributed to the lower CIF in BAS. The higher water content due to improved water retention in BAS resisted the generation of suction or the development of tensile stress by drying or evaporation as a results, lower cracks or CIF (Tang et al. 2010). The smaller size pores responsible for higher water retention in BAS holds water tightly and does not allow water to escape easily (lower evaporation) and hence resist the cracks formation. Among the biochar types tested (WHB, MB and SBB), the MB-amended soil showed the highest CIF and the amendment of SBB showed no cracks under both the 5% and 10% amendment rates. The zero CIF or no cracks in SBB-amended soil was attributed to the highest water retention after AEV as observed from the lowest value of n in SBB-amended soil (Table 6.1). Cracks generally start developing after AEV and extend further with increase in suction (Bordoloi et al. 2018b). Trend of decreased CIF or cracking tendency of soil due to biochar amendment was also reported in the literature (Zong et al. 2014; Bordoloi et al. 2018b). However, the effect of different biochar types that controls the biochar properties was not considered in the reported literature. The reduced desiccation

crack potential of BAS would be beneficial for bioengineered structures, in terms of controlling the infiltration rate, excess pore water pressure and maintaining the structural stability.

7.7 Summary and conclusions

The shear strength, load bearing capacity and desiccation crack potential of different types biochar-amended soils are presented. The undrained shear strength i.e., the UCS of soil was found to be decreased in the range of 22-56% after amendment of different types biochar. The amendment of SBB showed the highest decrease in UCS i.e., the lowest UCS among the biochar tested. The shear strength parameter cohesion (c) and angle of internal friction (ϕ) of the soils tested by direct shear test were found to be increased in the range of 22-227% after biochar (MB) amendment. However, the ϕ was observed to be decreased by 9-19% in pure sand with biochar amendment. Relatively higher increase of c after biochar amendment was found in silty sand over the pure sand. The increased c and ϕ after biochar amendment was observed to enhanced the factor of safety (FOS) or improved the stability of a hypothetical slope. The load-bearing capacity or the CBR value of the soils was found to be improved (20-190%) after biochar (MB) amendment. Comparatively higher improvement of CBR value was observed in silty sand over the pure sand. Although the required designed CBR value for embankments depends on the soil types used and the traffic or axel load, the RDSO 2018 (research design and standards organization) recommended a minimum CBR value of 5 for non-cohesive soil compacted at 100% of MDD which is satisfied by all the soil types tested with and without biochar in the present study. The desiccation crack potential of the soil was found to be decreased after biochar amendment i.e., the BAS exhibited lower cracks (CIF) compared to the bare soil. Even though, the shear strength parameters and the slope stability improved after biochar amendment, the undrained shear strength (UCS) of the soil was found to be decreased therefore, more comprehensive investigation of undrained shear strength of BAS need to be conducted. Noticeably, at lower biochar amendment rate (5%), the UCS values were found to be higher than the 200 kPa which is the recommended minimum UCS value for most of the bioengineered structures (USEPA, 1992; Bora et al., 2020).

CHAPTER 8
PERFORMANCE OF VEGETATION IN BAS

8.1 Introduction

The stability and function of bioengineered structures are highly dependent on the performance of vegetation. The vegetation covers the surface and protects the structures from surface erosion and failure (Coppin and Richards, 1990; Rebeca et al., 2010). The vegetation roots act as soil reinforcement and increases the strength and stability by anchoring the soil around (Wu et al., 1979; Mahannopkul and Jotisankasa, 2019). Further, the root water uptake to meet the plants need and compensate the water loss due to evapotranspiration generates suction in the root zone or soil which in turn contributes to the strength and stability (Garg et al., 2015; Fredlund et al., 2012). Therefore, proper growth or development along with healthy status of vegetation is crucial for the effective functioning of the bioengineered structures. The biochar amendment already showed impact on soil properties however the biochar effect on vegetation growth and health need to be investigated for application in bioengineered structures. Thus, the growth and health status of a non-crop, grass species in different types BAS were investigated and presented in this chapter. The growth was quantified by the vegetation density (VD), leaves count, and shoot and root biomass. The health status of the grass was evaluated by monitoring the stomatal conductance (SC), photosynthetic yield (PY) and drought stress or suction at the root zone.

8.2 Growth of vegetation in different types BAS

8.2.1 Variation of VD and leaves count with time

Fig. 8.1 (a-d) highlights the variation of vegetation growth parameters i.e., the vegetation density (VD) and leaves count in different biochar-amended silty sand and sand. The day zero in figure (x-axis) indicates the day of transplantation of the grass. The VD was observed to be increased with time and reached the maximum or peak where vegetation near completely covered the column surface. A higher VD in all the BAS compared to the bare soil was observed for the entire growth period after transplantation. The amendment of the biochar decreased the dry density (Fig. 4.3), and increased the water retention capacity i.e., higher plant available water (Fig. 6.1, Table 6.1 and Table 6.2), pH and EC (Table 4.3) of the soils which have enhanced the growth of roots and vegetation and hence the VD.

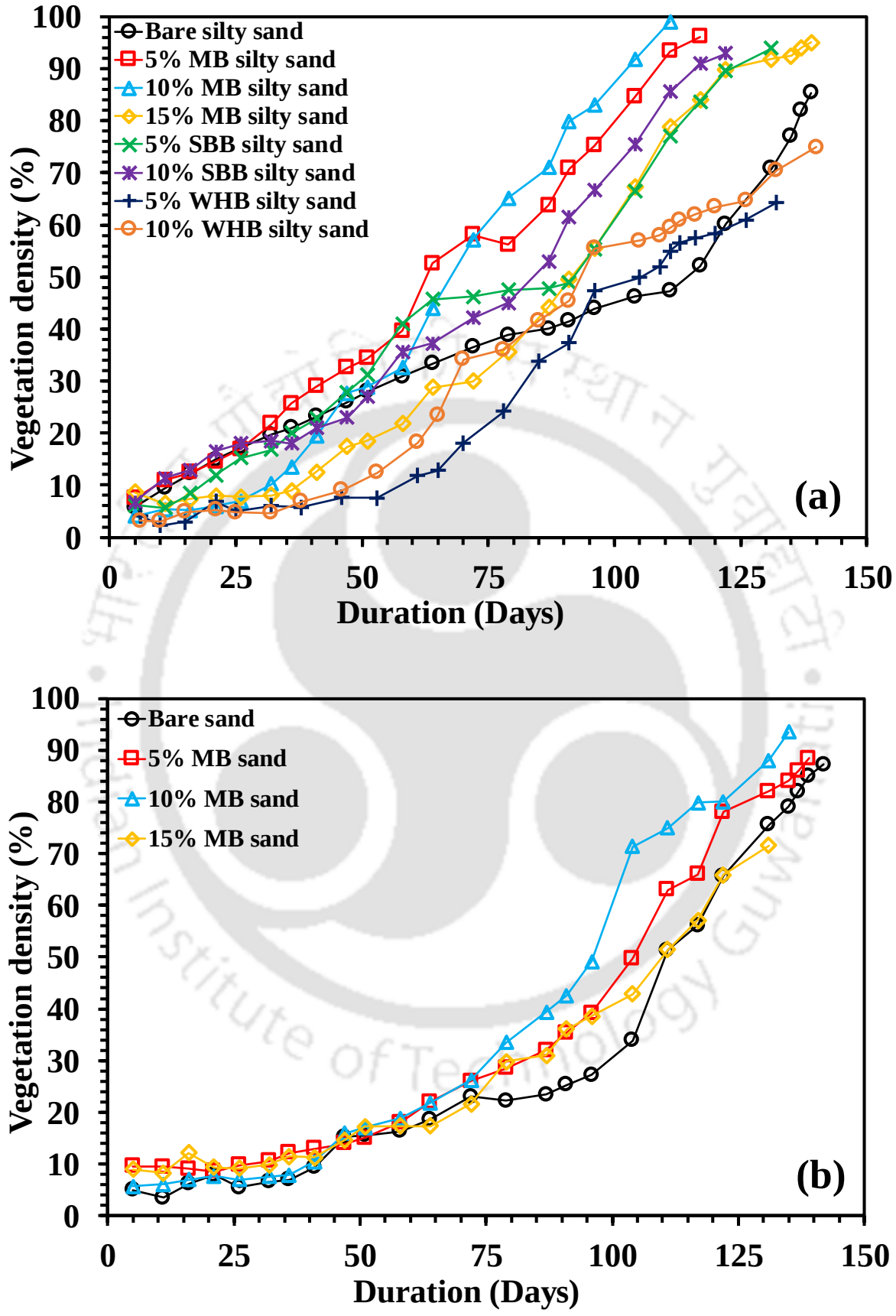

Fig. 8.1 Variation of VD in (a) different biochar-amended silty sand and (b) MB-amended sand.

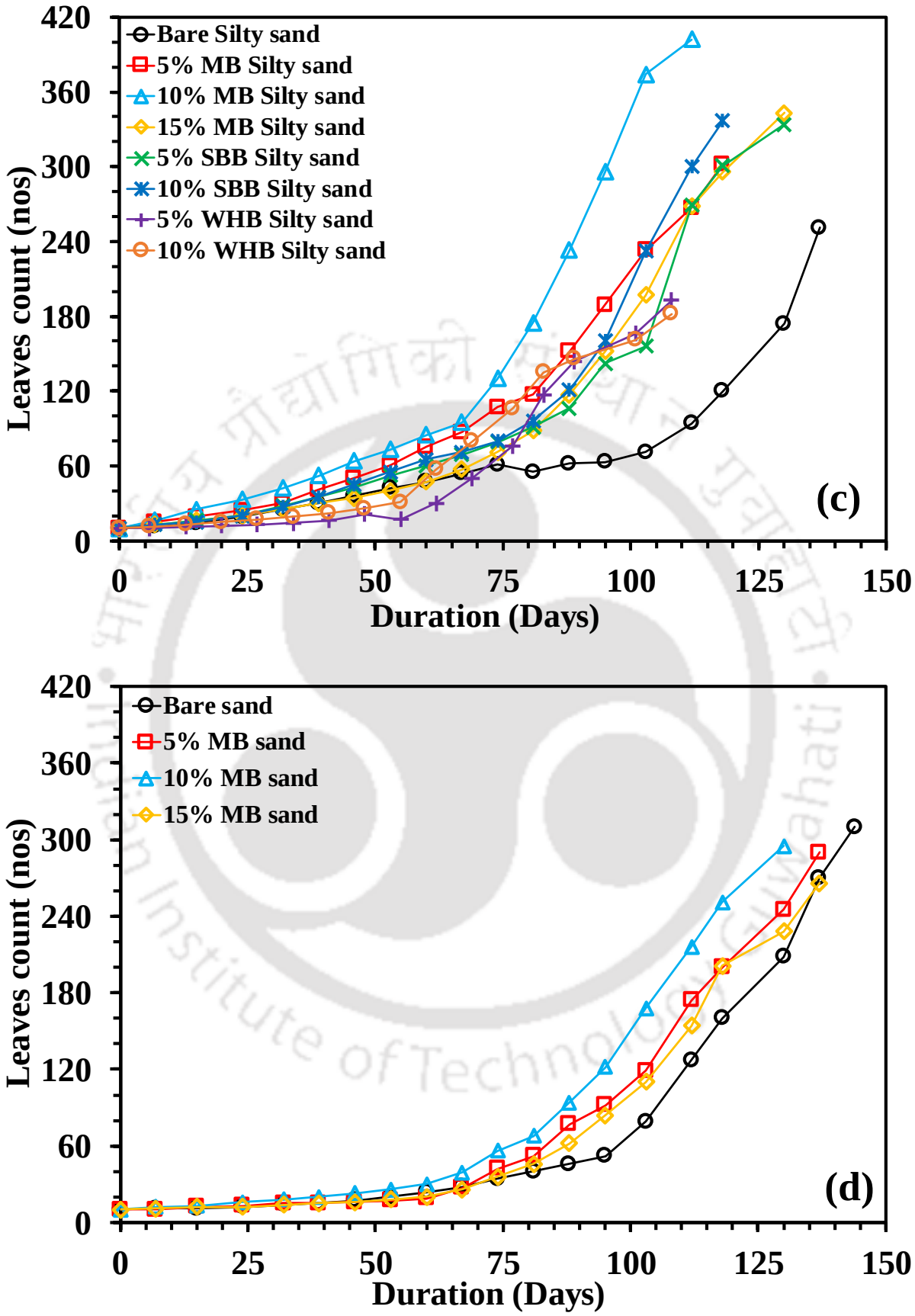

Fig. 8.1 Variation of leaves count in (c) different biochar-amended silty sand and (d) MB-amended sand.

Furthermore, the increase of biochar amendment rates from 5% to 10% found to be increased the VD and beyond i.e., at 15% no further improvement was observed (maximum at 10% biochar). The increase of amendment rates up to 15% found to increase the water retention and pH, and decrease the dry density of the soils. However, for the healthy growth of vegetation, there need to be an optimal soil pH value that might have reached at 10% biochar amendment rate and further increase of pH could cause no improvement, in fact adverse effect could be observed which has been occurred in 15% BAS. Considering the effect of biochar types, the MB-amended soil exhibited the highest VD among the different types biochar tested. Although, the SBB and WHB-amended soil showed the higher water retention capacity and lower dry density compared to MB-amended soil (Fig. 4.3 and Fig. 6.1), the pH and nutrient content in MB played the role in higher growth or increasing the VD. Comparing the effect on soil types, the amendment of MB exhibited a delayed growth of the vegetation or lower VD in pure sand with respect to that in the silty sand. The silty sand showed higher water retention capacity compared to the pure sand (Fig. 6.2) and the amendment of biochar in acidic silty sand and neutral sand changed the pH to neutral and basic state (Table 4.3) respectively. Therefore, the lower water retention and basic (pH) nature of biochar-amended sand compared to the biochar-amended silty sand led to the delayed vegetation growth or lower VD in sand.

The leaves count (Fig. 8.1c-d) of the vegetation obtained in different BAS represents the growth similar to the VD; however, the significance of leaves count lies in the evapotranspiration. The evapotranspiration and hence the evapotranspiration induced suction is dependent on the leaves area or leaves count. The stomata, responsible for transpiration is mostly located in the surface of leaves. The larger the leaves count, higher could be the evapotranspiration and induced suction in soil. The BAS irrespective of biochar types showed the higher leaves count compared with the bare soil. Depending on the soil hydraulic conductivity and water retention ability, the higher leaves count in BAS could lead to the higher evapotranspiration or quick removal of water from soil after wetting event (precipitation) in bioengineered structures.

8.2.2 Variation of VD with suction

Fig 8.2 (a-b) presents the variation of VD with suction for drought period (i.e., growth completion to wilting) in silty sand and sand amended with different types biochar.

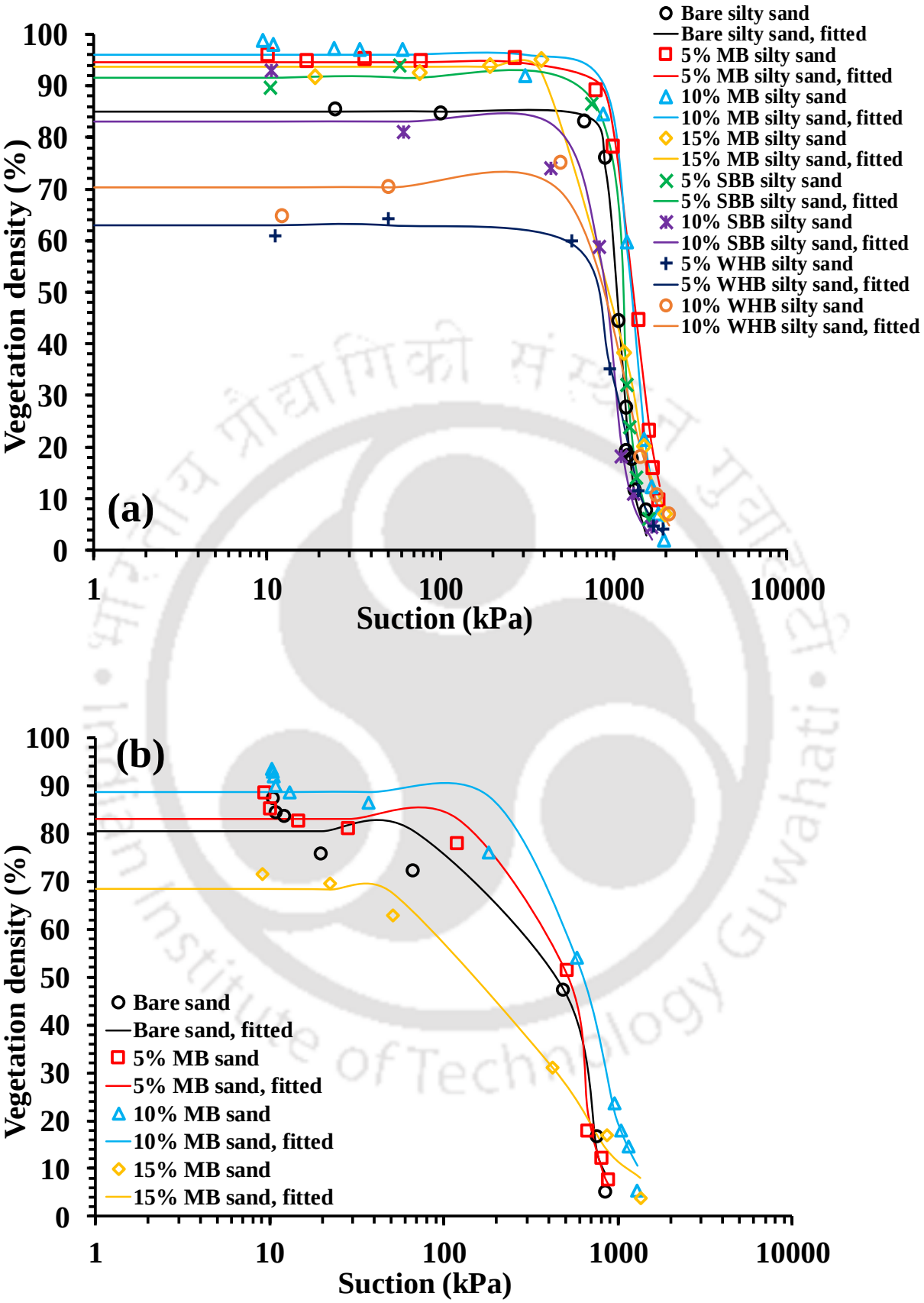

Fig. 8.2 Variation of VD with suction in different BAS (a) silty sand and (b) sand.

The VD versus suction plots were fitted to the correlation proposed by Gadi et al (2019) as given below:

$$\boldsymbol{VD(\Psi) = VD_{min} + \frac{VD_{max} - VD_{min}}{[1 + (\alpha(\Psi))^{n}]^{1-\frac{1}{n}}}} \qquad (\mathbf{8.1})$$

where VD (Ψ) is the vegetation density as function of suction (m^2/m^2), VD_{max} is the maximum vegetation density (m^2/m^2), VD_{min} is the minimum vegetation density (m^2/m^2), α is the fitting parameter related to the suction at which VD start decreasing or wilting starts ($\alpha > 0$) and n is the fitting coefficient associated with the curvature or the slope of the curve (n>1). The fitting parameters are presented in Table 8.1. The R^2 value was observed to be in the range of 0.97-0.99 which indicates the good fit of the equation. The suction at which the wilting start is termed as ψ_w and graphically measured from the curves.

Table 8.1 Fitting parameters of VD vs suction curve fitted using correlation proposed by Gadi et al (2019).

Type	Biochar (%, w/w)	VD_{max} (%)	VD_{min} (%)	α (kPa^{-1})	ψ_w (kPa)	n (-)	m (-)	R^2 value
Bare SS	0	85	0	0.001	800	10.1	0.9	0.99
WHB-SS	5	63	0	0.001	700	5.1	0.81	0.998
	10	70	0	0.001	650	5.1	0.81	0.986
SBB-SS	5	91.5	0	0.001	1000	8.1	0.88	0.998
	10	83	0	0.001	730	7	0.86	0.98
MB-SS	5	94.5	0	0.001	950	6.4	0.84	0.996
	10	96	0	0.001	900	7.55	0.87	0.996
	15	93.6	0	0.001	600	4.5	0.78	0.998
Bare sand	0	80.5	0	0.002	300	4.96	0.8	0.97
MB-sand	5	83	0	0.002	330	5.91	0.83	0.99
	10	88.7	0	0.002	310	3.61	0.72	0.98
	15	68.4	0	0.004	100	2.3	0.57	0.99

SS- silty sand, m=(1-1/n)

It could be observed from Fig. 8.2b that the increase of soil suction due to evapotranspiration caused no change in the VD up to a suction equivalent to ψ_w and further increase of suction beyond ψ_w decreased the VD and reached the minimum at permanent wilting point (PWP). The biochar amendment showed no consistent effect on ψ_w except the MB-amended soil,

where ψ_w increased relative to the bare soil. The VD gradually decreased in BAS as observed from the smaller *n* value (Table 8.1) whereas a steep decrease of VD (larger *n* value) could be observed in bare soil. Further, relatively gradual decrease in VD could be observed in bare and biochar-amended sand (Fig. 8.2b) over the silty sand (Fig 8.2a). The magnitude of ψ_w was found to be higher in silty sand compared to the sand (Table 8.1), indicating the longer stay of vegetation without wilting in silty sand compared to sand. The VD was observed to be negligible in all bare and BAS at PWP. The PWP where the vegetation completely wilted was decided based the negligible magnitude (reading) of plant health parameters (i.e., SC and PY). The variation of PWP in different biochar-amended soils is presented in Fig 8.3.

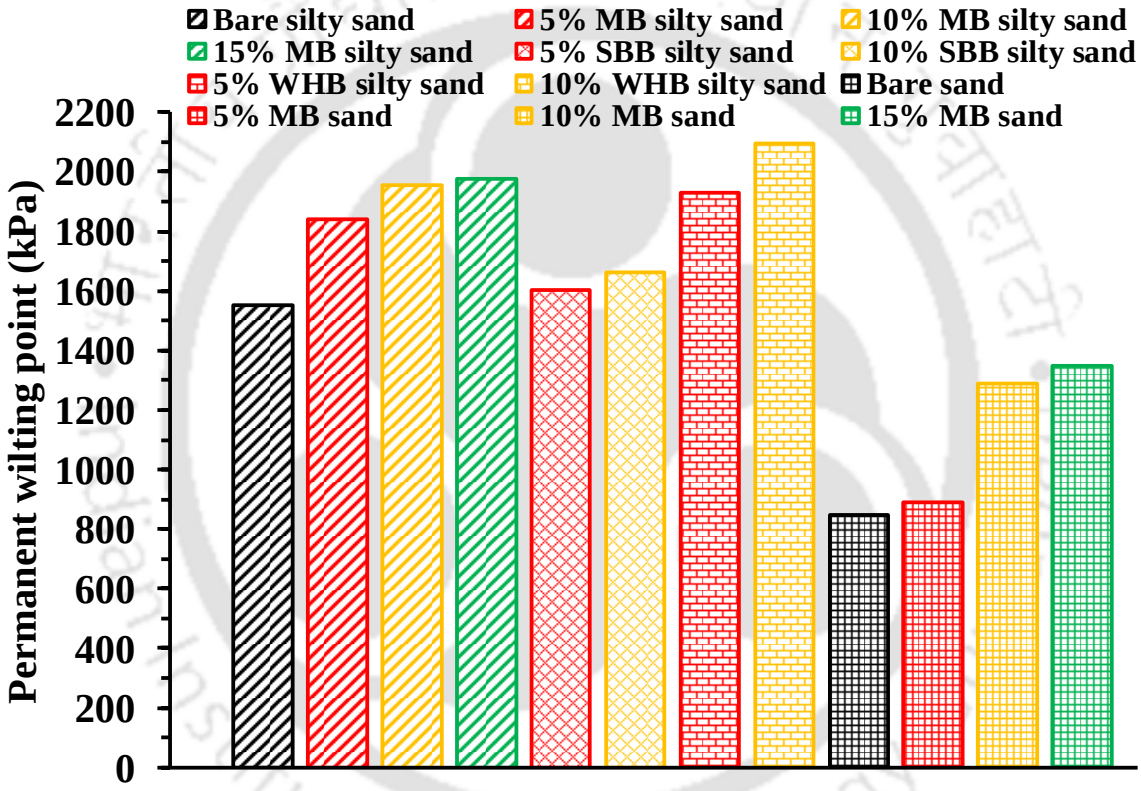

Fig. 8.3 Variation of permanent wilting point in different BAS.

The PWP was observed to be higher in BAS irrespective of biochar types compared to the bare soil. Further, the increase of biochar amendment rates irrespective of biochar types was found to increase the PWP. The amendment of biochar altered the pore size distribution of soils by decreasing the pore size or forming the smaller size pores which have stored water at a higher suction relative to the bare soil and hence the higher PWP. Among the different biochar types tested, the WHB-amended soil exhibited the largest PWP due to the smaller pore size in WHB-amended soil relative to other BAS that have stored water at larger suction and led to the largest PWP. The PWP was found to be soil specific as it was evident from the

smaller magnitude of PWP in bare and biochar-amended sand compared to the larger PWP in silty sand. Thus, the PWP was found to be varied with the soil and biochar types along with the biochar amendment rates. The larger magnitude of PWP or higher PWP in BAS signifies the survivability of vegetation a larger suction or drought stress in BAS compared to the bare soil which will be beneficial for the bioengineered structures.

8.2.3 Variation of shoot and root mass in BAS

Fig 8.4 (a-e) highlights the variation of dry shoot, roots and root mass density in different types biochar-amended soils. The root mass density i.e., the root mass variation with depth (Fig 8.4 a-b) showed a gradual decrease along the depth in both bare and biochar-amended soils. The grass species tested in the present study had fibrous root system due to which most of the roots were grown at the top surface. In addition, the higher soil confinement along the depth restricted the root growth at the deeper depth. Thus, the biochar amendment increased the root mass mainly at the shallow depth i.e., near top surface which is beneficial for anchoring the top soil from erosion and hence the failure. The total dry root mass presented in Fig. 8.4c was found to be higher in biochar-amended soils compared to the bare soil and the increase of amendment rate beyond 10% i.e., 15% showed no further increase in root mass. The decreased soil dry density or increased porosity after biochar amendment facilitated the roots to easily penetrate without resistance through soil. In addition, the higher plant available water content due to higher water retention capacity and the abundant microorganism due to improved urease activity in BAS assisted the higher and healthy root mass growth. The higher or near neutral pH of BAS offers a suitable medium for the enzymatic and microbial activity by enhancing the microbial diversity and community structure in the root zone that helps in the efficient cycling of nutrient for plant use. Previous studies on soil-biochar-microbial interaction found an enhanced microbial diversity and community structure along with improved physicochemical properties in soil after biochar amendment (Chen et al., 2013; Zhu et al., 2017; Wong et al., 2019). Soil enzymatic activities that controls the soil nutrient cycling ability were found to be increased after biochar amendment (Ghosh and Maiti, 2021; Ng et al., 2021).

The MB-amended soil showed the highest root mass among the biochar tested. The MB-amended soil exhibited lower water retention capacity and higher dry density compared to SBB and WHB-amended soil; however, the higher pH and nutrient content in MB-amended soil played the role in enhancing the root mass growth similar to VD.

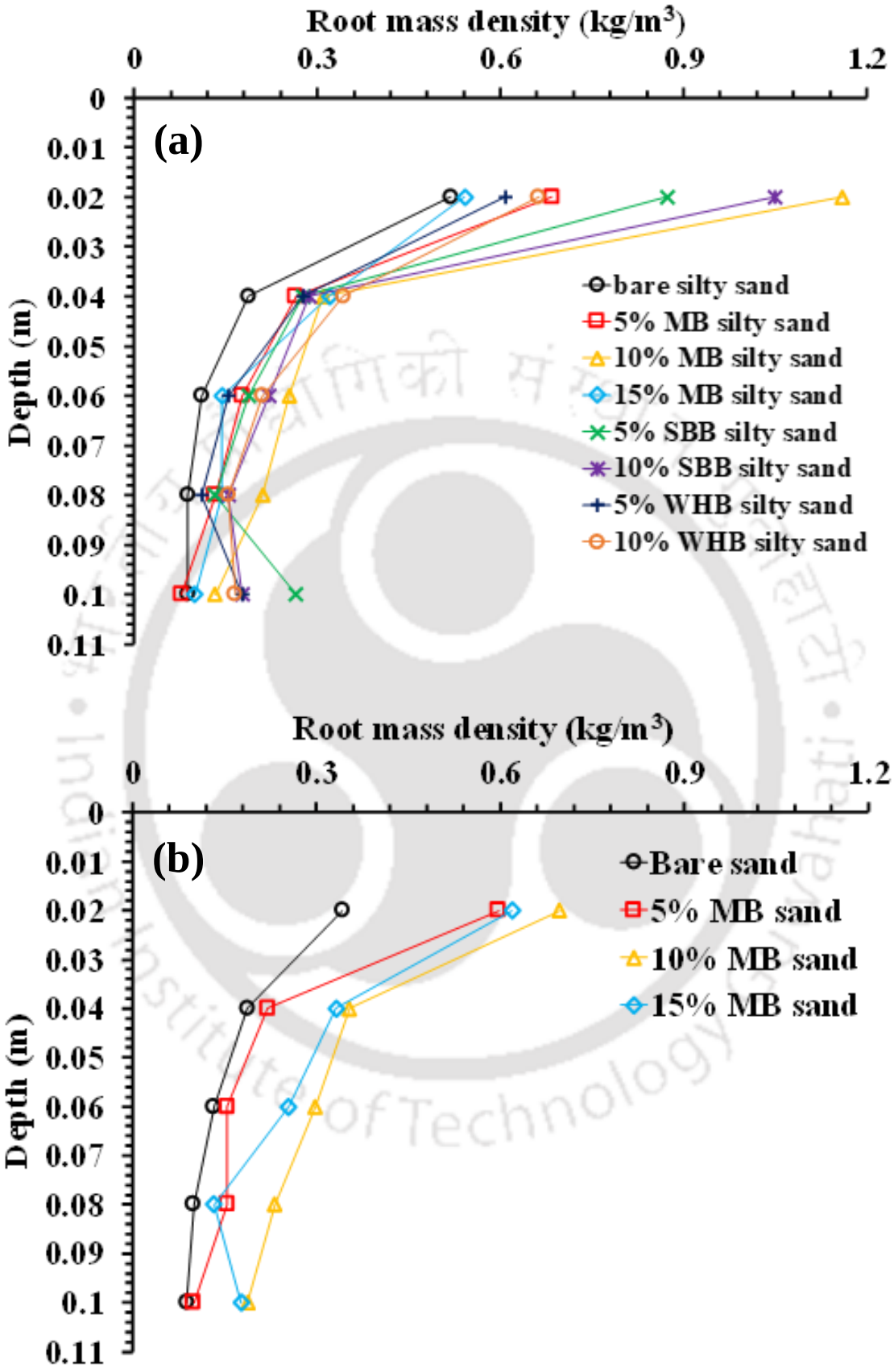

Fig. 8.4 Variation of root mass density in (a) different biochar-amended silty sand and (b) MB-amended sand.

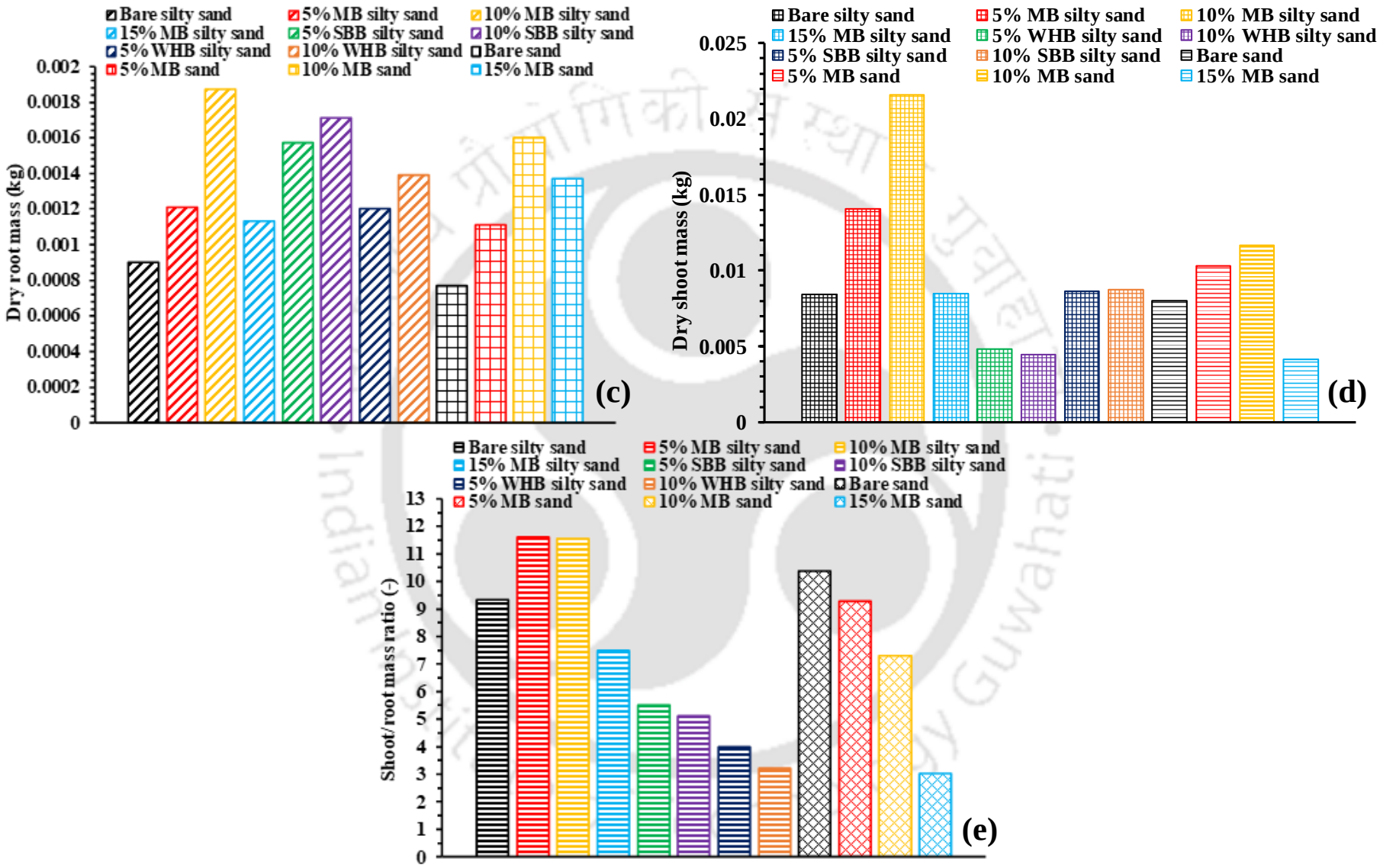

Fig. 8.4 Variation of root mass (c), shoot mass (d) and shoot to root mass ratio (e) in different biochar-amended soils.

The two different soil types tested, the higher root mass was observed in bare and biochar-amended silty sand compared with the sand. Although, the porosity in biochar-amended sand was higher relative to silty sand (Table 6.3), the suitable pH (neutral) and better microbial activity and nutrient cycling ability of silty sand (both bare and biochar-amended) let to the higher root mass growth in silty sand. The results of dry shoot mass (Fig 8.4d) followed the similar trend that of the VD. The amendment of the MB showed increase in dry biomass both in the silty sand and sand. However, the amendment of WHB and SBB showed no significant change in dry shoot biomass. As highlighted in Fig 8.4e, the shoot to root mass ratio was found to be decreased after biochar amendment due to the lower dry shoot mass and higher roots mass in BAS. In literature, the shoot and root mass of grass (*cynodon dactylon*) was found to be higher in peanut shell BAS after two years of monitoring (Ni et al., 2020). Similarly, higher growth of roots and shoot were also reported for *schefflera arboricola* grown in peanut shell and wood BAS by Ng et al. (2021). Therefore, the trends observed are consistent with the literature. The higher root mass or lower shoot to root mass ratio in BAS is advantageous of improve the anchorage of top soil and root water uptake, and hence the stability of the soil against failure (hydrologic and mechanical effect); thus, suggest the application of BAS in bioengineered structures.

8.3 Variation of SC and PY in BAS

8.3.1 Variation of SC and PY with time

Fig. 8.5(a-b) highlights the variation of SC with time in different biochar-amended silty sand and sand for the entire growing period (120 days). Considerable day to day variation in the SC could be observed in both the soil types even after maintaining the moisture level same at field capacity or regular irrigation for throughout the growth period. The fluctuation in the weather parameters as presented in Fig. 3.10, especially temperature was attributed to the variation in SC with time. The daily temperature was observed to be fluctuated in the entire growth period. The leaf porometer evaluates the SC based on the measurement of temperature and relative humidity where a small change in the temperature could lead to the big difference in the SC. The effect of diurnal variation of temperature and relative humidity on the SC was not expected as the measurements or readings were taken in a same time of the day for the entire monitoring period. Further, the variation could also be contributed by the aging of the leaves with time which was not quantified.

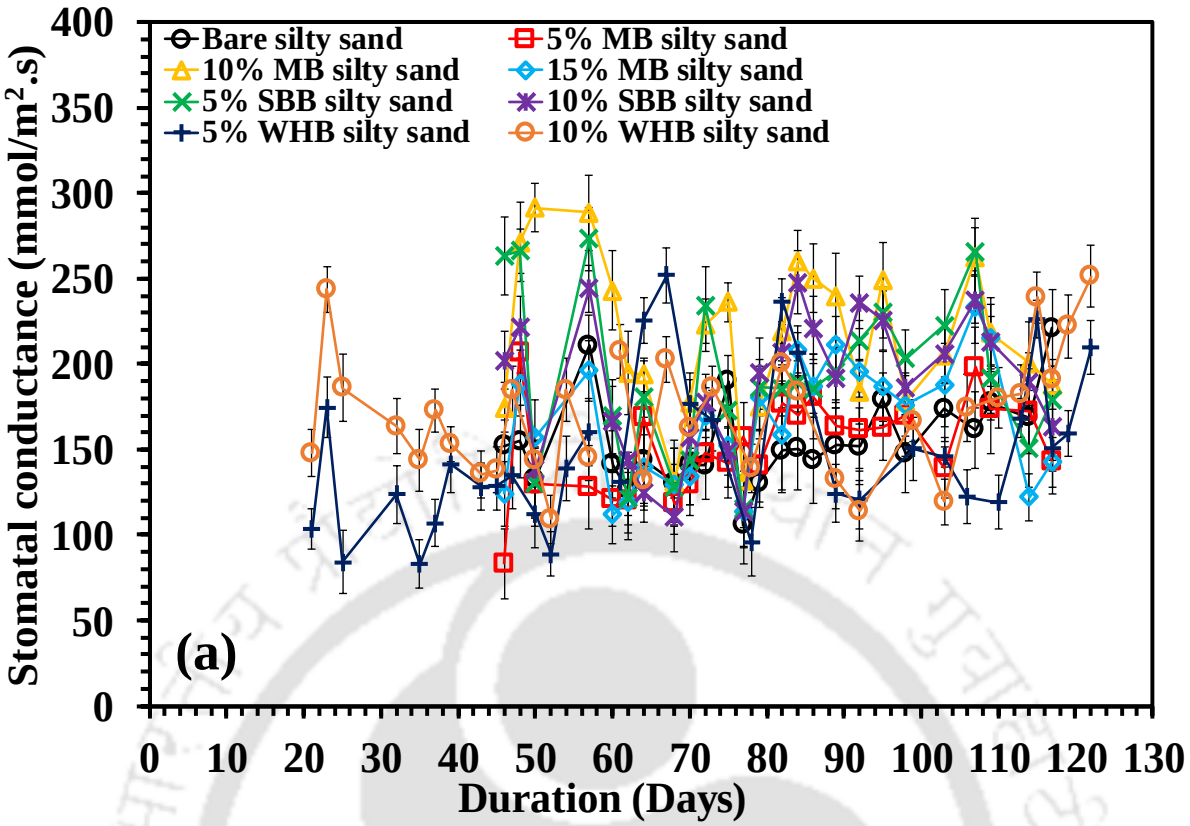

Fig. 8.5 (a) Variation of SC with time in different biochar-amended silty sand.

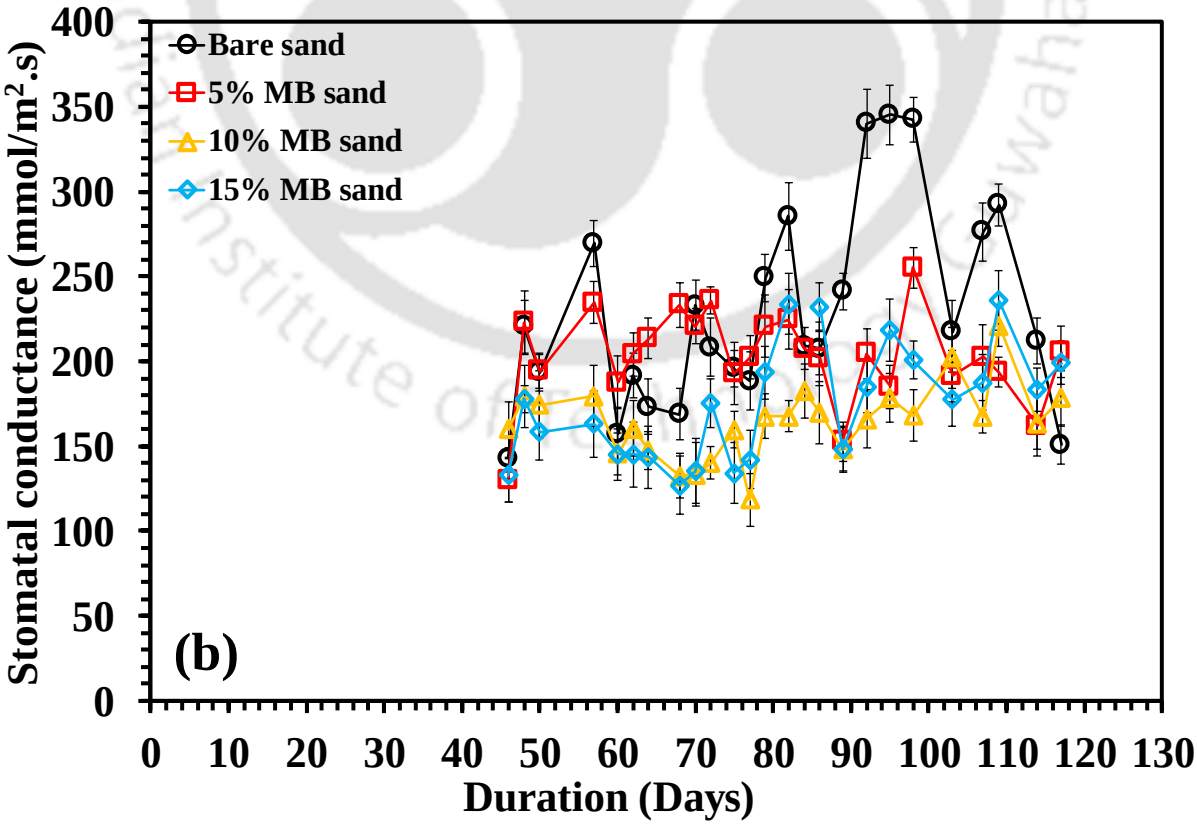

Fig. 8.5 (b) Variation of SC with time in MB-amended sand.

Fig. 8.6 (a-d) presents the daily variation of the photosynthetic yield (PY), F_v/F_m (maximum) and PY(II) (effective) in different biochar-amended soils for the entire growth period. The magnitude of the F_v/F_m and PY(II) was found to be in the range of 0.7-0.78 and 0.65-0.75 which are near to the maximum (0.84) and thus indicates the healthy status of the vegetation. The daily variation in both F_v/F_m and PY(II) was observed to be negligible. The MINI-PAM measures the PY based on the light fluorescence and the measurements of F_v/F_m and PY(II) were taken at the same time (10AM to 1PM) of the day for the entire growth period. Therefore, the variation in light or fluorescence in different days was expected to be negligible and hence its effect on PY was also expected to be negligible due to which the PY showed no major daily variation. A marginal difference between the PY of bare and different biochar-amended soils could be seen from the figure that have attributed the different leaves age among the bare and BAS.

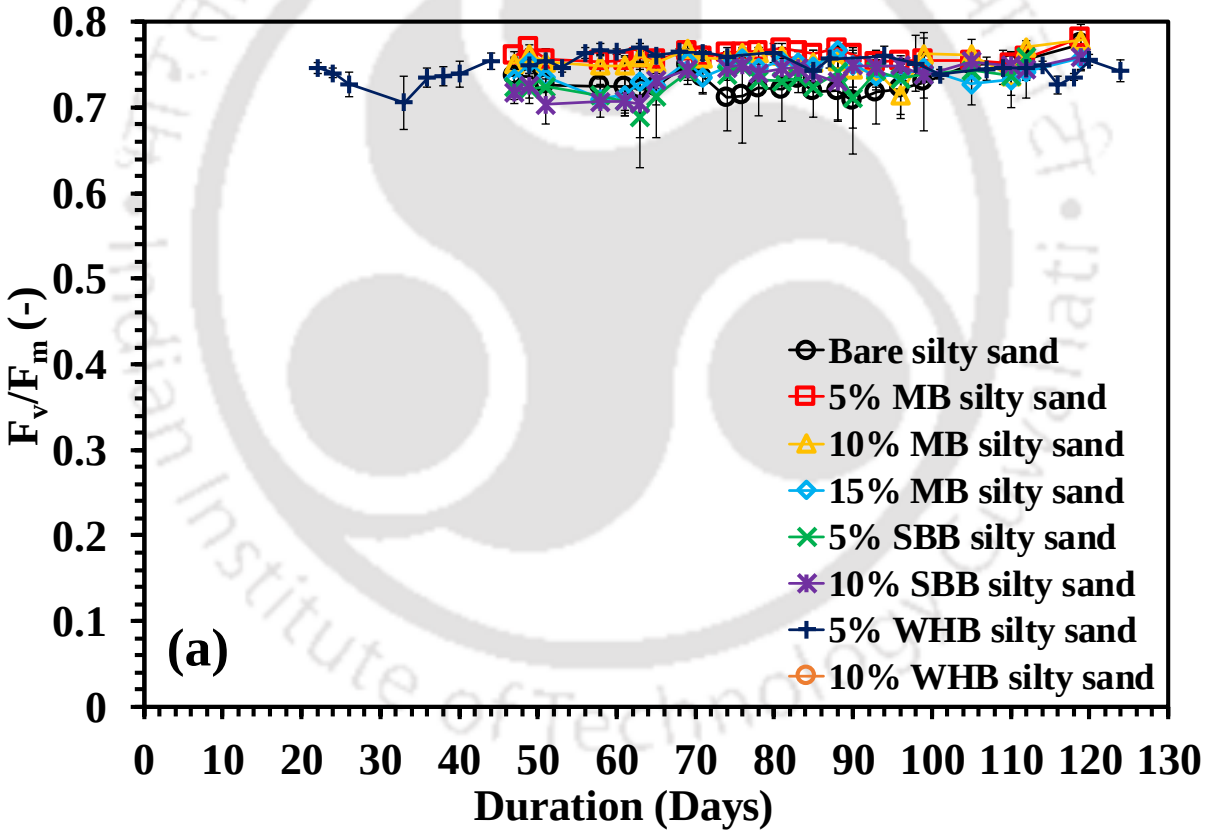

Fig. 8.6 (a) Variation of F_v/F_m with time in different biochar-amended silty sand.

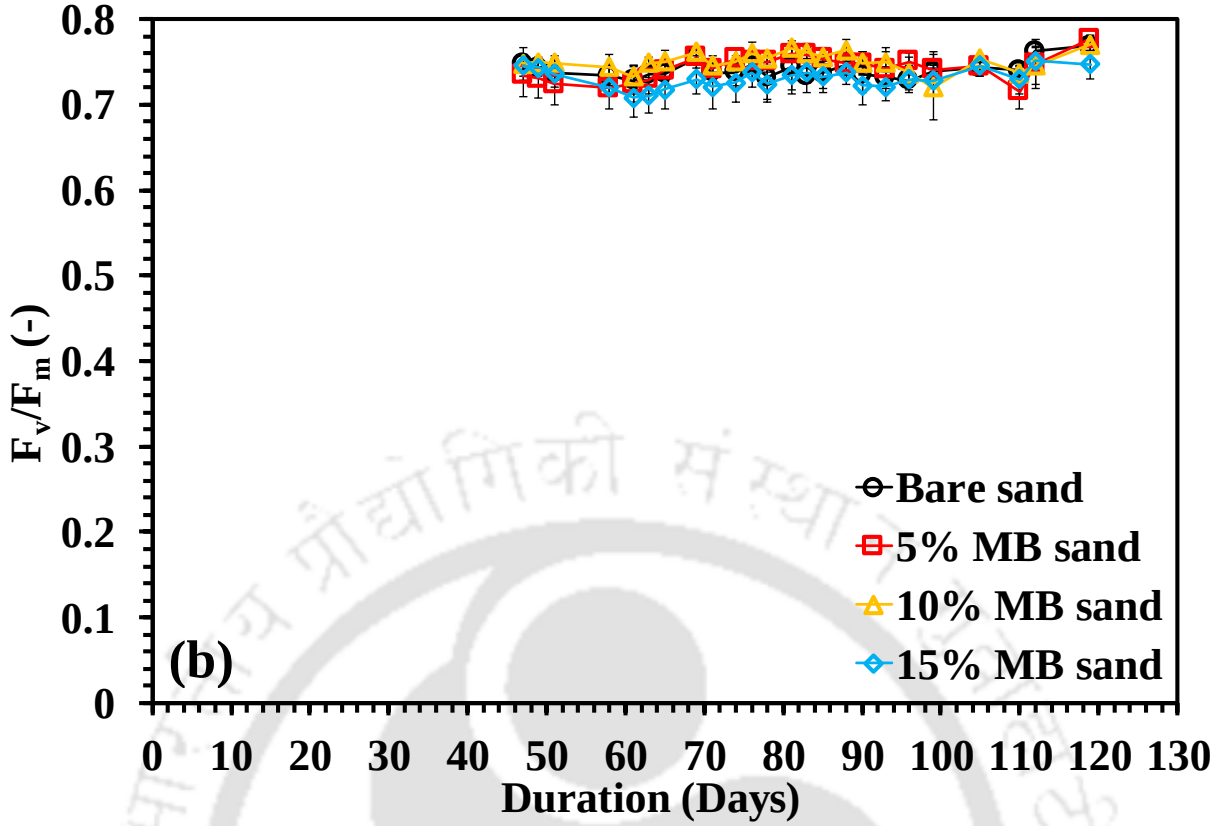

Fig. 8.6 (b) Variation of F_v/F_m with time in MB-amended sand.

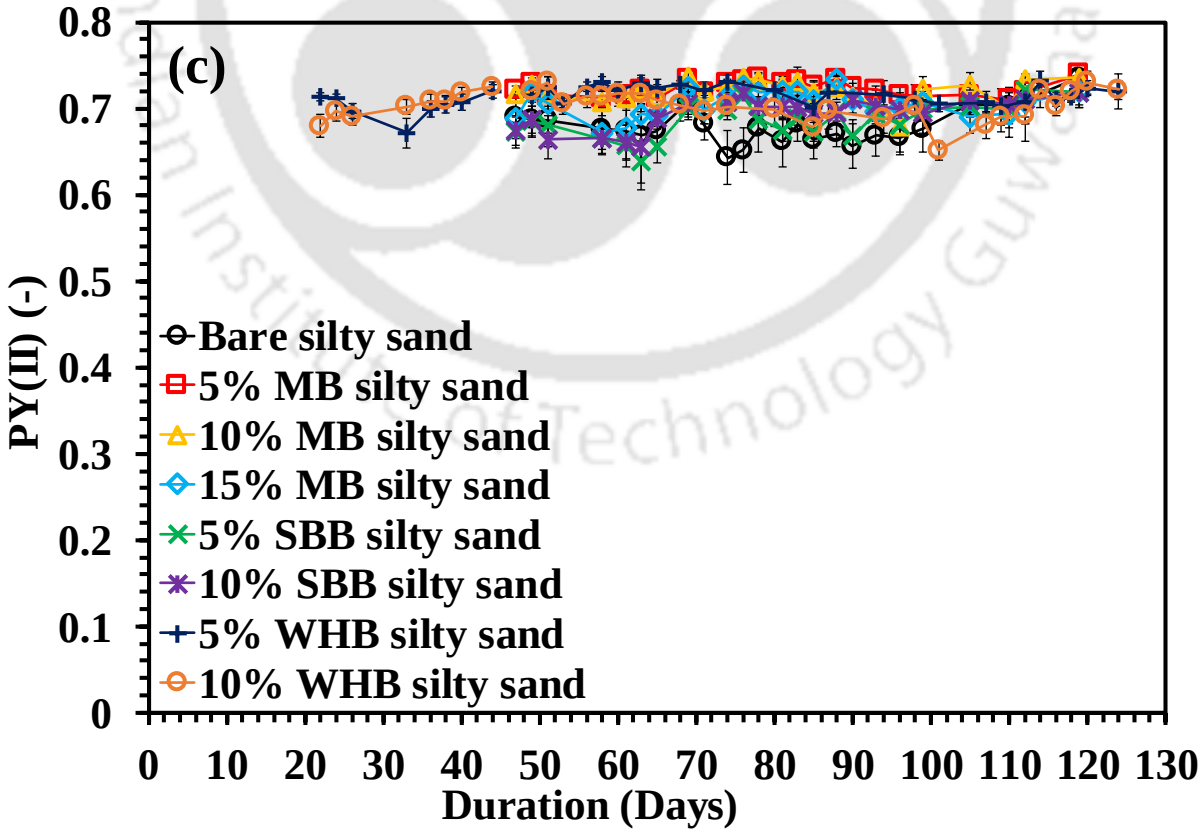

Fig. 8.6 (c) Variation of PY(II) with time in different biochar-amended silty sand.

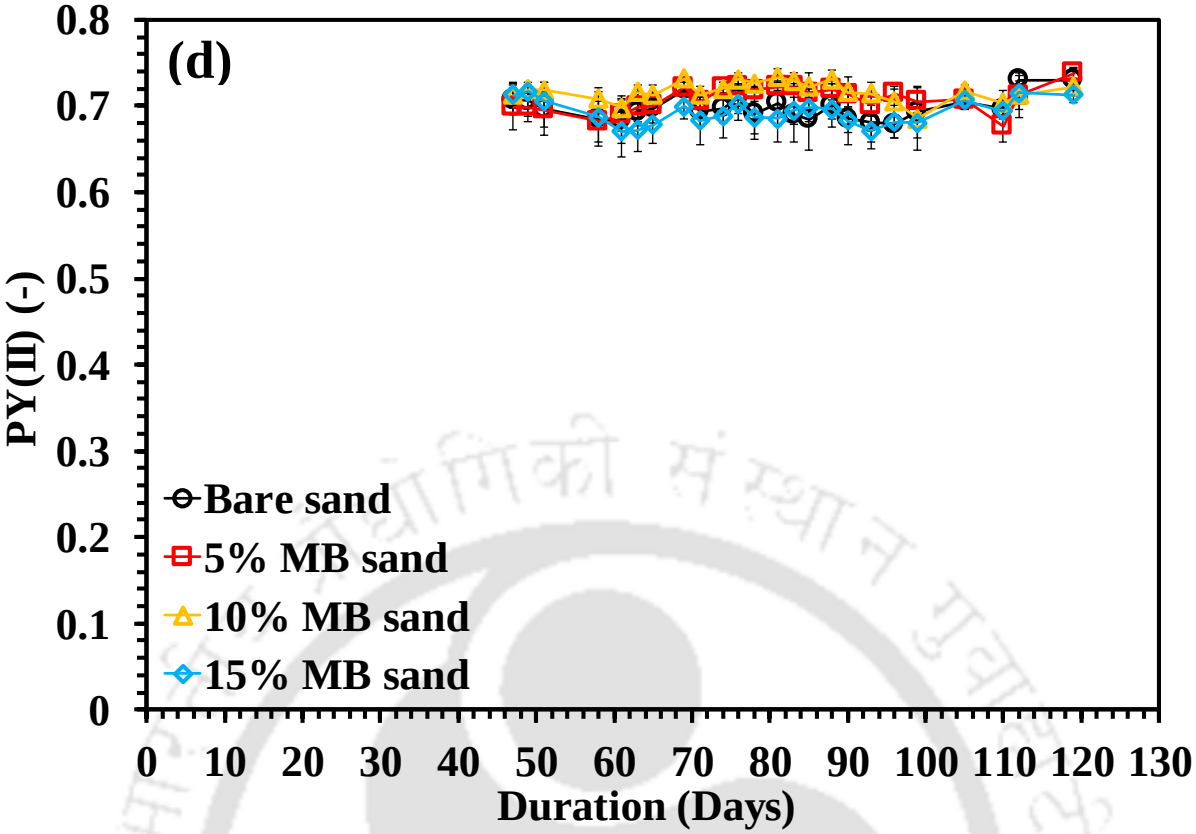

Fig. 8.6 (d) Variation of PY(II) with time in MB-amended sand.

8.3.2 Variation of SC with suction

Fig. 8.7 (a-b) highlights the SC variation with suction in different types biochar-amended silty sand and sand. The measured SC versus suction plot was found to fit better (R^2 of 0.93-0.99) the correlation proposed by Gadi et al (2019) given below

$$SC\,(\Psi) = SC_{min} + \frac{SC_{max} - SC_{min}}{[1 + (a(\Psi))^{n}]^{1-\frac{1}{n}}} \qquad (8.2)$$

where $SC\,(\Psi)$ is the stomatal conductance as a function of suction (mmol m^{-2} s^{-1}/mmol m^{-2} s^{-1}), SC_{max} is the maximum stomatal conductance (mmol m^{-2} s^{-1}/mmol m^{-2} s^{-1}), SC_{min} is the minimum stomatal conductance (mmol m^{-2} s^{-1}/mmol m^{-2} s^{-1}), α is the shape parameter related to the suction corresponding to peak SC ($\alpha > 0$) and n is the fitting coefficient associated with the curvature or the slope of the curve (n>1). The suction at which the SC start decreasing is termed as Ψ_{SCD} and measured graphically from the curve. The fitting parameters are presented in Table 8.2.

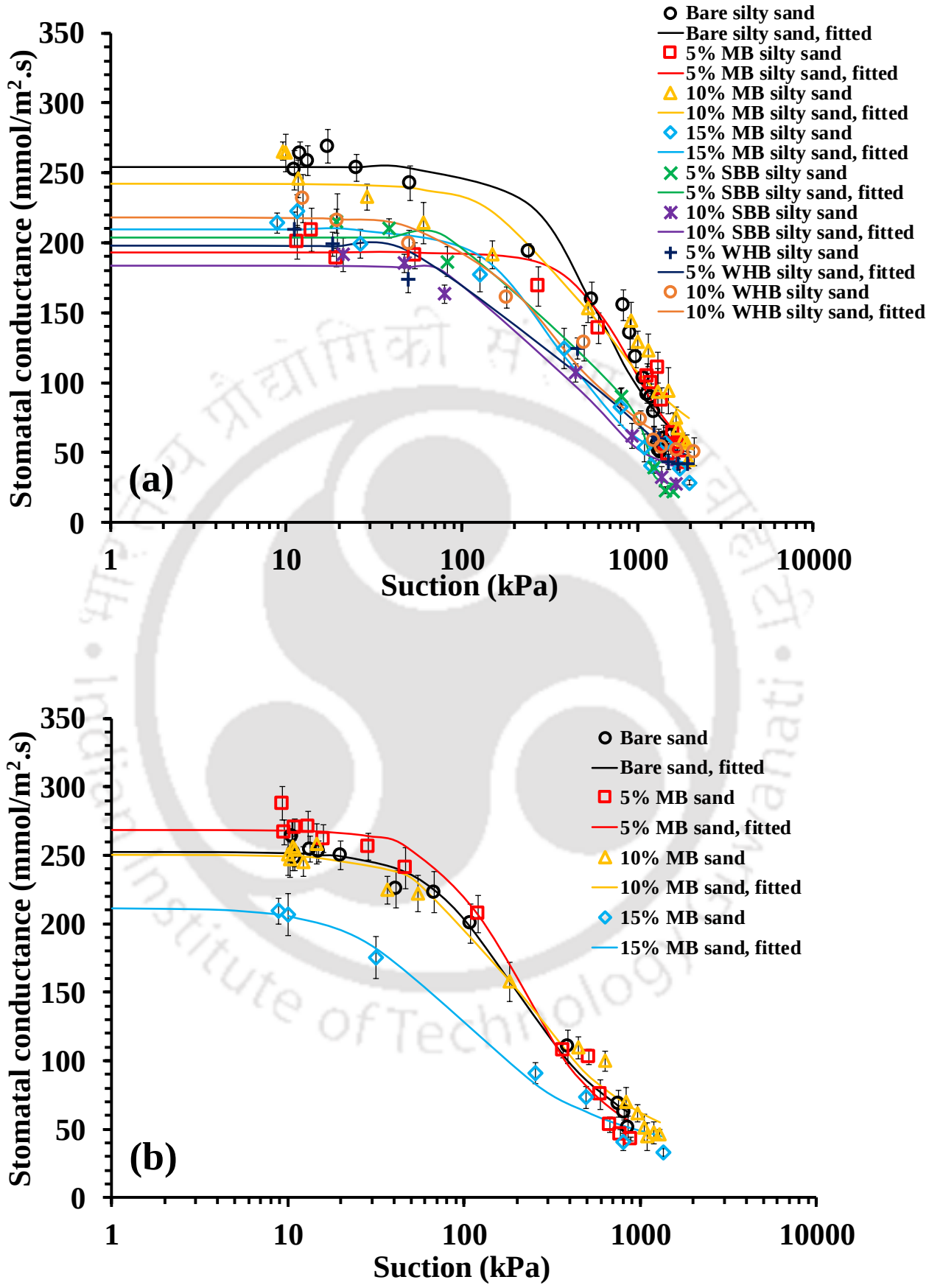

Fig. 8.7 Variation of SC with suction in biochar-amended silty sand (a) and sand (b).

Table 8.2 Fitting parameters of SC vs suction curve fitted using equation 8.2.

Type	Biochar (%, w/w)	SC_{max}	SC_{min}	α (kPa^{-1})	Ψ_{SCD} (kPa)	n (-)	m (-)	R^2 value
Bare SS	0	254	24	0.002	220	2.31	0.57	0.95
WHB-SS	5	198	24	0.004	55	1.95	0.49	0.97
	10	218	24	0.005	90	1.83	0.45	0.98
SBB-SS	5	211	24	0.006	72	2.42	0.59	0.99
	10	183	24	0.004	85	2.35	0.57	0.98
MB-SS	5	193	24	0.001	350	2.7	0.63	0.94
	10	242	24	0.003	150	1.81	0.45	0.93
	15	209	24	0.004	110	2.2	0.54	0.98
Bare sand	0	252	24	0.008	55	1.92	0.48	0.99
MB-sand	5	268	24	0.007	65	2.11	0.53	0.99
	10	250	24	0.008	45	1.85	0.46	0.99
	15	211	24	0.022	20	1.67	0.40	0.99

SS- silty sand, m=(1-1/n)

At relatively lower suction (10-50 kPa) or suction lower than Ψ_{SCD}, the measured SC was observed to be maximum or peak and unchanged with suction in all bare and BAS. However, with the further increase of soil suction beyond Ψ_{SCD}, the SC decreased and reached the minimum at PWP. The lower soil suction when abundant water is available in soil for the plants or roots to uptake facilitated the maximum transpiration rate or SC from the plants (Ng et al., 2021). As presented in Table 8.2, the maximum SC (SC_{max}) was observed to be lower in BAS compared to the bare soil. This could be attributed to the maximum utilization of the root up taken water in the growth of vegetation as the VD and roots mass were recorded to be higher in BAS thereby lower transpiration loss through stomata or lower SC. Early decrease of SC as suggested by the lower Ψ_{SCD} value (Table 8.2) could be observed in BAS relative to bare soil. However, further increase of suction beyond Ψ_{SCD}, the SC decreased gradually in BAS as quantified by lower *n* value in BAS (Table 8.2). With the increase of suction or decrease of water content in root zone, the vegetation gradually modifies its physiological activity like partial to complete closure of stomata to curb down the transpiration and meet the water deficiency in soil by releasing plant hormone (Garg et al., 2015; Munemasa et al., 2015). This modification of plant physiological activity with increased suction also represented as transpiration reduction function (Garg et al., 2015). The partial closure of

stomata due to the release of abscisic acid (ABA, plant hormone) attributed to the early decrease of SC in BAS, since the stomata are the only gateway to enter CO_2 and exit water vapor (transpiration) from the plants. The amendment of biochar increases the release of ABA by the plants for the intension of improving the roots growth and the resistance against drought stress and pathogen (Nguyen et al., 2016; Pei et al., 2020).

The SC_{min} was fixed at 24 mmol m^{-2} s^{-1} since the leaf porometer showed a minimum SC reading of in the range 20-25 mmol m^{-2} s^{-1} in completely wilted leaves. Ideally, in completely wilted leaves, zero to negligible SC reading is expected, however leaf porometer evaluates the SC based on the measured temperature and relative humidity, and a slight change in these parameter could yield large SC value due to which the negligible or zero reading was not observed. Considering the different biochar types, there was no distinct variation observed in SC among the different BAS. However, the MB-amended soil exhibited the higher SC_{max} and Ψ_{SCD} relative to other BAS. Similarly, considering the different soil types tested, the MB-amended sand exhibited the lower Ψ_{SCD} compared to the MB-amended silty sand. The lower water retention capacity of MB-amended sand caused an early wilting of the vegetation at relatively lower suction compared to the MB-amended silty sand i.e., lower PWP (Fig. 8.3) which have resulted in closure of stomata at relatively lower suction i.e., lower Ψ_{SCD} compared to the MB-amended silty sand. The SC versus suction relationship in BAS could be useful in the assessment of drought stress in root zone of bioengineered structures from the measured SC.

8.3.3 Variation of PY with suction

Fig. 8.8 highlights the variation of maximum (F_v/F_m) and effective (PY(II)) photosynthetic yield (PY) with suction in different biochar-amended silty sand and sand. PY(II) were observed to be above 0.7 (0-0.84) which indicates the healthy condition of the vegetation. The peak PY value of around 0.7 was also reported for the grass species in literature (Garg et al. 2020). The measured peak PY was observed to be unchanged for a suction up to around 1000 kPa and with further increase of suction the PY decreased abruptly. The peak PY indicates the green or fresh leaves or vegetation and the negligible or zero PY indicates the wilted leaves. The decrease of PY with increasing suction was attributed to the closure of reaction center or photo receptor in photosystem-II in chloroplast due to drought stress or water deficiency in the plants by the increased soil suction. The progressive wilting of leaves causes the destruction of chloroplast.

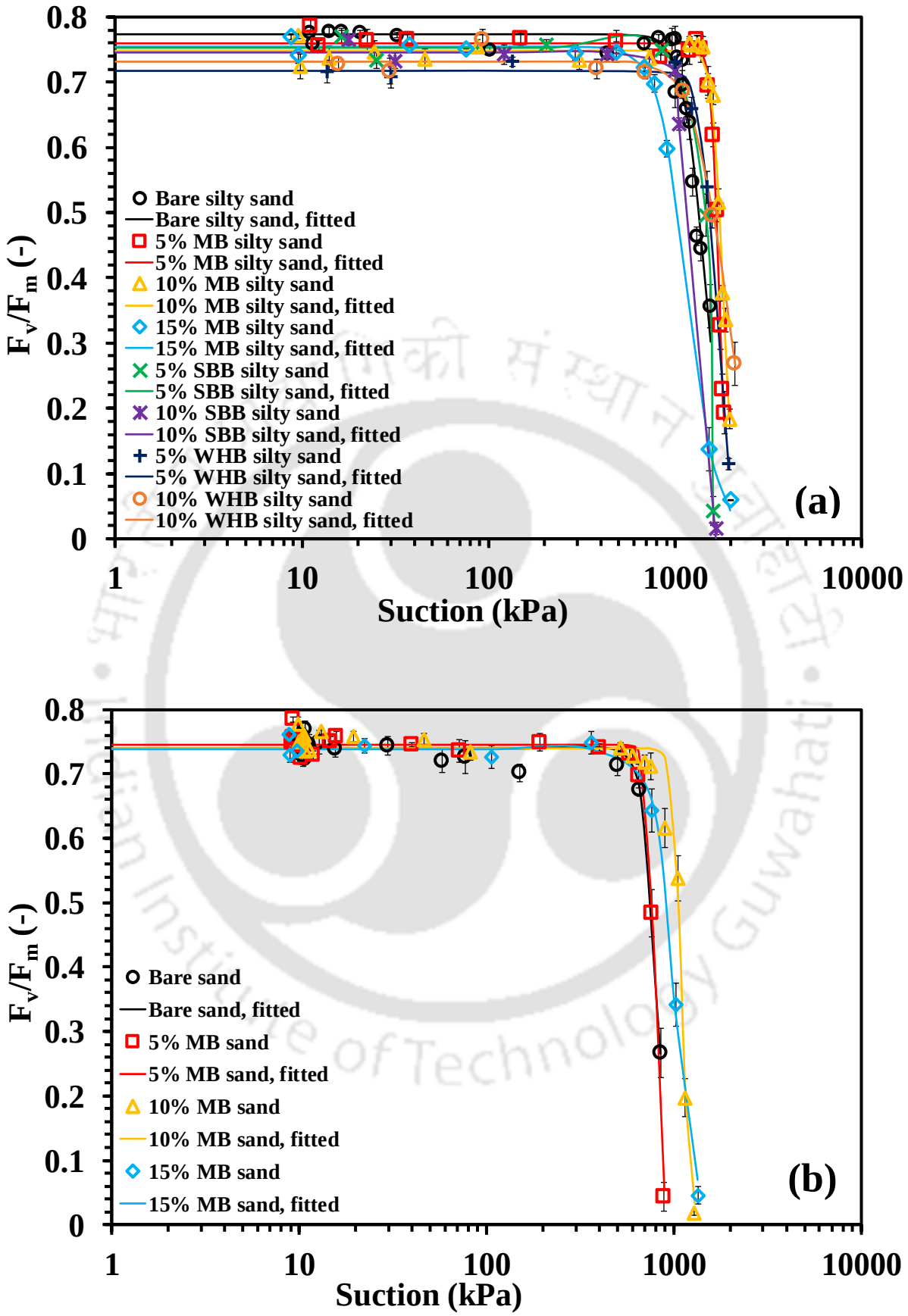

Fig. 8.8 Variation of F_v/F_m with suction in (a) different biochar-amended silty sand and (b) MB-amended sand.

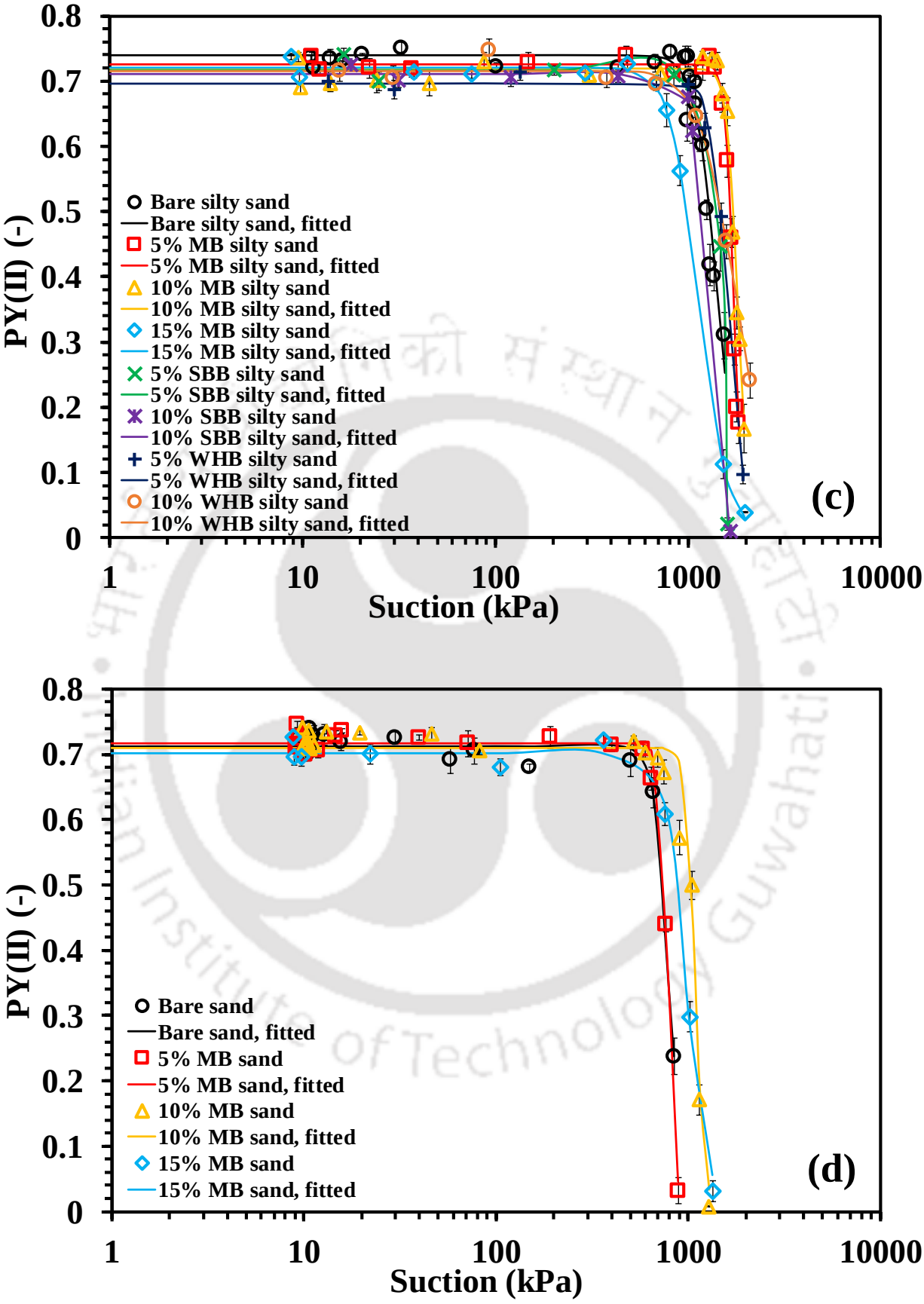

Fig. 8.8 Variation of PY(II) with suction in (c) different biochar-amended silty sand and (d) MB-amended sand.

The PY versus suction plot followed the similar pattern of SC versus suction. The peak value of (F_v/F_m) and to correlate the PY with suction and comparing among the treatments, the measured PY data was fitted to the correlation given below

$$\frac{F_v}{F_m}(\Psi) = \left(\frac{F_v}{F_m}\right)_{min} + \frac{\left(\frac{F_v}{F_m}\right)_{max} - \left(\frac{F_v}{F_m}\right)_{min}}{[1 + (\alpha(\Psi))^n]^{1-\frac{1}{n}}} \quad (8.3)$$

$$PY(II)(\Psi) = PY(II)_{min} + \frac{PY(II)_{max} - PY(II)_{min}}{[1 + (\alpha(\Psi))^n]^{1-\frac{1}{n}}} \quad (8.4)$$

where F_v/F_m (Ψ) and PY(II) (Ψ) are the maximum and effective photosynthetic yield as a function of suction (-), $(F_v/F_m)_{max}$ and $PY(II)_{max}$ are the peak value of the (F_v/F_m) and PY(II) (-), $(F_v/F_m)_{min}$ and $PY(II)_{min}$ are the minimum value of the (F_v/F_m) and PY(II) (-), α is the shape parameter related to the suction corresponding to peak (F_v/F_m) and PY(II) ($\alpha > 0$) and *n* is the fitting coefficient associated with the curvature or the slope of the curve (n>1). The fitting parameters are presented in Table 8.3. The R^2 value (0.94-1) indicates the best fit of the correlations. The suction where the (F_v/F_m) and PY(II) start decreasing is termed as $\Psi_{(Fv/Fm)D}$ and $\Psi_{(PY(II))D}$, and measured graphically from the curve.

Table 8.3 Fitting parameters of F_v/F_m and PY(II) vs suction curves.

		F_v/F_m						
Type	**Biochar (%, w/w)**	**$(F_v/F_m)_{max}$**	**$(F_v/F_m)_{min}$**	**α (kPa^{-1})**	**$\Psi_{(Fv/Fm)D}$ (kPa)**	**n (-)**	**m (-)**	**R^2 value**
Bare SS	0	0.77	0	0.0007	1050	7.4	0.86	0.94
WHB-SS	5	0.72	0	0.0006	1250	10.7	0.91	0.99
	10	0.73	0	0.0006	1070	5.1	0.80	0.99
SBB-SS	5	0.752	0	0.0007	1100	39.7	0.97	1
	10	0.746	0	0.0009	1000	31.4	0.97	1
MB-SS	5	0.76	0	0.0006	1550	19.3	0.95	0.99
	10	0.75	0	0.0005	1600	15	0.93	0.99
	15	0.754	0	0.0009	800	5.9	0.83	1
Bare sand	0	0.74	0	0.0013	630	11.7	0.91	0.98
MB-sand	5	0.745	0	0.0013	680	21.5	0.95	0.99
	10	0.74	0	0.0009	900	19.3	0.95	0.98

F_v/F_m								
Type	**Biochar (%, w/w)**	**$(F_v/F_m)_{max}$**	**$(F_v/F_m)_{min}$**	**α (kPa^{-1})**	**$\Psi_{(Fv/Fm)D}$ (kPa)**	**n (-)**	**m (-)**	**R^2 value**
	15	0.738	0	0.0010	780	8.1	0.88	1
PY(II)								
Type	**Biochar (%, w/w)**	**$PY(II)_{max}$**	**$PY(II)_{min}$**	**α (kPa^{-1})**	**$\Psi_{(PY(II))D}$ (kPa)**	**n (-)**	**m (-)**	**R^2 value**
Bare SS	0	0.74	0	0.0007	1050	7.9	0.87	0.94
WHB-SS	5	0.70	0	0.0006	1250	10.3	0.90	0.99
	10	0.71	0	0.0006	1070	4.8	0.79	0.99
SBB-SS	5	0.72	0	0.0007	1100	45.9	0.98	1
	10	0.71	0	0.0008	1000	15.9	0.94	1
MB-SS	5	0.73	0	0.0006	1550	19.3	0.95	1
	10	0.72	0	0.0006	1600	15.3	0.93	0.98
	15	0.72	0	0.0009	800	6.2	0.84	1
Bare sand	0	0.71	0	0.0013	630	11.7	0.91	0.98
MB-sand	5	0.72	0	0.0013	680	21.2	0.95	0.99
	10	0.71	0	0.0009	900	18.3	0.94	0.97
	15	0.70	0	0.0010	780	8.3	0.88	0.99

SS- silty sand, m=(1-1/n)

There was no comparable variation observed in the $(F_v/F_m)_{max}$ and $PY(II)_{max}$ after biochar amendment. The $(F_v/F_m)_{max}$ and $PY(II)_{max}$ were observed to be unchanged for suction in the range of 1000-1600 kPa i.e., up to $\Psi_{(Fv/Fm)D}$ and $\Psi_{(PY(II))D}$. The increase of suction beyond $\Psi_{(Fv/Fm)D}$ and $\Psi_{(PY(II))D}$, the vegetation starts fractionally losing the photosynthetic activity due to the closure of reaction center in the chloroplast. The amendment of biochar increased the $\Psi_{(Fv/Fm)D}$ and $\Psi_{(PY(II))D}$ compared to the bare soil (Table 8.3), indicating of complete photosynthetic activity even at higher suction in BAS. The higher plant available water due to smaller pores size and the delayed wilting (higher Ψ_W, Table 8.1) in BAS relative to bare soil allowed the complete photosynthetic activity or yield at comparatively higher suction i.e., higher $\Psi_{(Fv/Fm)D}$ and $\Psi_{(PY(II))D}$. The increase of suction beyond $\Psi_{(Fv/Fm)D}$ and $\Psi_{(PY(II))D}$ decreased the PY and ceased at PWP, where the vegetation fractionally lost the photosynthetic activity due to the permanent closure of reaction center in the chloroplast.

A steep or abrupt decrease of the (F_v/F_m) and PY(II) as quantified by the large *n* value (Table 8.3) could be observed in BAS relative to bare soil. The increase of soil suction or

drought stress beyond $\Psi_{(Fv/Fm)D}$ and $\Psi_{(PY(II))D}$ led to the water deficiency and wilting in the plants, which in turn, destroyed the reaction center or photo receptor in photosystem-II in the chloroplast and hence lower absorption of photon or lower PY (Wada et al., 2019; Garg et al., 2020). Considering the effect of biochar types on PY, the MB-amended soil exhibited the highest $\Psi_{(Fv/Fm)D}$ and $\Psi_{(PY(II))D}$ among the biochar tested due to the highest plant growth (root mass and VD) and delayed wilting in MB-amended soil. The different soil types tested, the sand exhibited relatively lower $\Psi_{(Fv/Fm)D}$ and $\Psi_{(PY(II))D}$ due to the large pore structure and lower water retention capacity that have caused the early wilting and permanent closure of the reaction centers in the plants. Thus, the biochar amendment extends the complete photosynthetic activity up to a large suction which implies the healthier status of vegetation in BAS compared to the bare soil and will be beneficial for the bioengineered structures.

8.4 Soil-biochar-root water retention curve

Fig. 8.9 (a-b) highlights the SWRC of different biochar-amended vegetated silty sand and sand. The measured suction and water content data were fitted to the van Genuchten (1980) model. The fitting parameters are presented in Table 8.4. The R^2 value was observed to be in the range of 0.98-0.99, indicates the good fit of the SWRC. As presented in Table 8.4, the amendment of different types biochar increased the θ_s in the range of 15-104%. The amendment of biochar decreased the pore size and increased the porosity as evident from the decreased dry density. The internally porous structure of biochar which is evident from the FESEM images (Fig. 4.4) and higher WAC (Table 4.1) as the WAC represents the internal porosity of the material, and the reformation of inter-pores between the different sized particles of soil and biochar attributed to the increased porosity. The higher porosity and the –OH and C=O functional groups in biochar surface (Fig. 4.6) which are polar in nature (Van der Spoel et al., 2006) attract and held higher volume of water in BAS and hence the higher θ_s. The SBB-amended soil exhibited the highest θ_s among the biochar tested. The higher porosity of SBB-amended soil compared to the other BAS as observed from the lowest dry density (Fig. 4.3) contributed to the highest θ_s. The higher porosity of SBB-amended soil is also evident from the higher WAC of SBB-amended soil (Table 4.1) due to large SSA of SBB over other biochar (Table 4.2). The increase of soil porosity after biochar amendment was also observed and reported by the past researchers (Blanco-Canqui, 2017; Nakhli and Imhoff, 2020; Hussain et al., 2021).

The amendment of biochar increased the AEV in the range of 133-400%.

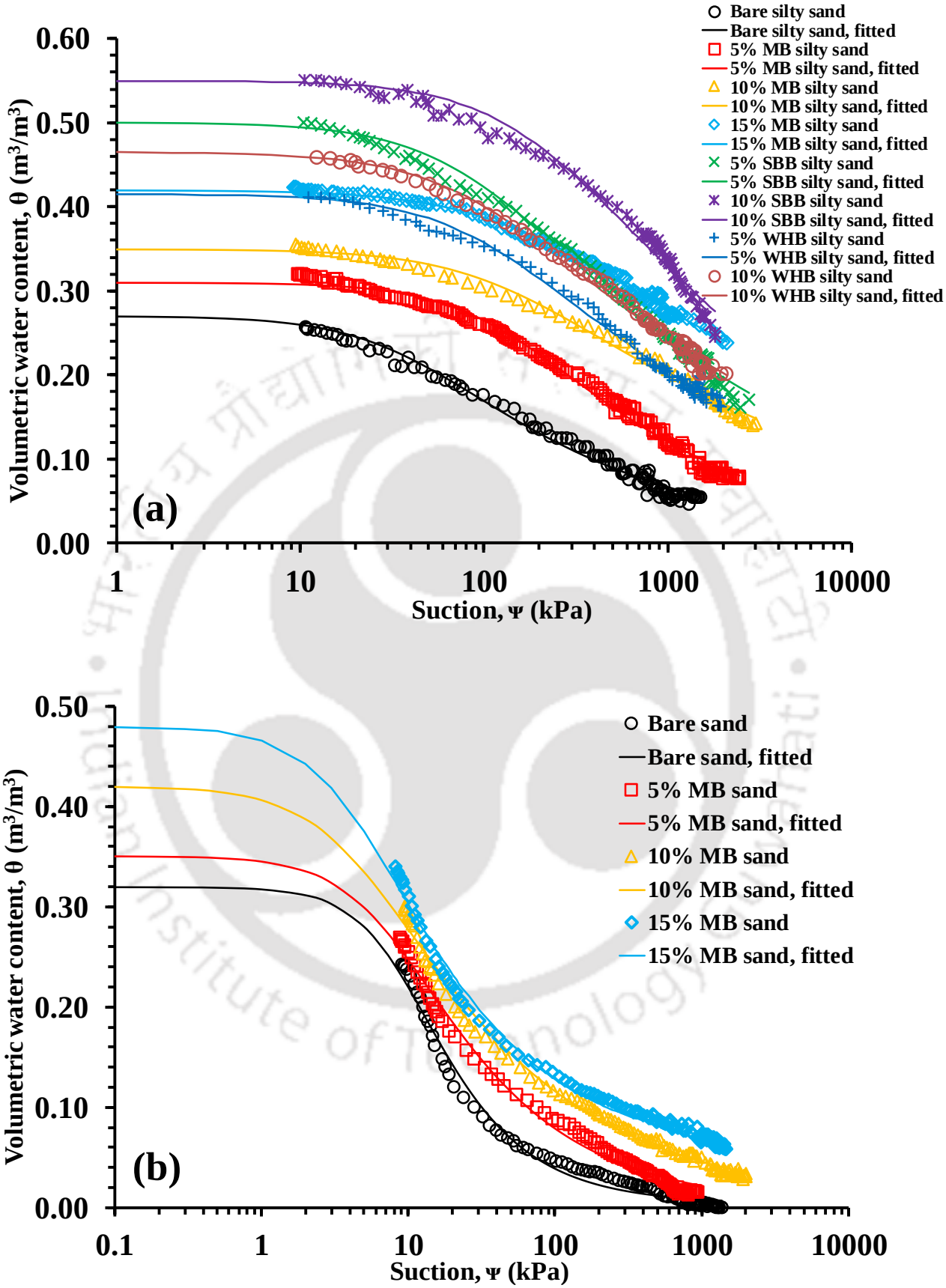

Fig. 8.9 SWRCs of biochar-amended vegetated soil (a) silty sand and (b) sand.

Table 8.4 Fitting parameters of the SWRCs of biochar-amended vegetated soil.

Type	Biochar (%, w/w)	θ_s (%)	θ_r (%)	α (kPa^{-1})	AEV (kPa)	n (-)	m (-)	R^2 value	θ_{1500} (%)	PAWC (%)
Bare SS	0	27	0	0.025	18	1.43	0.30	0.99	5.5	17
WHB-SS	5	41.5	0	0.009	46	1.32	0.24	0.99	18	23
	10	46.5	0	0.010	42	1.28	0.22	0.99	22	24.4
SBB-SS	5	50	0	0.010	42	1.3	0.23	0.99	22	26.4
	10	55	0	0.004	90	1.32	0.24	0.98	30	25.7
MB-SS	5	31	0	0.007	58	1.46	0.32	0.99	10	20.7
	10	35	0	0.007	62	1.28	0.22	0.99	18	17.3
	15	42	0	0.006	70	1.21	0.18	0.99	26	16.6
Bare sand	0	32	0.4	0.110	3.9	1.91	0.48	0.99	0.01	22.4
MB-sand	5	35	0	0.135	3	1.57	0.36	0.99	1	23.9
	10	42	0.2	0.223	2	1.42	0.29	0.99	3.5	25.4
	15	48	5	0.224	2	1.55	0.35	0.99	6	24.5

The AEV is related to the pore size of the soil and the increased AEV in BAS indicates the smaller size pores and strong held of water in the pores. The amendment of biochar with smaller size intra-pores made the pore size distribution of the soil tortuous or complex with pores of smaller size (Sun et al., 2015) which have not allowed water to evaporate easily and hence the higher AEV. The SBB-amended soil exhibited the highest AEV among the tested biochar due to the smaller size pores in SBB compared to the other biochar (Fig. 4.4).

Relatively lower value of *n* was observed in BAS compared to bare soil. The lower *n* value in BAS implies the reduction of pore size and a gradual or slow desaturation (release) of water from BAS relative to bare soil. The residual water content (θ_r) was found to be zero from the fitting and as the measured suction was not large enough to the residual suction, the θ_{1500} was evaluated for comparing the biochar effect at higher suction. The θ_{1500} was observed to be increased in the range of 82-445% after biochar amendment. The smaller size pores may be intra-pores or inter-pores, preferably the intra-pores which can hold water at larger suction due to their smaller size attributed to the higher θ_{1500} in BAS. The SBB-amended soil exhibited the highest θ_{1500} among the biochar tested due to their smallest intra-pores size as seen from the FESEM images (Fig. 4.4). The smaller-sized pores hold water tightly due to strong capillary action and resists the evaporation of water, and thus higher water retention (Fredlund et al., 2012). The PAWC, which was evaluated from the measured PWP found to

be increased in the range of 22-55% after biochar amendment. Relatively higher increase in PAWC was observed with SBB compared to the other biochar tested (Table 8.4). The two different soil types tested, the amendment of biochar showed higher improvement in the θ_s, AEV and PAWC of the silty sand compared to the sand. However, the magnitude of the θ_s and n were found to be higher in biochar-amended sand compared to the biochar-amended silty sand due to the larger size pores and higher porosity in sand.

The comparison of the SWRCs of the biochar-amended vegetated soil (Fig. 8.9a-b) with the SWRCs of BAS without vegetation (Fig. 6.1 and Fig. 6.2) revealed that the presence of vegetation or roots decreased the θ_s and increased the *AEV* (Table 6.1, 6.2, 8.4). The roots in vegetated soil occupied the pore spaces as a consequence, the pore throat or size reduced and the porosity decreased. The decreased porosity with reduced pore size in biochar-amended vegetated soil led to the lower θ_s and higher *AEV* relative to the BAS without vegetation. Overall, the biochar amendment showed positive impact on the water retention of soil both under vegetated and without vegetation state.

8.5 Summary and conclusions

The results of the vegetation performance evaluated in terms of vegetation growth and health parameters in different types biochar-amended soils are presented. The amendment of the biochar found to be improved the vegetation growth i.e., increased the vegetation density, roots mass and shoot mass in the range of 34-150%. Among the different types biochar tested, the amendment of MB showed the higher improvement in vegetation growth. Further, the amendment of biochar showed better or higher vegetation growth in silty sand relative to the sand. The amendment of biochar found to be improved the vegetation health status by delaying the vegetation wilting or increasing (by 50-546 kPa) the permanent wilting point, by maintaining the complete photosynthetic activity at a relatively larger (by 50-550 kPa with respect to bare soil) suction and by reducing (16-28%) the stomatal conductance through physiological (hormonal) modification to tackle the drought stress. Among the biochar types tested, the amendment of MB showed relatively higher improvement in the health status of the vegetation. The vegetation was found to be wilted at a relatively lower suction in sand i.e., lower permanent wilting point compared to the silty sand which have ensured the soil specific variation of permanent wilting point. Therefore, the improved vegetation growth and health status in biochar-amended soil indicates the better vegetation performance which is encouraging for bioengineered structures where vegetation have strong role.

CHAPTER 9
CONCLUSIONS AND FUTURE SCOPE

9.1 Conclusions

The multifunctional application of biochar such as soil amendment, energy source, toxic pollutant remover and water purifier was well established. The efficacy of biochar in improving the crop productivity and soil fertility of loose agricultural soil and removal of organic and inorganic pollutant from soil and water was well documented in literature. However, the influence of biochar on soil engineering properties and vegetation performance in compacted soil suitable for bioengineered structures, such as landfill final cover, vegetated slopes or embankment and green roofs was rarely reported. Therefore, in the present thesis work, biochar was produced from waste biomass and the effect of the biochar produced on the soil hydro-mechanical properties and the vegetation growth and health status (performance) was investigated and reported for application in bioengineered structures. The major conclusions drawn from the study are presented below

1) The biochar produced found to be carbon rich (53-72%), internally porous with <10 mm size intra-pores and large SSA (22-41 m^2/g), hydrophilic in nature with water absorptive surface functional groups, neutral to slightly basic in nature (pH 8 to 9.6) and exhibited CEC (10-44 meq/100g) suitable for plants growth. Moreover, these properties i.e., the physicochemical and microstructural properties were found to be varied with the biochar types. These results of the biochar produced ensured its suitability as soil amendment for bioengineered structures.
2) The amendment of biochar in soil improved the soil physicochemical properties i.e., increased the Atterberg limits (by 11-72%), water absorption capacity (30-190%), pH (28-77%), CEC (44-720%) and EC (200-1050%), and decreased the dry density (9-31%) and specific gravity (4-15%). The biochar-driven alteration of the soil physicochemical properties was found to be biochar and soil types specific. The improved soil physicochemical properties after biochar amendment ensured the suitable medium for the root zone or vegetation growth.
3) The amendment of biochar found to be reduced the K_{sat} by ~one order of magnitude and the I_r by up to two order of magnitude. The increase of tortuosity and reduction of porosity due to biochar amendment led to the reduced K_{sat} and I_r. The different biochar and soil types showed the similar effect or trend of decreased K_{sat} and I_r with variable magnitudes. The biochar particles size showed strong bearing on the K_{sat} i.e., the

amendment of biochar of different particles size affected the K_{sat} differently. The I_r in BAS was found to be decreased with increase in soil suction. The reduction of K_{sat} and I_r after biochar amendment is encouraging for bioengineered structures especially for landfill cover as lesser volume of water will ingress and hence generation of lesser pore water pressure and volume of leachate. The magnitudes of the K_{sat} and I_r are found to be within or smaller than the recommended value (1×10^{-7} m/s) for bioengineered structures and thus, satisfied the design criteria set by the united states environmental protection agency (USEPA).

4) The amendment of biochar improved the water retention characteristics of the soils by on an average 30-150% (as characterized by the fitting parameters) under both drying and wetting scenario. The alteration of soil pore size distribution and porosity after biochar amendment caused the improvement in the water retention. The different biochar types showed variable impact on improving the water retention. The impact of biochar on water retention was also found to be soil types dependent. The biochar amendment lowered the K_{unsat} of the soil by on an average one-two order of magnitude due to higher tortuosity in complex pores network of the soil after biochar amendment. The effect of biochar on K_{unsat} was found to be soil type specific. The improved water retention and decreased K_{unsat} of soil due to biochar amendment are the beneficial sign for the bioengineered structures as a higher amount of readily available water will be there for the growth of vegetation.
5) The amendment of biochar increased the shear strength and load bearing capacity and decreased the desiccation crack potential of the soil. However, the undrained shear strength (UCS) of the soil was found to be decreased after biochar amendment which is not favorable for the stability of bioengineered structures. The magnitude of UCS obtained with minimum biochar content (5%) in the present study was found to be higher than the minimum design UCS value (200 kPa) required for compacted landfill final cover soil and set by the USEPA (USEPA, 1996). The influence of the biochar on soil shear strength, load bearing capacity and crack potential was found to be biochar and soil types dependent. The results of shear strength suggest the application of soil amended with 5% (w/w) biochar in bioengineered structures.
6) The amendment of biochar improved the growth and health status of the vegetation. The above- and below-ground biomass of the vegetation was found to be increased on an average by 34-150%. The wilting of the vegetation was delayed due to the increased PWP by 50-546 kPa, decreased SC by 16-28% and facilitating the complete photosynthetic

activity at relatively larger suction by 50-550 kPa compared to that in bare soil. The influence of the biochar on the vegetation growth and health status was found to be biochar and soil types dependent. The improved growth and health status of vegetation grown in BAS directly encouraged the application of biochar in bioengineered structures where additional growth (roots) will empower the structures against failure.

7) Overall, the biochar amendment showed satisfactory results, except for the undrained shear strength. Therefore, based on the present research work, it is suggested to use 5% BAS for the construction of bioengineered structures. The increase of amendment rates beyond 5% decreased the undrained shear strength (below the minimum requirement). Further, the amendment of biochar decreased the soil dry density and hence the compaction of soils with biochar of large amendment rates (>5%) might not be possible in the field due to their lower dry density.

9.2 Major contributions of the study

The major contributions of the study are summarized below

1) Converted waste biomass namely water hyacinth weed, mesquite and sugarcane bagasse into an environment-friendly and value added material of biochar for soil applications.
2) Evaluated the engineering behavior of compacted soil after biochar amendment for intended application in bioengineered structures.
3) The performance of vegetation in compacted soil after biochar amendment was evaluated to see the suitability of compacted biochar-amended soil as an engineering material for bioengineered structures where vegetation has significant contribution.
4) Proposed a safe biochar amendment rate for the bioengineered structures based on the present study and the different criteria set by the international agencies.

9.3 Limitations and future scope of work

The suggestions made in the present thesis are based on the laboratory-scale tests and for implementing in the real field requires the field-scale trials which opens up the future scope of work. The other limitations and possible future scope of works are discussed below

1) In the present study, biochar influence on only silty sand and pure sand was explored. Hence, future studies are needed to explore the biochar effect on wide range of soil types especially clayey soil as clay is mostly used for the construction of landfill liner system, therefore biochar-amended clay could serve as an alternative liner system.

2) The biochar properties vary with the biochar feedstock types and pyrolysis temperature. Biochar produced at different pyrolysis temperature exhibits difference in physicochemical properties that in turn affects the soil properties differently. In the present study, only the effect of feedstock types was considered and therefore the effect of pyrolysis temperature on biochar properties and its corresponding influence on soil properties need to be investigated.
3) In the present study, the shear strength of BAS without vegetation or roots was investigated as a stability indicator. However, in bioengineered structures, soil is generally vegetated; therefore, for reliable stability assessment, the shear strength of biochar-amended rooted or vegetated soil need to be investigated which will give the actual stability of the bioengineered structures.
4) As the hydraulic properties of the BAS measured, the smaller size biochar particles and the compounds from biochar may leach with water which need to be investigated.

List of publication from the thesis

Journals

Hussain, R., Ravi, K., & Garg, A. (2020). Influence of biochar on the soil water retention characteristics (SWRC): potential application in geotechnical engineering structures. *Soil and Tillage Research, 204*, 104713.

Hussain, R., Garg, A., & Ravi, K. (2020). Soil-biochar-plant interaction: differences from the perspective of engineered and agricultural soils. *Bulletin of Engineering Geology and the Environment, 79*, 4461-4481.

Hussain, R., Bordoloi, S., Garg, A., Ravi, K., Sreedeep, S., & Sahoo, L. (2020). Effect of biochar type on infiltration, water retention and desiccation crack potential of a silty sand. *Biochar*, *2*(4), 465-478.

Hussain, R., Ghosh, K. K., & Ravi, K. (2021). Influence of biochar particle size on the hydraulic conductivity of two different compacted engineered soils. *Biomass Conversion and Biorefinery*, 1-11.

Hussain, R., Ghosh, K. K., Garg, A., & Ravi, K. (2021). Effect of biochar produced from mesquite on the compaction characteristics and shear strength of a clayey sand. *Geotechnical and Geological Engineering*, *39*(2), 1117-1131.

Hussain, R., Ghosh, K. K., & Ravi, K. (2021). Impact of biochar produced from hardwood of mesquite on the hydraulic and physical properties of compacted soils for potential application in engineered structures. *Geoderma*, *385*, 114836.

Muigai, H. H., Bordoloi, U., **Hussain, R**., Ravi, K., Moholkar, V. S., & Kalita, P. (2021). A comparative study on synthesis and characterization of biochars derived from lignocellulosic biomass for their candidacy in agronomy and energy applications. *International Journal of Energy Research*, *45*(3), 4765-4781.

Hussain, R., & Ravi, K. (2021). Investigating unsaturated hydraulic conductivity and water retention characteristics of compacted biochar-amended soils for potential application in bioengineered structures. *Journal of Hydrology*, 603, 127040.

Hussain, R., & Ravi, K. (2022). Investigating biochar-amended soil as a potential lightweight material for embankments. *Ecological Engineering*, 180, 106645.

Hussain, R., Kumar, H., Bordoloi, S., Jaykumar, S., Salim, S., Garg, A., Ravi, K., Sarmah, A.K., Gogoi, N., & Sreedeep, S. "Effect of biochar type and amendment rate on compacted soil physicochemical properties: potential application in green infrastructure". *Advance in civil engineering materials, ASTM* (*under review).*

Hussain, R., & Ravi, K. "Investigating soil properties and plant parameters in different biochar-amended vegetated soil at large suction for application in bioengineered structures". *Acta geotechnica* (*under review).*

Hussain, R., Muigai, H.H., Kalita, P., & Ravi, K. "Conversion of waste sugarcane bagasse into biochar and investigating its potential as soil amendment for bioengineered structures". *Bulletin of Engineering Geology and the Environment* (*under review).*

Conference

Ghosh, K. K., Patwa, D., **Hussain, R**., Ravi, K., (2019). "Effect of biochar on consistency behaviour of soil." Indian Conference on Geotechnical and Geo-Environmental Engineering (**ICGGE 2019*)*** MNNIT, Allahabad, India.

REFERENCES

Abbas T, Rizwan M, Ali S, Adrees M, Mahmood A, Zia-ur-Rehman M, ... & Qayyum MF (2018) Biochar application increased the growth and yield and reduced cadmium in drought stressed wheat grown in an aged contaminated soil. Ecotox Environ Safe 148: 825-833

Abdul RNF, Abdul RNS (2017) The effect of biochar application on nutrient availability of soil planted with MR219. Journal of Microbial and Biochemical Technology 9(2): 583-586

Abel S, Peters A, Trinks S, Schonsky H, Facklam M, Wessolek G (2013) Impact of biochar and hydrochar addition on water retention and water repellency of sandy soil. Geoderma 202: 183-191

Abid M, Lal R (2009) Tillage and drainage impact on soil quality: II. Tensile strength of aggregates, moisture retention and water infiltration. Soil Tillage Res 103(2): 364-372

Aharoni C (1997) The solid− liquid interface in capillary condensation. Sorption of water by active carbons. Langmuir 13(5): 1270-1273

Ahmad M, Rajapaksha AU, Lim JE, Zhang M, Bolan N, Mohan D, ... Ok YS (2014) Biochar as a sorbent for contaminant management in soil and water: a review. Chemosphere 99: 19-33

Ahmed A, Gariepy Y, Raghavan V (2017) Influence of wood-derived biochar on the compactibility and strength of silt loam soil. Int Agrophys 31(2): 149-155

Ajayi AE, Horn R (2016) Modification of chemical and hydrophysical properties of two texturally differentiated soils due to varying magnitudes of added biochar. Soil Tillage Res 164: 34-44

Ajayi AE, Holthusen D, Horn R (2016) Changes in microstructural behaviour and hydraulic functions of biochar amended soils. Soil Tillage Res 155: 166-175

Akhtar SS, Andersen MN, Naveed M, Zahir ZA, Liu F (2015) Interactive effect of biochar and plant growth-promoting bacterial endophytes on ameliorating salinity stress in maize. Funct Plant Biol 42(8): 770-781

Aksakal, E. L., Angin, I., & Oztas, T. (2013). Effects of diatomite on soil consistency limits and soil compactibility. *Catena*, *101*, 157-163.

Albright WH, Benson CH, Gee GW, Abichou T, McDonald EV, Tyler SW, Rock SA (2006) Field performance of a compacted clay landfill final cover at a humid site. J Geotech Geoenviron 132(11): 1393-1403

Allen RG, Pereira LS, Raes D, Smith M (1998) Crop evapotranspiration-Guidelines for computing crop water requirements-FAO Irrigation and drainage paper 56. Fao Rome 300(9): D05109

Amonette JE, Joseph S (2009) Characteristics of biochar: microchemical properties. Chapter 3. In: Lehmann J, Joseph S (eds) Biochar for environmental management science and technology. Earthscan London: pp 33–52

Andrenelli MC, Maienza A, Genesio L, Miglietta F, Pellegrini S, Vaccari FP, Vignozzi N (2016) Field application of pelletized biochar: Short term effect on the hydrological properties of a silty clay loam soil. Agr Water Manage 163: 190-196

Angulo-Jaramillo R, Vandervaere JP, Roulier S, Thony JL, Gaudet JP, Vauclin M (2000) Field measurement of soil surface hydraulic properties by disc and ring infiltrometers: A review and recent developments. Soil Tillage Res 55(1-2): 1-29

Angulo-Jaramillo R, Bagarello V, Iovino M, Lassabatere L (2016) Infiltration measurements for soil hydraulic characterization. Berlin, Germany: Springer

Anyanwu IN, Alo MN, Onyekwere AM, Crosse JD, Nworie O, Chamba E B (2018) Influence of biochar aged in acidic soil on ecosystem engineers and two tropical agricultural plants. Ecotox environ safe 153: 116-126

ASTM C128-15., 2015. Standard test method for relative density (specific gravity) and absorption of fine aggregate. ASTM International, West Conshohocken, PA.

ASTM D422–63., 2007. Standard test method for particle-size analysis of soils. ASTM International, West Conshohocken, PA.

ASTM D698-12., 2012. Standard Test Methods for Laboratory Compaction Characteristics of Soil Using Standard Effort. ASTM International, West Conshohocken, PA.

ASTM D854., 2010. Standard test method for specific gravity of soil solids by water pycnometer. ASTM International, West Conshohocken, PA.

ASTM D2487-11., 2011. Standard Practice for Classification of Soils for Engineering Purpose (Unified Soil Classification System). ASTM International, West Conshohocken, PA.

ASTM D4318-10., 2010. Standard Test Methods for Liquid Limit, Plastic Limit and Plasticity Index of Soils. ASTM International, West Conshohocken, PA.

ASTM D4972., 2018. Standard Test Method for pH of Soils. ASTM International, West Conshohocken, PA.

ASTM E1755-01., 2007. Standard method for the determination of ash in biomass. ASTM International, Philadelphia, PA.

Atkinson CJ, Fitzgerald JD, Hipps NA (2010) Potential mechanisms for achieving agricultural benefits from biochar application to temperate soils: a review. Plant Soil 337(1-2): 1-18

Bagarello V, Castellini M, Iovino M (2007) Comparison of unconfined and confined unsaturated hydraulic conductivity. Geoderma 137: 394–400

Baker R (1981) Tensile strength, tension cracks, and stability of slopes. Soils found 21(2): 1-17

Barnes RT, Gallagher ME, Masiello CA, Liu Z, Dugan B (2014) Biochar-induced changes in soil hydraulic conductivity and dissolved nutrient fluxes constrained by laboratory experiments. PLOS One 9(9): e108340

Baronti S, Vaccari FP, Miglietta F, Calzolari C, Lugato E, Orlandini S, ... Genesio L (2014) Impact of biochar application on plant water relations in Vitis vinifera (L.). Eur J Agron 53: 38-44

Basso AS, Miguez FE, Laird DA, Horton R, Westgate M (2013) Assessing potential of biochar for increasing water-holding capacity of sandy soils. Gcb Bioenergy 5(2): 132-143

Bazargan A, Rough SL, McKay G (2014) Compaction of palm kernel shell biochars for application as solid fuel. Biomass Bioenerg 70: pp. 489–497

Bengough AG, Mullins CE (1990) Mechanical impedance to root growth: a review of experimental techniques and root growth responses. J Soil Sci 41(3): 341-358

Bhave S, Sreeja P (2013) Influence of initial soil condition on infiltration characteristics determined using a disk infiltrometer. ISH J Hydraul Eng 19(3): 291-296

Blackwell P, Riethmuller G, Collins M (2009) Biochar application to soil. Biochar for environmental management: sci. technology 1: 207-226

Bordoloi S, Hussain R, Garg A, Sreedeep S, Zhou WH (2017) Infiltration characteristics of natural fiber reinforced soil. Transp Geotech 12: 37-44

Bordoloi S, Hussain R, Gadi VK, Bora H, Sahoo L, Karangat R, ... Sreedeep S (2018a) Monitoring soil cracking and plant parameters for a mixed grass species. Géotech Lett 8(1): 49-55

Bordoloi S, Gadi VK, Hussain R, Sahoo L, Garg A, Sreedeep S, ... Poulsen TG (2018b) Influence of Eichhornia crassipes fibre on water retention and cracking of vegetated soils. Géotech Lett 8(2): 130-137

Bordoloi S, Garg A, Sreedeep S, Lin P, Mei G (2018c) Investigation of cracking and water availability of soil-biochar composite synthesized from invasive weed water hyacinth. Bioresource technol 263: 665-677

Bouma JONGERIUS, Jongerius A, Schoonderbeek D (1979) Calculation of Saturated Hydraulic Conductivity of Some Pedal Clay Soils Using Micromorphometric Data 1. Soil Sci Soc Am J 43(2): 261-264

Bruun EW, Petersen CT, Hansen E, Holm JK, Hauggaard-Nielsen H (2014) Biochar amendment to coarse sandy subsoil improves root growth and increases water retention. Soil Use Manage 30(1): 109-118

Burland JB (1990) On the compressibility and shear strength of natural clays. Géotechnique 40 (3): 329-378

Busscher W, Novak J, Evans D, Watts D, Niandou M, Ahmedna M (2010) Influence of pecan biochar on physical properties of a Norfolk loamy sand. Soil Sci 175(1): 10–14

Cao CT, Farrell C, Kristiansen PE, Rayner JP (2014) Biochar makes green roof substrates lighter and improves water supply to plants. Ecol Eng 71: 368-374

Caplan JS, Yeakley JA (2010) Water relations advantages for invasive Rubusáarmeniacus over two native ruderal congeners. Plant Ecol 210(1): 169-179

Castellini M, Giglio L, Niedda M, Palumbo AD, Ventrella D (2015) Impact of biochar addition on the physical and hydraulic properties of a clay soil. Soil Tillage Res 154: 1-13

Chapuis RP (2012) Predicting the saturated hydraulic conductivity of soils: a review. Bull Eng Geol Environ 71(3): 401-434

Chen Y, Shinogi Y, Taira M (2010) Influence of biochar use on sugarcane growth, soil parameters, and groundwater quality. Soil Res 48(7): 526-530

Chen B, Yuan M, Qian L (2012) Enhanced bioremediation of PAH-contaminated soil by immobilized bacteria with plant residue and biochar as carriers. J Soil Sediment 12(9): 1350-1359

Chen XW, Wong JTF, Ng CWW, Wong MH (2016) Feasibility of biochar application on a landfill final cover—a review on balancing ecology and shallow slope stability. Environ Sci Pollut R 23(8): 7111-7125

Clark J, Hellin J (1996) Bio-engineering for effective road maintenance in the Caribbean.

Clarke JM, Townley-Smith TF (1986) Heritability and Relationship to Yield of Excised-Leaf Water Retention in Durum Wheat 1. Crop Sci 26(2): 289-292

Coles N, Trudgill S (1985) The movement of nitrate fertiliser from the soil surface to drainage waters by preferential flow in weakly structured soils, Slapton, S. Devon. Agr Ecosyst Environ 13(3-4): 241-259

Conz RF, Abbruzzini TF, de Andrade CA, Milori DM, Cerri CE (2017) Effect of Pyrolysis Temperature and Feedstock Type on Agricultural Properties and Stability of Biochars. Agr Sci 8(09): 914

Coppin NJ, Richards IG (Eds.) (1990) Use of vegetation in civil engineering. London: Construction Industry Research and Information Association. (pp. 23-36)

Corte A, Higashi A (1964) Experimental research on desiccation cracks in soil (No. RR-66). Cold Regions Research and Engineering Lab Hanover NH.

Costa S, Kodikara J, Shannon B (2013) Salient factors controlling desiccation cracking of clay in laboratory experiments. Géotechnique 63(1): 18

Cuenca RH, Ek M, Mahrt L (1996) Impact of soil water property parameterization on atmospheric boundary layer simulation. J Geophys Res-Atmos 101(D3): 7269-7277

de Melo Carvalho MT, Maia ADHN, Madari BE, Bastiaans L, Van Oort PAJ, Heinemann AB, ... Meinke H (2014) Biochar increases plant available water in a sandy soil under an aerobic rice cropping system. Solid Earth 6: 887-917

Downie A, Crosky A, Munroe P (2009) Physical properties of biochar. Biochar for environmental management: Sci Technology Routledge, London: pp 13–32

Du Z, Chen X, Qi X, Li Z, Nan J, Deng J (2016) The effects of biochar and hoggery biogas slurry on fluvo-aquic soil physical and hydraulic properties: a field study of four consecutive wheat–maize rotations. J Soil Sediment 16(8): 2050-2058

Egamberdieva D, Wirth S, Behrendt U, Abd_Allah EF, Berg G (2016) Biochar treatment resulted in a combined effect on soybean growth promotion and a shift in plant growth promoting rhizobacteria. Frontiers in microbiology 7: 209

Fredlund DG, Rahardjo H (1993) *Soil mechanics for unsaturated soils*. John Wiley & Sons

Fredlund DG, Rahardjo H, Fredlund MD (2012) *Unsaturated soil mechanics in engineering practice*. John Wiley & Sons

Gadi VK, Bordoloi S, Garg A, Kobayashi Y, Sahoo L (2016) Improving and correcting unsaturated soil hydraulic properties with plant parameters for agriculture and bioengineered slopes. Rhizosphere 1: 58-78

Gadi VK, Bordoloi S, Garg A, Sahoo L, Berretta C, Sekharan S (2017) Effect of shoot parameters on cracking in vegetated soil. Environmental Geotechnics 5(2): 1-31

Gadi VK, Garg A, Prakash S, Wei L, Andriyas S (2018) A non-intrusive image analysis technique for measurement of heterogeneity in grass species around tree vicinity in a green infrastructure. Measurement 114: 132-143

Gale NV, Sackett TE, Thomas SC (2016) Thermal treatment and leaching of biochar alleviates plant growth inhibition from mobile organic compounds. PeerJ 4: e2385

Gallage C, Kodikara J, Uchimura T, (2013) Laboratory measurement of hydraulic conductivity functions of two unsaturated sandy soils during drying and wetting processes. Soils Found 53(3): 417-430

Garg A, Coo JL, Ng CWW (2015) Field study on influence of root characteristics on soil suction distribution in slopes vegetated with Cynodon dactylon and Schefflera heptaphylla. Earth Surf Proc Land 40(12): 1631-1643

Garg A, Huang H, Kushvaha V, Madhushri P, Kamchoom V, Wani I, ... Zhu HH (2019) Mechanism of biochar soil pore–gas–water interaction: gas properties of biochar-amended sandy soil at different degrees of compaction using KNN modeling. Acta Geophys 1-11

Gavili E, Moosavi AA, Moradi Choghamarani F (2018) Cattle manure biochar potential for ameliorating soil physical characteristics and spinach response under drought. Arch Agron Soil Sci 1-14

GCO (Geotechnical Control Office) (2000) *Geotechnical manual for slopes*. Hong Kong, China: Geotechnical Control Office

Githinji L (2014) Effect of biochar application rate on soil physical and hydraulic properties of a sandy loam. Arch Agron Soil Sci 60(4): 457-470

Gravel V, Dorais M, Ménard C (2013) Organic potted plants amended with biochar: its effect on growth and Pythium colonization. Can J Plant Sci 93(6): 1217-1227

Gray DH (1974) Reinforcement and stabilization of soil by vegetation. J Geotech Geoenviron 100: (Proc Paper 10597 Tech Notes).

Gray DH, Leiser AT (1982) Biotechnical slope protection and erosion control. Van Nostrand Reinhold Company Inc.

Haque A, Tang CK, Islam S, Ranjith PG, Bui HH (2014) Biochar sequestration in lime-slag treated synthetic soils: a green approach to ground improvement. J Mater Civil Eng 26(12): 06014024

Hardie M, Clothier B, Bound S, Oliver G, Close D (2014) Does biochar influence soil physical properties and soil water availability? Plant Soil 376(1-2): 347-361

Haverkamp R, Parlange JY, Starr JL, Schmitz G, Fuentes C (1990) Infiltration under ponded condition.3. A predictive equation based on physical parameters. Soil Sci 149(5): 292–300

Herath HMSK, Camps-Arbestain M, Hedley M (2013) Effect of biochar on soil physical properties in two contrasting soils: an Alfisol and an Andisol. Geoderma 209: 188-197

Hillel D (1982) Introduction to Soil Physics. Academic Press, New York

Hillel D (2004) Introduction to environmental soil physics. San Francisco: Elsevier Science

Hopkins WG (1999) Introduction to plant physiology (No. Ed. 2). John Wiley and Sons

Horn R, Lebert M (1994) Soil compactability and compressibility. In Developments in agricultural engineering 11: pp. 45-69

Hunter B, Cardon GE, Olsen S, Alston DG, McAvoy D (2017) Preliminary screening of the effect of biochar properties and soil incorporation rate on lettuce growth to guide research and educate the public through extension. Journal of Agricultural Extension and Rural Development 9(1): 1-4

Ibrahim HM, Al-Wabel MI, Usman AR, Al-Omran A (2013) Effect of Conocarpus biochar application on the hydraulic properties of a sandy loam soil. Soil Sci 178(4): 165-173

Igalavithana AD, Ok YS, Niazi NK, Rizwan M, Al-Wabel MI, Usman AR, ... Lee SS (2017) Effect of corn residue biochar on the hydraulic properties of sandy loam soil. Sustainability 9(2): 266

International Biochar Initiative (2012) Standardized product definition and product testing guidelines for biochar that is used in soil. IBI biochar standards

International Biochar Initiative (2015) Standardized product definition and product testing guidelines for biochar that is used in soil. IBI biochar standards

Jeffery S, Verheijen FG, van der Velde M, Bastos AC (2011) A quantitative review of the effects of biochar application to soils on crop productivity using meta-analysis. Agr Ecosyst Environ 144(1): 175-187

Jeffery S, Meinders MB, Stoof CR, Bezemer TM, van de Voorde TF, Mommer L, van Groenigen JW (2015) Biochar application does not improve the soil hydrological function of a sandy soil. Geoderma 251: 47-54

Jindo K, Mizumoto H, Sawada Y, Sanchez-Monedero MA, Sonoki T (2014) Physical and chemical characterization of biochars derived from different agricultural residues. Biogeosciences 11(23): 6613-6621

Kameyama K, Miyamoto T, Shiono T, Shinogi Y (2012) Influence of sugarcane bagasse-derived biochar application on nitrate leaching in calcaric dark red soil. J Environ Qual 41(4): 1131-1137

Kammann CI, Linsel S, Gößling JW, Koyro HW (2011) Influence of biochar on drought tolerance of Chenopodium quinoa Willd and on soil–plant relations. Plant Soil 345(1-2): 195-210

Cammeraat E, van Beek R, Kooijman A (2005) Vegetation succession and its consequences for slope stability in SE Spain. Plant Soil 278(1-2): 135-147

Khademalrasoul A, Naveed M, Heckrath G, Kumari KGID, de Jonge LW, Elsgaard L, ... Iversen BV (2014) Biochar effects on soil aggregate properties under no-till maize. Soil Sci 179(6): 273-283

Kim WK, Shim T, Kim YS, Hyun S, Ryu C, Park YK, Jung J (2013) Characterization of cadmium removal from aqueous solution by biochar produced from a giant Miscanthus at different pyrolytic temperatures. Bioresource. Technol 138: 266-270

Kinney TJ, Masiello CA, Dugan B, Hockaday WC, Dean MR, Zygourakis K, Barnes RT (2012) Hydrologic properties of biochars produced at different temperatures. Biomass Bioenerg 41: 34-43

Klute A (1965) Laboratory measurement of hydraulic conductivity of saturated soil. Methods of soil analysis. Part 1. Physical and mineralogical properties, including statistics of measurement and sampling, (methodsofsoilana): 210-221

Klute A (1986) Methods of soil analysis, part 1, physical and mineralogical properties. American Society of Agronomy, Monograph: (9)

Kramer PJ (1969) Plant and soil water relationships: a modern synthesis. Plant and soil water relationships: a modern synthesis

Krupa S, McGrath MT, Andersen CP, Booker FL, Burkey KO, Chappelka AH, ... Zilinskas BA (2001) Ambient ozone and plant health. Plant Dis 85(1): 4-12

Kumar H, Cai W, Lai J, Chen P, Ganesan SP, Bordoloi S, ... Mei G (2020) Influence of in-house produced biochars on cracks and retained water during drying-wetting cycles: comparison between conventional plant, animal, and nano-biochars. J Soil Sediment 1-14

Kutilek M (2004) Soil hydraulic properties as related to soil structure. Soil Tillage Res 79(2): 175-184

Laird DA, Fleming P, Davis DD, Horton R, Wang B, Karlen DL (2010) Impact of biochar amendments on the quality of a typical Midwestern agricultural soil. Geoderma 158(3-4): 443-449

Lee FH, Lo KW, Lee SL (1988) Tension crack development in soils. J Geotech Eng 114(8): 915-929

Lehmann J, da Silva Jr JP, Steiner C, Nehls T, Zech W, Glaser B (2003) Nutrient availability and leaching in an archaeological Anthrosol and Ferralsol of the Central Amazon basin: fertilizer, manure and charcoal amendments. Plant Soil 249: 343–357

Lehmann J, Joseph S (2009) Biochar for environmental management: Sci. Technology. Earthscan, London: pp 1–12

Lehmann J, Rillig MC, Thies J, Masiello CA, Hockaday WC, Crowley D (2011) Biochar effects on soil biota–a review. Soil Biol Biochem 43(9): 1812-183

Lei O, Zhang R (2013) Effects of biochars derived from different feedstocks and pyrolysis temperatures on soil physical and hydraulic properties. J Soil Sediment 13(9): 1561-1572

Leung AK, Ng CWW (2013) Analyses of groundwater flow and plant evapotranspiration in a vegetated soil slope. Can Geot J 50(12): 1204-1218

Leung AK, Garg A, Coo JL, Ng CWW, Hau BCH (2015) Effects of the roots of Cynodon dactylon and Schefflera heptaphylla on water infiltration rate and soil hydraulic conductivity. Hydrol Process 29(15): pp.3342-3354

Leung AK, Coo JL, Ng CWW, Chen R (2016) New transient method for determining soil hydraulic conductivity function. Can Geot J 53(8): 1332-1345

Li JH, Zhang LM (2011) Study of desiccation crack initiation and development at ground surface. Eng Geol 123(4): 347-358

Liang B, Lehmann J, Solomon D, Kinyangi J, Grossman J, O'neill B, ... Neves EG (2006) Black carbon increases cation exchange capacity in soils. Soil Sci Soc Am J 70(5): 1719-1730

Lim TJ, Spokas KA, Feyereisen G, Novak JM (2016) Predicting the impact of biochar additions on soil hydraulic properties. Chemosphere 142: 136-144

Lipiec J, Horn R, Pietrusiewicz J, Siczek A (2012) Effects of soil compaction on root elongation and anatomy of different cereal plant species. Soil Tillage Res 121: 74-81

Liu X, Zhang A, Ji C, Joseph S, Bian R, Li L, ... Paz-Ferreiro J (2013) Biochar's effect on crop productivity and the dependence on experimental conditions—a meta-analysis of literature data. Plant Soil 373(1-2): 583-594

Liu Z, Chen X, Jing Y, Li Q, Zhang J, Huang Q (2014) Effects of biochar amendment on rapeseed and sweet potato yields and water stable aggregate in upland red soil. Catena 123: 45-51

Liu C, Colón BC, Ziesack M, Silver PA, Nocera DG (2016) Water splitting–biosynthetic system with CO2 reduction efficiencies exceeding photosynthesis. Science, 352(6290): 1210-1213

Liu Z, Dugan B, Masiello CA, Gonnermann HM (2017) Biochar particle size, shape, and porosity act together to influence soil water properties. Plos one, 12(6): e0179079

Lu N, Likos WJ (2004) Unsaturated soil mechanics. Wiley

Lu SG, Sun FF, Zong YT (2014) Effect of rice husk biochar and coal fly ash on some physical properties of expansive clayey soil (Vertisol). Catena 114: 37-44

Major J, Lehmann J, Rondon M, Goodale C (2010a) Fate of soil-applied black carbon: downward migration, leaching and soil respiration. Glob chang Biol 16: 1366– 1379

Major J, Rondon M, Molina D, Riha SJ, Lehmann J (2010b) Maize yield and nutrition during 4 years after biochar application to a Colombian savanna oxisol. Plant soil 333(1-2): 117-128

Major J, Rondon M, Molina D, Riha SJ, Lehmann J (2012) Nutrient leaching in a Colombian savanna Oxisol amended with biochar. J Environ Qual 41(4): 1076-1086

Malaya C, Sreedeep S (2010) A study on the influence of measurement procedures on suction-water content relationship of a sandy soil. J Test Eval 38(6): 691-699

Malaya C, Sreedeep S (2011) Critical review on the parameters influencing soil-water characteristic curve. J Irrig Drain E-ASCE 138(1): 55-62

Mbagwu JSC (1995) Saturated hydraulic conductivity in relation to physical properties of soils in the Nsukka Plains, southeastern Nigeria. Geoderma 68(1-2): 51-66

Moragues-Saitua L, Arias-González A, Gartzia-Bengoetxea N (2017) Effects of biochar and wood ash on soil hydraulic properties: A field experiment involving contrasting temperate soils. Geoderma 305: 144-152

Marinho FA, Stuermer MM (2000) The influence of the compaction energy on the SWCC of a residual soil. In Advances in unsaturated geotechnics: (pp. 125-141)

Marshall TJ (1958) A relation between permeability and size distribution of pores. J Soil Sci 9: 1-8

Masle J, Gilmore SR, Farquhar GD (2005) The ERECTA gene regulates plant transpiration efficiency in Arabidopsis. Nature, 436(7052): 866-870

Mathur N, Vyas A (1995) I. Influence of VA mycorrhizae on net photosynthesis and transpiration of Ziziphus mauritiana. J plant physiol 147(3-4): 328-330

Miller CJ (1988) Field Investigation of Clay Liner Movement. Hazard Waste Hazard 5(3): 231-238

Mualem Y (1986) Hydraulic conductivity of unsaturated soils: prediction and formulas. In Methods of soil analysis. Part 1. Physical and mineralogical methods. 2nd ed. Agronomy. *Edited* by A. Klute. American Society of Agronomy, Inc. and Soil Society of America, Inc., Madison, Wis, U.S.A: pp. 799-823

Mukherjee A, Lal R (2017) Biochar and soil characteristics. Encyclopedia of soil science: 183-188

Nearing MA, Parker SC, Bradford JM, Elliot WJ (1991) Tensile strength of thirty-three saturated repacked soils. Soil Sci Soc Am J 55(6): 1546-1551

Ng CWW, Leung AK (2011) Measurements of drying and wetting permeability functions using a new stress-controllable soil column. J Geotech Geoenviron 138(1): 58-68

Ng CW, Pang YW (2000) Experimental investigations of the soil-water characteristics of a volcanic soil. Can Geotech J 37(6): 1252-1264

Nimmo JR (1997) Modeling structural influences on soil water retention. Soil Sci Soc Am J 61: 712-719

Novak J, Sigua G, Watts D, Cantrell K, Shumaker P, Szogi A, ... Spokas K (2016) Biochars impact on water infiltration and water quality through a compacted subsoil layer. Chemosphere 142: 160-167

Obia A, Mulder J, Martinsen V, Cornelissen G, Børresen T (2016) In situ effects of biochar on aggregation, water retention and porosity in light-textured tropical soils. Soil Tillage Res 155: 35-44

Obia A, Børresen T, Martinsen V, Cornelissen G, Mulder J (2017) Effect of biochar on crust formation, penetration resistance and hydraulic properties of two coarse-textured tropical soils. Soil Tillage Res 170: 114-121

Ojeda G, Mattana S, Àvila A, Alcañiz JM, Volkmann M, Bachmann J (2015) Are soil–water functions affected by biochar application? Geoderma 249: 1-11

Omidi, G, Thomas J, Brown K (1996) Effect of desiccation cracking on the hydraulic conductivity of a compacted clay liner. Water Air Soil Pollut 89: 91–103

Omondi MO, Xia X, Nahayo A, Liu X, Korai PK, Pan G (2016) Quantification of biochar effects on soil hydrological properties using meta-analysis of literature data. Geoderma 274: 28-34

Ouyang L, Wang F, Tang J, Yu L, Zhang R (2013) Effects of biochar amendment on soil aggregates and hydraulic properties. J Soil Sci Plant Nut 13(4): 991-1002

Paetsch L, Mueller CW, Kögel-Knabner I, Lützow M, Girardin C, Rumpel C (2018) Effect of in-situ aged and fresh biochar on soil hydraulic conditions and microbial C use under drought conditions. Sci Rep-UK 8(1): 6852

Pandit NR, Mulder J, Hale SE, Martinsen V, Schmidt HP, Cornelissen G (2018) Biochar improves maize growth by alleviation of nutrient stress in a moderately acidic low-input Nepalese soil. Sci Total Environ 625: 1380-1389

Prober SM, Stol J, Piper M, Gupta VVSR, Cunningham SA (2014) Enhancing soil biophysical condition for climate-resilient restoration in mesic woodlands. Ecol Eng 71: 246-255

Qayyum MF, Liaquat F, Rehman RA, Gul M, ul Hye MZ, Rizwan M, ur Rehaman MZ (2017) Effects of co-composting of farm manure and biochar on plant growth and carbon mineralization in an alkaline soil. Environ Sci Pollut R 24(33): 26060-26068

Rahnama A, James RA, Poustini K, Munns R (2010) Stomatal conductance as a screen for osmotic stress tolerance in durum wheat growing in saline soil. Funct Plant Biol 37(3): 255-263

Ranjan G, Rao ASR (2007) Basic and applied soil mechanics. New Age International.

Rawls WJ, Gimenez D, Grossman R (1998) Use of soil texture, bulk density, and slope of the water retention curve to predict saturated hydraulic conductivity. Transactions of the ASAE 41(4): 983

Rayhani MH, Yanful EK, Fakher A (2007) Desiccation-induced cracking and its effect on the hydraulic conductivity of clayey soils from Iran. Can Geot J 44(3): 276-283

Reddy KR, Yargicoglu EN, Yue D, Yaghoubi P (2014) Enhanced microbial methane oxidation in landfill cover soil amended with biochar. J Geotech Geoenviron 140(9): 04014047

Reddy KR, Yaghoubi P, Yukselen-Aksoy Y (2015) Effects of biochar amendment on geotechnical properties of landfill cover soil. Waste Manage Res 33(6): 524-532

Rizwan M, Ali S, Abbas T, Adrees M, Zia-ur-Rehman M, Ibrahim M, ... Nawaz R (2018) Residual effects of biochar on growth, photosynthesis and cadmium uptake in rice (Oryza sativa L.) under Cd stress with different water conditions. J Environ Manage 206: 676-683

Rogovska N, Laird DA, Rathke SJ, Karlen DL (2014) Biochar impact on Midwestern Mollisols and maize nutrient availability. Geoderma 230: 340-347

Romero E, Gens A, Lloret A (1999) Water permeability, water retention and microstructure of unsaturated compacted Boom clay. Eng Geol 54(1-2): 117-127

Rondon MA, Lehmann J, Ramírez J, Hurtado M (2007) Biological nitrogen fixation by common beans (Phaseolus vulgaris L.) increases with bio-char additions. Biol Fert soils 43(6): 699-708

Sadasivam BY, Reddy KR (2014) Landfill methane oxidation in soil and bio-based cover systems: a review. Rev Environ Sci Bio 13(1): 79-107

Sadasivam BY, Reddy KR (2015a) Engineering properties of waste wood-derived biochars and biochar-amended soils. Int J Geot Eng 9(5): 521-535

Sadasivam BY, Reddy KR (2015b) Shear Strength of Waste-Wood Biochar and Biochar-Amended Soil Used for Sustainable Landfill Cover Systems. In From Fundamentals to Applications in Geotechnics IOS Press: pp. 745-752

Schiechtl HM (1980) Bioengineering for land reclamation and conservation. University of Alberta Press

Shwetha P, Varija K (2015) Soil water retention curve from saturated hydraulic conductivity for sandy loam and loamy sand textured soils. Aquatic Procedia 4: 1142-1149

Singh B, Singh BP, Cowie AL (2010) Characterisation and evaluation of biochars for their application as a soil amendment. Soil Res 48(7): 516-525

Sinha RK (2004) Modern plant physiology. CRC Press

Sinowski W, Scheinost AC, Auerswald K (1997) Regionalization of soil water retention curves in a highly variable soilscape, II. Comparison of regionalization procedures using a pedotransfer function. Geoderma 78(3-4): 145-159

Sorrenti G, Masiello CA, Dugan B, Toselli M (2016) Biochar physico-chemical properties as affected by environmental exposure. Sci Total Environ 563: 237-246

Sotir R (1990) Introduction to soil bioengineering restoration. Environmental Restoration: Science and Strategies for Restoring the Earth 146-148.

Spokas KA, Novak JM, Masiello CA, Johnson MG, Colosky EC, Ippolito JA, Trigo C (2014) Physical disintegration of biochar: an overlooked process. Environ Sci Tech Let 1(8): 326-332

Sreedeep S, Singh DN (2011) Critical review of the methodologies employed for soil suction measurement. Int J Geomech 11(2): 99-104

Steiner C, Glaser B, Geraldes Teixeira W, Lehmann J, Blum WE, Zech W (2008) Nitrogen retention and plant uptake on a highly weathered central Amazonian Ferralsol amended with compost and charcoal. J Plant Nutr Soil Sc 171(6): 893-899

Suleiman AA, Ritchie JT (2001) Estimating saturated hydraulic conductivity from soil porosity. Trans ASAE 44(2): 235

Suliman W, Harsh JB, Abu-Lail NI, Fortuna AM, Dallmeyer I, Garcia-Pérez M (2017) The role of biochar porosity and surface functionality in augmenting hydrologic properties of a sandy soil. Sci Total Environ 574: 139-147

Sun F, Lu S (2014) Biochars improve aggregate stability, water retention, and pore-space properties of clayey soil. J Plant Nutr Soil Sc 177(1): 26-33

Talbot JR, Deal CE (1993) Rehabilitation of cracked embankment dams. In Geotechnical Practice in Dam Rehabilitation, ASCE: pp. 267-283

Tan X, Liu Y, Zeng G, Wang X, Hu X, Gu Y, Yang Z (2015) Application of biochar for the removal of pollutants from aqueous solutions. Chemosphere 125: 70-85

Tan Z, Zou J, Zhang L, Huang Q (2018) Morphology, pore size distribution, and nutrient characteristics in biochars under different pyrolysis temperatures and atmospheres. J Mater Cycles Waste 20(2): 1036-1049

Tang C, Shi B, Liu C, Zhao L, Wang B (2008) Influencing factors of geometrical structure of surface shrinkage cracks in clayey soils. Eng geol 101 (3-4): 204-217

Tang CS, Pei XJ, Wang DY, Shi B, Li J (2014) Tensile strength of compacted clayey soil. J Geotech Geoenviron 141(4): 04014122

Thomas GW, Phillips RE (1979) Consequences of Water Movement in Macropores 1. J Environ Qual 8(2): 149-152

Tomczyk A, Sokołowska Z, Boguta P (2020) Biochar physicochemical properties: pyrolysis temperature and feedstock kind effects. Rev Environ Sci Biotechnol: 1-25

Tracy SR, Black CR, Roberts JA, Sturrock C, Mairhofer S, Craigon J, Mooney SJ (2012) Quantifying the impact of soil compaction on root system architecture in tomato (Solanum lycopersicum) by X-ray micro-computed tomography. Ann Bot 110(2): 511-519

Trupiano D, Cocozza C, Baronti S, Amendola C, Vaccari FP, Lustrato G, ... Scippa GS (2017) The effects of biochar and its combination with compost on lettuce (Lactuca sativa L.) growth, soil properties, and soil microbial activity and abundance. Int J Agron 2017

U.S. Environmental Protection Agency (USEPA). (1992). “U.S. EPA Subtitle D Clarification, 40 CFR 257 & 258, EPA/OSW-FR-92–4146–6.” Federal Register, 57(124), 28626–28632.

Uzoma KC, Inoue M, Andry H, Zahoor A, Nishihara E (2011) Influence of biochar application on sandy soil hydraulic properties and nutrient retention. J Food Agric Environ 9(3-4): 1137-1143

Van Zwieten L, Kimber S, Morris S, Chan KY, Downie A, Rust J, ... Cowie A (2010) Effects of biochar from slow pyrolysis of papermill waste on agronomic performance and soil fertility. Plant Soil 327(1-2): 235-246

Vaughn SF, Dinelli FD, Jackson MA, Vaughan MM, Peterson SC (2018) Biochar-organic amendment mixtures added to simulated golf greens under reduced chemical fertilization increase creeping bentgrass growth. Ind Crop Prod 111: 667-672

Vergani C, Graf F (2016) Soil permeability, aggregate stability and root growth: a pot experiment from a soil bioengineering perspective. Ecohydrology 9(5): 830-842

Verheijen F, Jeffery S, Bastos AC, Van der Velde M, Diafas I (2010) Biochar application to soils. A critical scientific review of effects on soil properties, processes, and functions. EUR 24099: 162.

Wall K, Zeiss C (1995) Municipal landfill biodegradation and settlement. J Environ Eng 121 (3): 214-224

Wang ZF, Li JH, Zhang LM (2011) Influence of cracks on the stability of a cracked soil slope. In Proc., 5th Asia-Pacisif Conf. on Unsaturated Soils (AP-UNSAT 2011): pp. 721-728

Wang J, Pan X, Liu Y, Zhang X, Xiong Z (2012) Effects of biochar amendment in two soils on greenhouse gas emissions and crop production. Plant soil 360(1-2): 287-298

Waqas M, Li G, Khan S, Shamshad I, Reid BJ, Qamar Z, Chao C (2015) Application of sewage sludge and sewage sludge biochar to reduce polycyclic aromatic hydrocarbons (PAH) and potentially toxic elements (PTE) accumulation in tomato. Environ Sci Pollut R 22(16): 12114-12123

Wiemer, G., & Kopf, A. (2017). Influence of diatom microfossils on sediment shear strength and slope stability. *Geochemistry, Geophysics, Geosystems*, *18*(1), 333-345.

Wong JTF, Chen Z, Ng CWW, Wong MH (2016) Gas permeability of biochar-amended clay: potential alternative landfill final cover material. Environ. Sci Pollut R 23(8): 7126-7131

Wong JTF, Chen Z, Chen X, Ng CWW, Wong MH (2017) Soil-water retention behavior of compacted biochar-amended clay: a novel landfill final cover material. J Soil Sediment 17(3): 590-598

Wong JTF, Chen Z, Wong AYY, Ng CWW, Wong MH (2018) Effects of biochar on hydraulic conductivity of compacted kaolin clay. Environ Pollut 234: 468-472

Wooding RA (1968) Steady infiltration from a shallow circular pond. Water Resour Res 4(6): 1259-1273

Wu TH, McKinnell III WP, Swanston DN (1979) Strength of tree roots and landslides on Prince of Wales Island, Alaska. Can Geotech J 16(1): 19-33

Xie T, Reddy KR, Wang C, Xu K (2014) Effects of amendment of biochar produced from woody biomass on soil quality and crop yield. In Geoenvironmental Engineering: pp. 170-180

Xie T, Sadasivam BY, Reddy KR, Wang C, Spokas K (2015) Review of the effects of biochar amendment on soil properties and carbon sequestration. Journal of Hazardous, Toxic, and Radioactive Waste 20(1): 04015013

Yargicoglu EN, Reddy KR (2015) Characterization and surface analysis of commercially available biochars for geoenvironmental applications. In IFCEE 2015: pp. 2637-2646

Yu L, Tang J, Zhang R, Wu Q, Gong M (2013) Effects of biochar application on soil methane emission at different soil moisture levels. Biol Fert Soils 49(2): 119-128

Zeleke TB, Si BC (2005) Scaling relationships between saturated hydraulic conductivity and soil physical properties. Soil Sci Soc Am J 69(6): 1691-1702

Zhang J, Huang HW, Zhang LM, Zhu HH, Shi B (2014) Probabilistic prediction of rainfall-induced slope failure using a mechanics-based model. Eng Geol 168: 129-140

Zhang Y, Gu K, Li J, Tang C, Shen Z, Shi B (2020) Effect of biochar on desiccation cracking characteristics of clayey soils. Geoderma 364: 114182

Zhou H, Long Y, Meng A, Li Q, Zhang Y (2015) Classification of municipal solid waste components for thermal conversion in waste-to-energy research. Fuel 145: 151-157

Zhu XG, Long SP, Ort DR (2010) Improving photosynthetic efficiency for greater yield. Annu Rev Plant Biol 61: 235-261

Zong Y, Chen D, Lu S (2014) Impact of biochars on swell–shrinkage behavior, mechanical strength, and surface cracking of clayey soil. J Plant Nutr Soil Sc 177(6): 920-926

Zong Y, Xiao Q, Lu S (2016) Acidity, water retention, and mechanical physical quality of a strongly acidic Ultisol amended with biochars derived from different feedstocks. J soils sediments 16(1): 177-190